Characterizing the Role of the CRISPR-Cas system in Biofilm Formation and Pathogenicity of *Salmonella enterica* subspecies *enterica* serovar Typhimurium

THESIS

Submitted in partial fulfillment

of the requirements for the degree of

DOCTOR OF PHILOSOPHY

by

Nandita Sharma

2017PHXF0019P

Under the Supervision of

Dr. Sandhya Amol Marathe

BIRLA INSTITUTE OF TECHNOLOGY AND SCIENCE

PILANI (RAJASTHAN)- 333031

2022

BIRLA INSTITUTE OF TECHNOLOGY AND SCIENCE, PILANI

CERTIFICATE

This is to certify that the thesis entitled **"Characterizing the Role of the CRISPR- Cas system in Biofilm Formation and Pathogenicity of *Salmonella enterica* subspecies *enterica* serovar Typhimurium,"** submitted by **Ms. Nandita Sharma**, ID No. **2017PHXF0019P** for the award of Ph.D. Degree of the Institute embodies the original work done by her under my supervision.

Signature of the Supervisor:

Name: Dr. Sandhya Amol Marathe

Designation: Associate Professor

Date: 17.07.2023

Place: Pilani

Dedicated to the loving memories of my grandfathers
Ganga Prasad Sharma and Dr. Hari Shankar Sharma

Acknowledgments

"A smooth sea never made a skilled sailor" applies to all aspects of life in general, being at the culmination of some of the most important years of my scientific career and looking back, I realize that my path toward this point has been filled with some of the most amazing individuals who have helped me overcome obstacles at various points and to whom I would like to offer my humble gratitude.

I would like to start by thanking my family members- Mumma, papa, my little Anadi, and my partner in crime, Satish. As overprotective as my parents can be at times, I can never be thankful enough to my parents for all the love, support, and sacrifice they have endured to get me to where I am today. I'm lucky to have a fun-loving brother like Anadi, who inspires me to be positive even during crucial hours. I feel blessed to have someone like my husband, Satish, who perfectly completes my madness. A person whom I have always looked up to for everything, be it partaking in crazy deeds, sharing gossip, planning trips, and surprises, talking about food all day long, too serious scientific discussions, and lastly serving as my thesis reviewer. He has been my pillar over the years. I'm indebted for all the care, support, and love from my Appa and Amma who always looked up to me as their daughter. I would also like to thank my close friends – Moti (Devika), Dv (Divya), and Suriya. The one who makes the world a little less chaotic and a whole lot more meaningful. Right from video chats, talking nonsense all day long to bugging each other. The thought that they are always there by my side was enough to keep me going.

This journey wouldn't have been possible without the immense help of my supervisor, Dr. Sandhya Marathe. I still remember the day I discussed with her my master's dissertation in her lab. The excitement and encouragement she showed during the discussion were something that inspired me. I feel fortunate to have had a mentor like her, who is extremely friendly, caring, thoughtful, open, and welcoming to new ideas and more importantly believed in me and my abilities to overcome barriers when things didn't go as planned. I cannot be thankful enough for all that I have learned under her guidance (both professionally and personally) and I'm grateful for her support throughout my Ph.D. years.

I express my sincere thanks to my Doctoral Advisory Committee (DAC Members), Dr. Jitendra Panwar, and Dr. Prabhat Nath Jha for the critical reading of my thesis manuscript and for suggesting valuable inputs.

I am greatly thankful to Prof. Souvik Bhattacharyya (Vice-Chancellor), Prof. Sudhir Kumar Barai (Director), Col Soumyabrata Chakraborty (Registrar), Prof. S. K. Verma (Dean, Administration), Prof. M. B. Srinivas (Dean, AGSRD), Prof. Shamik Chakraborty (Associate Dean, AGSRD, Pilani Campus), Dr. Rajdeep Chowdhary (Head of the Department, Biological Sciences, Pilani Campus) for allowing me to pursue my doctoral studies by providing necessary facilities.

As important as a supervisor or a project is, the lab atmosphere plays an equally important role in defining a Ph.D. career, and in this regard, I feel fortunate to have been surrounded by a few crazy bunches of people who were part of this journey. I would like to start by thanking Tripti, a chirpy soul whose stupidity knows no bound. Be it making fun, laughing at quirky jokes, or singing aloud inside the hood. She played a major role in keeping the lab environment hilarious. Moving further here comes my three musketeers, google drive Ankita (baby Das), crazy little Shreya and Simran. Be it helping each other or partaking in unwanted laboratory-related chores, they always stood by my side. I would like to thank Harshita for her cheerful presence during food and tea time.

As with many things in life, there will be people who indirectly facilitate or make our work easier and I feel that it is important to recognize their contribution. In this regard, I thank all the non-teaching staff of the Department of Biological Sciences, Mr. Naresh, Mr. Ajay, and Mr. Subhash. It would be incomplete without extending my gratitude to Girdhari uncle, especially for those refreshing cups of extra tea, and the light-hearted conversation in Skylab during boredom.

I would like to conclude by stating that this is not an exhaustive list of people whom I acknowledge and that I sincerely thank everyone I have encountered and not mentioned here, who has helped me grow into the person I am today and guided me to places that matter.

(Nandita Sharma)

Table of Contents

List of Tables

List of Abbreviations

Symbol	Abbreviation
WHO	World Health Organization
CDC	Centers for Disease Control and Prevention
NTS	Non-typhoidal *Salmonella*
T3SS-1	type III secretion system 1
SPI-1	*Salmonella* pathogenicity island 1
SPI-2	*Salmonella* pathogenicity island 2
MHC	Major histocompatibility complex
AMPs	Antimicrobial peptides
SCV	*Salmonella*-containing vacuole
Ssa	Secretion system apparatus
Ssc	Secretion system chaperones
Sse	Secretion system effector
Ssr	Secretion system regulator proteins
Sop	*Salmonella* outer proteins
Sif	*Salmonella*-induced filament
RNI	Reactive nitrogen species
ROS	Reactive oxygen species
PIP	Pathogenicity island-encoded proteins
Spv	*Salmonella* plasmid virulence genes
PP	Peyer's patch
MLN	Mesenteric lymph nodes
M-cells	microfold cells
DC	Dendritic cells
ECM	Extracellular matrix
e-DNA	Extracellular DNA
RAW 264.7	Ralph And William’s cell line 264.7
IHF	Integration host factor
H-NS	Histone-like nucleoid structuring protein
LPS	Lipopolysaccharide
OMP	Outer membrane protein
c-di-GMP	Cyclic diguanosine monophosphate
c-di-AMP	Cyclic diadenosine monophosphate
cAMP	Cyclic adenosine monophosphate
CRP	cAMP receptor protein

CRISPR	Clustered Regularly Interspaced Short Palindromic Repeats
Cas	CRISPR-associated
crRNA	Clustered regularly interspaced short palindromic repeats RNA
PAM	Protospacer adjacent motif
MGE	Mobile genetic elements
LB	Luria Bertani
YESCA	Yeast extract casamino acid
GOI	Gene of interest
CV	Crystal violet
PBS	Phosphate buffer saline
RT	Room temperature
PI	Propidium iodide
RNA	Ribonucleic acid
DNA	Deoxyribonucleic acid
EPS	Exopolymeric substances
CR	Congo red
CLSM	Confocal laser scanning electron microscopy
SEM	Scanning electron microscopy
Tht	Thioflavin-T
CTAB	Cetyltrimethylammonium bromide
cDNA	Complementary Deoxyribonucleic acid
mg	Milli gram
g	Grams
ng	Nanograms
µg	Microgram
mL	Millilitre
µL	Microlitre
bp	Base pair
kDa	Kilo dalton
min	Minutes
h	Hours
cm	Centimeter
M	Molar
mM	Milli molar
µM	Micromolar

C	Celsius
SD	Standard deviation
UV-vis	Ultraviolet-visible
OD	Optical density
PCR	Polymerase Chain Reaction
qRT-PCR	Quantitative real-time polymerase chain reaction
SDS-PAGE	Sodium Dodecyl Sulphate–Polyacrylamide Gel Electrophoresis
CF	Calcofluor
OM	Outer membrane
OS	Oligosaccharides
BLP	Bacterial Lipoprotein
sca-RNA	Small, CRISPR/Cas-associated RNA
mRNA	Messenger ribonucleic acid
H_2O_2	Hydrogen peroxide
rpm	Revolutions per minute
CFU	Colony formation unit
AU	Arbitrary unit
SA	Site Accessibility
MFE	Minimum Free Energy
EMFE	Extended Minimum Free Energy
H_2DCFDA	2′,7′-dichlorodihydrofluorescein diacetate
MH	Muller Hinton
BATH	Bacterial adhesion to hydrocarbon
NGM	Nematode growth medium
FBS	Fetal bovine serum
RPMI	Roswell Park Memorial Institute 1640 media
MOI	Multiplicity of infection
NED	N-1-naphthyl ethylenediamine dihydrochloride
TLRs	Toll-like receptors
PAMPs	Pathogen-associated molecular patterns
NRAMP	Natural resistance-associated macrophage protein

List of Figures

Abstract

The **C**lustered **R**egularly **I**nterspaced **S**hort **P**alindromic **R**epeats with CRISPR-associated proteins (CRISPR-Cas) system, found in bacteria and archaea, provides adaptive immunity against mobile genetic elements, including phages and plasmids. In addition to being implicated in bacterial immunity and genome editing, the CRISPR-Cas system has recently been demonstrated to regulate bacterial physiology and virulence in many pathogenic bacteria, including *Salmonella.* However, the endogenous gene regulatory mechanisms of the *Salmonella* type IE system remain elusive. Thus, we decided to explore the role of the CRISPR-Cas system-mediated biofilm formation in *Salmonella enterica* subspecies *enterica* serovar Typhimurium. The role of the CRISPR-Cas system in *Salmonella* biofilm formation was investigated by deleting CRISPR-Cas components Δ*crisprI*, Δ*crisprII*, ΔΔ*crisprI crisprII*, and Δ*cas op.* We determined that the system positively regulates surface biofilm while inhibiting pellicle biofilm formation. Results of real-time PCR suggest that the flagellar (*fliC, flgK*) and curli (*csgA*) genes were repressed in knockout strains, causing reduced surface biofilm. The CRISPR-Cas mutants displayed altered pellicle biofilm architecture. They exhibited bacterial multilayers and a denser extracellular matrix with enhanced cellulose and less Curli, ergo weaker pellicles than those of the wildtype. The cellulose secretion was more in the knockout strains due to the upregulation of *bcsC*, a gene necessary for cellulose export. We hypothesized that the secreted cellulose quickly integrates into the pellicle, leading to enhanced pellicular cellulose in the knockout strains. We determined that the global regulator cAMP-regulated protein (CRP) was upregulated in the knockout strains, thereby inhibiting the expression of *csgD* and, hence, also of *csgA* and *bcsA*. The conflicting upregulation of *bcsC*, the last gene of the *bcsABZC* operon, could be caused by independent regulation by the CRISPR-Cas system owing to a partial match between the CRISPR spacers and the *bcsC* gene. The CRP-mediated regulation of the flagellar genes in the knockout strains was probably circumvented through the regulation of Yddx governing the availability of the sigma factor σ^{28} that further regulates class 3 flagellar genes (*fliC, fljB,* and *flgK*). Additionally, the variations in the lipopolysaccharide (LPS) profile and expression of LPS-related genes (*rfaC, rfbG,* and *rfbI*) in knockout strains could also contribute to the altered pellicle architecture. Collectively, we establish that the CRISPR-Cas system differentially regulates the formation of surface-attached and pellicle biofilm.

We further show that the alteration in the LPS profile of the knockout strains impacted the membrane characteristics in these strains. The CRISPR-Cas knockout strains showed reduced cell surface hydrophobicity, increased membrane permeability, and increased sensitivity against an antimicrobial peptide (Polymyxin B). *In-silico* analysis suggests *ompW* gene as one of the targets for the CRISPR1-spacer, indicating its regulation by the CRISPR1 array. OmpW acts as an influx pump for hydrogen peroxide. We show that *ompW* is upregulated in the knockout strains. Increased *ompW* expression in the CRISPR-Cas knockout strains resulted in the increased uptake of hydrogen peroxide, thereby leading to their increased sensitivity against hydrogen peroxide. Through these results, we deduce that the CRISPR-Cas system positively regulates outer membrane protein, OmpW, and LPS in *S.* Typhimurium, thereby protecting the bacterial cell against antimicrobial compounds like hydrogen peroxide and polymyxin B.

The CRISPR-Cas knockout strains show impaired motility, altered LPS profile, reduced expression of Curli, and sensitivity against the antimicrobial peptide and hydrogen peroxide. These traits are some of the important contributors to virulence in *Salmonella*. Thus, we assessed the role of the CRISPR-Cas system in *Salmonella* pathogenesis by using *in vitro* and *in vivo* infection models. Our study showed that the CRISPR-Cas knockout strains have impaired invasion and proliferation efficiency in both the intestinal and phagocytic cell lines. This was further iterated by the attenuated systemic dissemination of the knockout strains in BALB/c mice. Additionally, the CRISPR-Cas knockout strains displayed increased sensitivity against innate immune barriers like antimicrobial and complement proteins. The reduced expression of SPI-1 encoded HilA, SipA, SipD, and SopB could have contributed to the impaired invasion of the knockout strains in intestinal epithelial cells. Furthermore, the expression of SPI-2 encoded effector proteins like SpiC, PipB2, and other virulence genes like *mgtC, katG, sod,* and *ahpC* was decreased in the knockout strains. This could have compromised their survival within the host impacting colonization in *Caenorhabditis elegans* and BALB/c mice infection model. Overall, the results suggest that the CRISPR-Cas system positively regulates two important *Salmonella* pathogenicity islands i.e. SPI-1 and SPI-2, impacting the pathogenicity of *Salmonella*.

In a nutshell, the CRISPR-Cas system of *S.* Typhimurium regulates biofilm formation, membrane properties, and pathogenesis by regulating the expression of endogenous genes.

Chapter 1

Introduction

1. Background

Annually, ~1 in 10 people get sick with foodborne illness, and effectively 33 million healthy life years are lost (*Food Safety*, 2022). Most foodborne illnesses result in diarrhea, and *Salmonella* is one of the four global reasons for such cases (World Health Organization (WHO), 2018). It causes salmonellosis with symptoms of gastroenteritis that may progress to enteric fever. Organizations like World Health Organization (WHO), the Centers for Disease Control and Prevention (CDC), and several research groups are working toward controlling disease occurrence and developing drugs/vaccines to eradicate diarrhea diseases. With the advent of drug-resistant strains, it is all the more important to look out for novel therapeutic strategies. To devise novel therapeutic strategies against infectious diseases, it is essential to gain mechanistic insights into the pathogenesis and physiology of the pathogen. A recent study on *Pseudomonas aeruginosa, Klebsiella pneumonia,* and *Escherichia coli* K12 suggest the remodeling of bacterial pathogenicity by endogenous CRISPR-Cas systems (R. Li et al., 2016). Insights into the gene regulation by endogenous CRISPR-Cas systems in pathogenic bacteria can strongly influence the design of effective therapeutic strategies against bacterial diseases (R. Li et al., 2016).

In the following thesis, we have aimed to test the extent of CRISPR-Cas mediated regulation of pathogenicity and biofilm formation in *Salmonella*. In the succeeding sections, we have briefly discussed the concepts of *Salmonella* infection and the mechanistic details of the CRISPR-Cas system.

1.1 *Salmonella* classification and epidemiology

Salmonellae, a Gram-negative, facultatively anaerobic, flagellated intracellular pathogen, is a member of the *Enterobacteriaceae* family. The bacilli-shaped bacteria were named after a veterinary surgeon, Dr. Daniel E Salmon. This genus comprises two species, *Salmonella enterica,* and *Salmonella bongori,* which are further divided into six subspecies. The majority of salmonellosis cases are due to *S. enterica* accounts for the majority of Salmonellosis. *Salmonella* consists of three antigens, namely, flagellar (H), somatic/LPS (O), and capsular (Vi) antigens (R. A. Cheng et al., 2019). The variations in these antigens on the bacteria are harnessed in the Kauffmann-White scheme to classify *Salmonella* subspecies into more than 2600 serovars (Ranieri et al., 2013). These serovars can be grouped into host-adapted, host-restricted, and broad-host-range serovars based on host specificity. The host-adapted serovars infect specific host species causing systemic

infection; and, they sporadically infect other hosts. The host-restricted serovars infect a specific host and cause systemic infection. In contrast, the broad-host-range serovars infect diverse host species, causing mild enteric diseases or persisting within the host without any symptoms. Most of the serovars that cause infections in humans and warm-blooded animals belong to the subspecies *enterica* (Gal-Mor, 2019).

The distinct clinical responses in humans dictate the typhoidal and non-typhoidal serovar (NTS:non-typhoidal *Salmonella*) faction (Gal-Mor et al., 2014). In NTS infection, the clinical manifestation includes abdominal pain, diarrhea, and vomiting (Darwin & Miller, 1999). The WHO estimated that approximately 550 million people worldwide become ill with diarrhea yearly. According to the CDC, 1.35 million *Salmonella* infections and 420 deaths were reported in the United States (*Salmonella* Homepage | CDC). Unlike the NTS serovars, typhoidal serovars are invasive and cause systemic infection and enteric fever. In countries like Africa, the southeastern part of Asia, the western pacific region, and America, enteric fever remains a concern. Annually, 14.3 million individuals suffer from typhoid fever, with 135,000 estimated deaths worldwide (World Health Organization (WHO), 2018). In 2017, the global burden accounted for 95% of NTS cases (Stanaway et al., 2019). Furthermore, CDC reported an estimated 5,700 cases of typhoid infection with a 25% mortality and 10% relapse rate among treated patients(Information for Healthcare Professionals | Typhoid Fever | CDC). Moreover, an epidemiological survey in 2014 from South America and South Asia has shown that 90%cases of typhoid are asymptomatic carriers (di Domenico et al., 2017; Jahan et al., 2022). The NTS serovar is globally recognized as zoonotic and ubiquitous. The diversity of *Salmonella* serovars allows it to thrive under a broad host spectrum, collectively accounting for diversified reservoirs in the environment. It occurs independently as a population of individual bacteria or in the form of biofilms (a consortium of microbial cells forming a mat-like structure) in different ecological niches.

1.2 Sources of *Salmonella*

Salmonella is present in marine and coastal areas, and freshwater in the river, ponds, lakes, aquatic and groundwater ecosystems (Abulreesh & Abulreesh, 2012; H. Liu et al., 2018). Fish feed houses various *Salmonella* serovars like *Salmonella enterica* subspecies *enterica* serovar Senftenberg, serovar Agona, serovar Montevideo, and serovar Kentucky (Lunestad et al., 2007). *Salmonella* usually thrives on fish's gills, skin, and intestinal tracts (Bibi et al., 2015). Once infected, the marine life serves as a passive exporter of *Salmonella*.

Additionally, the terrestrial environment also forms a favorable niche for *Salmonella*, making groundwater amenable to contamination with the foodborne pathogen. Diverse *Salmonella* serovars have been identified in ground and irrigation water, making their home in farm-produced crops (Abulreesh & Abulreesh, 2012). Apart from this, the presence of *Salmonella* is widespread among wild, domestic, and farm animals. Cattle, sheep, fowls, and chickens are natural hosts for *Salmonella* serovars. Moreover, cattle have been reported as an 'active carrier' of *Salmonella* (Demirbilek & Demirbilek, 2017). Many domestic fowls like chickens, geese, turkeys, and guinea fowl are natural presenters of serovars like Gallinarum and Pullorum (Abulreesh & Abulreesh, 2012). Collectively, *Salmonella* is regarded as an important livestock colonizer. Furthermore, poultry farms also foresee the presence of *Salmonella* serovars like *Salmonella enterica* subspecies *enterica* serovar Typhimurium (*S*.Typhimurium), serovar Choleraesuis, serovar Gallinarum, and serovar Pullorum. The occurrence of *Salmonella* extends to pests (rodents, rats, and mice), exotic pets, domestic animals, and reptiles like lizards, snakes, and turtles, that act as carrier animals (Demirbilek & Demirbilek, 2017).

Salmonella can also be present in the natural environment as biofilms on biotic and abiotic substrates (Steenackers et al., 2012). It adheres to glass, plastic, rubber, and stainless steel used in various industrial settings, manufacturing units, food processing units, and hospitals. It also colonizes multiple medical devices like stents, catheters, and prosthetics, forming biofilms on poultry and meat products. Furthermore, *Salmonella* colonizes various parts of the plant, making the plant a vehicle for pathogen spread (Steenackers et al., 2012). Numerous *Salmonella* outbreaks reported in underdeveloped countries have been associated with contaminated seeds and sprouts like alfalfa, beans, celery, broad leafy vegetables, tomatoes, radish, carrots, and mushrooms. It thrives on various parts of plants, like sprouts, seeds, leaves, roots, and fruits, while forming a biofilm (Steenackers et al., 2012). In addition, human epithelial cells (Ledeboer et al., 2006) and gallstones also provide a scaffold for *Salmonella* biofilm (Crawford, Rosales-Reyes, et al., 2010). Various studies have also reported *Salmonella* biofilm formation in laboratory settings. The presence of enteric bacteria under terrestrial, aquatic, groundwater, and food ecosystems are related to environmental threats posed by runoff from agricultural discharge, sewage treatment plants, sludge, and fecal pollution. Besides this, improper handling and lack of disinfection in industries, food processing, livestock production, and hospital units

aggravate the release of pathogens in the environment, where it remains dormant and virulent.

1.3 Clinical manifestations and pathogenesis of *Salmonella*

Salmonella infections can be classified as foodborne or hospital-acquired, depending on their source. Unhygienic conditions coupled with biofilm formation contribute to an increased probability of disease. In addition, biofilm formation on medical devices accounts for 50% of general infections (Paredes et al., 2014). Biofilms cater to long-term bacterial survival and provide a replicative niche to the pathogen. In addition, they provide antibiotic tolerance and permit the dissemination of planktonic cells in the environment causing clinical complications (Mah, 2001). *Salmonella* infection can be acute or chronic. At times chronic illnesses cause malignancies (Harrell et al., 2021). For example, *Salmonella enterica* subspecies *enterica* serovar Typhi (*S*.Typhi) is associated with gallbladder cancer (Koshiol et al., 2016). Additionally, latent infection of *Salmonella* has also been reported in patients surviving *Salmonella* infection (Harrell et al., 2021).

Salmonella transmission happens by ingesting contaminated food, while human-to-human and animal-to-human transmissions result *via* the faeco-oral route. The incubation period within the human body ranges from 6 to 72 h, followed by gastrointestinal symptoms - headache, fever, abdominal pain, diarrhea, and vomiting (Darwin & Miller, 1999). Typically, *Salmonella* pathogenesis is sequentially orchestrated into five steps – attachment to the intestinal epithelium, invasion in intestinal epithelial cells, proliferation inside macrophages, systemic dissemination in various organs, persistence in the gallbladder, and transmission by fecal shedding.

1.3.1 The gastro-intestinal infection process

After ingesting contaminated food, *Salmonella* travels through the gut to the intestine (Fig. 1.1). While acidic conditions of the stomach usually kill most bacteria, a few bacteria that survive are then transported to the intestine, colonizing the terminal ileum and colon. After adhesion to the epithelium lining, bacterial cells initiate invasion by host-mediated or cell-mediated pathways (Fig. 1.1).

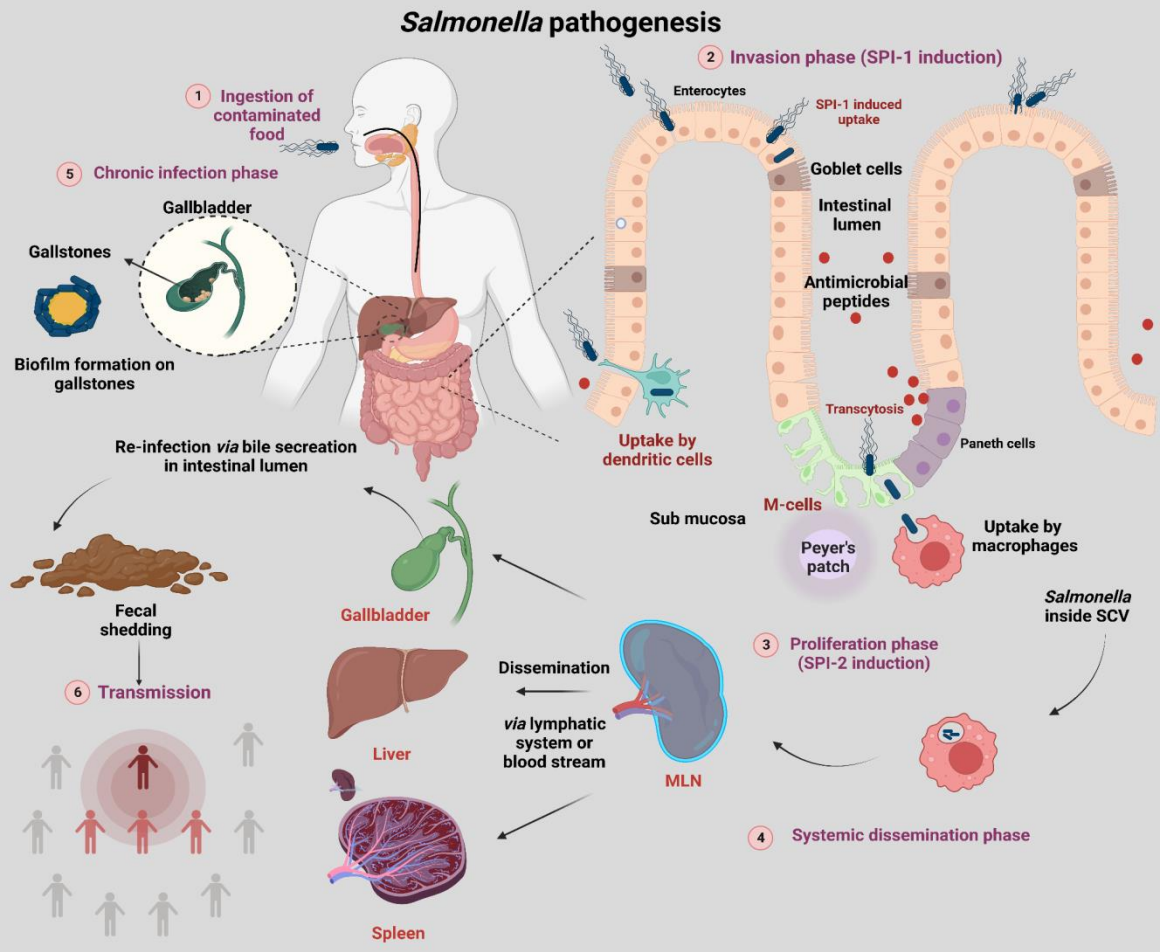

Fig. 1.1: Schematic representation of the *Salmonella* infection cycle in humans (1) The infection cycle begins with ingesting contaminated food. *Salmonella* passes through the gastric barrier and reaches intestine. **(2)** The intestinal invasion is achieved either through M-cells *via* transcytosis or direct uptake by enterocytes (requires SPI-1 system). In addition, uptake by dendritic cells is an alternative pathway. The invasion process is followed by bacterial replication inside epithelial *Salmonella* containing vacuole (SCV). Next, *Salmonella* breaches the intestinal epithelial barrier and enters the sub-mucosa, where macrophages capture them. **(3)** Inside macrophages, *Salmonella* resides within SCV, and the vacuolar niche triggers SPI-2 encoded genes to aid intracellular proliferation and survival. Macrophages act as a vehicle for systemic dissemination of *Salmonella*. **(4)** During its systemic phase, the pathogen spreads from the intestine to the mesenteric lymph node (MLN) and eventually colonizes the liver, spleen, and gallbladder. **(5)** Upon reaching the gallbladder, *Salmonella* forms biofilms on gallstones, causing the carriage stage. **(6)** *Salmonella* carriers shed bacteria into the small intestine through bile from gall bladder. The fecal shedding in the environment marks the beginning of *Salmonella* transmission to a new host and the process continues. The figure was created using Biorender.

The host-mediated pathways include uptake by transcytosis (Velge et al., 2012a), i.e., invasion of apical cells (microfold cells or enterocytes) followed by exocytosis to the

basal side of the intestine. Additionally, *Salmonella* is randomly phagocytosed by $CD18^{+}$cells (Niedergang et al., 2000) (Fig. 1.1). **The cell-mediated** invasion pathway is initiated by remodeling the cellular cytoskeleton (Velge et al., 2012a). The membrane remodeling can be receptor-mediated (Zipper mechanism), for example, *via* the Rck system, or can be *via* membrane ruffling (Trigger mechanism) by one of the type III secretion system 1 (T3SS-1) (Manon et al., 2012). This T3SS-1 secretion apparatus is assembled on the bacterial surface, spanning the inner and outer bacteria membrane (Fig. 1.2). It is encoded by a pathogenicity island, *Salmonella* pathogenicity island 1 (SPI-1).

1.3.1.1 *Salmonella* pathogenicity island 1 (SPI-1) secretion system regulates the initial phase of infection

SPI-1, a 40 kb chromosomal region, is composed of 39 genes encoding the components of the T3SS-1 (Kombade et al., 2021). These include exporter apparatus (Basal body) encoded by *prg/org* and *inv/spa* operon and needle complex encoded by *prg* and *inv* operon (Fig. 1.2). The needle is capped by a tip/translocon composed of SipB, SipC, and SipD (Fig. 1.2). The other components include effectors (Avr, Sips, and SptP), chaperons (SicA, InvB, and SicP), and regulators (HilA, HilC, HilD, and InvF) (Gao et al., 2019; Manon et al., 2012). The SPI-1 also translocates other effectors like *Salmonella* outer proteins (Sops) that are located outside the SPI-1 encoding region.

Pathogen entry is initiated upon bacteria-host cell contact. This energy-driven process is sequentially mediated by the action of SpaO, OrgA, OrgB, InvI, and InvC (Manon et al., 2012). These five proteins, along with molecular chaperons, deliver translocases that form a pore in the host cell to transport bacterial effectors (Manon et al., 2012). The event causes membrane ruffling and cytoskeleton remodeling within the host epithelial cells leading to bacterial uptake. The role of SPI-1 is not only restricted to membrane trafficking and plays a role in other processes. It aids in apoptosis, cell division, macrophage polarisation, downregulation of early proinflammatory cytokines (Pavlova et al., 2011), and suppression of major histocompatibility complex (MHC-II) presentation (Lou et al., 2019). In addition to this, SPI-1 also helps the bacteria to cross the blood-brain barrier (Chaudhuri et al., 2018).

In the intestinal environment, SPI-1 proteins also induce an inflammatory response helping *Salmonella* to generate novel electron acceptors, tetrathionate, and nitrate (utilizable only by *Salmonella*) to outcompete the intestinal microbiota (Khan, 2014). The

inflammatory cytokines released during infection activate the infected macrophages inducing the killing of intracellular *Salmonella*, causing neutrophil infiltration at the site of infection and stimulating epithelial cells to release antimicrobial peptides (AMPs) into the intestinal lumen (Ibarra & Steele-Mortimer, 2009). One of the AMP secreted in the lumen includes lipocalin-2, which sequesters iron, depriving the pathogens of iron (Broz et al., 2012). *Salmonella* produces two siderophores, enterochelin and salmochelin, to acquire

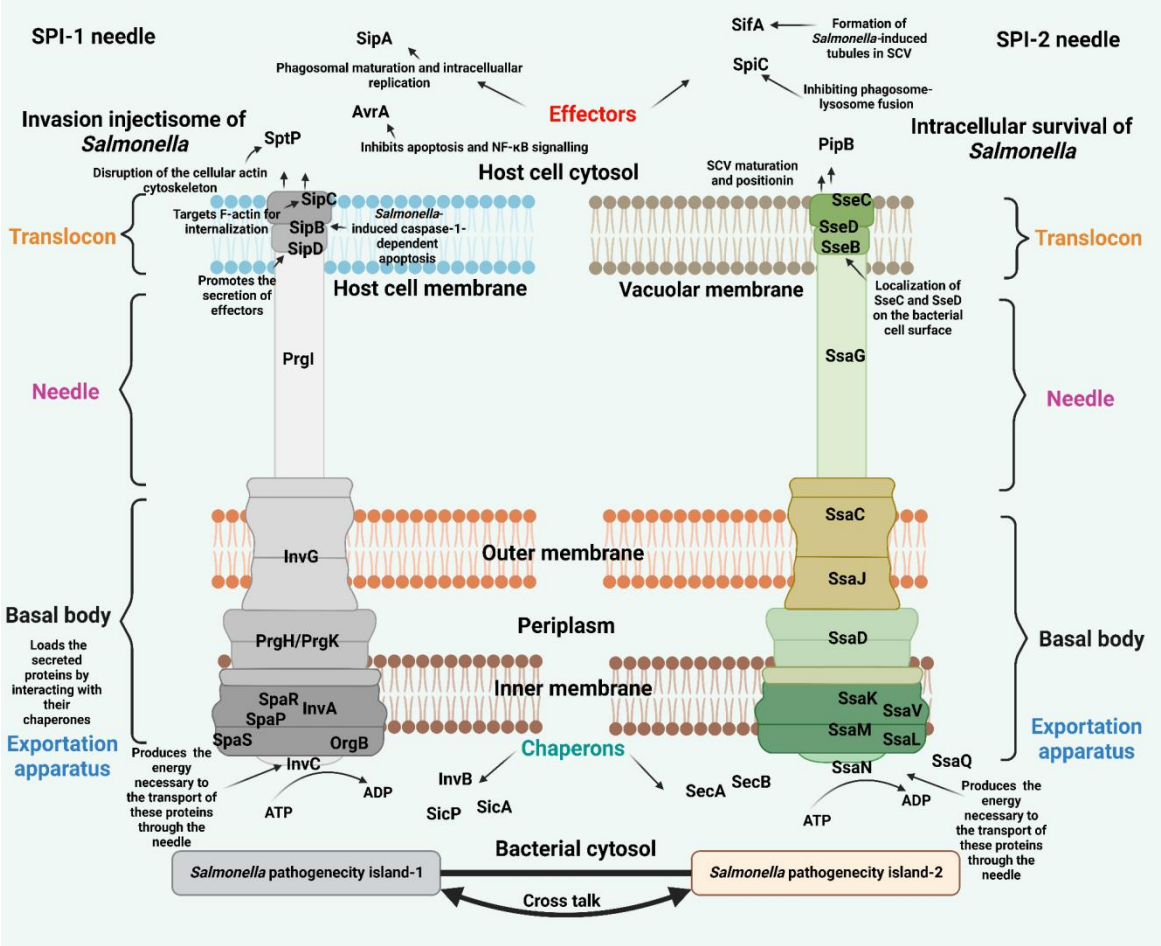

Fig. 1.2: Model for the function of two injectosomes involved in host-pathogen interaction during *Salmonella* infection. The *Salmonella* pathogenicity island-1 (SPI-1) and *Salmonella* pathogenicity island-2 (SPI-2) encode a distinct set of effector proteins involved in the invasion and intracellular survival of *Salmonella*, respectively. The coordinated action of these two virulence loci governs the fate of *Salmonella* pathogenesis. The complex structure of T3SSs includes a basal body that holds the secretion apparatus into the inner and outer membrane. Anchored to the basal body, the needle protrudes from the outer membrane. The extreme end of the needle comprises a translocon, which forms a pore in the host cell or vacuolar membrane. Finally, the translocation of effector proteins requires an export apparatus located at the inner membrane. The unfolded effector proteins together with chaperons are targeted to the export apparatus, while ATP production aids the transport of these proteins through the needle to deliver them inside the target host-cell cytosol. The figure was created using Biorender.

iron from the iron-limiting intestinal lumen. Lipocalin-2 inhibits iron uptake through enterochelin. However, lipocalin-2 cannot bind to salmochelin, thus, allowing *Salmonella* to replicate in the intestinal lumen while starving the gut microbiota of iron (Ibarra & Steele-Mortimer, 2009).

1.3.1.2 *Salmonella* pathogenicity island 2 (SPI-2) secretion system regulates the proliferation phase

Salmonella is an intracellular pathogen majorly surviving and replicating within a modified phagosome known as the *Salmonella*-containing vacuole (SCV). Within the SCV, it acquires nutrients and avoids host antibacterial activities. In intestinal epithelial cells, a few SCVs transcytose *Salmonella* across the intestinal barrier (Malik-Kale et al., 2012). *Salmonella* is phagocytosed by macrophages upon crossing the epithelial barrier and internalized within SCVs. At this stage, the bacteria shut down its SPI-1 system and activate the SPI-2 system. The virulence proteins secreted by the SPI-2 system aid the intracellular survival and proliferation of *Salmonella*. However, *Salmonella* majorly replicates within the epithelial cells replicates (Malik-Kale et al., 2012), where the SPI-2 system has no role in cytosolic replication.

SPI-2 is divided into two segments, 15 kb and 25 kb (Kombade et al., 2021), encoding genes necessary for tetrathionate metabolism (Winter et al., 2010) and virulence (Kombade et al., 2021), respectively. The SPI-2 secretion apparatus is encoded by four categories of virulence genes - (i) *ssa* (secretion system apparatus), (ii) *ssc* (secretion system chaperones), (iii) *sse* (secretion system effector), and (iv) *ssr* (secretion system regulator proteins (Figueira & Holden, 2012)) (Fig. 1.2). Some SPI-2 effector proteins like SseI, SifA, SseJ, and SspH2 are encoded outside the SPI-2 island. SPI-2 plays a vital role in replication, followed by systemic dissemination of the pathogen. The expression of the system is induced as the bacterial cells encounter low osmolarity, low pH, and low concentration of Mg^{2+}, Ca^{2+}, and PO_3^{3-} inside SCV. The two-component regulators like the SsrA-SsrB, OmpR-EnvZ, and PhoP-PhoQ (Fass & Groisman, 2009a) activate the SPI-2, which uses its translocon SseBCD to maintain the biogenesis of vacuolar compartments (Nikolaus et al., 2001). The function of SPI-2 effector proteins is synced with SPI-1 effectors (SipA, SipD, SopA, and SopB) present in the cytosol after the invasion (Gao et al., 2019). Together, these effectors help *Salmonella* to secure a replicative niche inside the macrophages. The effector proteins protect *Salmonella* by hindering intracellular trafficking, safeguarding against the oxidative killing (NADPH-dependent) and reactive

nitrogen species (RNS) (Vazquez-Torres et al., 2000), inducing apoptosis (van der Velden et al., 2000), enhancing cholesterol esterification (Catron et al., 2002), and forming F-actin assembly around SCV (Méresse et al., 2001). In addition, SPI-2 enhances bacterial cell proliferation by modulating host cytoskeleton (Méresse et al., 2001), *Salmonella*-induced filament (*sif*) formation, and localization in proximity to Golgi probably to acquire nutrients (Méresse et al., 2001).

1.3.1.3 Other virulence determinants of *Salmonella*

Gene clusters responsible for *Salmonella* virulence are present either on chromosomes or plasmids. Twenty-one pathogenicity islands are identified on the chromosomal locus, including SPI-1 and SPI-2. The SPI-3, a 17kb locus, harbors the *mgtCB* operon and aids bacterial proliferation within SCVs (Blanc-Potard et al., 1999; Blanc-Potard & Groisman, 1997). The gene *mgtC* gets triggered under low Mg^{2+} conditions, helping the growth and systemic dissemination by maintaining bacterial cytosolic pH, increasing phosphate uptake, and repressing cellulose production inside the host (Choi et al., 2019). SPI-4 is a 27 kb locus encoding six genes *siiABCDFE* (Kiss et al., 2007). The secretory protein, SiiE, functions as an adhesin, facilitating the apical invasion of enterocytes (X. Li et al., 2019). SPI-5 (Gao et al., 2019b) encodes the bacterial pathogenicity island encoded proteins (PIP), PipA, PipB, PipD. SPI-6 encodes for invasion proteins and a type 6 secretion system that acts as an antibacterial antagonist in the gut (Sana et al., 2016). *Salmonella enterica* subspecies *enterica* serovars like serovar Dublin, Typhi, and Paratyphi harbours the 133 kb SPI-7 locus, which codes for Vi antigen, SopE and type IVB pili. SPI-16 is associated with LPS O-antigen modifications (Singh et al., 2018). The rest of the *Salmonella* pathogenicity islands, like SPI-8, SPI-9, SPI-10, SPI-11, SPI-12, SPI-13, SPI-14, and SPI-15, are not well characterized but encode putative virulence proteins.

Apart from the pathogenicity islands, *Salmonella* also possesses virulence genes [*Salmonella* plasmid virulence genes (*spv* genes)]- on the plasmid (Guiney & Fierer, 2011). The plasmid consists of five genes - *spvR, spvA, spvB, spvC,* and *spvD* (Singh et al., 2018). The regulatory gene (*spvR*) and the operon *spvABCD* is controlled by the RpoS, which gets induced under the intravascular condition. *spvB* contributes to cytoskeleton destabilization and cell cytotoxicity, while *spvC* inhibits hosts' mitogen-activated protein kinases. In addition, fimbrial genes like *pef* and *lpf* contribute to intestinal adhesion (Ledeboer et al., 2006) and colonization in Peyer's patch (PP), respectively (Edwards & Puente, 1998).

Furthermore, serum resistance is conferred by plasmid-encoded genes like *traT*, *rck*, and *rsk* (Koczerka et al., 2021a). Besides resistance against complement-mediated killing, *rck* also aids in epithelial cell invasion (Koczerka et al., 2021a; Velge et al., 2012b).

1.3.2 Systemic dissemination of *Salmonella*

Salmonella employs various strategies to evade the immune system and colonize reticuloendothelial organs like the MLN, liver, and spleen. *Salmonella* traverses the gastrointestinal lining and disseminates systemically in two ways (Fig. 1.1). The first one is through the non-phagocytic cells, enterocytes, and microfold cells (M-cells) that serve to transport the bacteria through lymph vessels and PP. The second one is through $CD18^{+}$ phagocytic cells that directly capture the bacteria from the intestine and disseminate them to systemic organs through the bloodstream (Worley et al., 2006). *Salmonella* infects M-cells present in mucosa-associated lymphoid tissue. It induces epithelial-mesenchymal transition, providing an additional invasion route (Tahoun et al., 2012). The bacterial cells proliferate in PP (Watson & Holden, 2010)and as the microbial load increases, the bacterial subpopulation is captured by phagocytic cells like dendritic cells (DCs). DCs transport the bacteria to the MLN *via* the lymphatic system (Watson & Holden, 2010). In addition, the intestinal DCs serve as a carriage for transporting *Salmonella* directly from the intestinal lumen and from lamina propria to MLN (Rescigno et al., 2001), followed by its dissemination to the liver and spleen.

The SPI-1 and SPI-2 effectors aid the early systemic spread of *Salmonella*. For example, *sipB* activates caspase-1, which activates IL-1β and IL-18 production and causes pyroptosis. Pyroptosis damages the epithelial barrier whereby the pathogen invades and disseminates to different organs. SPI-2 protein, SrfH influences the motility of infected cells to enhance the dissemination of bacteria from the intestinal lumen (Worley et al., 2006). Prolonged infection in the host leads to the dissemination of *Salmonella* in other organs like the gallbladder.

1.3.3 Persistence phase in the gallbladder

The gall bladder serves as a reservoir for serovar Typhi and Typhimurium during the chronic-infection stage in humans and mice, respectively. The pathogen enters the gall bladder *via* the vasculature or ducts emanating from the liver (Gonzalez-Escobedo et al., 2011). Approximately 90% of chronic carrier cases of typhoid *Salmonella* reside as a biofilm on the gallstones (di Domenico et al., 2017). Bacteria are glued to each other and

substrate within the biofilm through an extracellular matrix (ECM). Biofilm-embedded gallstones represent a favorable environment for *Salmonella* persistence leading to reseeding of the intestine and fecal shedding, ensuing transmission to a new host (di Domenico et al., 2017). The gallbladder contains bile, a lipid-rich, detergent-like digestive antimicrobial secretion. Bile induces the production of an exopolysaccharide matrix O-antigen that facilitates biofilm formation by *Salmonella* on human gallstones (Crawford et al., 2008). Bile also regulates the expression of bacterial genes necessary for pathogenesis and bile resistance (Prouty et al., 2002).

1.4 Models for studying *Salmonella* pathogenesis

Various virulence determinants employed by *Salmonella* have been identified using *in vitro* and *in vivo* models providing insights into host-pathogen interactions. A few of these models are discussed below.

1.4.1 *In vitro* cell line models

In vitro models allow an understanding of the cell biology of the infection process. The enteropathogenesis of *Salmonella* begins with invasion into M-cells and enterocytes. This may be followed by colonization of the polarised gallbladder epithelial cells. Various human intestinal cell lines like HT-29, Caco-2, Hep-2 have been used to study *Salmonella* and epithelial cell interactions (Douce et al., 1991). Among all, HT-29 provides a close resemblance with gut epithelium. These cell lines are also used to investigate the adhesion, invasion, and immune responses during *Salmonella* infections. HT-29 can be differentiated into mature and polarised enterocytes by replacing glucose with galactose in the culture medium (le Bivic et al., 1988). Following the invasion of intestinal epithelial cells, *Salmonella* establishes its niche in phagocytic cells like macrophages and DCs. *Salmonella* uses macrophages as a carriage for systemic dissemination. Thus, the following cell lines RAW264.7, U937, and THP-1 serve as cell-culture models to study the defense mechanisms and cellular responses active during the intravacuolar life of *Salmonella*. Primary macrophages like peritoneal and bone marrow-derived macrophages are also used as models to study *Salmonella* pathogenesis. Furthermore, LPS stimulates macrophages to produce RNI and mitochondrial ROS production (Canton et al., 2021; Taciak et al., 2018). *In vitro* models are useful for studying the initial steps of infection, but these models provide no information on the crosstalk between different cell types and immune systems.

1.4.2 *In vivo* models: *Mus musculus* and *Caenorhabditis elegans*

Infection studies with *in-vivo* models closely resemble clinical settings, hence providing better insights into the pathogenesis (Verma et al., 2020). Although gastroenteritis is self-limiting compared to typhoid fever, *Salmonella* serovars causing these diseases *viz* Typhi and Typhimurium, respectively, share a few pathogenic characteristics (Chaudhuri et al., 2018). These include the induction of inflammation at the site of bacterial entry and the mode of invasion. Nevertheless, *S.* Typhimurium infection in mice models mimics typhoidal fever in humans (Santos et al., 2003). The two standard mice models for *Salmonella* infection studies (Hurley et al., 2014) are the Natural resistance-associated macrophage protein (Nramp $^{-/-}$), C57BL/6, and BALB/c as they mimic typhoidal symptoms followed by intestinal lesions, enterocolitis, and enlarged PP post-oral infection (S. Zhang et al., 2003). The intestinal pathology and immune responses in infected mice are similar to that of human typhoid patients. Systemic infection with serovar Typhimurium in mice results in hepatomegaly and splenomegaly (Gal-Mor et al., 2014; Santos et al., 2001). However, C57BL/6 and BALB/c mice are not suited for chronic/persistent infection studies, as these mice usually die of infection from relatively low doses of *Salmonella*. Chronic infection is usually studied in *Nramp*$^{+/+}$ mice. Oral inoculation of *S.* Typhimurium in these mice resulted in an acute phase of infection followed by fecal shedding and persistence in MLN (Monack et al., 2004).

The soil nematode *Caenorhabditis elegans* (*C. elegans*) serves as a model host for studying *Salmonella* pathogenesis and intestinal biofilm formation (Ruby et al., 2012; Desai et al., 2019; Labrousse et al., 2000). Its small size, shorter generation time, and close resemblance with the mammalian immune system makes it an attractive model for studying host-pathogen interactions. Recently, the role of *Salmonella* virulence factors (SPI-2 effectors and PhoP/Q) has been implicated in governing pathogenesis in *C. elegans* (Ruby et al., 2012). Moreover, *Salmonella* exists as a biofilm in *C. elegans* gut (Desai et al., 2019). The biofilm formation in *C. elegans* reprograms the innate immune system to colonize the intestinal niche during persistent infection (Desai et al., 2019).

1.5 *Biofilm* formation by *Salmonella*

Salmonella form biofilms to adapt to harsh environmental conditions like the presence of bile. Biofilm confers bacteria with an ability of persistence and antimicrobial resistance. *Salmonella* forms biofilms on biotic (gallstones, plant, and animal tissues) and

abiotic surfaces (glass, plastic, rubber, and stainless steel (Steenackers et al., 2012)). The different types of biofilms formed by it include - surface-attached (ring biofilm at the solid-liquid-air interface), pellicle (air-liquid interface), and bottom (solid-liquid interface) biofilm (Paytubi et al., 2017). The multicellular behaviors of *Salmonella* biofilm are in response to varied physiological conditions sensed by *Salmonella.* These conditions trigger the production of different ECM components like aggregative fimbriae, cellulose, colanic acid, biofilm-associated protein (BapA), extracellular DNA (eDNA), and other exopolymeric substances. The development of biofilm occurs in four stages - (i) adhesion to the substratum (reversible and irreversible attachment), (ii) microcolony formation, (iii) maturation, and (iv) dispersion followed by colonization of a new niche. At the adhesion stage, planktonic cells transit to a sedentary mode, trigger monolayer formation, and produce ECM for protection. The bacteria establish cellular communication, contact, and growth in the next stage. Following microcolony formation, polysaccharide and protein production potentiates cementing of the neighboring cells. Finally, the microcolony shapes into a mature 3-D structure. Some bacterial cells disseminate to the environment, starting the biofilm cycle all over again. The transition of the bacteria from planktonic mode to a surface-associated lifestyle triggers the activation of biofilm-associated genes.

1.6 Regulation of *Salmonella* biofilm and pathogenesis

Salmonella biofilm formation is predominantly coordinated by CsgD (Gerstel & Römling, 2003), a regulatory protein from the LuxR family (Z. Liu et al., 2014). Unphosphorylated CsgD (Zakikhany et al., 2010) binds to the promoter region of *csgBAC* operon and *adrA*, activating the production of biofilm components, Curli, and cellulose, respectively (Fig. 1.3). The cyclic dimeric GMP (c-di-GMP) synthesized by AdrA binds to the Pilz domain of BcsA protein and activates the cellulosic machinery (Morgan et al., 2014). CsgD also regulates *bapA* and O-antigen gene expression (Gibson et al., 2006)(Fig. 1.3). Given that CsgD lies amidst the complex biofilm regulatory network, its induction is governed by a multitude of environmental cues (temperature, envelope stress, nutrient switch, amino acid metabolism, pH, and starvation) (Brombacher et al., 2006)*via* response regulators (OmpR, RpoS, HNS, IHF, MlrA, and CpxR,) (Chambers & Sauer, 2013) and secondary messengers (c-di-GMP and cAMP-CRP) (Ahmad et al., 2017; Hufnagel et al., 2016).

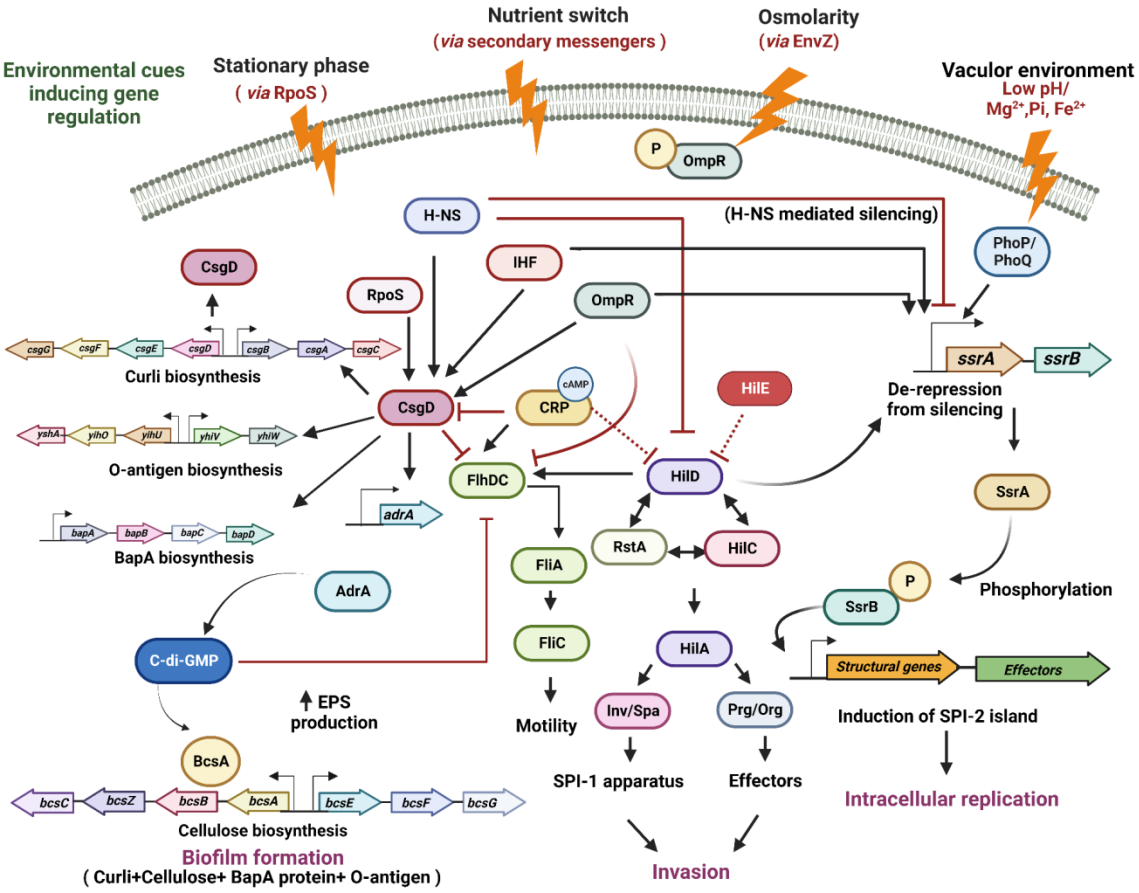

Fig. 1.3: Regulatory networks controlling the biofilm formation and virulence traits in *Salmonella*. An overview of different environmental stimuli affecting major response regulators and secondary messengers, which in turn regulate the expression of global regulators. Various regulatory pathways operating in bacterial cells play an essential role in controlling the major virulence-associated traits needed for biofilm formation, invasion, survival, replication, and colonization inside the host. → represents activation; —| represents direct inhibition; - - -| represents indirect inhibition; ↔ represents feedback loop. The figure was created using Biorender.

During biofilm formation, conditions in the stationary phase induce the production of sigma factors (e.g.: RpoS and RpoE). RpoS activates *csgD* expression that triggers the production of Curli and cellulose in *S.* Typhimurium (Römling et al., 1998) (Fig. 1.3). RpoS also enhances bacterial endurance during the adaptation stage of biofilm formation (Cabeza et al., 2007). Similarly, the deletion of *rpoE* leads to impaired biofilm formation and reduced *csgD* expression (Peng, 2016). The intergenic region of *csgBAC* and *csgDEFG* operon forms a platform for other transcriptional factors like OmpR, integration host factor (IHF), the histone-like nucleoid structuring protein (H-NS), and the MerR-like regulator (MlrA) (Gerstel et al., 2003; Steenackers et al., 2012) (Fig. 1.3). A change in osmolarity or

pH is sensed by the sensor kinase EnvZ that phosphorylates OmpR (Gerstel et al., 2003). The phosphorylated OmpR upregulates CsgD expression (Gerstel et al., 2003). IHF competes with the phosphorylated OmpR for binding to the *csgD* promoter region. Under microaerophilic conditions, IHF activates *csgD* expression (Gerstel et al., 2003), while phosphorylated OmpR represses it under aerobic conditions. On the other hand, H-NS binds to AT-rich sites lying in the intrinsic region of the curli operon and contributes to the activation of *csgD* (Ogasawara, Yamada, et al., 2010). The other positive regulator, MlrA, gets induced in the presence of metal ions (Ogasawara, Yamamoto, et al., 2010) and contributes to RpoS-dependent Curli production in *Salmonella* (Brown et al., 2001). Apart from transcriptional factors, the secondary messengers like c-di-GMP and cAMP-CRP also govern biofilm formation (Fig. 1.3). Like CsgD, the secondary messenger, c-di-GMP also acts as a molecular switch for two lifestyles - planktonic and biofilm. Increased concentration of c-di-GMP in the intracellular milieu of cells promotes ECM production and represses flagellar motility (Simm et al., 2004; Valentini & Filloux, 2016). It regulates virulence, biofilm formation, cell cycle, and motility (Ahmad et al., 2013). Taken together, CsgD, along with c-di-GMP, aids in colonization and virulence (Hall & Lee, 2018). Another secondary messenger, cAMP-CRP, negatively regulates *csgD* expression (Fig. 1.3) and promotes pellicle biofilm formation in *Salmonella* (Paytubi et al., 2017).

The metabolic sensor CRP negatively regulates the SPI-1 T3SS system of *Salmonella* (el Mouali et al., 2018a) (Fig. 1.3). CsgD and c-di-GMP impact T3SS effector (SipA) expression and the flagellin secretion (Fig. 1.3), thus hampering epithelial cell invasion and pro-inflammatory responses of the host (Ahmad et al., 2011; Lamprokostopoulou et al., 2010). Furthermore, at the epithelial cell lining, c-di-GMP mediates the switch between biofilm formation and virulence in *S*. Typhimurium *via* CsgD through the regulation of cellulose expression (Lamprokostopoulou et al., 2010).

The virulence of *Salmonella* is influenced by the pathogenicity determinants encoded by SPI-1 and SPI-2. The modulation of SPI-1 expression is through global regulators, and transcriptional regulators like HilA, HilC, HilD, and InvF encoded within the pathogenicity island (Lou et al., 2019) (Fig. 1.3). Most of the environmental stimuli focalize on *invF* and *hilA* for induction of SPI-1genes. The regulatory feedback loop formed by HilC-RtsA-HilD controls the transcription of *hilA* (Ellermeier et al., 2005) (Fig. 1.3). The central regulator HilA activates the two gene clusters - *inv/spa* and *prg/org* - each encoding effectors and secretion apparatus, respectively (Gerlach & Hensel, 2007) (Fig.

1.3). InvF can also function in a HilA-independent manner to activate the SPI-1 system (Gerlach & Hensel, 2007). Among all regulators, HilA and HilD are the key mediators contributing to the expression of invasion machinery. However, few transcriptional regulators like H-NS, LeuO, (Espinosa & Casadesús, 2014), and HilE (Paredes-Amaya et al., 2018) negatively regulate SPI-1 expression (Fig. 1.3). Moreover, these transcriptional regulators are in turn controlled by environmental cues *via* two-component regulators and secondary messengers.

CRP-cAMP regulates the SPI-1 gene expression at post-transcriptional level (el Mouali et al., 2018b) by controlling the *hilD* mRNA *via* a small RNA named Spot42. Under nonpermissive conditions, CRP represses the expression of Spot 42, which activates HilD expression by binding to the regulatory motif at the 3'UTR of *hilD* mRNA (el Mouali et al., 2018b). However, under the permissive condition, CRP represses *csrA* (*hilD* repressor) and promotes SPI-1 expression (Altier et al., 2000). The two-component system, SsrA/B, contributes to SPI-1 silencing during the transition from invasion to the intravacuolar environment while activating the SPI-2 expression (Fig. 1.3). The SCV conditions (low Mg^{2+}, acidic pH, and presence of AMPs) trigger EnvZ/OmpR and PhoP/Q (Fass & Groisman, 2009a) which in turn regulate the transcription of *ssrA/B* (Garmendia et al., 2003; Tang et al., 2013) (Fig. 1.3). Phosphorylated SsrB mediates SPI-2 expression (Desai & Kenney, 2019). However, under neutral conditions, unphosphorylated SsrB binds to the promoter of the biofilm master regulator, CsgD, and relieves H-NS-mediated silencing (Desai & Kenney, 2019). Thus, SsrA/B acts as a molecular switch controlling the interplay between virulence and biofilm of *Salmonella*.

1.7 Clustered Regularly Interspaced Short Palindromic Repeats -CRISPR-associated (CRISPR-Cas) system

The CRISPR-Cas system is an adaptive immune system in bacteria that confers protective immunity against invading mobile genetic elements (MGE) (Hille & Charpentier, 2016). Recent findings indicate the regulation of bacterial pathogenicity by the CRISPR-Cas system of *Salmonella* and other bacteria. But the mechanisms have just begun to be elucidated (Hille & Charpentier, 2016).

This system has also been suggested to govern bacterial physiology and pathogenesis by regulating the expression of various genes (Hille & Charpentier, 2016).

1.7.1 Overview and classification of the CRISPR-Cas system

The CRISPR-Cas system is encoded by approximately 40% sequenced bacterial genomes and nearly 90% archaea (Marraffini & Sontheimer, 2010). It comprises an AT-rich leader sequence, CRISPR array, and *cas* genes (Medina-Aparicio et al., 2018). Based on the locus organization and *cas* gene content, the CRISPR-Cas systems are classified into six main types (I, II, III, IV, V, VI) and 33 subtypes (Makarova et al., 2020; Seed et al., 2013). Each type is characterized by the presence of signature nucleases - *cas3* (Type I system), *cas9* (Type II system), *cas10* (Type III system), *csf1* (Type 1V system), *cas12* (Type V system), and *cas13* (Type VI system) (Koonin & Makarova, 2019; Makarova et al., 2011). The CRISPR-Cas mediated defense is divided into three stages (Hille & Charpentier, 2016; Newsom et al., 2021) (Fig. 1.4): (i) Adaptation/acquisition stage - Cas proteins are involved in acquiring spacers. They recognize a distinct small motif called protospacer adjacent motif (PAM) in the invading DNA, thereby cleaving it and incorporating a piece of the genetic material (called as protospacer) in the CRISPR locus. (ii) CRISPR RNA (crRNA) biogenesis - on encountering a new MGE, the CRISPR-Cas system expresses the Cas proteins followed by transcription of long precursor crRNA (pre-crRNA). Cas, along with accessory proteins, processes pre-crRNA into mature crRNA. (iii) Interference - crRNA-Cas protein complex recognizes the target DNA and the crRNA base pairs with the protospacer. Lastly, the recruited Cas nuclease cleaves the invader's genetic material. Although the basic mechanism of adaptive immunity is shared by all the CRISPR-Cas systems, they exhibit extraordinary diversity in spacer composition, crRNA biogenesis, and interference.

1.7.2 Gene regulation by the CRISPR-Cas system in bacteria

Apart from its promising role in providing bacterial immunity, the CRISPR-Cas system is being implicated in modulating bacterial stress factors like starvation, low pH, or insults from host-immune responses. For example, Cas9 from the type II CRISPR-Cas system is involved in regulating various virulence traits of pathogens like *Campylobacter jejuni* (Louwen et al., 2013), *Neisseria meningitides* (Louwen et al., 2013), *Francisella novicida* (Sampson & Weiss, 2013), etc. In intracellular *F. novicida*, Cas9 influenced the degradation of bacterial lipoprotein (BLP), inhibiting the activation of TLR2, and thus the initiation of an antibacterial pro-inflammatory response (Sampson et al., 2013). In *C. jejuni* and *N. meningitidi*s Cas9 interfered with the ability to attach, invade and replicate within epithelial cells (Sampson & Weiss, 2014a). Another study demonstrated the requirement

of Cas2 in *Legionella pneumophila* (Gunderson et al., 2015) for successfully causing intracellular infection in amoebae. In *Listeria monocytogenes*, the CRISPR array controlled the virulence without any involvement of the *cas* gene (Mandin et al., 2007). A CRISPR-mediated Cas-independent regulation of virulence genes is recently reported for *Streptococcus agalactiae* (Dong et al., 2021). The type IF CRISPR-Cas system regulates the physiology of *P. aeruginosa* (Louwen et al., 2014). It targets an mRNA of a quorum-sensing regulator, helping the bacteria to evade host defenses (Wiedenheft & Bondy-Denomy, 2017). It also regulates biofilm formation but only in the DMS3 lysogenic strain of *P. aeruginosa* (Zegans et al., 2009). Moreover, in a virulence study of *Enterococcus faecalis*, the deletion of the CRISPR-Cas system affected colonization and biofilm formation (Bourgogne et al., 2008; Louwen et al., 2014). Contrary to this, CRISPR-Cas strains showed enhanced biofilm formation and colonization ability. Off late, the role of the CRISPR-Cas system in regulating endogenous genes of *Salmonella* and hence certain physiological characteristics has been demonstrated.

1.7.3 Role of the CRISPR-Cas in *Salmonella*

Salmonella possesses a type IE CRISPR-Cas system with two CRISPR loci, CRISPR-I and CRISPR-II, comprising 29 nt long direct repeats separating spacers of ~32 nt length (Shariat et al., 2015). The CRISPR-Cas system contains a single *cas* operon with 8 *cas* genes, namely, *cas1, cas2, cas5, cas7, cas6e, cas3, cse1*and *cse2*. This system, mainly the CRISPR-I loci, is well-conserved across different *Salmonella* serovars (Shariat et al., 2015).

Surprisingly, many of its matching proto-spacers were traced on chromosomes instead of its general target, phages, and plasmids, suggesting the regulation of some endogenous genes by the CRISPR-Cas system. Transcriptome profiles of five clinical isolates of *S*. Typhi displayed altered expression of multiple *cas* genes *via* induction of *cas3* and repression of *cas6*, suggesting the involvement of the CRISPR-Cas system in modulating *S*. Typhi's survival inside the host(Sheikh et al., 2011). Exposure to intracellular mimicking conditions (growth in N-minimal medium) induced the expression of *cas* genes in *S*. Typhi, indicating the CRISPR-Cas system's role in the intracellular survival of *S*. Typhi (Medina-Aparicio et al., 2011).

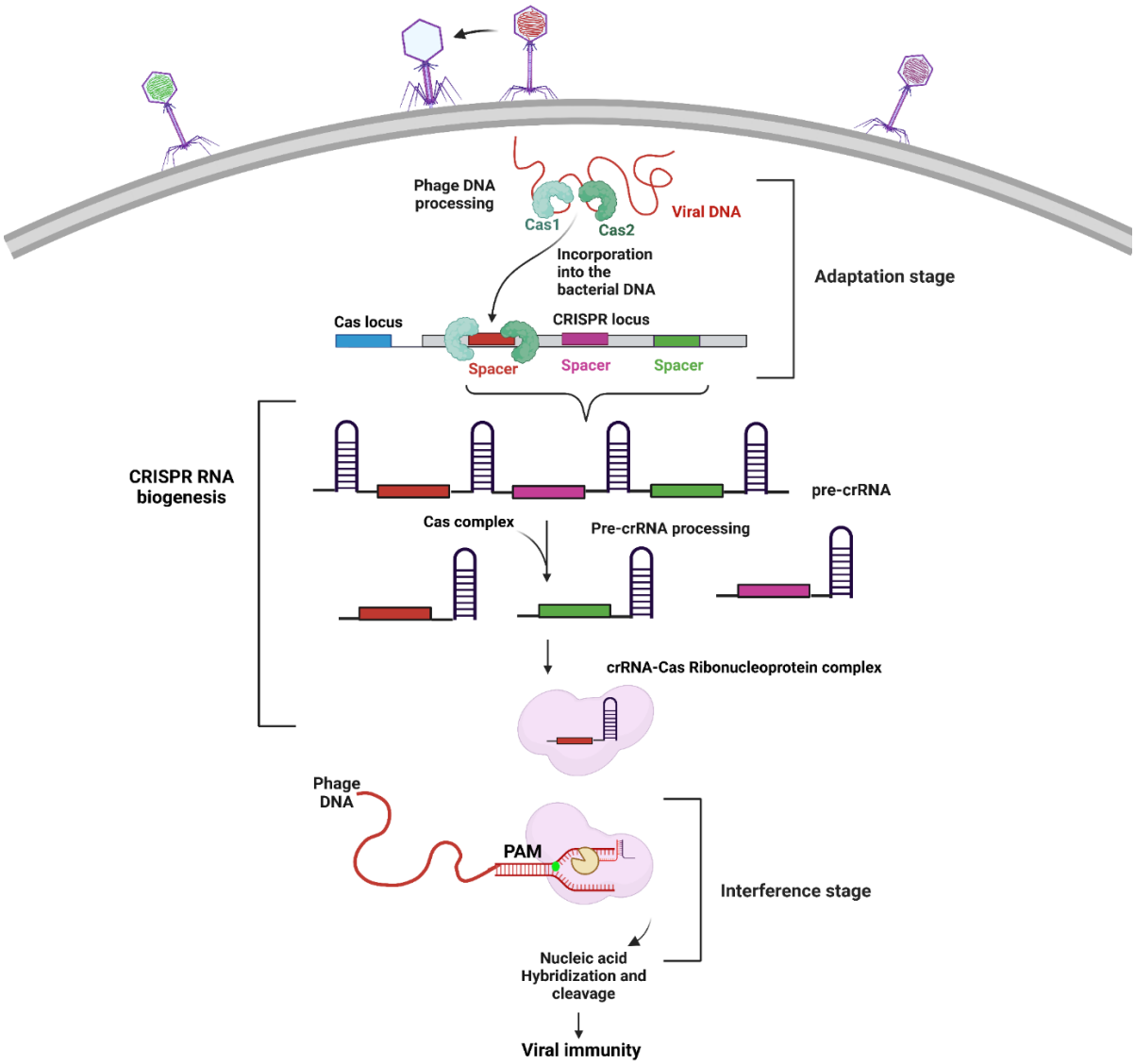

Fig. 1.4: Diagrammatic representation of CRISPR-Cas mediated nucleic acid targeting mechanism. The entire process is divided into three stages: **(1) Acquisition/adaptation:** In the acquisition phase, upon infection, a part of the invader DNA is processed by Cas1 and Cas2 and is finally incorporated into the CRISPR locus as a new spacer. **(2) crRNA biogenesis:** The CRISPR array is transcribed into pre-crRNA resulting in mature crRNA. The mature crRNA and Cas proteins function as a surveillance system for the bacterial genome. **(3) Interference:** When phage DNA invades again, the Cas: crRNA complex identifies a PAM. This leads to a complementary base pairing between the spacer and target (e.g., phage DNA). Finally, the target gets cleaved by signature Cas to provide viral immunity. The figure was created using Biorender.

A similar study by Eriksson et al. for *Salmonella* that monitored the transcriptional profile of intracellular bacteria from macrophages did not detect any change in *cas* gene expression except for *cas3* (Eriksson et al., 2003). In another study by Eswarappa et al., the introduction of *lacI* into *S.*Typhimurium resulted in increased transcription of *cas* genes

viz. cas1, cas2, cas3, cas5, cas6, and cas7 with consequent attenuation of virulence in a mice model (Eswarappa et al., 2009). Furthermore, recent studies on serovar *S.* Enteritidis demonstrated the role of *cas3* in indirectly regulating biofilm and SPI-1 genes by inhibiting the quorum sensing gene, *lsrF* (Cui et al., 2020). In this serovar, Cas3 represses the expression of *lsrF* (involved in the degradation of autoinducer, AI-2). Increased AI-2 levels upregulate *lsr* operon, thereby increasing the expression of biofilm and SPI-1-associated genes, regulating biofilm formation and pathogenicity in *S.* Enteritidis. Medina et al. reported that the CRISPR-Cas system of *S.*Typhi positively regulates bacterial outer membrane protein (OmpR) (Medina-Aparicio et al., 2021). Deletion of CRISPR-Cas locus resulted in the repression of two other porins i.e.- *ompC* and *ompF*. Additionally, the CRISPR-Cas system also regulates biofilm formation and bile salt resistance (Medina-Aparicio et al., 2021). Thus, it can be hypothesized that the CRISPR-Cas system could directly or indirectly regulate the endogenous genes of *Salmonella*.

1.8 Gaps in existing research and thesis objectives

Based on the literature cited in section 1.7, there are pieces of evidence that the CRISPR-Cas system regulates the physiology and pathogenicity of bacterial species like *Salmonella* by directly or indirectly regulating endogenous genes. As many of the matching proto-spacers of the CRISPR-Cas system in *Salmonella* traced to chromosomes instead of its general targets, phages, and plasmids, ***we hypothesized that the CRISPR-Cas system could regulate Salmonella physiology and pathogenicity. On analysis, we found that some of the protospacer were genes involved in biofilm formation and pathogenicity of Salmonella.*** Moreover, while the thesis work was in progress, there were reports citing the role of the CRISPR-Cas system in regulating the biofilm and pathogenicity of *Salmonella* serovars Enteritidis and Typhi (Cui et al., 2020; Medina-Aparicio et al., 2021).

Although the mechanistic details of the CRISPR-mediated adaptive immune system are well documented, the molecular details of its alternative functions (virulence and physiology regulation) have just begun to be elucidated (Louwen et al., 2014; Sampson & Weiss, 2014a). For instance, the type IF system of *P. aeruginosa* is known to regulate quorum sensing *via* regulating the degradation of *lasR* (transcriptional activator of quorum sensing) transcript, and the molecular details have been elucidated (Wiedenheft & Bondy-Denomy, 2017). However, the endogenous gene regulatory mechanisms of the *Salmonella* type IE system were unknown during the inception of this thesis. ***Therefore, we aimed to study and dissect the role of the CRISPR-Cas system in the biofilm formation and***

pathogenicity of S. Typhimurium. In 2020, a study by Cui et al. showed that the type Cas3 protein of *S.* Enteritidis targets *lsrF*, thereby positively regulating biofilm formation, yet the molecular details are unknown (Cui et al., 2020)**.** ***In our study, we sought to characterize the role of the cas operon and its functional partner, the CRISPR array, in biofilm and pathogenicity regulation*****.*** *In addition, we also explored the role of the CRISPR-Cas system in modulating different stages of biofilm formation.*

The CRISPR-Cas system is known to regulate cell envelope integrity by repressing BLP mRNA in *F. novicida* (Gholizadeh et al., 2020), suggesting the role of CRISPR-Cas in maintaining cell membrane homeostasis. ***Thus, in the present work, we also intended to elucidate the CRISPR-Cas system's role in modulating membrane properties, thereby impacting different phenotypes*****.** In support of our work proposal, Medina et al., in 2021, reported that the CRISPR-Cas system regulates a two-component regulator, OmpR, that affects the downstream synthesis of other porins like OmpF, OmpC, and OmpS2 in *S.* Typhi. Furthermore, the CRISPR-Cas system regulates the expression of virulence factors (Q. Wu et al., 2022) in some pathogenic bacteria like *Enterococcus faecali*s (Gholizadeh et al., 2020), *L. pneumophi*la (Gunderson & Cianciotto, 2013), *F. novicida* (Sampson et al., 2013), etc. In *S.* Enteritidis, Cas3 indirectly regulates SPI-1 expression *via* quorum sensing related genes, thereby impacting its pathogenicity (Cui et al., 2020). However, the detailed regulatory mechanism is unclear. ***Through our current study, we also aimed to decipher the role of the CRISPR-Cas system in Salmonella pathogenesis and its virulence determinants.***

Considering the gaps mentioned above, we have formulated the following research objectives:

1. Gaining mechanistic insights into the CRISPR-Cas mediated biofilm regulation in *Salmonella enterica* subspecies *enterica* serovar Typhimurium.

   The research outcomes of this objective are discussed in Chapter 2: The CRISPR-Cas System Differentially Regulates Surface- Attached and Pellicle Biofilm in *Salmonella enterica* serovar Typhimurium.

2. Investigating the modulation of membrane properties of *Salmonella enterica* subspecies *enterica* serovar Typhimurium by the CRISPR-Cas system.

*The research findings of this objective are elaborated in Chapter 3:*The CRISPR-Cas system of *Salmonella enterica* serovar Typhimurium modulates its membrane properties.

3. Characterising the CRISPR-Cas system's role in the pathogenesis of *Salmonella enterica* subspecies *enterica* serovar Typhimurium.

   The results of this objective are elaborated in Chapter 4: Deletion of the CRISPR-Cas system attenuates the virulence of *Salmonella enterica* serovar Typhimurium.

Chapter 2

The CRISPR-Cas System Differentially Regulates Surface-Attached and Pellicle Biofilm in *Salmonella enterica* serovar Typhimurium

Publication from this objective:

Sharma, N., Das, A., Raja, P., and Marathe, S. A. (2022). The CRISPR-Cas System Differentially Regulates Surface-Attached and Pellicle Biofilm in Salmonella enterica serovar Typhimurium. Microbiology Spectrum, e00202-22.

2.1 Introduction

The Clustered Regularly Interspaced Short Palindromic Repeats (CRISPR)-CRISPR - associated (Cas) system bestows adaptive immunity to bacteria against invading mobile genetic elements (MGE). It captures proto-spacers from invading MGEs and incorporates them in the CRISPR array with the help of Cas proteins. The system has also been implicated in alternative functions like governing virulence and bacterial physiology. This system has been demonstrated to regulate biofilm formation in the *Salmonella enterica* subspecies *enterica* serovar Enteritidis (*S.* Enteritidis) by regulating the quorum-sensing system (Cui et al., 2020). It also regulates the expression of outer membrane proteins in *Salmonella enterica* subspecies *enterica* serovar Typhi (*S.*Typhi), thereby impacting biofilm formation and resistance to bile (Medina-Aparicio et al., 2021). *Salmonella* forms biofilms on various surfaces, including medically important surfaces like medical devices (catheters, endoscopy tubes, etc.), as well as gallstones (Crawford, Rosales-Reyes, et al., 2010). This complicates the treatment processes. Biofilm formation on cholesterol-rich gallstones is conceived as a significant factor influencing the establishment of a chronic carrier state, accounting for 1 to 4% of total typhoid cases; (WORLD HEALTH ORGANIZATION Geneva, 2008; Parry et al., 2002). Biofilm aids *Salmonella* virulence by facilitating evasion of the host's immune response and increasing antibiotic tolerance, as biofilms can be impenetrable to antibiotics (Mah, 2001). *Salmonella* biofilms are a concern in the food and packaging industries and act as a pathogen transmission source in food processing units (Frank & Chmielewski, 2001; Galié et al., 2018). Biofilms lead to *Salmonella's* persistence in the environment (Steenackers et al., 2012). Improper disinfection and cleaning leave behind food particles that act as substrates for surface-attached biofilm formation (Lamas et al., 2021). Environmental conditions like low temperature and pH in the food production chain favor biofilm formation (Lamas et al., 2021). These biofilms are resistant to common disinfectants used in the food industry, thus safeguarding *Salmonella* throughout food processing (Corcoran et al., 2014; Silva et al., 2014). This magnifies the problems and spread of infection.

Biofilm formation is a tightly regulated process requiring adhesins such as pili (Petrova &Sauer, 2012), flagella (Petrova & Sauer, 2012), and Curli (Debenedictis et al.,2016; Jonas et al., 2007) for substrate adhesion (Fig. 2.1). Flagellum acts as a mechanosensor triggering surface-associated motility and polysaccharide synthesis (Petrova & Sauer, 2012), while Curli is required for cell-cell cohesion (Prigent-Combaret

et al., 2000), forming a biofilm monolayer and microcolonies (Fig. 2.1). The monolayer matures by gradually embedding extracellular polymeric substances (EPS), forming a 3-dimensional structure like the pellicle (Armitano et al., 2014).

Salmonella can form different types of biofilms, including surface-attached (ring biofilm at the solid-liquid-air interface), pellicle (air-liquid interface), and bottom (solid-liquid interface) biofilm. Different biofilm components play a crucial role in various types of biofilm formation. These are listed in table 2.1.

Role of different biofilm components:

Flagella plays a vital role in biofilm formation by *Salmonella* (F. Wang et al., 2020). Mutation in genes encoding flagellar regulator (*flhC*) and hook protein (*flgE*), impairs biofilm formation in the presence of bile (Crawford, Reeve, et al., 2010), while a mutation in flagellar sigma factor (*fliA*), and motor stator protein (*motA*) showed impaired biofilm formation on glass (Prouty & Gunn, 2003). Deleting flagellar regulon (*flhE)* and flagellin (*fliC)* resulted in impaired adhesion, colonization, and biofilm formation (F. Wang et al., 2020). However, these mutants showed increased aggregation and a denser biofilm matrix at later stages. Flagella mediates cell-cell interactions and microcolonies formation at an early stage of biofilm formation (F. Wang et al., 2020). Along with type I pili which aid cohesion in the biofilm matrix, flagella provide structural stability to biofilm (Petrova & Sauer, 2012).

In addition to flagella and pili, the *Salmonella* genome encodes fimbrial genes, namely *pef, lpf, bcf, stf, saf,* type 1 fimbriae, and thin aggregative fimbriae (Tafi) (also known as Curli fimbriae) (Steenackers et al., 2012). Fimbriae are necessary for the initial phase of bacterial attachment on a solid surface. However, their precise role remains unelucidated. Among all, Curli forms an important proteinaceous component of the biofilm matrix. It aids adhesion, colonization, and persistence (Tursi & Tükel, 2018). The *csgBAC* and *csgDEFG* operons govern the production of Curli. The *csgBAC* encodes for structural unit CsgA, nucleation protein CsgB, and chaperone-like protein CsgC. Defects in *csgA* and *pef* production affected biofilm formation on plastic and intestinal tissues (Steenackers et al., 2012). The CsgA and CsgB proteins are secreted outside and assembled on the bacteria's surface. They initiate initial cell-surface and subsequent cell-cell interactions during the biofilm formation (Prigent-Combaret et al., 2000). They exist as a complex with cellulose and the O-Ag-capsule, physically linking the cells (Steenackers et al., 2012).

Cellulose, an important EPS, supports long-range cell-cell interactions while conferring resistance against chlorine and desiccation (Cristina Solano, 2002). It has been reported that both Curli and cellulose enhance the survival and persistence of *Salmonella* in the environment, thus aiding its transmission to a new host (White et al., 2006). The other polysaccharide component, colanic acid, confers resistance against desiccation, oxidative stress, and hyperosmolarity. Under environmental stress, the *rcsCBD* operon induces the production of colanic acid, which is important for the complete maturation of biofilm on the eukaryotic cell surface (Pando et al., 2017). The other extracellular matrix (ECM) components include BapA and O-antigen capsule. BapA is encoded by the *bapA* and secreted through the BapBCD secretion system. The surface protein, BapA is crucial for bacterial aggregation and pellicle formation at the air-liquid interface (Steenackers et al., 2012). It is also implicated in playing a role in host colonization and connecting individual cells within the biofilm, either directly through homophilic interactions or by strengthening Curli-mediated associations. The precise mechanism underlying this process remains unknown (Latasa et al., 2005). The synthesis of the O-antigen capsule, another ECM component, is governed by *yihU-yshA* and *yihVW* operons. The O-antigen capsule serves as an important component for biofilm formation on gallstones (Crawford et al., 2008). It also aids serum resistance and systemic dissemination of *Salmonella*. Further, it inhibits immune recognition of T3SS, reduces the inflammatory response, and modulates flagella's (*fliC*) expression (Marshall & Gunn, 2015).

The present study evaluated if and how the endogenous CRISPR-Cas system regulates different biofilm phenotypes of *Salmonella enterica* subspecies *enterica* serovar Typhimurium (*S.* Typhimurium). We found that the CRISPR-Cas system differentially regulated surface-attached and pellicle biofilm formation by altering the expression of biofilm-associated genes.

2.2 Material and methods

2.2.1 Bacterial strains and culture conditions

S. Typhimurium str. 14028s was used as a parent strain (wildtype, WT 14028s). The wildtype, CRISPR, and *cas* knockout strains (the knockout construction is explained below) and their corresponding complement strains were routinely grown in Luria-Bertani (LB, HiMedia) with appropriate antibiotics (Table 2.2) at 37°C, 120 rpm. Bacterial strains were grown in biofilm media (LB without NaCl) to observe growth patterns up to 12 h.

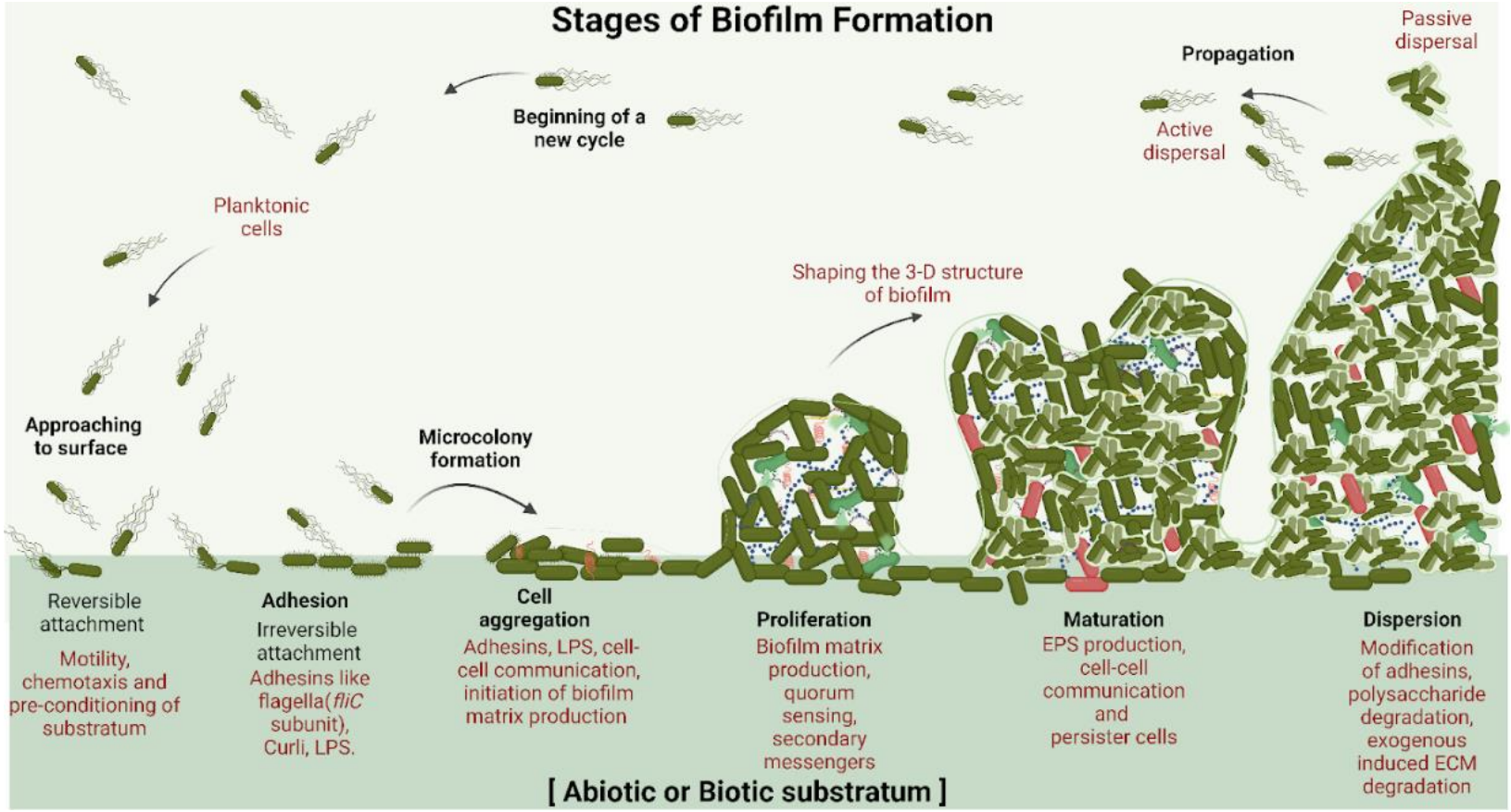

Fig. 2.1: Biofilm formation process in *Salmonella.* Biofilm formation begins with the interaction of planktonic cells with an abiotic or biotic substrate, followed by their irreversible attachment to the surface by adhesins. Bacterial adhesion triggers cell aggregation, and soon the bacteria start forming monolayers, followed by ECM production (Curli, LPS, etc.). With time, the developing biofilm enters the proliferation stage. During later stages, the biofilm shapes itself into a 3-D structure encapsulated by biofilm matrix components such as e-DNA, enzymes, proteins, polysaccharides, bacterial cells, dead cells, and persister cells (indicated as red rod-shaped bacteria). Changes in the environmental conditions cause dispersion wherein a small population of bacterial cells encapsulated into thick EPS start to slough off from the biofilm niche and disperse in the environment with the aim of beginning a new biofilm cycle. The Figure was created using Biorender.

Table 2.1: The conditions and critical biofilm components required for different biofilm types:

Biofilm type	Condition in Environment	Conditions in laboratory	Major components	Temperature and incubation
Surface-attached biofilm (ring) (Cristina Solano, 2002)	Medical devices, food processing units (Zhao et al., 2017), standing and flowing water ecosystems (Serra & Hengge, 2014).	Liquid media (LB, YESCA) in microtiter wells, flow cells, or test tubes at static or dynamic conditions.	Cellulose, LPS, Curli, Type III secretion apparatus, and flagella (Steenackers et al., 2012)	25-37°C, 12-24 h
Pellicle biofilm (Armitano et al., 2014; Cristina Solano, 2002; Serra & Hengge, 2014)	Stagnant water ecosystem, vinegar production, and drainage system (Serra & Hengge, 2014)	Liquid YESCA media in tubes, flasks, or microtiter wells under static conditions.	Curli, LPS, and cellulose (Serra & Hengge, 2014)	25-28°C, 3-4 days

Table 2.2: List of bacterial strains and plasmids used in this study

Bacterial Strain	Genotype and Characteristics	Source/ref
Salmonella enterica serovars Typhimurium 14028s	WT 14028s	A kind gift from Prof. Dipshikha Chakravorty, IISc, India
Δ*crisprI*	WT 14028s Δ*crisprI*:: Chl (Chl^r)	This study
Δ*crisprII*	WT 14028s Δ*crisprII*:: Chl (Chl^r)	This study
Δ*cas op*	WT 14028s Δ*cas operon* :: Chl (Chl^r)	This study
ΔΔ*crisprI crisprII*	WT 14028s Δ*crisprI*:: Kan :Δ*crisprI*::Chl (Kan^r, Chl^r)	This study
Δ*fliC*	WT 14028s Δ*fliC*::Kan (Kan^r)	Marathe et al., 2016
Δ*csgD*	WT 14028s Δ*csgD* : : Chl (Chl^r)	A kind gift from Prof. Dipshikha Chakravorty, IISc, India
WT60	WT 14028s transformed with empty pQE60 vector	This study
Δ*crisprI 60*	Δ*crisprI* transformed with empty pQE60 vector	This study
Δ*crisprII 60*	Δ*crisprII* transformed with empty pQE60 vector	This study
Δ*cas op 60*	Δ*cas op* transformed with empty pQE60 vector	This study
ΔΔ*crisprI crisprII 60*	ΔΔ*crisprI crisprII* transformed with empty pQE60 vector	This study
Δ*crisprI +pcrisprI*	Δ*crisprI* complemented with functional CRISPR I array cloned in pQE60	This study
Δ*crisprII +pcrisprII*	Δ*crisprII* complemented with functional CRISPR II array cloned in pQE60	This study

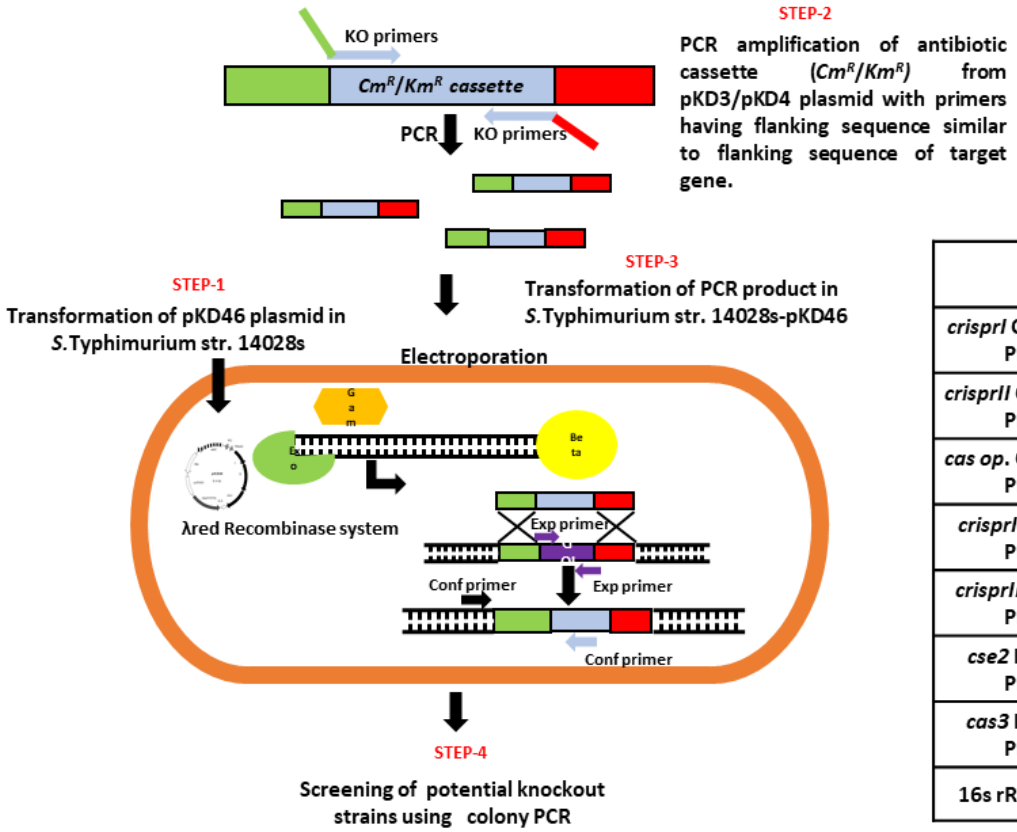

	WT	*Δcrispr1*	*ΔcrisprII*	*Δcas op*	*ΔΔcrispr1 crisprII*
***crispr1* Confirmatory Primers**	-	1067 bp	-	-	1579 bp
***crisprII* Confirmatory Primers**	-	-	1132 bp	-	1132 bp
***cas op*. Confirmatory Primers**	-	-	-	1204 bp	-
***crispr1* Expression Primers**	202 bp	-	-	-	-
***crisprII* Expression Primers**	183 bp	-	-	-	-
***cse2* Expression Primers**	182 bp	-	-	-	-
***cas3* Expression Primers**	177 bp	-	-	-	-
16s rRNA Primers	171 bp	171 bp	171 bp	171 bp	171 bp

Fig. 2.2: Schematic representation for generating and confirming the knockout strains. The successful generation of knockout strains (Δ*crisprI*, Δ*crisprI*, Δ*cas op*, and ΔΔ*crisprI crisprII*) would require homologous recombination between the gene of interest (GOI) and the antibiotic resistance cassette. For Δ*crisprI*, Δ*crisprII*, and Δ*cas op* the genes were replaced with chloramphenicol resistance cassette, whereas for generation of ΔΔ*crisprI crisprII*, the *crisprI* gene was replaced with kanamycin resistance cassette in the Δ*crisprII* strain.

2.2.2 Generation of knockout and their respective gene complement strains for the knockout

We generated an in-frame deletion of Δ*crisprI*, Δ*crisprII*, and Δ*cas op* in the *Salmonella enterica* subspecies *enterica* serovar Typhimurium (str. 14028s) genome, as described by Datsenko and Warner with minor modifications (Datsenko & Wanner, 2000). This method involves replacing the desired gene with an antibiotic (chloramphenicol/kanamycin) resistance cassette using the bacteriophage lambda red recombinase system (Fig. 2.2). *S.* Typhimurium strain carrying the recombinase system in pKD46 plasmid was grown in LB containing 10 mM arabinose at 30°C till the $OD600_{nm}$ of 0.3-0.4. Electrocompetent cells were then prepared. The chloramphenicol/kanamycin cassette was amplified from the pkD3/pkD4 plasmid with the primer set mentioned in Table 2.2. The purified Cm^R/Km^R cassette (1µg) was electro-transformed into *S.* Typhimurium, having pKD46, using a 2 mm diameter Biorad cuvette using gene pulser II (Bio-Rad) at 2.5 kV. Transformants of *S.* Typhimurium were screened using PCR from the LB plate supplemented with appropriate antibiotics. The confirmatory primers (binding to a region flanking the knockout primers and within the chloramphenicol/ Kanamycin cassette) and expression primers used for confirming the knockout strains are mentioned in Table 2.3.

The *crisprI* and *crisprII* genes were amplified using the respective cloning primers listed in Table 2.3. The amplified products were cloned into BamHI and HindIII sites of pQE60 (a kind gift from Dipshikha Chakravorty, Indian Institute of Science, India). The positive constructs were transformed into the respective knockout strains to obtain corresponding complement strains, Δ*crisprI* with Δ*crisprI* and Δ*crisprII* with Δ*crisprII*.

2.2.3 Biofilm quantification using crystal violet assay

(i) *Tube biofilm assay* - Overnight-grown bacterial cultures were subcultured at 1:100 ratios in LB supplemented with 3% ox bile (HiMedia). These cultures were added in 1.5 mL microcentrifuge tubes coated with 1 mg cholesterol and subsequently incubated at 37°C under static conditions for 96 h. Every day, the medium was replaced with fresh media (LB with 3% ox bile). The biofilms were quantified using a crystal violet (CV) assay.

(ii) *Ring and pellicle biofilm* - Overnight-grown bacterial cultures were subcultured at a 1:100 ratio in LB without NaCl in test tubes and incubated at 25°C under static conditions for 24 h, 48 h, and 96 h. The biofilms were quantified using a CV assay.

(iii) *Crystal violet assay* - The biofilms formed were given washes with phosphate-

buffered saline (PBS), dried at 56°C for 30 min, and stained with 1% (wt/vol) CV solution for 20 min. After washing with distilled water, biofilms were quantified by solubilizing the biofilm-bound CV with 30% (vol/vol) glacial acetic acid and recording the absorbance of the solution at 570 nm using Multiskan GO (Thermo Scientific, USA).

2.2.4 Biofilm dry mass and viability assay

After the designated time period of incubation, the planktonic culture was decanted and replaced with 50 mL of water. The floating biofilm pellicles were carefully collected with the help of a toothpick into microfuge tubes. These collected pellicles were washed and dried in a hot air oven at 56°C, after which their dry weight was measured.

Resazurin-based viability assay - The pellicle biofilms were washed twice with distilled water and stained with resazurin (HiMedia) dye (0.337 mg/mL) for 30 min at room temperature (RT). The resazurin fluorescence was measured using a Fluoroskan Ascent (Thermo Scientific, USA) instrument at excitation (λ_{ex}) of 550 nm and emission (λ_{em}) of 600 nm.

2.2.5 Biofilm architecture using field emission scanning electron microscopy

The pellicle biofilms were allowed to form in the glass tube containing an immersed glass slide. The pellicle biofilms fixed with 2.5% glutaraldehyde were dehydrated with increasing ethanol concentrations. The samples were air-dried, sputter coated with gold, and visualized with FEI ApreoS field emission scanning electron microscope (Oxford Instruments, Netherland).

2.2.6 Confocal laser scanning microscopy for surface-attached and pellicle biofilm

The surface-attached and pellicle biofilm was stained with 5 mM SYTO9 (Thermo Scientific), 5 mM propidium iodide (PI) (Thermo Scientific), and 50 mM calcofluor white (Sigma-Aldrich) solution for 30 min, in the dark at RT. Slides were imaged with an LSM 880 confocal microscope (Zeiss, Germany) using Z-stack (ZEN 2.3 lite).

2.2.7 Motility assay

Five microliters of overnight culture were spot inoculated at the center of swarm petri plates (20 g/L Luria Broth, 0.5% [wt/vol] agar, and 0.5% [wt/vol] glucose). After 45 to 50 min of air drying, the plates were incubated at 37°C for 9 h. The swarm rate was estimated by calculating the radius of the growth front using ImageJ Software (U.S. National Institutes of Health, USA).

2.2.8 Evaluation of the expression of flagellar proteins

Planktonic bacterial cells and pellicle biofilms were lysed in Laemmli buffer (50 mM Tris-HCl, pH 6.8, 2% SDS, 10% glycerol, 5% b-mercaptoethanol, and 0.05% bromophenol blue). Pellicle biofilms (96 h) were homogenized with TissueLyser LT (Qiagen, Germany) at 50 kHz for 10 min. An equal amount of each lysate (50 mg protein from planktonic and 400 mg from pellicle biofilm) was processed for immunoblotting using an anti-flagellin antibody (Difco). The immunoblots were developed, and images were captured with the ChemiDoc XRS1 system (Bio-Rad Laboratories, USA). Each immunoblot band was normalized to Coomassie-stained bands, and the relative ratio of each with WT was quantified using Image Lab software (Bio-Rad Laboratories, USA).

Table 2.3: List of Primers used in this study

Sl. No.	Primer Name	Nucleotide Sequence
1	*crispr*1 Knockout (Forward)	5' GAGCTGGCGAAGGCGGAAAAAACGTCCTGATA TGCTGGTGGTGTAGGCTGGAGCTGCTTCG 3'
2	*crispr*1 Knockout (Reverse)	5' AAATATATAGTTTTAGTGTGTTCCCCGCGCCAG CGGGGCATATGAATATCCTCCTTA 3'
3	*crispr*1 confirmatory (Forward)	5' CGGATAATGCTGCCGTTGGT 3'
4	*crispr*2 Knockout (Forward)	5' CTGCCATTACTGGTACACAGATTATGATTATGC AACGGCTGTGTAG GCTGGAGCTGCTTCG 3'
5	*crispr*2 Knockout (Reverse)	5' GCCTGCCGATGCCGTCTGTGACTCATCCATTACC TTGC CATATGAATATCCTCCTTA 3'
6	*crispr*2 confirmatory (Forward)	5' GCAATACCCTGATCCTTAACGC 3'
7	*cas op*. Knockout (Forward)	5' AGGCGTAGAGTGCTTTTATTATCCACATGCTGG AGTTTACGTGTAG GCTGGAGCTGCTTCG 3'
8	*cas op*. Knockout (Reverse)	5' CAACAGGAAGAAAAGAAACCAAACGCAGTCCA TCCAAATC CATATGAATATCCTCCTTA 3'
9	*cas op*. confirmatory (Forward)	5' CTTTGAGCGCTTCTTCCAG 3'
10	Confirmatory Internal Primer	5' CCTCCTTAGTTCCTATTCCG 3'
11	*fliC* (Forward)	5' GATAAGACGAACGGTGAGG 3'
12	*fliC* (Reverse)	5' AGCCTCTGTCAAATCAGC 3'
13	*flgK* (Forward)	5' GGATAACACCACCTTCACG 3'

14	*flgK* (Reverse)	5' CAATCTCGGCTTCATTTGTC 3'
15	*csgA* (Forward)	5' GGATTCCACGTTGAGCATT 3'
16	*csgA* (Reverse)	5' TACTGTTATCCGCACCCT 3'
17	*csgD* (Forward)	5' AACTGGCCTCATATTAACGG 3'
18	*csgD* (Reverse)	5' GTGCGTAATCAGGTAACTGG 3'
19	*bcsA* (Forward)	5' GATGGACATTTGTTCTCCTG 3'
20	*bcsA* (Reverse)	5' GCGTTGGAAAGACATATTCC 3'
21	*bcsC* (Forward)	5' GACCAGTTGAGCGGTAAA 3'
22	*bcsC* (Reverse)	5' GTCGTAATGCCAGATCATGT 3'
23	*rpoD* (Forward)	5' GATAAGACGAACGGTGAGG 3'
24	*rpoD* (Reverse)	5' AGCCTCTGTCAAATCAGC 3'
25	*rfaC* (Forward)	5' TACGATAAACCGCAGTCG 3'
26	*rfaC* (Reverse)	5' CTTCCGGCCAGTGTTTA 3'
27	*rfbG* (Forward)	5' CTTGATGCGCCAACTGTTC 3'
28	*rfbG* (Reverse)	5' AAAGGCTGGGCTGCCATA 3'
29	*yddX* (Forward)	5' AAATACCTCAGCAGCACAACC 3'
30	*yddX* (Reverse)	5' TCTTCAGTGACAACGCCTAAC 3'
31	*crp* (Forward)	5' GGTTCTTGTCTCATTGCCA 3'
32	*crp* (Reverse)	5' CGGAGCCTTTAACGATGTAG 3'
33	*flgJ* (Forward)	5' CGCAATCTCTGAACGAACTG 3'
34	*flgJ* (Reverse)	5' CGCATACTTTTCAGCATCATC 3'
35	*rfbI* (Forward)	5' TATCGGGCTGGTATCCATCTTGA 3'
36	*rfbI* (Reverse)	5' CTTTGGAGTCAACAACTTCTCC 3'
37	*fljB* (Forward)	5' GAGCGTCTGTCTTCTGGT 3'
38	*fljB* (Reverse)	5' TTACGGGAAGCCTGAGTC 3'
39	16s rRNA (Forward)	5' CCTGGACAAAGACTGACGCT 3'
40	16s rRNA(Reverse)	5' TTTAACCTTGCGGCCGTACT 3'
41	*crispr1* expression (Forward)	5' GATAAACCGTGAGCAACGACAG 3'
42	*crispr1* expression (Reverse)	5' GCCCTGCAACGGTTTATCC 3'
43	*crispr2* expression (Forward)	5' GCGTTTGACATGAGCGTGTT 3'
44	*crispr2* expression (Reverse)	5' GGTATAGACCAGCGTCACGG 3'
45	*cas3* expression (Forward)	5' AACATGCCGGTTGGATTTGC 3'
46	*cas3* expression (Reverse)	5' CCACAGCGTGACAGACTCTT 3'
47	*cse2* expression (Forward)	5' TGATGCCTGTTTGGCTGAGG 3'
48	*cse2* expression (Reverse)	5' TGTCGCCACCTTTCTTCTGT 3'

2.2.9 Analysing lipopolysaccharide (LPS) profiles

LPS lysis buffer (2 mL of 20% SDS, 800 µL ß-Mercaptoethanol, 200 µL bromophenol, 2 mL glycerol, 15 mL of 1M Tris-HCl) was added to the pellicle biofilms, and rinsed twice with distilled water. The samples were then lysed using TissueLyser LT (QIAGEN, Germany) at 50 Hz for 10 min. The lysates were heated at 100°C, for 10 min followed by DNase (1 µg/µL), RNase (20 µg/µL), and Proteinase-K (20 µg/µL) treatment. Crude LPS thus obtained was resolved using SDS–polyacrylamide gel electrophoresis (SDS-PAGE) with 15% separating gel(H. Li & Benghezal, 2017). The LPS profile was detected using ProteoSilver Silver Stain Kit (SIGMA-ALDRICH, USA).

2.2.10 Determining pellicle strength

The strains were cultured in LB without NaCl media for 96 h, at 25°C, in static condition. The pellicle biofilm strength was determined by the addition of glass beads (1 mm, HiMedia) using a tweezer until disruption (collapse of the pellicle to the bottom). The weight of glass beads that collapsed the pellicle was recorded (Srinandan et al., 2015).

2.2.11 Quantification of extracellular matrix (ECM) components

The 96 h pellicle biofilms were washed with sterile water and sonicated on ice, 15 kHz for 30 secs. The samples were centrifuged and the supernatant was used for the analysis. The DNA and protein concentrations in the supernatants of each sample were estimated spectrophotometrically using BioSpectrometer® basic (Eppendorf, Germany). The exopolysaccharides were quantified by the phenol-sulphuric acid method followed by absorbance at 490 nm (Masuko et al., 2005).

2.2.12 Cellulose determination

Cellulose dry weight estimation, calcofluor binding, and anthrone assay were used to estimate cellulose content in the planktonic culture and pellicle biofilm. For cellulose dry weight estimation, pellicle biofilms were washed twice with distilled water and hydrolyzed with 0.1 M sodium hydroxide (NaOH) at 80°C for 2 h. The samples were dried and weighed.

(i) *Cellulose quantification by calcofluor* - The pellicle biofilms were rinsed twice with distilled water and stained with a 50 mM calcofluor white stain (Sigma-Aldrich) for 40 min in the dark at RT. The bound calcofluor was measured at λ_{ex} of 350 nm and emission λ_{em} of 475 nm with a Victor3 1420 multilabel counter (PerkinElmer, USA).

(ii) *Cellulose quantification by anthrone*- Planktonic bacteria were pelleted via centrifugation, and the culture supernatant was lyophilized in a lyophilizer (ScanVac freeze dryer). The bacterial pellet, lyophilized supernatant, and pellicle biofilm were resuspended in 300 mL of an acetic-nitric reagent and incubated for 30 min at boiling temperatures. The pellets were then washed twice with sterile water, followed by adding 67% sulfuric acid with intermittent mixing, and incubated at RT for 1 h. The samples were placed in an ice bath, and 1 mL of cold anthrone reagent (Fisher Scientific) was added and mixed gently. The tubes were incubated in a boiling water bath for 15 min, after which they were placed on ice. The absorbance at 620 nm was recorded with Multiskan GO.

2.2.13 Whole-cell Congo red depletion assay

The planktonic culture and pellicle biofilm after 24 h, 48 h, and 96 h were pelleted at 10,000 × g for 5 min and resuspended in Congo red solution (10 mg/mL). After 10 min incubation at RT, the cells were centrifuged at 10,000 × g for 10 min. The absorbance of the supernatant was measured at 500 nm with Multiskan GO.

2.2.14 Curli estimation by Thioflavin-T fluorescence

The pellicle biofilms were lysed with a lysis buffer (Tris-EDTA, pH 7.5, and 2% SDS) at 95°C for 45 min. The insoluble pellet was washed twice with autoclaved water and resuspended in PBS containing DNase (1 mg/mL; HiMedia) and RNase (20 mg/mL; HiMedia). After 6 h of incubation at RT, the samples were treated with 2 mM ThT (Sigma-Aldrich) for 15 to 20 min in the dark. The absorbance was measured at (λ_{ex}) of 440 nm and (λ_{em}) at 482 nm with the Victor3 1420 multilabel counter.

2.2.15 Quantitative real-time PCR

Total RNA from 24 h (bacterial culture) and pellicle biofilm in LB without NaCl was isolated using TRIzol reagent (HiMedia) and the method described below, respectively. The RNA extraction was followed by cDNA synthesis using ProtoScript II reverse transcriptase (NEB). Quantitative real-time (qRT-PCR) was performed using PowerUp SYBR Green master mix (Thermo Fisher Scientific). Relative expression of the gene was calculated using the threshold cycle method ($2^{-\Delta\Delta CT}$) by normalizing to reference gene *rpoD*. The primers used in RT-qPCR are listed in Table 2.3.

RNA isolation from pellicle biofilm - Pellicle biofilms were resuspended in a solution containing 70% ammonium sulfate and 10% cetyltrimethylammonium bromide (CTAB). The pellicles were crushed with the help of a toothpick and incubated at RT for

10 min. The suspensions were then centrifuged and resuspended in 500 mL of lysis solution (10 mM Tris, 10 mM EDTA, and 1 mg/mL lysozyme) and incubated at RT for 10 min. A mixture of 10% SDS and 3 M sodium acetate was added to the samples. Finally, the RNA was purified using phenol-chloroform-isoamyl alcohol extraction. The RNA in the aqueous phase was then precipitated overnight at 280°C using isopropanol. The purified RNA was then used for cDNA synthesis.

2.2.16 Statistical analysis.

Statistical analysis was performed using Prism 8 software (GraphPad, California). Unpaired Student's t-test was performed. Error bars indicate standard deviation (SD). Statistical significance is shown as follows: *,P ≤ 0.05; **, P ≤ 0.01; ***, P ≤0.001; ****, P < 0.0001; and ns, not significant.

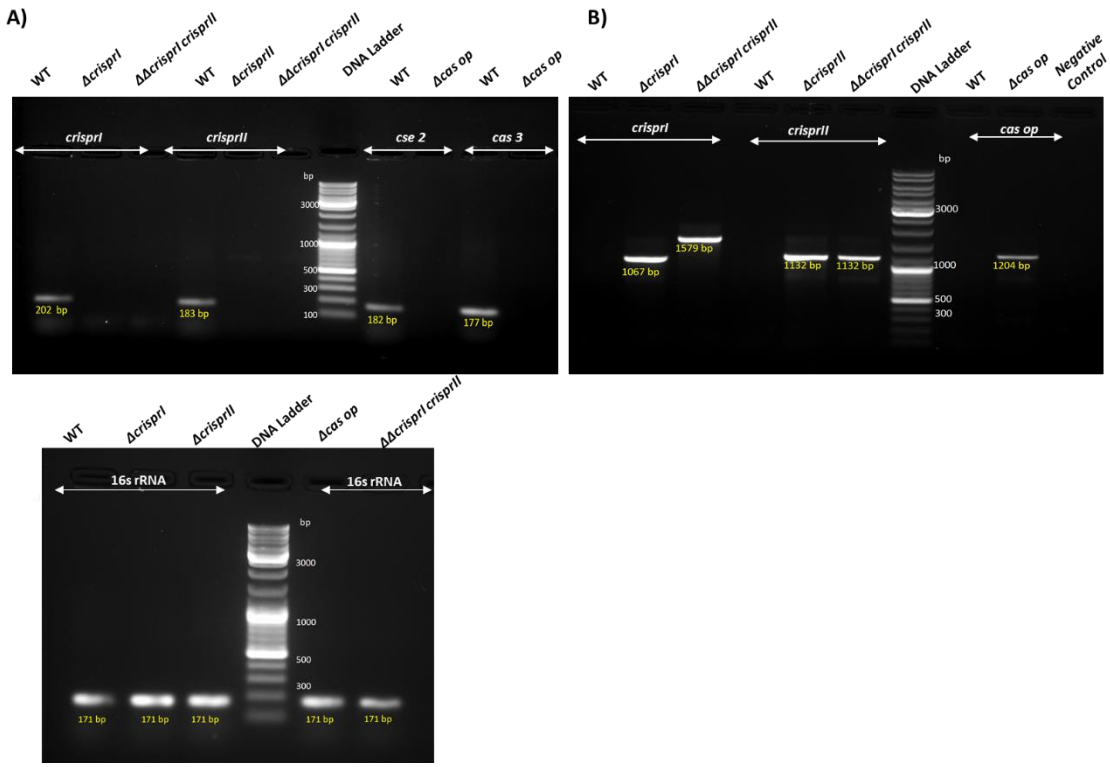

Fig. 2.3: Deletion of the CRISPR-Cas components was confirmed through PCR using expression primers (A), and confirmatory primers (B). The colony PCR of potential knockout strains was done using respective primers mentioned in Table 2.3, and the amplicons were visualized using agarose electrophoresis. **A.** The presence of CRISPR-Cas genes was checked in WT and knockout strains (Δ*crisprI*, Δ*crisprII*, Δ*cas op*, and ΔΔ*crisprI crisprII*), while 16srRNA was used as a positive control for each strain. **B.** Amplicons of appropriate sizes were obtained for each knockout strain, whereas WT did not yield any bands.

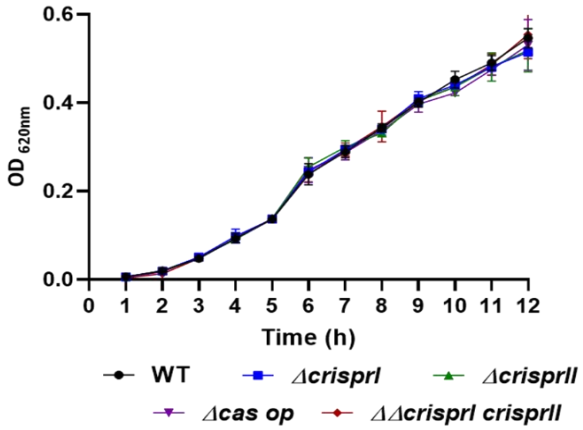

Fig. 2.4: The CRISPR-Cas knockout strains of *S. enterica* subsp. *enterica* serovar Typhimurium 14028s showed a similar growth trend to wildtype in LB without NaCl media. The *S.* Typhimurium strain 14028s wildtype (WT), CRISPR (Δ*crisprI*, Δ*crisprII*, and ΔΔ*crisprI crisprII*), and *cas operon* (Δ*cas op*) knockout strains were cultured in LB without NaCl media at 37°C. The graph represents OD_{620nm} for each strain.

2.3 Results

2.3.1 CRISPR-Cas knockout strains show temporal variations in the biofilm formation

We began with knocking out the CRISPR arrays (*crisprI* and *crisprII*) individually or both and the *cas* operon using a single-step gene knockout strategy (Fig. 2.2). The successful generation of the respective knockout strains were confirmed by PCR-based approach using the confirmatory and expression primers (Fig. 2.2 and 2.3).

We tested the biofilm-forming ability of the CRISPR and *cas* operon knockout strains (Δ*crisprI*, Δ*crisprII*, Δ*cas op.*, and ΔΔ*crisprI crisprII*) of *S.* Typhimurium strain 14028s under gallstone-mimicking conditions. For this purpose, cholesterol-coated tubes that create a uniform surface mimicking gallstones were used, and biofilm formation was tested in the presence of 3% ox bile (Crawford et al., 2008). At the end of the 96 h, all the knockout strains showed reduced biofilm formation compared to wildtype (WT) (Fig. 2.5A). The phenotypes exhibited by the knockout strains were restored on the complementation of corresponding genes in Δ*crisprI* and Δ*crisprII* (Fig. 2.5A). This outcome confirms that the gene deletions were clean without any side effects.

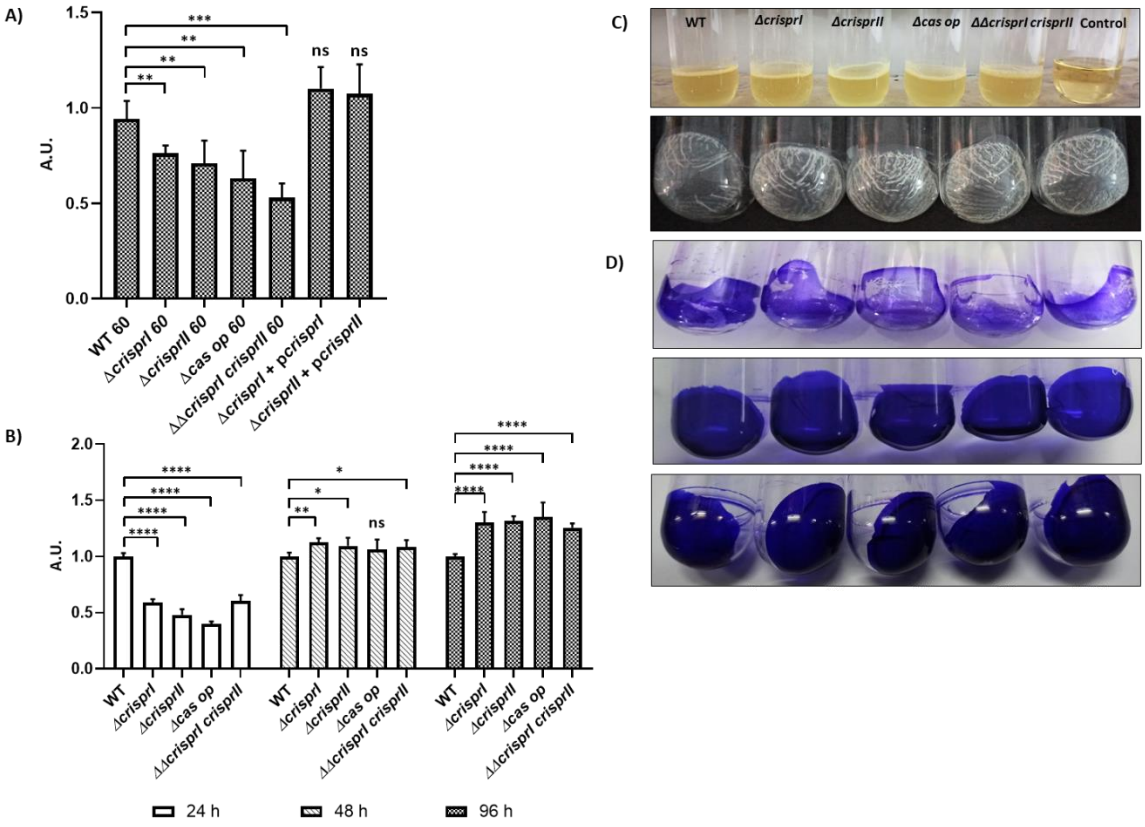

Fig. 2.5: The CRISPR-Cas knockout strains of *S. enterica* subsp. *enterica* serovar Typhimurium 14028s showed reduced biofilm formation under gallstone mimicking condition (A), while these strains showed temporal variations in biofilm at solid-liquid and air interface (B). Representative images of pellicle Biofilms. (C and D). **A.** The biofilm formed by Wildtype, CRISPR, and *cas operon* knockout strains transformed with empty vector pQE60 (WT60, Δ*crisprI 60*, Δ*crisprII 60*, Δ*cas op 60*, and ΔΔ*crisprI crisprII 60*), and the complement strains (Δ*crisprI*+p*crisprI*, Δ*crisprII*+p*crisprII*) was tested using tube biofilm assay. **B.** The *S.* Typhimurium strain 14028s wildtype (WT), CRISPR (Δ*crisprI*, Δ*crisprII*, and ΔΔ*crisprI crisprII*), and *cas operon (*Δ*cas op*) knockout strains were cultured in LB without NaCl media for different time periods (24 h, 48 h, and 96 h) and the biofilm formation was estimated using the crystal violet staining method. The graph represents OD_{570nm} for each strain, normalized by OD570nm of WT. An unpaired t-test was used to determine significant differences between the WT and knockout strains. Error bars indicate SD. Statistical significance: *, P≤ 0.05, **, P≤ 0.01, ***, P≤ 0.001, ****, P <0.0001, ns = not significant. A.U., arbitrary units.**C.Top:** Biofilm formation by *S. enterica* subsp. *enterica* serovar Typhimurium 14028s wildtype and CRISPR-Cas system knockout strains at the air-liquid interface (pellicle). **Bottom:** Unstained pellicle biofilm of *S. enterica* subsp. *enterica* serovar Typhimurium 14028s wildtype and CRISPR- Cas system knockout strains. **D. Top:** CV-stained, 24 h old pellicle biofilm of *S. enterica* subsp. *enterica* serovar Typhimurium 14028s wildtype and CRISPR-Cas system knockout strains. **Middle:** CV-stained, 48 h old pellicle biofilm of *S. enterica* subsp. *enterica* serovar Typhimurium 14028s wildtype and CRISPR-Cas system knockout strains. **Bottom:** CV-stained, 96 h old pellicle biofilm of *S. enterica* subsp. *enterica* serovar Typhimurium 14028s wildtype and CRISPR-Cas system knockout strains.

Next, a time-dependent study determining the biofilm formation by the knockout strains in low osmotic conditions (LB without NaCl) showed temporal variations in biofilm phenotypes compared to that of the WT (Fig. 2.5B). The knockout strains formed a thin biofilm ring on the solid-liquid-air interface (surface biofilm) at 24 h (Fig. 2.5B) and 96 h (Fig, 2.6A). However, as time progressed, the knockout strains displayed a gradual increase in the biofilm formation, with a 1.3-fold increase in the biofilm at 96 h (Fig. 2.5B and Fig. 2.6 B). The difference in observed biofilm phenotype was not accredited to the difference in bacterial growth, as testified by the similar growth patterns of all the strains in LB without NaCl media (Fig. 2.4).

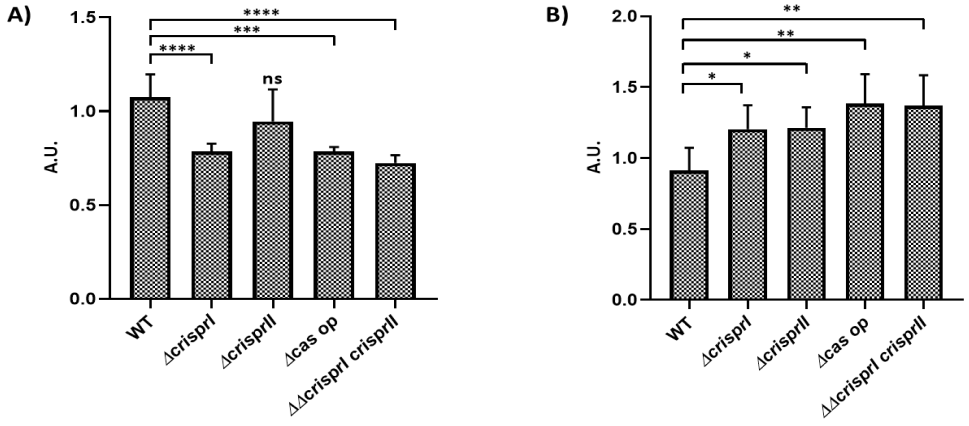

Fig. 2.6: The CRISPR-Cas knockout strains of *S. enterica* subsp. *enterica* serovar Typhimurium 14028s showed reduced biofilm formation at the solid-liquid interface(A), while these strains showed increased biofilm (pellicle) at the solid-liquid and air interface (B).
The S. Typhimurium strain 14028s wildtype (WT), CRISPR (Δ*crisprI*, Δ*crisprII*, and ΔΔ*crisprI crisprII*), and *cas operon* (Δ*cas op*) knockout strains were cultured in Tryptic Soy Broth (TSB) media for 96 h, at 25°C, static condition in 24-well plastic plate. The biofilm formation was estimated using the crystal violet staining method. The graph represents OD570nm for each strain, normalized by OD570nm of WT. An unpaired t-test was used to determine significant differences between the WT and knockout strains. Error bars indicate SD. Statistical significance: *, P≤ 0.05, **, P≤ 0.01, ***, P≤ 0.001, ****, P<0.0001, ns = not significant. A.U., arbitrary units.

2.3.2 Scanning electron microscopy depicts the difference in biofilm architecture of CRISPR-Cas knockout strains

Scanning electron microscopy (SEM) was used to investigate biofilm architecture at early (24 h) and late (96 h) time points. At 24 h, the micro-graphs of the WT showed more

aggregated and tightly packed bacterial cells covering the large surface area (Fig. 2.7A). In contrast, the micrographs of all the knockout strains showed patchy bacterial aggregates (Fig. 2.7A). Distinct bacterial cells were more evident in the Δ*cas* op. strain than those of other *Salmonella* strains. Small dome-like structures were observed only in the WT micrograph, indicating the formation of the multilayered structure. The biofilm formed by the knockout strains displayed clumped cells without any slimy material in their vicinity. On average, all the strains had similar lengths at 24 h (Fig. 2.7B). However, a few elongated cells (marked in the micrograph) were observed in the knockout strains at 24 h (Fig. 2.7A). SEM analysis of 96 h pellicle biofilm revealed that, in general, the air-exposed side of the pellicle biofilm had a dry but smooth mat-like structure composed of dense fibrous networks with tightly packed bacterial cells. However, compared to WT biofilm, the biofilms formed by knockout strains had thicker extracellular matrix (ECM) coatings and consisted of "hilly" structures of different sizes (Fig. 2.7C, arrowheads). The liquid-submerged side of the pellicle biofilm was rough, consisting of a dome- and valley-like arrangement made up of loosely packed bacterial cells entrapped in EPS. The knockout strains also displayed discrete regions with EPS lumps (marked in micrographs) and pronounced bacterial density (Fig. 2.7D).

2.3.3 Factors Contributing to differential biofilm formation by CRISPR-Cas knockout strains

To understand the knockout strains' temporal variations in biofilm formation, we assessed the expression of essential biofilm components like flagella, cellulose, LPS, and curli.

2.3.3.1 CRISPR-Cas knockout strains show reduced motility and flagellin expression

Motility is crucial for the initial surface colonization during biofilm formation. As the CRISPR and *cas* deletion mutants showed reduced biofilm formation at 24 h, we assessed their motility by using a swarming assay. There was at least a 20% reduction in swarming rates of all the knockout strains compared to WT (Fig. 2.8A). The complementation of Δ*crisprI* and Δ*crisprII* with corresponding genes restored the defect in their motility (Fig. 2.8A). We next analyzed the expression of flagellin protein (FliC) for the planktonic and pellicle bacteria. The FliC expression in planktonic bacteria was less for knockout strains than that for the WT. However, in the 96 h pellicle, no FliC expression was observed in all the strains (Fig. 2.8B).

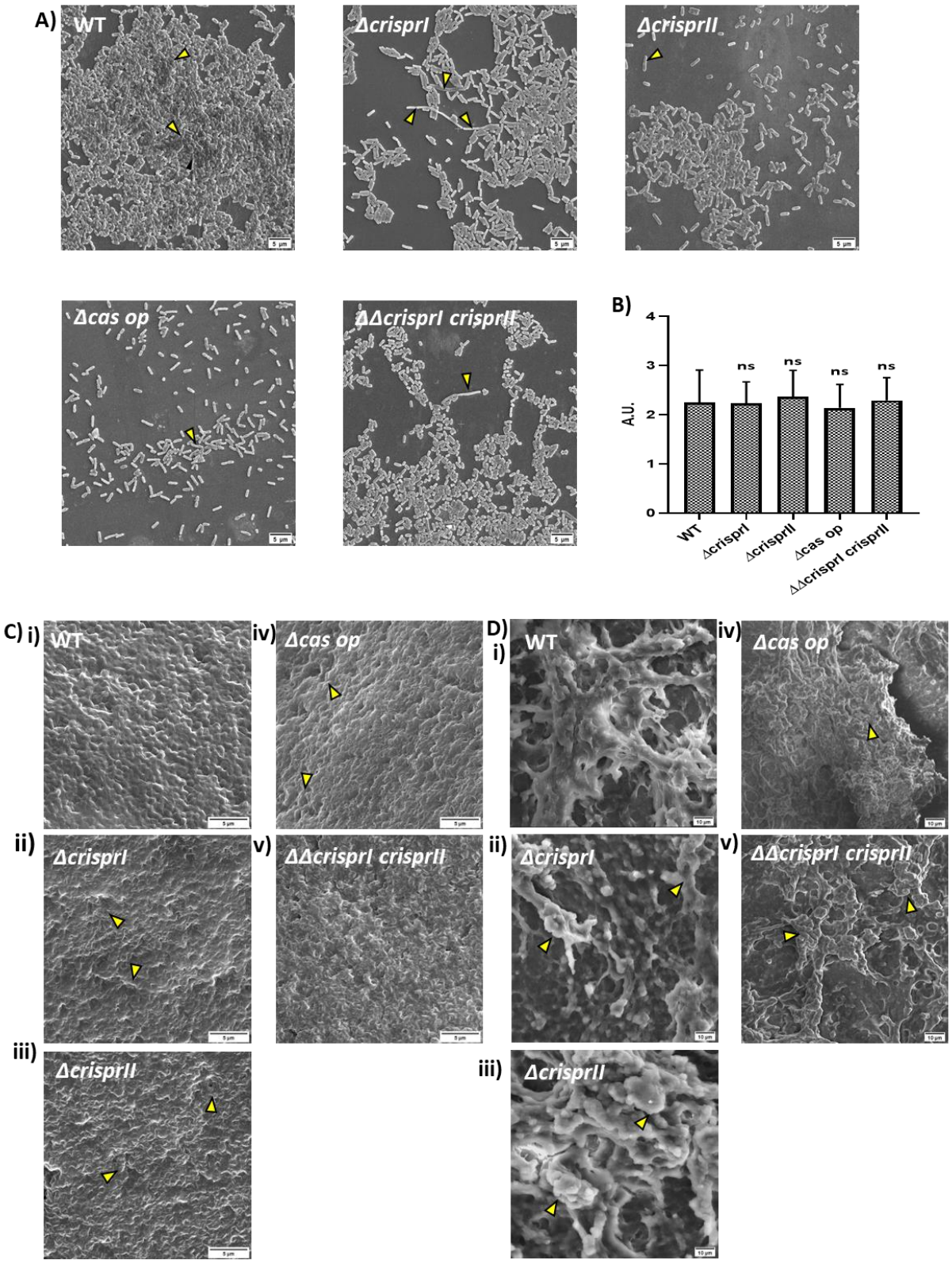

Fig. 2.7: Morphology of air-exposed side of surface-attached (glass) biofilm at early (24 h) and pellicle biofilm at late time point (96 h) at the air-exposed side (C) and liquid-submerged side

(D). A. At 24 h, the knockout (Δ*crisprI*, Δ*crisprII*, Δ*cas op*, and ΔΔ*crisprI crisprII*) strains formed patchy bacterial aggregates, in comparison to wildtype (WT), which had tightly packed bacterial aggregates covering a larger area, with a few dome-like structures (arrow-head in the WT micrograph). Few elongated cells (arrowheads in the micrographs) were also observed in the biofilms of the knockout strains. The images were captured at 5000x magnification and scaled to the bar. **B.** The graph represents the average size (in µm) of WT and Knockout strains. An unpaired t-test was used to determine significant differences between the WT and knockout strains. Error bars indicate SD. Statistical significance: *P≤ 0.05, **P≤ 0.01, *** P≤ 0.001, ****P<0.0001, ns = not significant. A.U., arbitrary units. **C.** SEM image analysis of 96 h biofilm depicts the difference in the pellicle biofilm architecture of CRISPR-Cas knockout (Δ*crisprI*, Δ*crisprII*, Δ*cas op.*, and ΔΔ*crisprI crisprII*) strains and that of the wildtype (WT) for both air-exposed side (captured at 10,000x magnification), and liquid-submerged (captured at 2500x magnification) side of pellicle biofilm. The air-exposed surface of the pellicle biofilm of CRISPR-Cas knockout strains had denser mat-like ECM. It consisted of "hilly" structures (marked with arrowheads), indicating more layering of the biofilm. **D.** The liquid-submerged surface of the pellicle biofilm of CRISPR-Cas knockout strains had more EPS lumps (marked with arrowheads) than the wild type. Images were scaled to the bar.

2.3.3.2 Deletion of CRISPR-Cas genes affects the LPS structure

The reduction in swarming motility in the knockout strains is not consistent with FliC expression. For example, expression of FliC protein was minimum in the ΔΔ*crisprI crisprII* strain, but its swarming rate was not the lowest. This anomaly could partially be attributed to the variations in the wettability factor, like LPS, that governs the swarming rate. Additionally, the O-antigen of LPS plays a crucial role in biofilm formation (Peng, 2016), and Gram-negative bacteria modify their LPS while in the biofilm (Maldonado et al., 2016). Thus, we assayed the LPS profiles of all the knockout strains and compared them with that of the WT (Fig. 2.9). The intensity of the lipid A band was similar in all the strains except for Δ*cas op.* and ΔΔ*crisprI crisprII*. The O-antigen profile showed variations where the ladder-like banding patterns in Δ*crisprII* and ΔΔ*crisprI crisprII* were less intense than those of the other strains. The band corresponding to very long O-antigen was absent in Δ*crisprI*, whereas the WT and Δ*cas op*. bands had comparable intensities. The very long O-antigen band intensity was similar for Δ*crisprII* and ΔΔ*crisprI crisprII* but was less than that of WT. As for the banding pattern of core glycoforms, Δ*crisprII* and WT were similar to ΔΔ*crisprI crisprII* and Δ*cas op*., respectively. Δ*crisprI* had a distinct pattern of core glycoforms. All these observations point to alterations of the O-antigen chain in the knockout strains during biofilm formation.

2.3.3.3 The CRISPR-Cas knockout strains show increased pellicle formation due to increased bacterial biomass and its respective components

The dry weights of the pellicle biofilms by all the knockout strains were similar to those of the WT at 48 h, whereas they were significantly higher at 96 h (Fig. 2.10 A). The temporal variations in the dry weight of all the strains were similar to that of the biofilm formation as estimated using crystal violet assay. As the dry mass comprises bacterial cells and ECM, we independently assessed the bacterial cell mass (by assessing viability) and concentration of the ECM components.

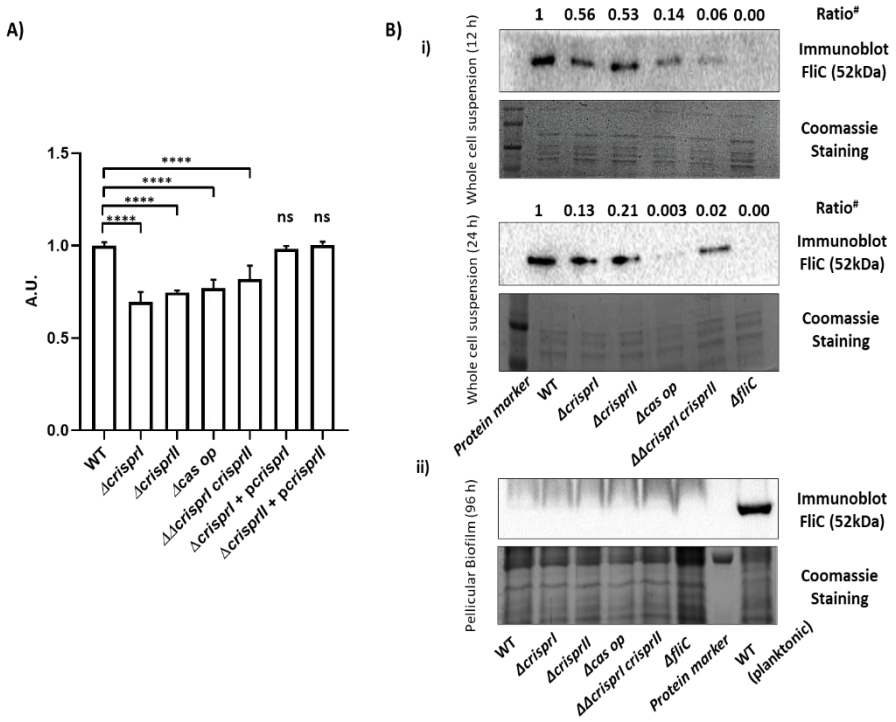

Fig. 2.8: Reduced swarming motility (A) and expression of the flagellar protein, FliC (B), was observed in the CRISPR-Cas system knockout strains. A. Swarming rate (cm/h) of the wildtype (WT), the knockout strains (Δ*crisprI*, Δ*crisprII*, Δ*cas op*, and ΔΔ*crisprI crisprII*), and the complement strains (Δ*crisprI* + p*crisprI*, Δ*crisprII*+ p*crisprII*) was calculated after 9 h. The graph represents the swarming rate (cm/h) relative to that of WT. **B.** The expression of the flagellar protein in planktonic bacteria (B) at early time points (12 h and 24 h) and in pellicle biofilm (B) at a late time point (96 h) was assessed using western blot analysis. Even at higher protein concentrations, FliC was not detected in the blot for pellicle sample of any strain, indicating repression of FliC expression in pellicle biofilm. Δ*fliC*was used as a negative control. An unpaired t-test was used to determine significant differences between the WT and knockout strains. Error bar indicates SD. Statistical significance: *P≤ 0.05, **P≤ 0.01, ***P≤ 0.001, ****P<0.0001, ns = not significant. A.U., arbitrary units. #The ratio above the Immunoblots (B(i)) indicates the relative intensity of the bands with respect to wildtype, observed in the blots, normalized by the relative intensity of the bands with respect to wildtype, observed on the gel.

ratio: $\frac{\frac{[FliC\ intensity}{coomassie\ band\ intensity]_{strain}}}{\frac{[FliC\ intensity}{coomassie\ band\ intensity]_{WT}}}$

The resazurin cell viability assay results show that the knockout strains were more viable than the WT (Fig. 2.10 B), hinting at more bacterial mass. We also validated high bacterial abundance within the pellicle biofilm of knockout strains using SYTO9 staining while also assaying the total bacterial abundance within the surface-attached biofilm at 24 h (Fig. 2.10 C). The surface-attached biofilm of all the knockout strains (at an early time point, 24 h) had lower SYTO9 intensity than that of the WT (Fig. 2.10 C; Fig. 2.11A), whereas, at 96 h, SYTO9 intensity was higher than that of the WT (Fig. 2.10 C; Fig. 2.11B).

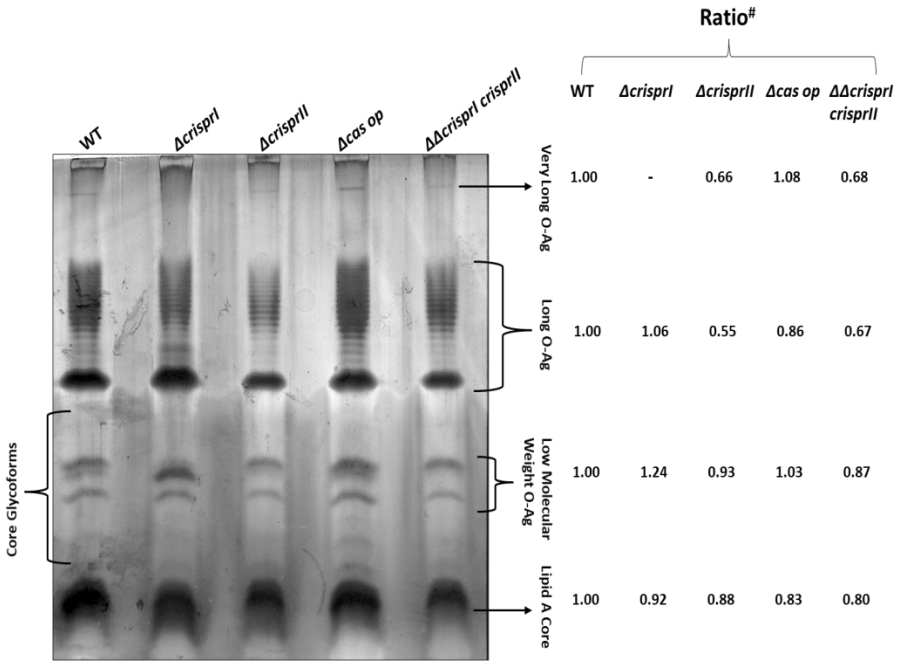

Fig. 2.9: Silver-stained Lipopolysaccharide (LPS) profiling of wildtype (WT), and CRISPR-Cas system knockout strains. The variation in O-antigen was analyzed by LPS profiling of the strains grown in LB without NaCl media for 96 h. The crude LPS samples were resolved using loaded SDS-PAGE and stained using a silver staining kit. Variations in banding pattern and intensity between knockout (Δ*crisprI*, Δ*crisprII*, Δ*cas op*, and ΔΔ*crisprI crisprII*) strains and WT were observed in long O-Ag, low molecular weight O-Ag, and core glycoforms regions. #Ratio indicates the intensity of the bands observed on the gel for all strains normalized by the intensity of the band wildtype.

Further, the SYTO9/propidium iodide (PI) ratio was less for surface-attached biofilm (Fig. 2.11A) and more for pellicle biofilm (Fig. 2.11B) of all the knockout strains except Δ*cas op*. This indicates that the knockout strains have fewer viable bacteria than the WT in surface-attached biofilm (24 h), while the opposite was true for the pellicle biofilm at 96 h (Fig.2.11B and Fig. 2.12B). The thicknesses of the surface-attached biofilm (Fig. 2.12A to D) for WT, Δ*crisprI*, Δ*crisprII*, Δ*casop*., and ΔΔ*crisprI crisprII* were 102 mm, 82 mm, 62 mm, 56 mm, and 68 mm, respectively, whereas, for the pellicle biofilm, the

observed thicknesses were 82 mm, 96 mm, 88 mm, 120 mm, and 124 mm, respectively (Fig. 2.13A to D).

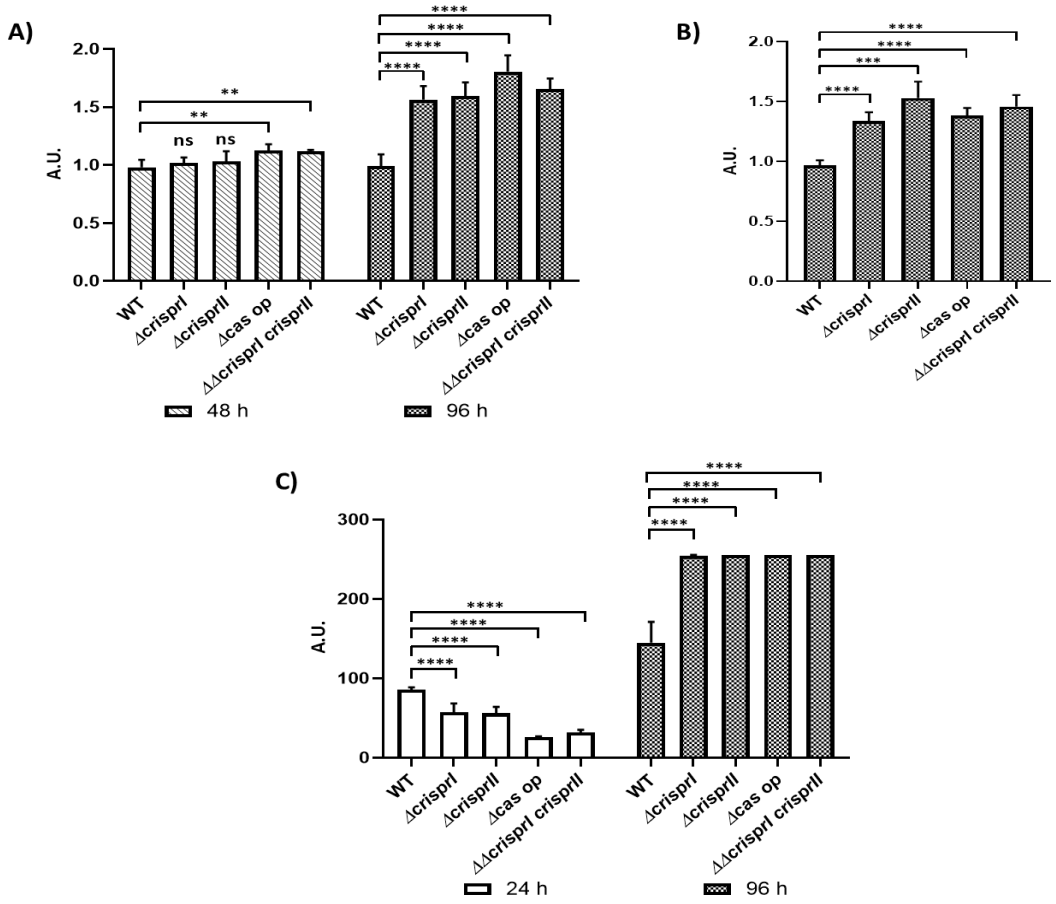

Fig. 2.10: Compared to WT, CRISPR-Cas system knockout strains show differences in their bacterial biomass (A), metabolic activity (B), bacterial cell concentration (C), A. The *S.* Typhimurium strain 14028s wildtype (WT), CRISPR (Δ*crisprI,* Δ*crisprII,* and ΔΔ*crisprI crisprII*) and *cas operon (*Δ*cas op*) knockout strains were cultured in LB without NaCl media for different time periods (48 h, and 96 h). The biomass of the strains was estimated with the help of dry weight of pellicle biofilms. The graph represents dry pellicle biofilm weight (in gms) of each strain normalized by the dry pellicle biofilm weight (in gm) of WT at respective time points. **B.** The metabolic activity of *S.* Typhimurium strain 14028s wildtype (WT), CRISPR (Δ*crisprI,* Δ*crisprII,* and ΔΔ*crisprI crisprII*) and *cas operon (*Δ*cas op*) knockout strains was assessed using resazurin assay. The graph represents the fluorescence intensity observed for each strain normalized by the fluorescence intensity of WT. **C.** The pellicle biofilm formed by the strains was stained with SYTO 9, for 30 mins in the dark, at RT. The graph represents the mean intensity of SYTO9 observed for each strain.

We next estimated the net content of the extracellular polymeric substances like proteins, DNA, and polysaccharides that comprise the ECM. The pellicle biofilms of all the knockout strains had significantly higher polysaccharide concentrations than those of

the WT (Fig.2.14A). Similarly, the protein concentrations were significantly high in the pellicle biofilms of all the knockout strains except in ΔΔ*crisprI crisprII* (Fig. 2.14B). The DNA content was significantly higher only in the pellicle biofilm of Δ*crisprI* and Δ*cas op*. (Fig. 2.14C).

We further evaluated the expression of individual biofilm components like curli and cellulose. Curli, thin aggregative fimbriae, aid surface adhesion and provide cell-cell interactions while framing the biofilm architecture (Reichhardt et al., 2015). Less curli production could also be one of the reasons for reduced ring biofilm formation by the knockout strains. Thus, we assessed the curli production (24 h, 48 h, and 96 h) using whole-cell Congo red (CR) depletion assay for planktonic culture and pellicle biofilm. The CR depletion (Fig. 2.15A and Fig. 2.15B) was less for both the planktonic culture and pellicle biofilm of all the knockout strains, suggesting low levels of curli protein. The results were further validated using an amyloid-specific indicator dye, Thioflavin-T (ThT) (Perov et al., 2019). The results confirm that the curli production is less in all four knockout strains for all the time points tested (Fig. 2.15C). The cellulose production in surface-attached biofilm was evaluated by quantifying the calcofluor white intensity in the images captured using confocal laser scanning microscopy (CLSM). There was no difference in the cellulose content except for that of Δ*crisprII* (Fig. 2.11 A, Fig. 2.16 B, and Fig.2.12 C) for surface-attached biofilm.

However, for pellicle biofilm at 96 h, the cellulose content was higher for the knockout strains. We further estimated the cellulose dry weight for the pellicle biofilm at 48 h and 96 h. Interestingly, the cellulose dry weight of the knockout strains was lower than that of the WT at 48 h but was significantly higher at 96 h (Fig. 2.16A). The analysis of the orthogonal projections of CLSM images suggests that the cellulose is mainly deposited in the region with mature (multilayered) biofilm containing both the live and dead bacteria (Fig. 2.12 and Fig.2.13). The areas with fresh bacterial growth (less PI staining) have less cellulose (Fig. 2.12 and Fig.2.13). Curli content in the pellicle biofilm is related to surface elasticity, thereby providing mechanical strength to the biofilm (C. Wu et al., 2012). As Curli protein was less in the pellicles of knockout strains, we determined the pellicle biofilm strength using a glass bead assay (Srinandan et al., 2015). The pellicles of the knockout strains were easily disrupted with lesser weight while enduring 50% less weight than the WT pellicles could sustain (Fig. 2.17B). The results suggest that knockout strains' pellicles are weaker due to less Curli production.

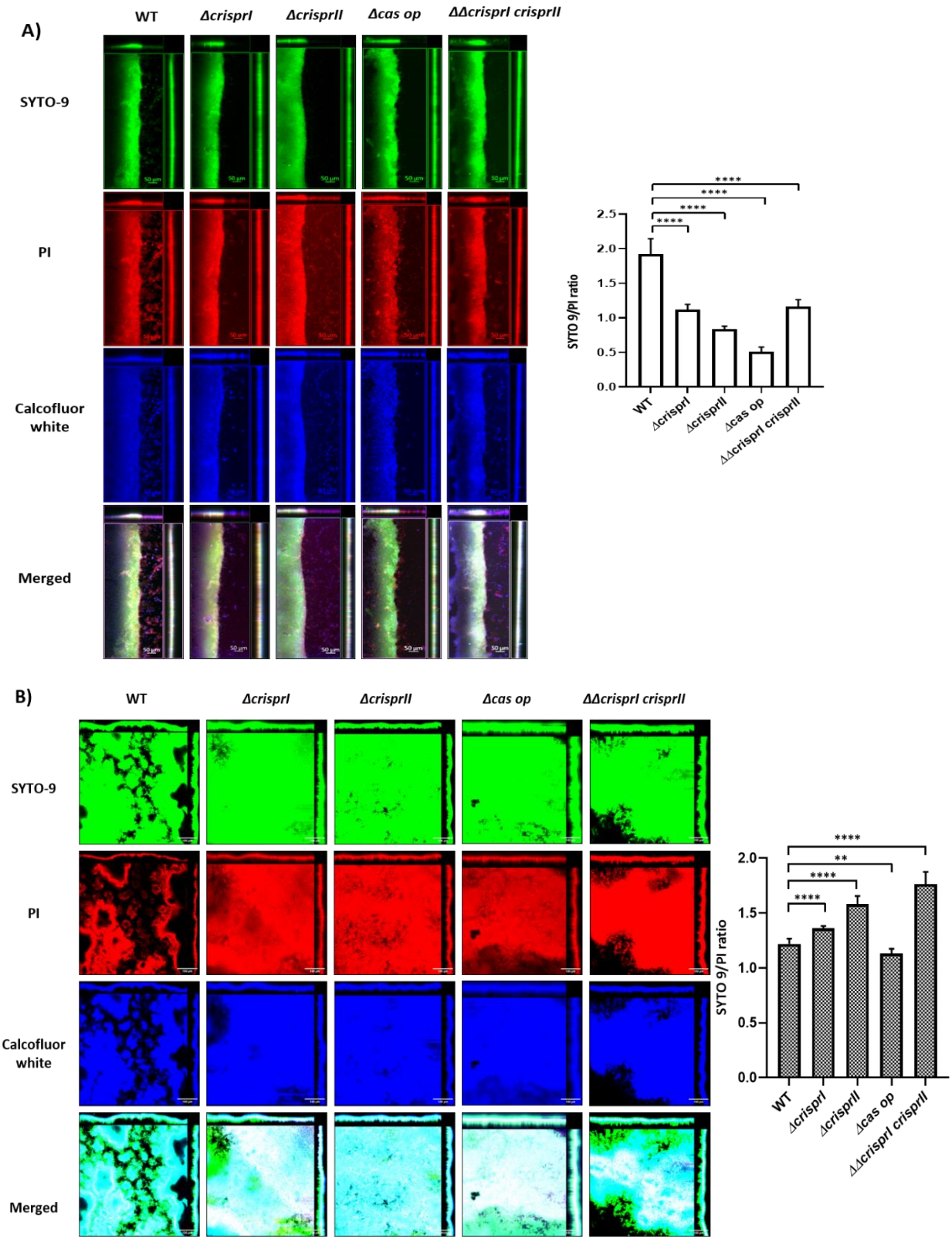

Fig. 2.11: The CRISPR- Cas knockout strains showed temporal variations in their bacterial cell concentration, cellulose content, and SYTO 9/ PI ratio compared to WT at early (24 h) (A) and late (96 h) time points (B). A& B. The *S.* Typhimurium strain 14028s wildtype (WT), CRISPR (Δ*crisprI,* Δ*crisprII* and ΔΔ*crisprI crisprII*) and *cas operon (*Δ*cas op*) knockout strains were cultured in LB without NaCl media for 24 h (A), and 96 h (B), at 25°C, static condition. The biofilm formed was stained

with SYTO 9, Propidium Iodide (PI), and Calcofluor white for 30 mins in the dark, at RT. The CLSM images were captured, and orthogonal projections of wildtype and CRISPR- Cas knockout strains were obtained. The graph on the right of CLSM images represents the ratio of the mean intensity of SYTO 9the to the mean intensity of PI for respective strains at 24 h **(A)** and 96 h **(B)**. An unpaired t-test was used to determine significant differences between the WT and knockout strains. Error bars indicate SD. Statistical significance: *P≤ 0.05, **P≤ 0.01, ***P≤ 0.001, ****P<0.0001, ns = not significant. A.U., arbitrary units.

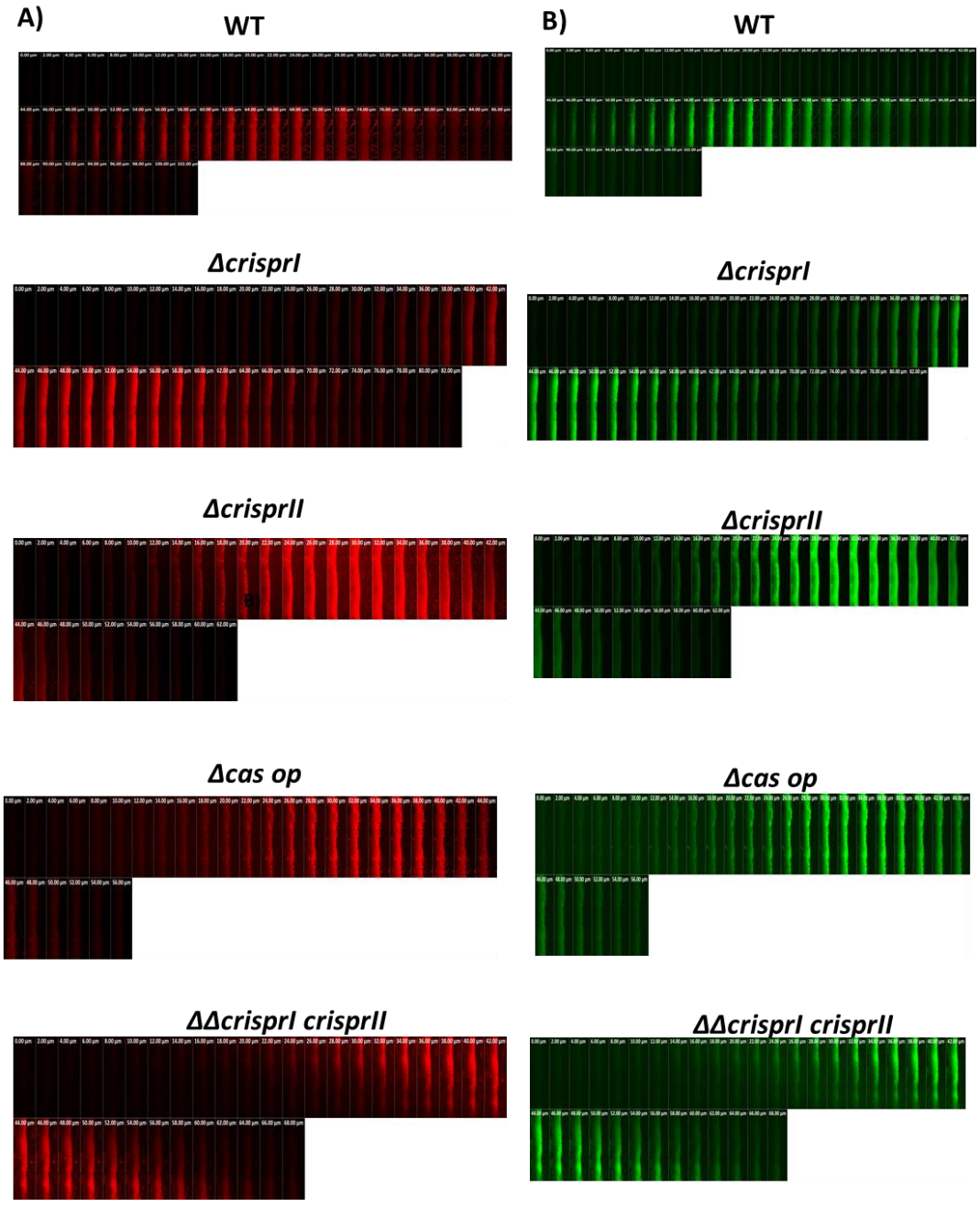

Fig. 2.12: A, B. CLSM images (stacks) of wildtype and CRISPR- Cas knockout strains stained with Propidium Iodide(A), SYTO 9 (B). The pellicle biofilm formed by the *S.* Typhimurium strain 14028s wildtype (WT), CRISPR (Δ*crisprI,* Δ*crisprII* and ΔΔ*crisprI crisprII*) and *cas operon (*Δ*cas op*) knockout strains was stained with Propidium Iodide (PI), SYTO 9 and images were captured using CLSM.

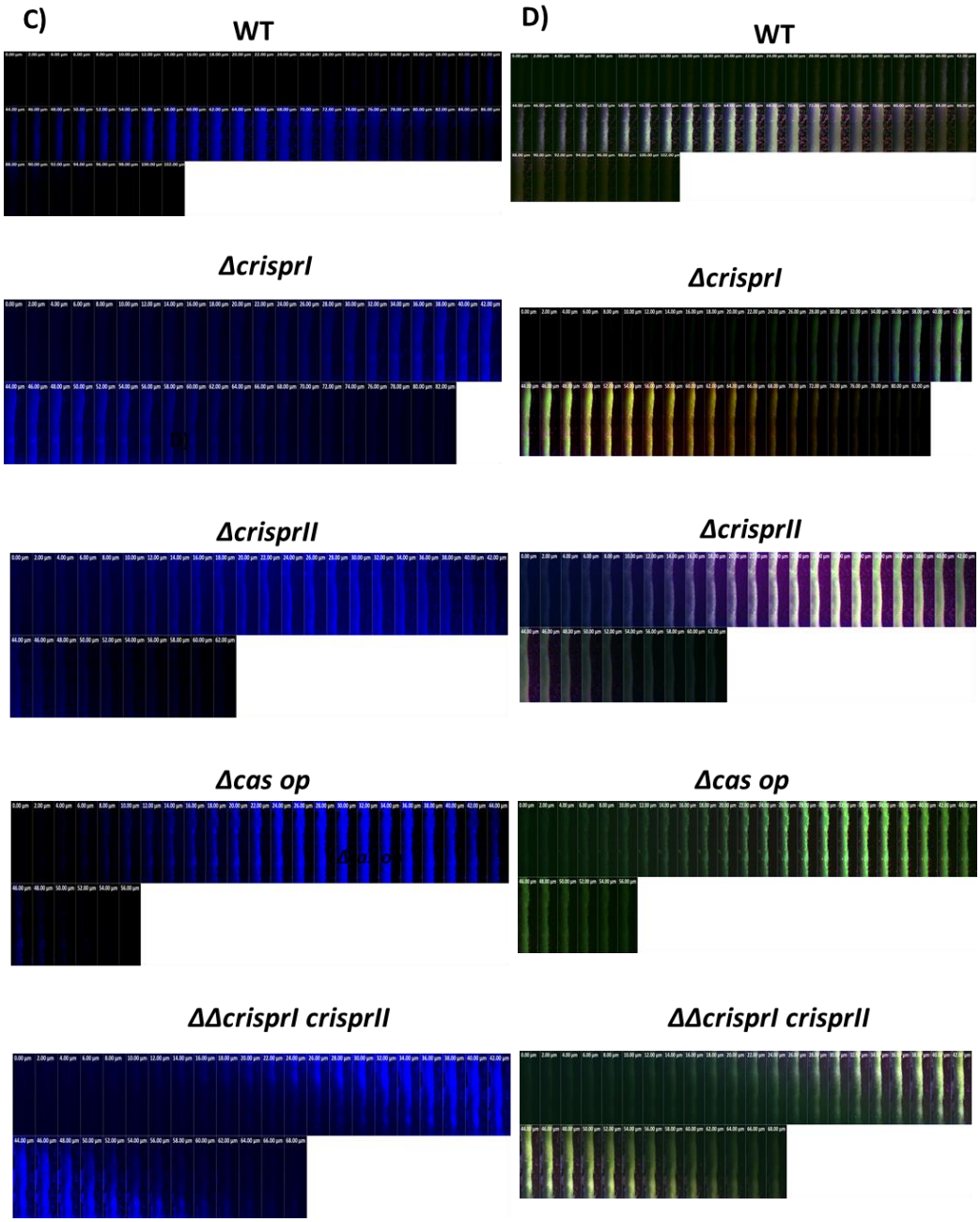

Fig. 2.12: C, D. C. CLSM images (stacks) of wildtype and CRISPR- Cas knockout strains stained with Calcofluor white. D. Represents the merged CLSM stacks for all three components. The pellicle biofilm formed by the *S.* Typhimurium strain 14028s wildtype (WT), CRISPR (Δ*crisprI*, Δ*crisprII* and ΔΔ*crisprI crisprII*) and *cas operon (*Δ*cas op*) knockout strains was stained with Calcofluor white and images were captured using CLSM.

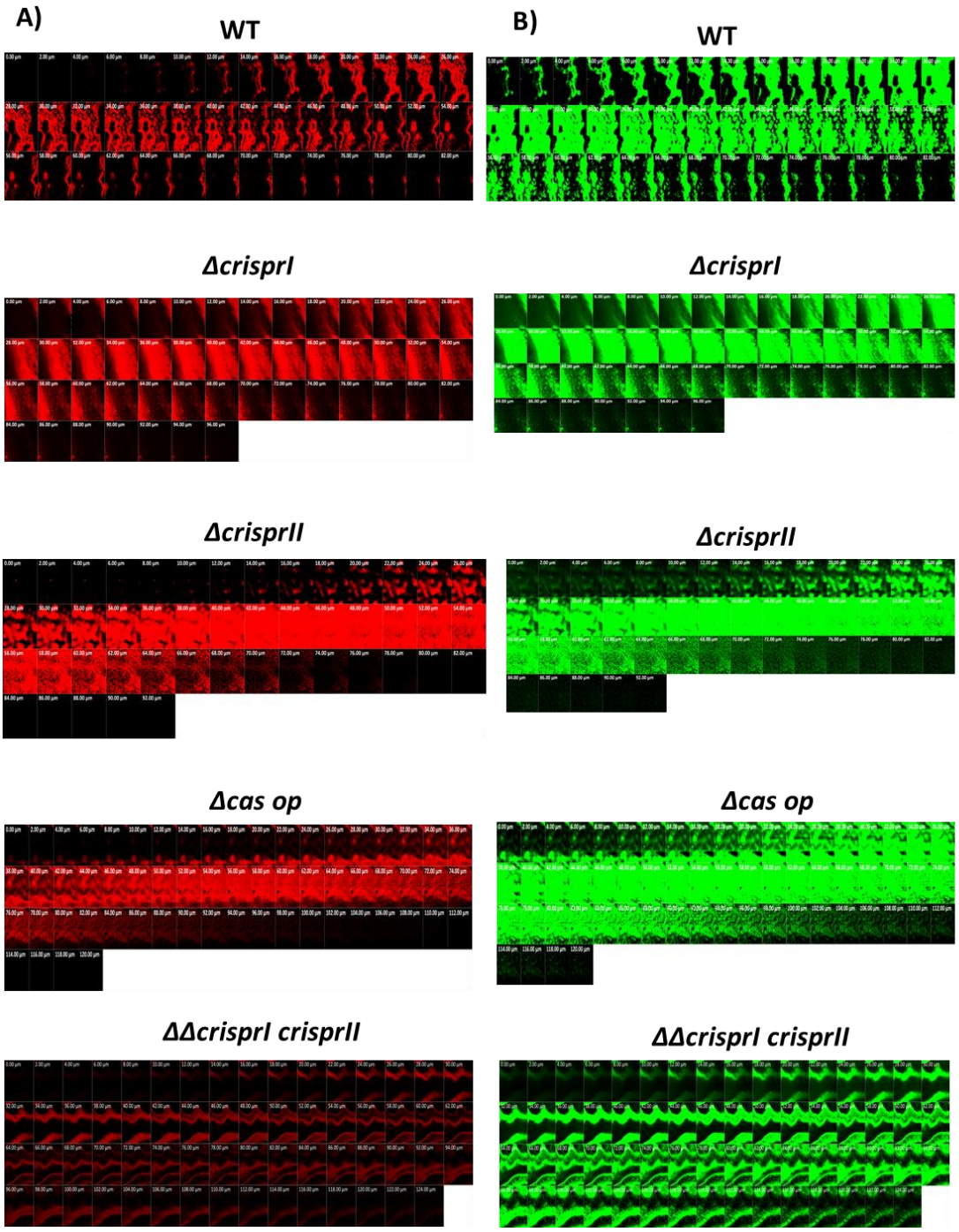

Fig. 2.13: A, B. CLSM images (stacks) of wildtype and CRISPR- Cas knockout strains stained with Propidium Iodide (A), SYTO 9 (B). The pellicle biofilm formed by the *S.* Typhimurium strain 14028s wildtype (WT), CRISPR (Δ*crisprI*, Δ*crisprII* and ΔΔ*crisprI crisprII*) and *cas operon* (Δ*cas op*) knockout strains was stained with Propidium Iodide (PI), SYTO 9 and images were captured using CLSM.

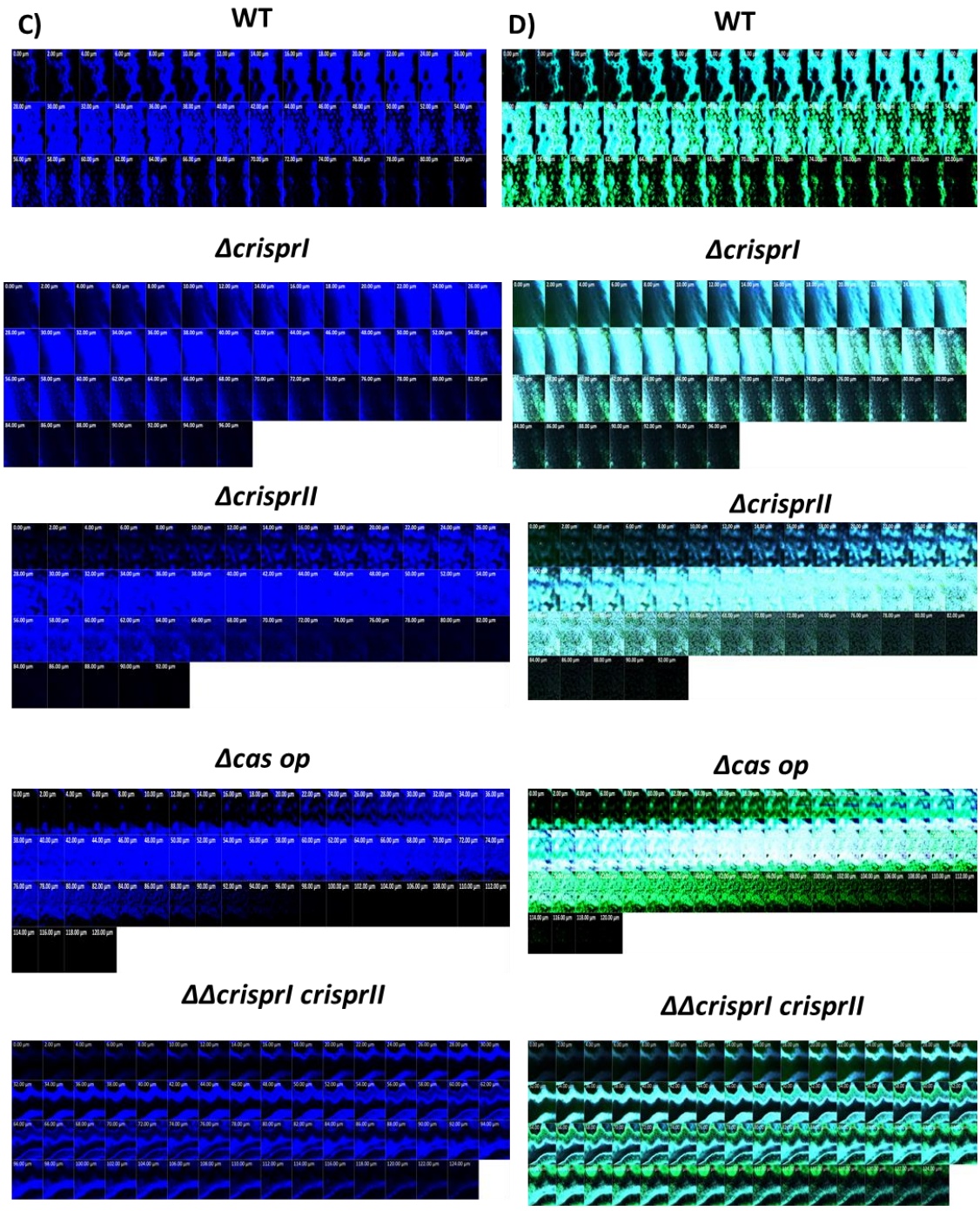

Fig. 2.13: C, D. C. CLSM images (stacks) of wildtype and CRISPR- Cas knockout strains stained with Calcofluor white. D. Represents the merged CLSM stacks for all three components The pellicle biofilm formed by the *S.* Typhimurium strain 14028s wildtype (WT), CRISPR (Δ*crisprI*, Δ*crisprII* and ΔΔ*crisprI crisprII*) and *cas operon (*Δ*cas op*) knockout strains was stained with Calcofluor white and images were captured using CLSM.

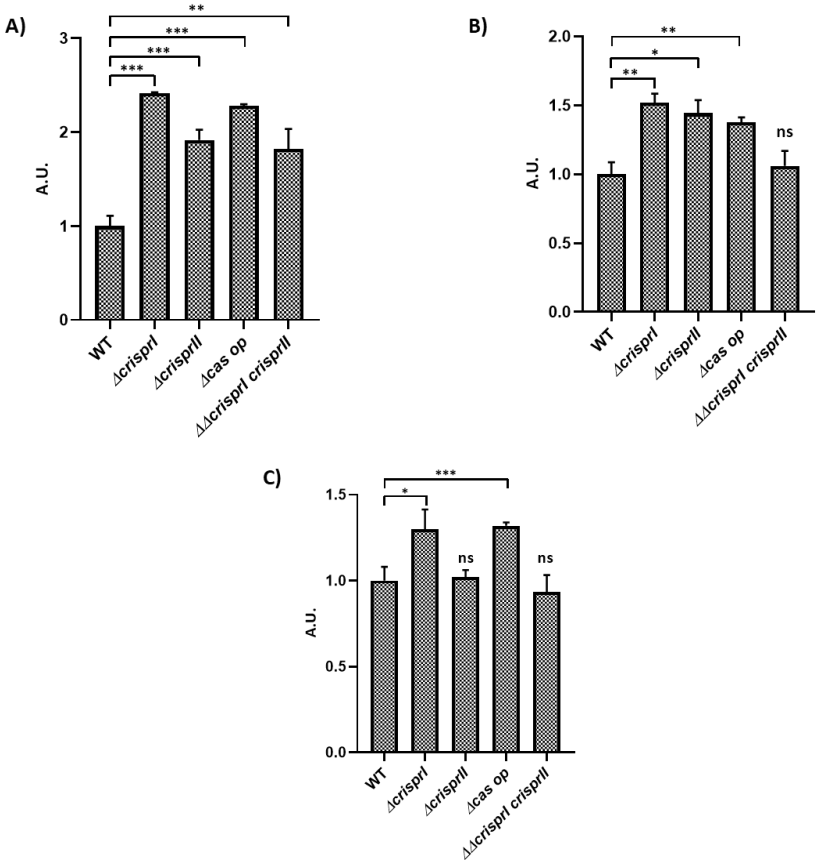

Fig. 2.14: Compared to WT, CRISPR-Cas system knockout strains show differences in ECM components like polysaccharides (A), protein (B), and DNA (C). *S.* Typhimurium strain 14028s wildtype (WT), CRISPR (Δ*crisprI,* Δ*crisprII,* and ΔΔ*crisprI crisprII*), and *cas operon (*Δ*cas op*) knockout strains were cultured in LB without NaCl media for 96 h. **A.** The exopolysaccharides were quantified by the phenol-sulfuric acid method. The graph represents absorbance observed at 490 nm for each strain normalized by absorbance observed at 490 nm for WT. **B and C.** The protein and DNA concentrations in the supernatants of each sample were estimated spectrophotometrically and were further normalized by absorbance for WT in each case. An unpaired t-test was used to determine significant differences between the WT and knockout strains. Error bars indicate SD. Statistical significance: *P≤ 0.05, **P≤ 0.01, ***P≤ 0.001, ****P<0.0001, ns = not significant. A.U., arbitrary units.

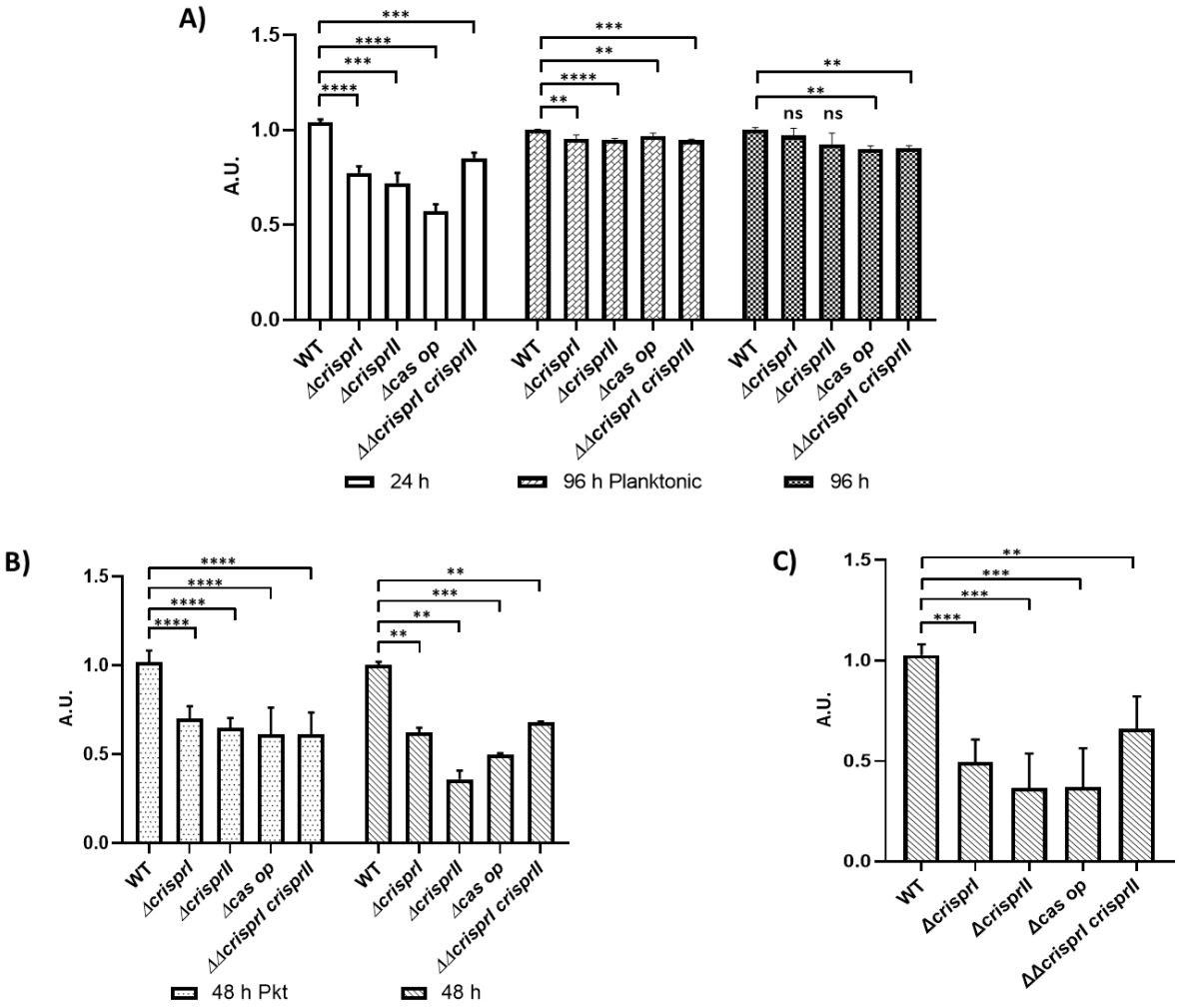

Fig. 2.15: The CRISPR- Cas knockout strains showed variations in the production of Curli. Curli production in the planktonic culture and pellicle biofilms of wildtype, CRISPR, and *cas* operon knockout strains was assessed with the help of Congo red depletion (A-B) and Thioflavin (ThT) Fluorescence intensity (C). The *S.* Typhimurium strain 14028s wildtype (WT), CRISPR (Δ*crisprI*, Δ*crisprII*, and ΔΔ*crisprI crisprII*), and *cas operon* (Δ*cas op*) knockout strains were cultured in LB without NaCl media for different time periods (24 h, 48 h, and 96 h), at 25°C, static condition. **A-B.** Congo red depletion was determined by measuring absorbance at 500nm. The graph represents absorbance at 500nm of each strain, normalized by absorbance at 500 nm of WT. **C.** Thioflavin (ThT) fluorescence intensity was determined by measuring absorbance at excitation 440 nm and emission of 482 nm. Δ*csgD* was used as a negative control. The graph represents the intensity readings of each strain, normalized by intensity readings of WT.

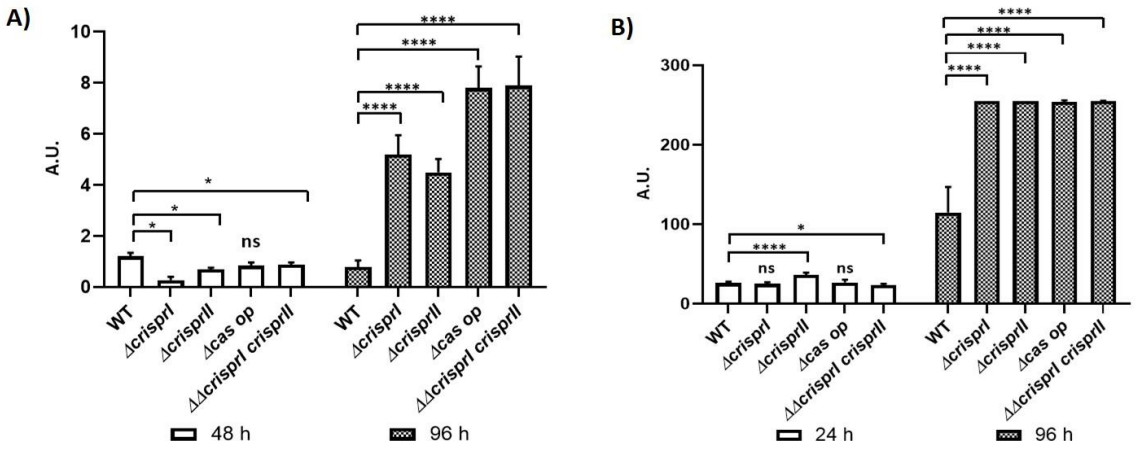

Fig. 2.16: The CRISPR- Cas knockout strains showed variations in the production of cellulose A. Cellulose production in the pellicle biofilms of wildtype, CRISPR (Δ*crisprI,* Δ*crisprII* and ΔΔ*crisprI crisprII*), and *cas operon (*Δ*cas op*) knockout strains was quantitatively assessed by determining the cellulose dry-weight in the pellicle biofilm. **B.** Qualitative analysis of the amount of cellulose present in the biofilm was done by measuring the calcofluor intensity of the CLSM images (represented in Fig. 2.11 A & B). An unpaired t-test was used to determine significant differences between the WT and knockout strains. The error bar indicates SD. Statistical significance: *P≤ 0.05, **P≤ 0.01, ***P≤ 0.001, ****P<0.0001, ns = not significant. A.U., arbitrary units.

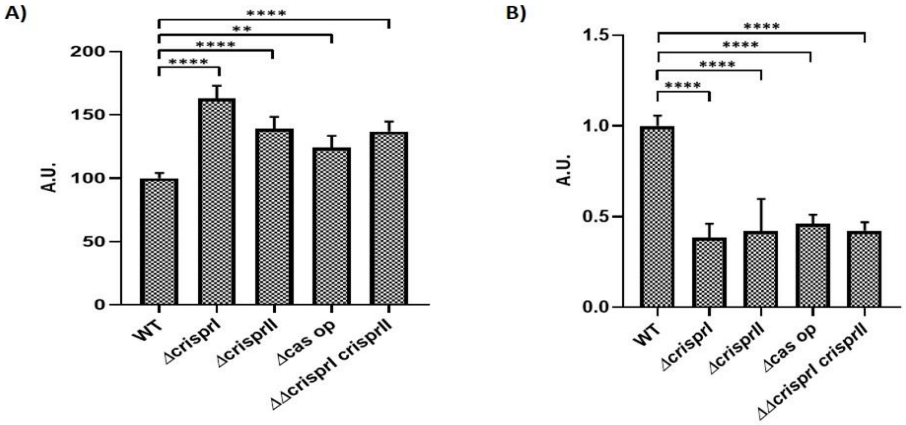

Fig. 2.17: Compared to WT, CRISPR-Cas system knockout strains show differences in their cellulose content in pellicle biofilm. Though thicker than wildtype, pellicle biofilms formed by CRISPR- Cas knockout strains were found to be more delicate. A. The *S.* Typhimurium strain 14028s wildtype (WT), CRISPR (Δ*crisprI,* Δ*crisprII* and ΔΔ*crisprI crisprII*), and *cas operon (*Δ*cas op*) knockout strains were cultured in LB without NaCl media for 96 h. **A.** Qualitative analysis of the amount of cellulose present in the pellicle biofilm was done by measuring the bound calcofluor. **B.** The pellicle biofilm strength was determined by the addition of glass beads (1 mm, HiMedia) using a tweezer until disruption (collapse of pellicle biofilm to the bottom). The glass bead weight tolerated by the pellicle biofilm of each strain was normalized to that of WT. An unpaired t-test was used to determine significant differences between the WT and knockout strains. The error bar indicates SD. Statistical significance: *P≤ 0.05, **P≤ 0.01, ***P≤ 0.001, ****P<0.0001, ns = not significant. A.U., arbitrary units.

2.3.4 The CRISPR-Cas knockout strains show altered expression of biofilm-related genes

To understand the temporal variations in biofilm formation by the CRISPR-Cas knockout strains, we checked the regulation of biofilm-related genes for early (24 h) and late (96 h, pellicle biofilm) time points using RT-PCR.

We assessed the expression of genes governing motility, like *fliC* (phase 1 flagellin subunit), *fljB* (phase 2 flagellin), *flgK* (hook protein), *yddX* (biofilm modulation protein, controlling regulatory pathway of flagellar assembly), and *flgJ* (peptidoglycan-hydrolyzing flagellar protein). All the knockout strains showed reduced expression of these genes (Fig.2.18A) except *flgJ* (Fig.2.18A). Next, to comprehend the observed variations in the LPS profile of the knockout strains (Fig. 2.9), we analyzed the expression of a few representative LPS genes within the *rfa* (LPS core synthesis) and *rfb* (O-antigen synthesis) gene clusters. *rfaC* (lipopolysaccharide heptosyltransferase I) was upregulated at both time points (Fig. 2.18B).

However, *rfbG* (DP-glucose 4,6-dehydratase) was upregulated at 24 h (Fig. 2.18B) and undetected at 96 h, while *rfbI*, coding for the core LPS region was downregulated at both time points in all the knockout strains except for Δ*cas op*. at 24 h (Fig. 2.18B). The *csgA* gene responsible for producing the curli fibers was downregulated at both time points in knockout strains (Fig.2.18C). The expression of *csgA* is controlled by the master regulator *csgD*, which too, had reduced expression in the knockout strains at 24 h and 96 h (Fig. 2.18C). The expression of the *crp* gene coding for cAMP receptor protein, a *csgD* repressor (C. Liu et al., 2020), was high in the knockout strains at 24 h (Fig. 2.18C) and showed no difference at 96 h. *csgD* also controls the expression of cellulose synthesis genes (*bcsABZC*). Notably, the expression of *bcsA* (cellulose synthase catalytic subunit A) was slightly less (1.5-fold) in the knockout strains at 24 h (Fig. 2.18C) and showed no difference at 96 h. *bcsC* (subunit involved in the export of cellulose to the extracellular matrix(Abidi et al., 2022)) was 2-fold upregulated in knockout strains at 24 h (Fig. 2.18C), and at 96 h, the expression was comparable to WT. The observed results hint at *csgD*-independent regulation (da Re & Ghigo, 2006) of *bcsC* in the knockout strains.

2.3.5 The CRISPR-Cas knockout strains export more cellulose in the extracellular milieu

Since the expression of the cellulose exporter gene, *bcsC*, was high in the knockout strains

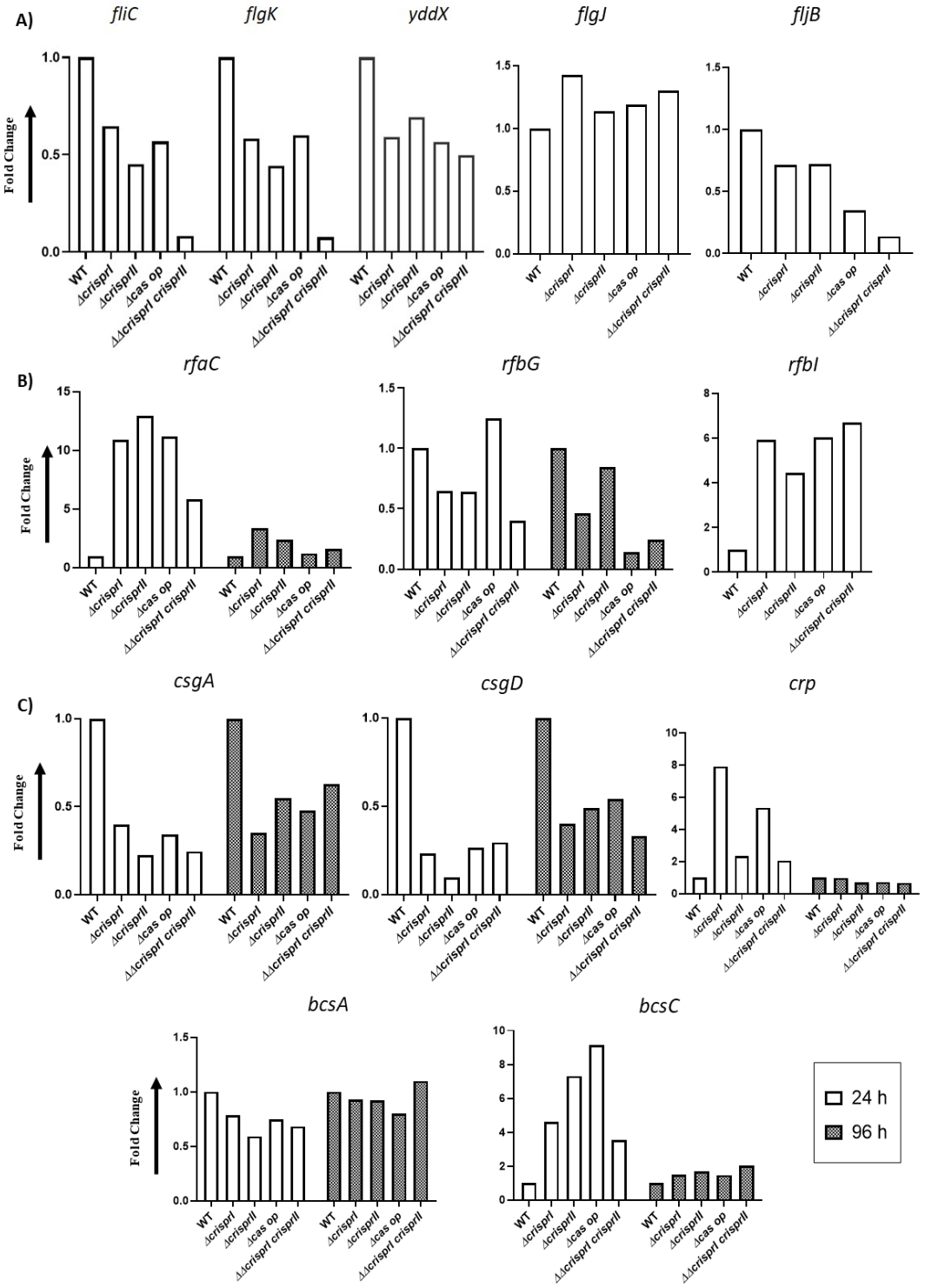

Fig. 2.18: Fif CRISPR-Cas system knockout strains showed differences in the expressions of flagellar genes (A), LPS genes (B), the production of curli-*csgA*&*csgD*, cAMP-regulated protein (*crp*) and cellulose-*bcsA* and *bcsC* (C) when compared to WT. The *S.* Typhimurium strain 14028s wildtype (WT), CRISPR (Δ*crisprI*, Δ*crisprII*, and Δ*crisprI* Δ*crisprII*) and *cas operon (*Δ*cas op*) knockout strains were cultured in LB without NaCl media for different time periods (24 h and 96 h). Relative expression of the gene was calculated using the $2^{-\Delta\Delta Ct}$ method and normalized to reference gene *rpoD.*

at 24 h, we estimated the cellulose production, secretion, and incorporation into the pellicle using anthrone assay (Table 2.4). In accordance with the trend in *bcsA* expression, the total cellulose production was less in the knockout strains at an early time point (24 h), and at the later time points (48 h and 96 h), it became comparable to that of the WT. Intriguingly, at all the time points tested, the intracellular cellulose content was less in the knockout strains than in the WT. In contrast, more cellulose was secreted to the extracellular milieu (culture supernatant). The knockout strains had higher cellulose content in the pellicle biofilm (48 and 96 h) than the WT.

2.4 Discussion

Biofilm formation in *Salmonella* is finely regulated, helping the bacteria to sustain various environmental insults while aiding in their persistence within and outside the host (Steenackers et al., 2012). Recently, the CRISPR-Cas system has been implicated to play a role in endogenous gene regulation (Bozic et al., 2019) and biofilm formation in various bacteria, including *Salmonella* (Cui et al., 2020; Sampson & Weiss, 2014b). Cui et al. demonstrated that Cas3 positively regulates biofilm formation in *S.* Enteritidis (Cui et al., 2020). However, our study determined that the Cas proteins negatively regulate biofilm formation in *S.* Typhimurium. This discrepancy in the results could be related to the differences in CRISPR spacers within these serovars (Kushwaha et al., 2020) or differences in *cas* gene expression observed in both studies. The *cas* genes were upregulated in the *cas3* mutant strain of serovar Enteritidis. This implies that the increased expression of Cas proteins (except Cas3) could have suppressed biofilm in serovar Enteritidis, while in our study, the entire operon was deleted; thereby, there was no *cas* gene expression and, hence, enhanced biofilm formation. Furthermore, our study also demonstrated that CRISPR-I and CRISPR-II arrays negatively regulated pellicle biofilm formation in *S.* Typhimurium. Correspondingly, a study by Medina et al. suggests that the CRISPR-Cas system suppresses the surface biofilm formation (at 24 h) in *S.* Typhi (Medina-Aparicio et al., 2021). Intriguingly, we found that the CRISPR-Cas system of *S.* Typhimurium positively regulates surface biofilm while repressing pellicle biofilm. We speculate that the difference in our data on surface biofilm and that of Medina et al. could be because serovars Typhi and Typhimurium differ in the arrangement and sequence of *cas* genes, as well as in the CRISPR-I array (Cui et al., 2020; Medina-Aparicio et al., 2021). Could the differential evolution of the CRISPR-Cas system possibly be the reason for the two serovars' distinct biofilm phenotypes? Or could it be due to differences in the CRISPR spacers? These

deductions need further exploration.

We next explored the underlying mechanisms of biofilm regulation by the CRISPR-Cas system. Biofilm formation is a complex mechanism requiring coordination between multiple factors and processes. Flagellar motility is essential for cell-cell adhesion and the formation of microcolonies at the initial stages (F. Wang et al., 2020). Our study showed that the CRISPR-Cas knockout strains are less motile, thereby explaining less surface-attached biofilm formation at 24 h by CRISPR-Cas knockout strains. The observations were further validated by the CLSM data of SYTO9 intensity of surface-attached biofilm. Nevertheless, as the biofilm progresses, the requirement of flagella becomes negligible, and its expression is repressed (Hung et al., 2013). In accordance, we found that FliC expression was absent in pellicle biofilms of all the strains at 96 h. The FliC subunit is also crucial for cholesterol binding and biofilm development on gallstones (Crawford, Reeve, et al., 2010; Prouty & Gunn, 2003). The decreased biofilm formation by the CRISPR-Cas knockout strains in tube biofilm assay could be attributed to decreased FliC expression. The reduction in FliC expression is also reflected in the reduced swarming motility of the knockout strains, but it is not proportionate to the observed trend in FliC expression. For example, despite showing minimal FliC expression among all knockout strains, ΔΔ*csprI csprII* had considerable swarming motility. This disparity could be due to variations in the production of LPS and exopolysaccharides. LPS acts as a wettability factor, favoring swarming while inhibiting biofilm formation (Mireles 2nd et al., 2001). Interestingly, our study displayed such a relation; all the knockout strains showed reduced swarming but enhanced biofilm formation. Exopolysaccharides, including O-antigen (W. Kim & Surette, 2005), and cellulose(Costa et al., 2017), function as antidesiccants for the swarmer cells. Together with LPS, these polysaccharides provide a hydration shell around the bacteria, promoting flagellar rotation during swarming (W. Kim & Surette, 2005). Thus, the disparity in the correlation between the FliC expression and swarming motility could possibly be attributed to the differences in the LPS profile and secretion of exopolysaccharides by the knockout and WT strains.

The CRISPR-Cas knockout strains had altered the LPS profile with a difference in the LPS gene expression. The *rfaC* (part of *rfa* gene cluster, responsible for LPS core synthesis) and *rfbG* (part of *rfb* gene cluster, responsible for O-antigen synthesis) genes were upregulated in the knockout strains (24 h). At the same time, *rfbI* was significantly downregulated only in ΔΔ*csprI csprII*. Also, studies suggest the plausible conversion

of LPS to exopolysaccharides that contribute to external slime (Toguchi et al., 2000). The increased exopolysaccharides in the pellicle of CRISPR-Cas knockout strains may also be attributed to this, along with the observed increase in cellulose production.

Table 2.4: Cellulose production and secretion as estimated by anthrone assay

24 h	**WT**	**Δ*crisprI***	**Δ*crisprII***	**Δ*cas op***	**ΔΔ*crisprI crisprII***
Bacterial Pellet	0.210 ± 0.049	0.044 ± 0.004***	0.064 ± 0.009**	0.094 ± 0.007**	0.042 ± 0.010***
Culture Supernatant	0.109 ± 0.015	0.075 ± 0.012**	0.063 ± 0.012***	0.048 ± 0.013***	0.067 ± 0.007***
Pellicle Biofilm	N/A	N/A	N/A	N/A	N/A
Total Cellulose[#]	0.324 ± 0.057	0.119 ± 0.010***	0.127 ± 0.004***	0.143 ± 0.012***	0.109 ± 0.012***
% Secretion in Planktonic	35.26	63.40	49.73	33.86	61.43

48 h	**WT**	**Δ*crisprI***	**Δ*crisprII***	**Δ*cas op***	**ΔΔ*crisprI crisprII***
Bacterial Pellet	0.173 ± 0.012	0.040 ± 0.007****	0.075 ± 0.007****	0.090 ± 0.007****	0.070 ± 0.009****
Culture Supernatant	0.539 ± 0.051	0.674 ± 0.030***	0.584 ± 0.108*	0.603 ± 0.0701*	0.59 ± 0.073^{ns}
Pellicle Biofilm	0.060 ± 0.004	0.16 ± 0.045****	0.173 ± 0.059****	0.129 ± 0.032**	0.119 ± 0.010****
Total Cellulose[ff]	0.753 ± 0.084	0.874 ± 0.022*	0.832 ± 0.055^{ns}	0.822 ± 0.093^{ns}	0.779 ± 0.070^{ns}
% Secretion in Planktonic	77.71	94.43	88.58	86.95	89.32

96 h	**WT**	**Δ*crisprI***	**Δ*crisprII***	**Δ*cas op***	**ΔΔ*crisprI crisprII***
Bacterial Pellet	0.301 ± 0.038	0.187 ± 0.014**	0.133 ± 0.044**	0.224 ± 0.042*	0.208 ± 0.039*
Culture Supernatant	0.141 ± 0.024	0.126 ± 0.031^{ns}	0.168 ± 0.034^{ns}	0.154 ± 0.034^{ns}	0.140 ± 0.042^{ns}
Pellicle Biofilm	0.145 ± 0.020	0.267 ± 0.040**	0.287 ± 0.071***	0.209 ± 0.011**	0.218 ± 0.045**
Total Cellulose	0.586 ± 0.043	0.580 ± 0.073^{ns}	0.587 ± 0.066^{ns}	0.587 ± 0.033^{ns}	0.565 ± 0.049^{ns}
% Secretion in Planktonic	31.68	40.23	55.82	40.74	40.14

The values represent mean±SD. Statistical significance: *P≤ 0.05, **P≤ 0.01, ***P≤ 0.001, ****P<0.0001, ns = not significant.

[#] The total cellulose corresponds to the sum of absorbance for planktonic bacteria (pellet) and culture supernatant

[ff] The total cellulose corresponds to the sum of recorded absorbance for planktonic bacteria (pellet), culture supernatant, and pellicle biofilm.

The percentage secretion of cellulose was calculated a $\frac{[Planktonic\ Supernatant]_{train}}{[Planktonic\ Supernatant+Bacterial\ pellet]_{strain}} \times 100$

The pellicles formed by the CRISPR-Cas knockout strains are thicker (owing to more bacterial mass and EPS secretion (F. Wang et al., 2020)) than the pellicle formed by

the WT, confirming the formation of multi-layered pellicle biofilms, as evidenced by SEM and CLSM analysis. As per SEM analysis, the air-exposed pellicle biofilm architecture of Δ*crisprII* and ΔΔ*crisprI crisprII* appears similar, indicating that *crisprII* could act upstream of *crisprI*. This observation is seconded by our LPS profiling data, where the banding patterns of Δ*crisprII* and ΔΔ*crisprI crisprII* are similar.

The EPS-overproducing variants reportedly have rough and wrinkled biofilm (Limoli et al., 2015). This supports our observation that the CRISPR-Cas knockout strains overproduce EPS and display intricate wrinkled patterns in the pellicle biofilm. These wrinkled patterns appeared fractal-like (Fig. 2.4C bottom), as reported for *Vibrio cholera* (Qin et al., 2021). Such morphology could aid bacterial growth of the CRISPR-Cas knockout strains due to the increased surface area that presumably facilitates the nutrient supply (Qin et al., 2021). Consistently, the bacterial mass was higher in the knockout strains with more viable bacteria, as evidenced by the resazurin assay and SYTO9-PI staining. The ECM scaffold of pellicle biofilm majorly comprises cellulose and curli that define the long-range and short-range interactions, respectively, thereby providing mechanical integrity (White et al., 2006). The pellicle biofilms of CRISPR-Cas knockout strains have higher cellulose but less curli content. This could probably be the reason for the weaker pellicle biofilm of the CRISPR-Cas knockout strains that quickly collapsed in the glass bead assay. Further, high cellulose in the pellicles of the CRISPR-Cas knockout strains means high water retention that can hamper intermolecular forces in the matrix by decreasing the hydrogen bond interactions. Additionally, less curli could lead to the low tensile strength of the pellicle biofilm of the CRISPR-Cas knockout strains. Higher cellulose and less curli could also explain reduced surface biofilm (ring biofilm at 24 h and 96 h) in the CRISPR-Cas knockout strains. High cellulose may inhibit the formation of surface biofilm, as it can coat the curli fibers required for surface attachment (Gualdi et al., 2008). Though the cellulose content was high in pellicle biofilms of the CRISPR-Cas knockout strains, the expression of cellulose synthase, *bcsA*, was 1.5-fold lower in all the knockout strains at 24 h, whereas it was unaltered at 96 h. This corroborates with less cellulose production by the knockout strains at 24 h, which, with time, becomes comparable to that of the WT. However, the intracellular cellulose content in the CRISPR-Cas knockout strains was less than that of the WT, and the percentage secretion of cellulose was higher in the knockout strains for all the tested time points. This could be explained through the upregulated *bcsC* (at 24 h), encoding an exporter of cellulose subunits that could export cellulose units to the

```
Alignment of
Sequence_1:  [bcsC-reverse complement] with  Sequence_2: [CRISPR1 array-spacer11]

Similarity : 14/3543 (0.40 %)

Seq_1  1     ttaccagtcagcgtaaggcaccagaggctgcggcggtaaatccatatccccctgccagcc  60
Seq_2  1     ------------------------------------------------------------  0

-------------------------------------------------------------------------

Seq_1  1321  ggcggcgtcacgcaataccatcggcgctttccattgatggcggctgtgcttttgcctgcgg  1380
                                  |||||||||||  |   |     |
Seq_2  1     ---------------ATATTCGCCGCTTTCCATTTACCGAACGTAAC-------------  32

-------------------------------------------------------------------------

Seq_1  3481  taaggcgtttcgaccgccagccggcaaaaaagcgtgcatgagacttaacgtgaacttacg  3540
Seq_2  33    ------------------------------------------------------------  32

Seq_1  3541  cat  3543
Seq_2  33    ---  32

Alignment of
Sequence_1:  [bcsC] with  Sequence_2: [CRISPR1 array-spacer15]

Similarity : 21/3543 (0.59 %)

Seq_1  1     atgcgtaagttcacgttaagtctcatgcacgctttttgccggctggcggtcgaaacgcc  60
Seq_2  1     ------------------------------------------------------------  0

-------------------------------------------------------------------------

Seq_1  1321  aataccaatgctgtacgcgggctggcgaatctttatcgccagcagtcgccgcaaaaagcc  1380
                                                 |||  ||  ||||  |||  ||
Seq_2  1     ------------------------------------AGCCGTTTCCGCTAAATACC  20

Seq_1  1381  gccgcgtttatcgcttctctttccgccagccagcggcgcagtatcgacgatatcgaacgc  1440
               ||||   | ||
Seq_2  21    CCCGCAGTGATT-------------------------------------------------  32

Seq_1  3481  gcgggctggcaggggatatggatttaccgccgcagcctctggtgccttacgctgactgg  3540
Seq_2  33    ------------------------------------------------------------  32

Seq_1  3541  taa  3543
Seq_2  33    ---  32


Alignment of
Sequence_1:  [bcsC-reverse complement] with  Sequence_2: [CRISPR1 array-spacer15]

Similarity : 19/3543 (0.54 %)

Seq_1  1     ttaccagtcagcgtaaggcaccagaggctgcggcggtaaatccatatccccctgccagcc  60
Seq_2  1     ------------------------------------------------------------  0

-------------------------------------------------------------------------

Seq_1  661   tttggtgccggtattgctgctggcatccttttgcccgccaaacgccagcagcgagctgga  720
                                     | ||  |||  | |    | ||  ||  ||||  ||
Seq_2  1     ----------------------AGCCGTTTCCGCTAAATACCCCCGCAGTGATT----  32

-------------------------------------------------------------------------
Seq_1  3481  taaggcgtttcgaccgccagccggcaaaaaagcgtgcatgagacttaacgtgaacttacg  3540
Seq_2  33    ------------------------------------------------------------  32

Seq_1  3541  cat  3543
Seq_2  33    ---  32
```

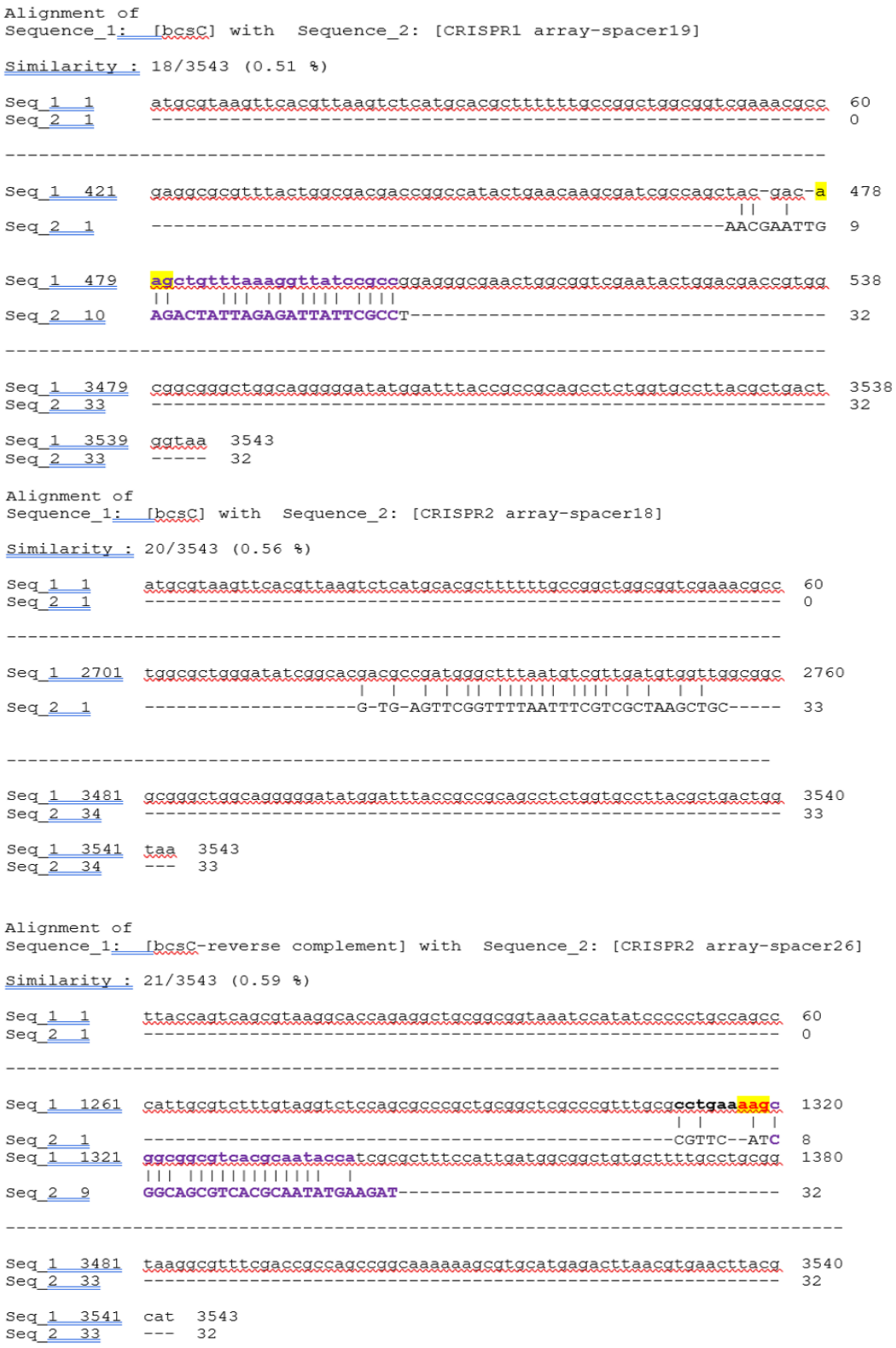

Fig. 2.19: Partial complementarity between spacers (spacer 11, 15 and 19 in CRISPRI array and 18 and 26 in CRISPRII array) and *bcsC* gene. The coding and the reverse complement (template) sequence of the *bcsC* gene were extracted from a complete-genome sequence of Typhimurium str. 14028s, NCBI (GenBank: CP001363.1). The spacer sequences of CRISPRI and CRISPRII arrays were then aligned with coding and reverse complement of *bcsC* gene using serial cloner version 2.6 software. The putative PAM sequences are highlighted in yellow.

extracellular mileu (Whitney & Howell, 2013). We hypothesized that this secreted cellulose (Acheson et al., 2019; Zimmer, 2019) is quickly incorporated into the pellicle, increasing cellulose content in the pellicles of the knockout strains.

Apart from reduced expression of *csgA* and marginal repression of *bcsA*, we found that *csgD*, the activator of *csgBAC* and *bcsABZC*, was also downregulated in the knockout strains. In order to gain mechanistic insight into the CRISPR-Cas-mediated biofilm regulation, we checked the expression of the further upstream regulator, CRP. CRP negatively regulates *csgD* in *S*. Typhimurium (Paytubi et al., 2017). The expression of *crp* was significantly upregulated in the knockout strains at an early time point (24 h), explaining the repression of *csgA* and *bcsA*. The conflicting upregulation of *bcsC*, the last gene of *bcsABZC*, could be through the crRNA binding to the *bcsC* gene. The CRISPR spacers (spacers 11, 15, and 19 of the CRISPR-I array and spacers 18 and 26 of the CRISPR-II array) show partial complementarity (43.75% to 65.6%) to the *bcsC* gene (Fig. 2.19) and, hence, could regulate the expression of *bcsC*. Such a kind of regulation is reported in *Pseudomonas aeruginosa*, where spacer 12 of the CRISPR-I array has partial complementarity to the *lasR* gene, and the *lasR* gene is regulated by the CRISPR array (Wiedenheft & Bondy-Denomy, 2017). CRP also activates *flhDC*, a flagellar master operon(Soutourina et al., 1999) that further activates the expression of class 2 genes, including *fliA*. The *fliA* gene encodes the flagellar-specific transcription factor σ^{28}, which directs the expression of class 3 genes like *fliC* and *flgK*. Before the assembly of the hook-basal body structure, it is held inactive by the anti- σ^{28} factor, *flgM* (Frye et al., 2006). YddX, a biofilm-dependent modulation protein (BDM) homolog, interacts with FlgM to repress its function as an anti-σ^{28}factor (J. Lee et al., 2017). Our study observed a significant downregulation of *yddX* in the knockout strains. Low YddX would mean that FlgM would sequester σ^{28}, inhibiting the transcription and expression of class 3 genes, including *fliC* and flgK. This explains the impaired motility of the CRISPR-Cas knockout strain. In a nutshell, the CRISPR-Cas system facilitates surface-attached biofilm formation while repressing the pellicle biofilms by acting on different biofilm regulators. The mechanism is summarized in Fig 2.20.

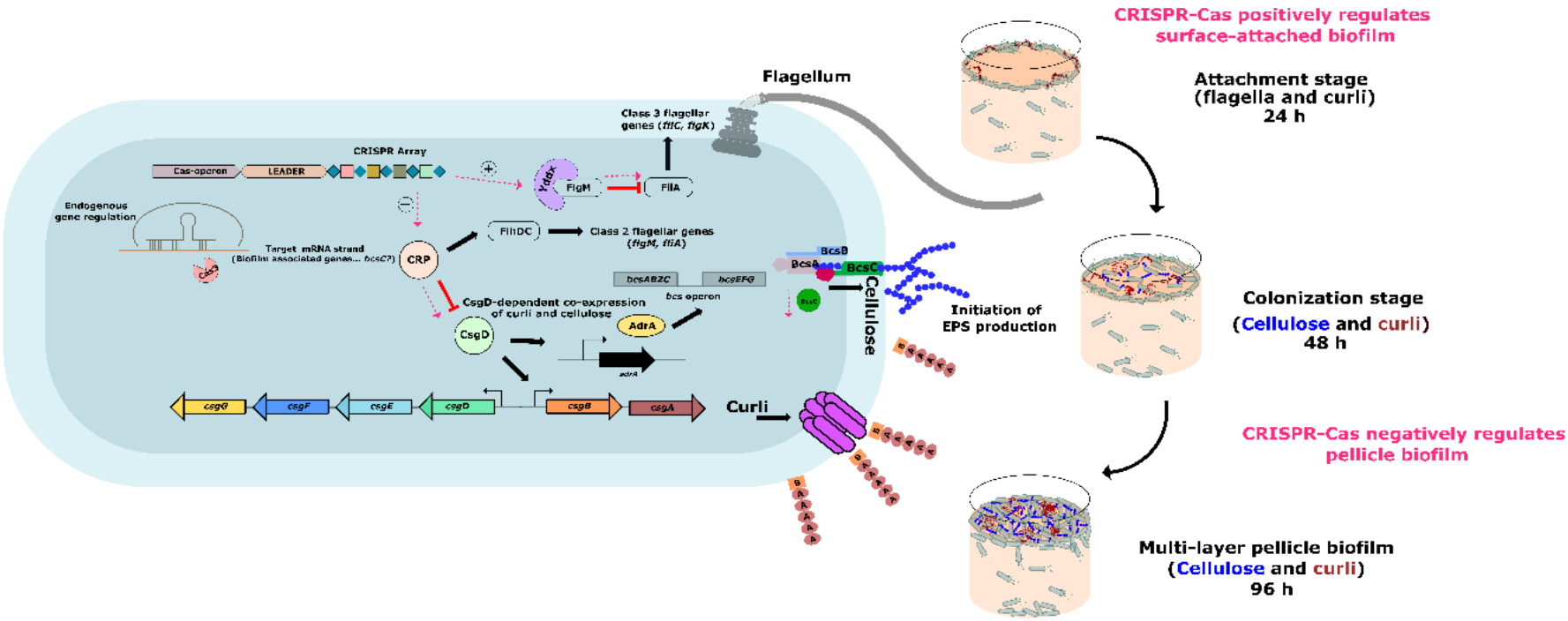

Fig. 2.20: Differential regulation of surface-attached and pellicle-biofilm formation in *Salmonella* Typhimurium by the CRISPR-Cas system. The CRISPR-Cas system differentially regulates surface-attached and pellicle-biofilm formation via modulation (pink dotted lines) of biofilm-associated genes (*crp, yddx, and bcsC*). CRP acts on FlhDC, which further governs the expression of class 2 flagellar genes (*flgM* and *fliA*). FlgM inhibits FliA-mediated expression of class 3 flagellar genes. Yddx relieves the inhibition of FliA by binding to FlgM, thereby inactivating it. We propose that CRISPR-Cas positively regulates *yddx*, whereby it sequesters FlgM and upregulates the expression of the flagellar subunit. CRP also inhibits CsgD, which in turn governs the production of Curli and cellulose. Our study suggests that the CRISPR-Cas system mediates the expression of CsgDby suppressing *crp* expression and independently represses the expression of cellulose exporter, BcsC. Taken together, the CRISPR-Cas system enhances flagella and Curli production and hence surface-attached biofilm formation. Additionally, it suppresses cellulose export to the extracellular milieu, thus negatively regulating pellicle biofilm formation.The figure was created using inkscape.

Chapter 3

The CRISPR-Cas system of *Salmonella enterica* serovar Typhimurium modulates its membrane properties

3.1 Introduction

Maintaining membrane architecture is an important prerequisite for the survival of bacterial cells, especially for Gram-negative bacteria (G. Zhang et al., 2013). The bacterial outer membrane (OM) shields the bacteria against a myriad of toxic compounds like antibiotics, bile salts, antimicrobial drugs, etc. (Delcour, 2009). Any change in the OM integrity increases bacterial sensitivity to such toxic compounds. A thorough understanding of the factors affecting this integrity may help improve antibacterial drug design(Halder et al., 2015). The OM in Gram-negative bacteria is an asymmetric bilayer composed of an inner leaflet of phospholipids and an outer leaflet of outer membrane proteins (OMPs) and lipopolysaccharide (LPS) (Silhavy et al., 2010). Specific interaction between the LPS and OMPs is essential for maintaining OM permeability, thereby maintaining outer membrane integrity and protecting against antimicrobial drugs (Delcour, 2009). LPS consists of lipid A linked to O-antigen by a conserved core oligosaccharide unit (Core-OS) (Silhavy et al., 2010). This oligosaccharide unit also affects cell surface hydrophobicity, adhesion, auto-aggregation, and biofilm formation (Z. Wang et al., 2015). The Core-OS of *Pseudomonas aeruginosa* and *Salmonella* determines bacterial susceptibility to aminoglycosides and antimicrobial peptides, respectively (Martynowycz et al., 2019; Poole, 2005). In *Escherichia coli,* defects in the outer core reduced tolerance towards erythromycin and novobiocin (Z. Wang et al., 2015). Alteration in LPS structure affects cell membrane permeability, swarming motility, biofilm formation, tolerance against heavy metals, cationic peptides, and antimicrobial drugs, as well as the expression of OMPs (Z. Wang et al., 2015).OMPs are composed of lipoproteins and β-barrel proteins, namely porins(K. H. Kim et al., 2012). They play multifarious roles in processes including biofilm formation, adhesion, invasion, phagocytosis, biogenesis of outer membrane, etc. (Horne et al., 2020). Alteration of OMPs confers cross-resistance to β-lactam antibiotics and, in conjunction with modified LPS, it causes invasion defects in the *Salmonella enterica* subspecies *enterica* serovarParatyphi (Gutmann et al., 1988). Moreover, LPS and OMPs also confer resistance to complement-mediated killing in *Salmonella* (Futoma-Kołoch et al., 2015; Krzyżewska-Dudek et al., 2022).

Among the OMPs, porins are the most abundant (A. Sharma et al., 2022). These channel proteins facilitate antibiotic diffusion, thereby contributing to drug resistance. For example, the Δ*ompA* mutants of *Acinetobacter baumannii* showed reduced antibiotic tolerance (Sugawara & Nikaido, 2012). In *E. coli,* OmpA and OmpF maintain membrane

structure and antibiotic transport, respectively, while OmpC is known to assist both functions (U. Choi & Lee, 2019). OmpA and PagC aid the intracellular survival of *Yersinia pestis* in macrophages (Bartra et al., 2012). OmpA and OmpX in *E.coli* (Weiser & Gotschlich, 1991), while PagC and Rck in *Salmonella* (Koczerka et al., 2021b) provide resistance against serum. Furthermore, OmpA and OmpX in *Cronobacter* (K. Kim et al., 2010), Ail in *Y. pestis*(Busch et al., 2008), and NspA in *Neisseria meningitides* (Lewis et al., 2010) are reported to assist in bacterial invasion and the establishment of infection inside the host. Several studies have also reported that porin expression is regulated by factors like oxidative stress, temperature, salinity, and nutritional switches that alter membrane properties.

The role of the CRISPR-Cas system has been implicated in enhancing bacterial envelope (outer membrane) integrity and resistance against antibiotics (Sampson et al., 2013). In *Francisella novicida, the* type II CRISPR-Cas system regulates BLP, an OMP, thereby controlling the integrity of the cell envelope. The partial complementarity of small, CRISPR/Cas-associated (Sca) RNA to mRNA transcript of BLP causes degradation of the transcript. The CRISPR-Cas mediated regulation of OMPs has also been reported in *Salmonella enterica* subspecies *enterica* serovar Typhi (*S.* Typhi) (Medina-Aparicio et al., 2021). The system positively regulates the porin response regulator, *ompR,* which in turn induces the expression of *ompA, ompF,* and *ompS2.* Moreover, the CRISPR and *cas* mutants showed increased biofilm formation in *S.* Typhi, suggesting other physiological roles of the CRISPR-Cas system. Additionally, the role of the CRISPR-Cas system has been implicated in governing responses against oxidative stress. For example, the deletion of *cas* show increased susceptibility to stress induced by hydrogen peroxide(H_2O_2), Sodium dodecyl sulfate (SDS), or temperature in *Streptococcus mutans* (Gong et al., 2020). Furthermore, the microarray data showed an increased expression of the CRISPR-1 array and decreased expression of CRISPR-2 in *cdaA* mutants of *S. mutans*, leading to increased sensitivity to H_2O_2 and exopolymeric substances (EPS) production(X. Cheng et al., 2016).

In the previous chapter, we demonstrated that the deletion of the CRISPR-Cas system impairs surface-attached biofilm formation in the *Salmonella enterica* subspecies *enterica* serovarTyphimurium (*S.* Typhimurium). This was attributed to altered LPS profile, motility, more secretion of polysaccharides, etc. by the knockout strains. In the context of the above-mentioned studies, we decided to assess the H_2O_2 tolerance and membrane properties of the CRISPR-Cas knockout strains of *S.* Typhimurium. We have

attempted to establish the role of the CRISPR-Cas system in maintaining membrane integrity through the regulation of two important outer membrane components, OMP and LPS.

3.2 Material and methods

3.2.1 Bacterial strains and growth conditions

S. Typhimurium str. 14028s was used as a parent strain (wildtype). The wildtype, CRISPR (Δ*crisprI, ΔcrisprII, and ΔΔcrisprI crisprII*), and *cas operon* (Δ*cas op*) knockout strains and their corresponding complement strains (Δ*crisprI*+p*crisprI* and Δ*crisprII*+p*crisprII*) were grown in Luria Bertani (LB) broth (Himedia) at 37°C in a shaking incubator with 150 revolutions per minute (rpm). Whenever required, the media was supplemented with appropriate antibiotics (Table 3.1).

Table 3.1 List of bacterial strains and plasmids used in this study

Bacterial Strain	Genotype and Characteristics	Source
Salmonella enterica serovar Typhimurium 14028s	WT 14028s	A kind gift from Prof. Dipshikha Chakravortty, IISC, Bangalore India
Δ*crisprI*	WT 14028s Δ*crisprI*:: Chl (Chl^r)	This study
Δ*crisprII*	WT 14028s Δ*crisprII*:: Chl (Chl^r)	This study
Δ*cas op*	WT 14028s Δ*cas* operon:: Chl (Chl^r)	This study
ΔΔ*crisprI crisprII*	WT 14028s Δ*crisprI*:: Kan :Δ*crisprI*::Chl (Kan^r, Chl^r)	This study
Δ*crisprI* +p*crisprI*	Δ*crisprI* complemented with functional CRISPR I array cloned in pQE60	This study
Δ*crisprII* +p*crisprII*	Δ*crisprII* complemented with functional CRISPR II array cloned in pQE60	This study

3.2.2 Bacterial sensitivity to hydrogen peroxide

Bacterial strains were grown overnight in LB media and washed with PBS. Equal amounts (10^7) of bacteria were subcultured in F-media (5mM KCl, 7.5 mM NH_4SO_4, 0.5 mM K_2SO_4, 10mM MES buffer, 0.27% glycerol, 0.1% Casein Acid hydrolysate and 10 µM $MgCl_2$), pH-5.4. The bacteria were incubated with 0 mM, 0.2 mM, 1 mM, 2 mM, and 4 mM of hydrogen peroxide (H_2O_2) at 37°C in the dark at 100 rpm. After 8 h, the bacterial

growth was determined by measuring the optical density (OD) at 600 nm using Multiskan GO (Thermo Scientific, USA). Alternatively, overnight grown bacterial cultures of wildtype, Δ*crisprI*, Δ*crisprII*, Δ*cas op*, ΔΔ*crisprI crisprII*, Δ*crisprI*+p*crisprI*, and Δ*crisprII*+p*crisprII* strains were treated with 1 mM H_2O_2 in Muller Hinton (MH, Himedia, pH- 5.4) media for 2 h. The bacterial suspensions were plated onto LB-agar plates containing appropriate antibiotics to determine Colony Forming Units (CFU). The percentage survival was calculated using the following formula:

$$\% \text{ Survival} = \frac{CFU\ of H_2O_2\ treated\ samples}{CFU\ of\ untreated\ samples} \times 100$$

3.2.3 Priming assay with Hydrogen peroxide

The overnight bacterial cultures were subcultured in MH Media and grown to $OD_{600nm} \sim 0.4$. Following incubation for 30 min with 0.1 mM H_2O_2 (priming) in dark at 37˚C with shaking. The H_2O_2 was removed by centrifugation at 5000 x g for 10 min and cells were allowed to recover for 2 h. Equal amounts (10^7) of bacteria were subcultured in MH media The bacteria were incubated with 0 mM and 1 mM (trigger), of H_2O_2 at 37°C in the dark at 100 rpm. After 8 h, the bacterial growth was determined by measuring the OD_{600nm} using Multiskan GO (Thermo Scientific, USA).

3.2.4 Bioinformatic analysis of gene target prediction

RNA can exist as a double-stranded structure due to intramolecular bonding between complementary bases inside a single strand of RNA. Thus, for a crRNA to bind to the target RNA both the target RNA and the crRNA must be single-stranded and complementary. To calculate the binding efficiency of the crRNA to its target we considered two parameters: Site Accessibility (SA)(Busch et al., 2008)and Minimum Free Energy (MFE). SA calculates the amount of energy (KCal/mol) required to convert a stretch of RNA into a single-stranded structure. While MFE is the energy released when the two single-stranded RNA form a stable dimer. The net free energy of the reaction to be stable should be negative. We assume that the CRISPR-RNA (crRNA) produced from the CRISPR array upon transcription is single-stranded due to its short length. We calculate Extended Minimum Free Energy (EMFE) to analyze if the RNA dimer formed is energetically favorable. A stable structure should have a negative EMFE.

$$EMFE = MFE_n + SA$$

SA is the difference in energy of the ensemble of all structures and the structure where the target stretch is single-stranded. The low value of SA signifies that a small amount of energy is required to make the target RNA single-stranded, and hence, RNA targets with low SA would favor the required interaction between the two RNAs. To calculate SA, the binding site of the spacer (crRNA) on the RNA was identified through local alignment of the respective spacer sequence with the *S.* Typhimurium. The top-scoring alignments (with no mismatch, but gaps allowed) were used to get the positions where the spacer is attached to the transcribed mRNA. The SA was calculated using the formula: $SA = -RT\ ln\ (Pr)$, where *Pr* is the probability that a stretch is single-stranded (Lorenz et al., 2011). The value of *Pr* is found by using RNA fold (Lorenz et al., 2011), a Unix command line tool in which the '-u′ option allows to find the probability that a consecutive set of nucleotides of length 'u′ is single-stranded. The value of parameter '-u′ was the maximum length of local alignment between a spacer and transcribed mRNA.

MFE is defined to be the minimum amount of free energy a stable RNA structure can release. Free Energy (also called Gibbs Free Energy) is the energy released when an unfolded RNA is folded into a secondary structure. MFE was calculated using an online web server, RNAcofold, that predicts the secondary structure of two single-stranded RNA upon dimerization and also generates the MFE of the most stable structure. As MFE increases linearly with the sequence length, to allow comparison, we normalized the MFE as, $MFE_n = \frac{MFE}{log(mn)}$, where m, n is the length of the spacer RNA and the target mRNA, respectively (Rehmsmeier et al., 2004). We align crRNA with RNA sequences of all the identified genes in *S.* Typhimurium to get a preliminary list of target genes. We then find out the EMFE of *ompW*mRNA. We then remove dimer interactions where EMFE is positive from the potential dimers.

3.2.5 Quantitative real-time (q-RT) PCR analysis

Bacterial strains were grown overnight and subcultured in F-media with and without 1 mM H_2O_2 for 8 h in dark at 37°C with constant shaking. Total RNA was isolated from bacteria using TRIzol reagent (Himedia) as per the manufacturer′s instructions. 2 µg of RNA was used for cDNA synthesis using the iScript™ cDNA synthesis kit (Biorad). qRT-PCR was performed using PowerUp™ SYBR™ Green Master Mix (Thermo Fisher Scientific). Relative expression of the gene was calculated using the $2^{-\Delta\Delta Ct}$ method by normalizing to reference gene *rpoD*. The primers used in RT-qPCR are listed in Table 3.2.

Table 3.2: List of Primers used in this study

Sl. No.	Primer Name	Nucleotide Sequence
1	*rpoD* (Forward)	5′ACATGGGTATTCAGGTAATGGAAGA3′
2	*rpoD* (Reverse)	5′CGGTGCTGGTGGTATTTTA3′
3	*ompW*(Forward)	5′CGGGTTTGATGTGAGTAATAAC3′
4	*ompW*(Reverse)	5′GAAGTACCACTGCGCCATT3′

3.2.6 *In vitro* determination of hydrogen peroxide influx

In vitro diffusion of H_2O_2 into the bacterial strains was assessed as described previously (Calderón et al., 2011). Overnight cultures were diluted and cells were grown to $OD_{600nm} \sim 0.5$ in F-media, following incubation for 5 min with 1 mM H_2O_2 in dark. The bacterial cultures were centrifuged for 5 min at 4500 x *g*. The supernatant was collected and filtered using 0.2 µm filters (Millipore). Both the extracellular (supernatant) and intracellular (bacterial pellet) fractions were incubated separately with 5 µM of 2′,7′-dichlorodihydrofluorescein diacetate (H_2DCFDA, Sigma). The fluorescence intensity was measured at (λ_{ex}) of 485 nm and (λ_{em}) at 535 nm using Fluoroskan (Thermo scientific).

3.2.7 Measurement of membrane damage by crystal violet uptake assay

The alteration in the membrane permeability was evaluated by crystal violet (CV) uptake assay with some modifications (Devi et al., 2010). Overnight-grown bacterial strains (wildtype, Δ*crisprI,* Δ*crisprII,* Δ*cas op, and* ΔΔ*crisprI crisprII)* were subcultured at a 1:100 ratio in F-media with or without H_2O_2 (1 mM) and were grown at 37°C, 150 rpm. After 8 h bacterial cells were harvested by centrifugation at 5000 rpm for 10 min at 4°C. The cells were washed twice and resuspended in PBS containing 10 µg/ml of CV (Thermofisher) followed by incubation at 37°C for 20 min. The suspension was then centrifuged at 13000 g for 15 min and the OD_{590nm} of the supernatant was recorded. The percentage CV uptake of all the samples was calculated using the following formula:

$$\%\text{Uptake of CV} = \frac{A_{\text{crystal violet}} - A_{\text{sample}}}{A_{\text{crystal violet}}} \times 100, \text{ where}$$

A_{sample}- O. D value of the sample and $A_{crystal\ violet}$- O.D value of crystal violet solution

3.2.8 Hydrophobicity assay using bacterial adhesion to hydrocarbons(BATH) method

The absorbance of overnight cultures was measured at $OD600_{nm}$. 3 mL of bacterial culture was mixed with 1 mL of xylene (Himedia). The mixture was vortexed and incubated at room temperature for 30 min. The absorbance of the aqueous phase was measured at 600 nm (Xu et al., 2009).

$$\%\ hydrophobicity = \frac{A_{600nm}\ \text{of intitial culture} - A_{600nm}\ \text{of aqueous phase}}{A_{600nm}\ \text{of intitial culture}} \times 100$$

3.2.9 Antimicrobial peptide killing assay

Overnight-grown bacterial cultures were subcultured at a ratio of 1:40 in LB at 37°C. 10^5 bacterial cells were resuspended in tryptone-NaCl (0.5% tryptone and 0.5% NaCl) media. The diluted bacterial suspension was treated with polymyxin B (0.5 μg/mL, Himedia), and incubated at 37°C for 1 h. Following the incubation, the mixture was plated onto LB-agar plates supplemented with appropriate antibiotics. Percentage survival was calculated by normalizing the CFU of treated samples to those of the untreated controls.

3.2.10 Statistical analysis

Statistical analysis was performed using Prism 8 software (GraphPad, California). Unpaired Student's t-test was performed. Error bars indicate standard deviation (SD). Statistical significance is shown as follows: *,$P \leq 0.05$; **, $P \leq 0.01$; ***, $P \leq 0.001$; ****, $P < 0.0001$; and ns, not significant.

3.4 Results

3.4.1 CRISPR-Cas knockout strains show reduced survival to an oxidative stressor, hydrogen peroxide

We evaluated the sensitivity of the CRISPR-Cas knockout strains (Δ*crisprI,* Δ*crisprII,* Δ*cas op,* and ΔΔ*crisprI crisprII*) against H_2O_2. As a first step, we checked the sensitivity of the knockout strains against different concentrations of H_2O_2 (0 mM, 0.1 mM, 0.5 mM, 1 mM, and 2 mM). The CRISPR-Cas knockout strains showed increased sensitivity to H_2O_2, showing a gradual decrease in survival with increasing H_2O_2 concentration when compared to the wildtype (Fig. 3.1A). The difference in the survival of the CRISPR-Cas knockout strains and wildtype was significant in the presence of H_2O_2. We next assessed the viability of the knockout strains in the presence of H_2O_2 by estimating their percentage survival at 1 mM H_2O_2 using CFU assay. The percentage survival of the knockout strains was significantly reduced by ~60-70% for Δ*crisprI,* Δ*crisprII,* Δ*cas op,*

and ΔΔ*crisprI crisprII* when compared to that of the wildtype (Fig. 3.1B). The percentage survival for complement strains (Δ*crisprI+pcrisprI* and Δ*crisprII+pcrisprII*) was the same as that of the wildtype confirming that the knockout generation process was clean without any side effects.

3.4.2 CRISPR-Cas knockout strains regain resistance against oxidative stress after H_2O_2 pre-treatment

Many organisms have a common trait: the ability to elicit a stress response after repeated stress relies on ′remembering′ a similar event from the past (Hilker et al., 2016). For example, Imlay et al. reported that the pre-treatment of *E. coli* with a low dose (60 μM) of H_2O_2 increased bacterial survival upon subsequent exposure to high doses of H_2O_2 (Imlay & Linn, 1986). This process also aids the evolution of H_2O_2 resistance in H_2O_2-primed *E.coli* cells (Rodríguez-Rojas et al., 2020). As the CRISPR-Cas knockout strains show reduced survival in the presence of H_2O_2, we decided to assess the survival of the CRISPR-Cas knockout strains after priming with 0.1 mM H_2O_2, non-toxic dose to the strains of this study (Fig. 3.1A). The percentage survival of the primed Δ*crisprI* and Δ*crisprII* knockout strains was the same as that of the primed wildtype (Fig 3.2). While Δ*cas op* and ΔΔ*crisprI crisprII* showed marginal differences in survival compared to the wildtype (Fig 3.2).

3.4.3 CRISPR-Cas knockout strains show increased expression of *ompW*

It is known that the outer membrane porin, OmpW aids the influx of H_2O_2 in *Salmonella*(Calderón et al., 2011), and the *ompW* null mutants of *E. coli* and *Salmonella* are resistant to oxidative stress(Morales et al., 2012; P. Zhang et al., 2020). Additionally, the *ompW* null mutants show enhanced surface-attached biofilm in *Cronobacter sakazakii* (Ye et al., 2018; X. Zhang et al., 2019). We observed that the CRISPR and *cas* knockout strains showed reduced H_2O_2 tolerance (Fig. 3.1B) and lesser surface-attached biofilm compared to that of wildtype (Fig 2.4B). Thus, we hypothesized that the *ompW* is upregulated in the CRISPR-Cas knockout strains leading to the observed phenotypes. Moreover, *in-silico* analysis suggests that spacer 3 of the CRISPR1 array has partial complementarity to *ompW* (Fig 3.3A). The interaction between the CRISPR1-spacer3 and the *ompW* mRNA represents favorable binding kinetics (with the negative mean free energy, -8.045 kcal/mol, of the interaction) (Fig 3.3A), suggesting *ompW* regulation by the CRISPR1 array. No spacer of the CRISPR2 array had any complementarity with the *ompW*

sequence. With this antecedent, we assessed the expression of *ompW* in the knockout strains in the presence and absence of 1 mM H_2O_2. In H_2O_2 untreated samples, the *ompW* expression was 2-fold higher for Δ*crisprI* and Δ*cas op*, while in Δ*crisprII* and ΔΔ*crisprI crisprII* it was 3-fold higher than that of the wildtype (Fig. 3.3B). H_2O_2 is known to repress the expression of *ompW* in *S.* Typhimurium (Morales et al., 2012). As expected, the H_2O_2 treatment reduced the expression of *ompW,* and the difference in the expression between the knockout strains and wildtype reduced to 1 to 1.3-fold (Fig. 3.3B).

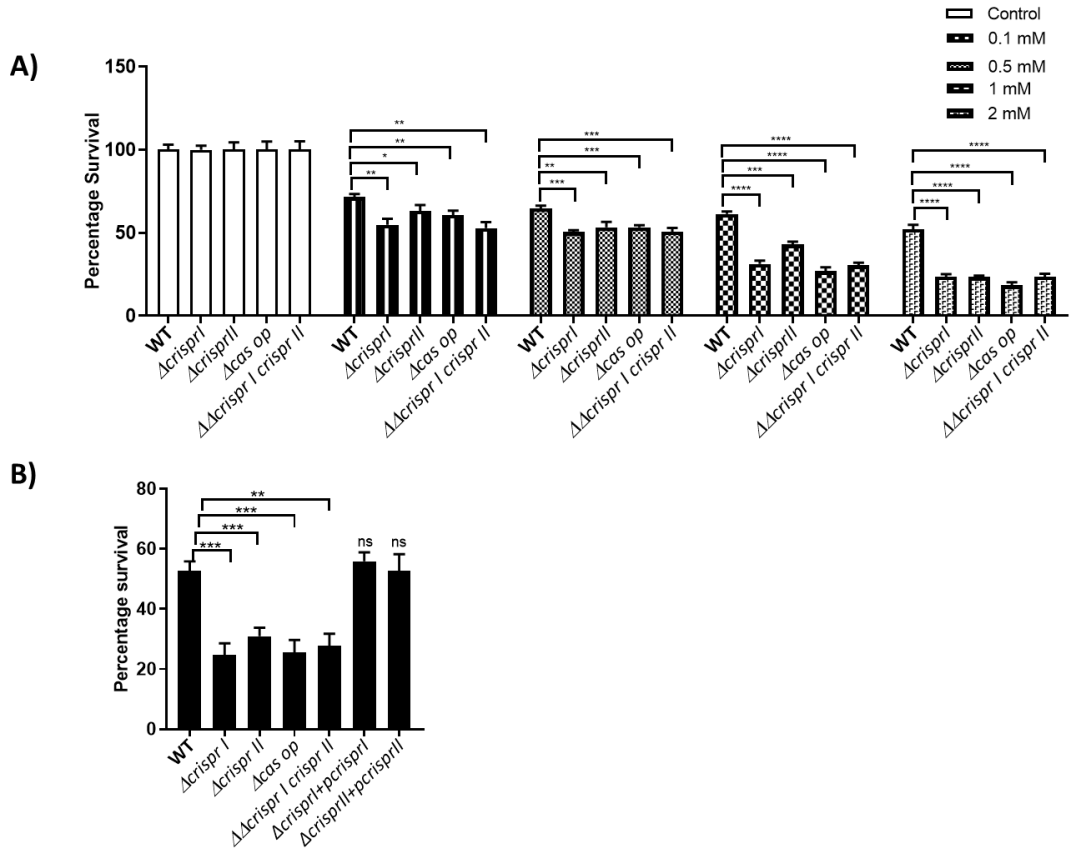

Fig. 3.1: Hydrogen peroxide inhibits growth and reduces the survival of the CRISPR-Cas knockout strains. A. The concentration-dependent inhibition by hydrogen peroxide (0 mM, 0.1 mM, 0.5 mM,1 mM, and 2 mM) on the growth of mutant strains was tested by observing the bacterial Optical density (OD_{600nm}) after 8 h. The *S.* Typhimurium strain 14028s wildtype (WT), CRISPR (Δ*crisprI*, Δ*crisprII* and ΔΔ*crisprI crisprII)* and *cas operon* (Δ*cas op*) knockout strains were exposed to different concentrations of H_2O_2 and percentage survival was plotted with respect to H_2O_2 untreated cells. **B.** The strains grown overnight in Luria Bertani were resuspended in MH media (pH 5.4), and 10^7 cells were treated with 1 mM H_2O_2 for 2 h at 37°C, in dark, after this CFU were determined. Percentage survival was calculated by normalizing the treated samples to those of the untreated controls. An unpaired t-test was used to determine significant differences between the WT and knockout strains. Error bars indicate SD. SD. Statistical significance is shown as follows: *,P ≤ 0.05; **, P ≤ 0.01; ***, P a≤ 0.001; ****, P < 0.0001; and ns, not significnt.

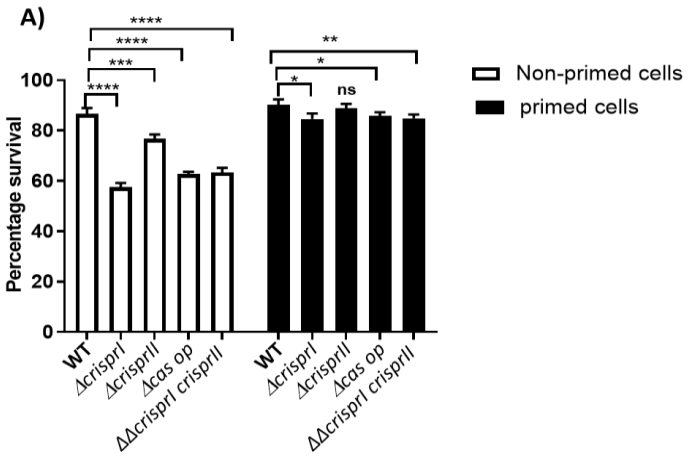

Fig. 3.2: Pre-treatment with H_2O_2 improves survival of the CRISPR-Cas knockout strains. The *S.* Typhimurium strain 14028s wildtype (WT), CRISPR (Δ*crisprI*, Δ*crisprII*and ΔΔ*crisprI crisprII*), and *cas* operon(Δ*cas op*) knockout strains were grown to OD_{600nm}~0.4 in MH media. The bacterial cells were primed with 0.1 mM H_2O_2 for 30 min. The primed bacterial cells were exposed to 0 mM and 1 mM H_2O_2 for 8 h at 37°C in dark. Percentage survival was calculated by normalizing the treated samples to those of the untreated controls. An unpaired t-test was used to determine significant differences between the WT and knockout strains. Error bars indicate SD. SD. Statistical significance is shown as follows: *, P ≤ 0.05; **, P ≤ 0.01; ***, P ≤0.001; ****, P < 0.0001; and ns, not significant.

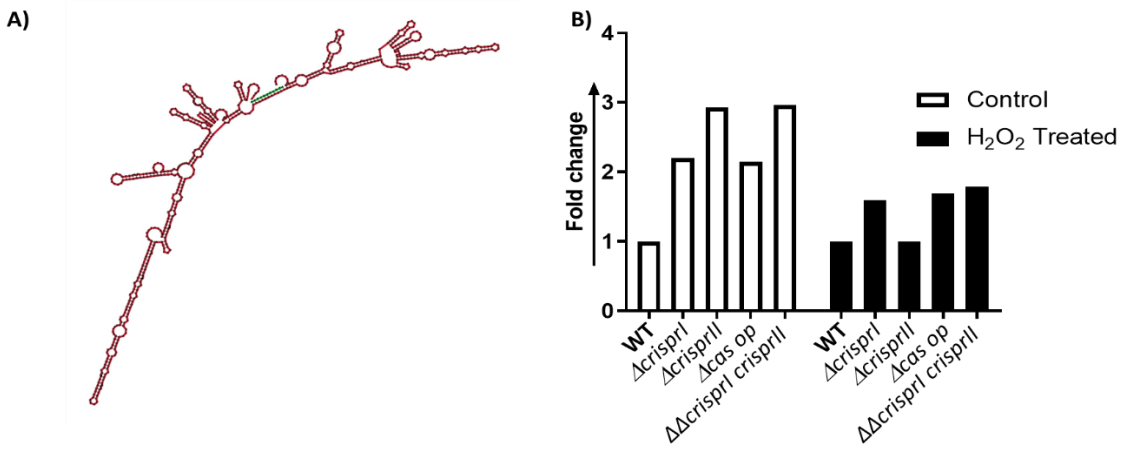

Fig. 3.3: The CRISPR-Cas system regulates *ompW* expression

A. The diagram represents the binding between the spacer represented in green (CRISPR-1, spacer-3) and the gene represented in red (*ompW*). The methodology used for bioinformatic analysis is mentioned in the material and methods section. **B.** RT-PCR gene expression analysis of outer membrane porin gene (*ompW*), was evaluated for the wildtype and CRISPR-Cas system knockout strains grown in F-media with and without hydrogen peroxide (1 mM) for 8 h. The *S.* Typhimurium strain 14028s wildtype (WT), CRISPR (Δ*crisprI*, Δ*crisprII*, and ΔΔ*crisprI crisprII*), and *cas operon* (Δ*cas op*) knockout strains were grown in F-media with and without hydrogen peroxide (1 mM) for 8 h, followed by qRT-PCR analysis. Relative expression of the gene was calculated using the $2^{-\Delta\Delta Ct}$ method and normalized to reference gene *rpoD*.

3.4.4 Increased expression of *ompW* potentiated H_2O_2 influx in the CRISPR-Cas knockout strains

As the *ompW* expression was upregulated in the CRISPR-Casknockout strains, we expected an increased H_2O_2 influx in the strains, leading to their reduced survival. With this context, we qualitatively estimated the intracellular and extracellular H_2O_2 after exposing the strains to 1 mM H_2O_2. The knockout strains had increased intracellular H_2O_2 compared to that of the wildtype; at the same time, the H_2O_2 in the extracellular milieu was less in these strains compared to that of the wildtype (Fig 3.4).

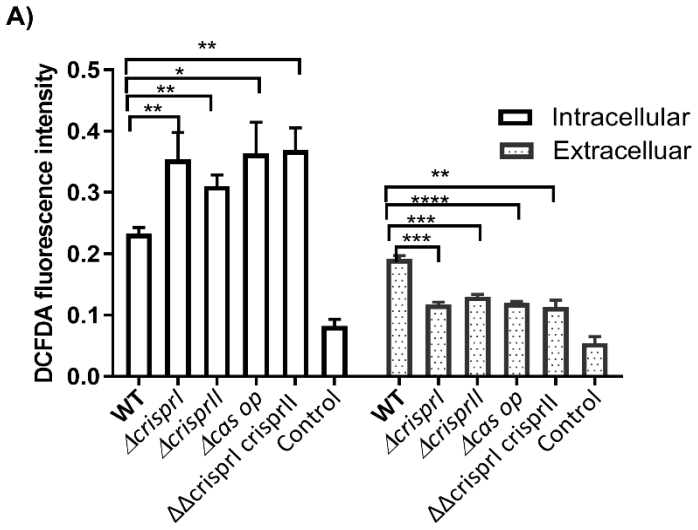

Fig. 3.4: *In vitro* determination of H_2O_2 influx in the CRISPR-Cas knockout strains. The *S.* Typhimurium strain 14028s wildtype (WT), CRISPR (Δ*crisprI*, Δ*crisprII* and ΔΔ*crisprI crisprII*), and *cas operon* (Δ*cas op*) knockout strains were grown to OD_{600nm}~0.5 in F-media media and incubated for 5 min with 1 mM H_2O_2 in dark. The H_2O_2 in the extracellular (supernatant) and intracellular (bacterial pellet) fractions were determined using H_2DCFDA. The H_2O_2 untreated sample was used as a control. An unpaired t-test was used to determine significant differences between the WT and knockout strains. Error bars indicate SD. Statistical significance is shown as follows: *, $P \leq 0.05$; **, $P \leq 0.01$; ***, $P \leq 0.001$; ****, $P < 0.0001$; and ns, not significant.

3.4.5 Deletion of CRISPR-Cas genes altered membrane characteristics making the strains susceptible to polymyxin B

Outer membrane porins along with LPS, restrict the entry of molecules across the membrane, thereby contributing to its selective permeability. In Chapter 2, we observed altered LPS profiles of the knockout strains. Thus, we anticipate altered membrane permeability in these strains. Furthermore, *ompW*-deficient mutants are reported to have decreased influx of H_2O_2 (Morales et al., 2012). The increased influx of H_2O_2 due to the

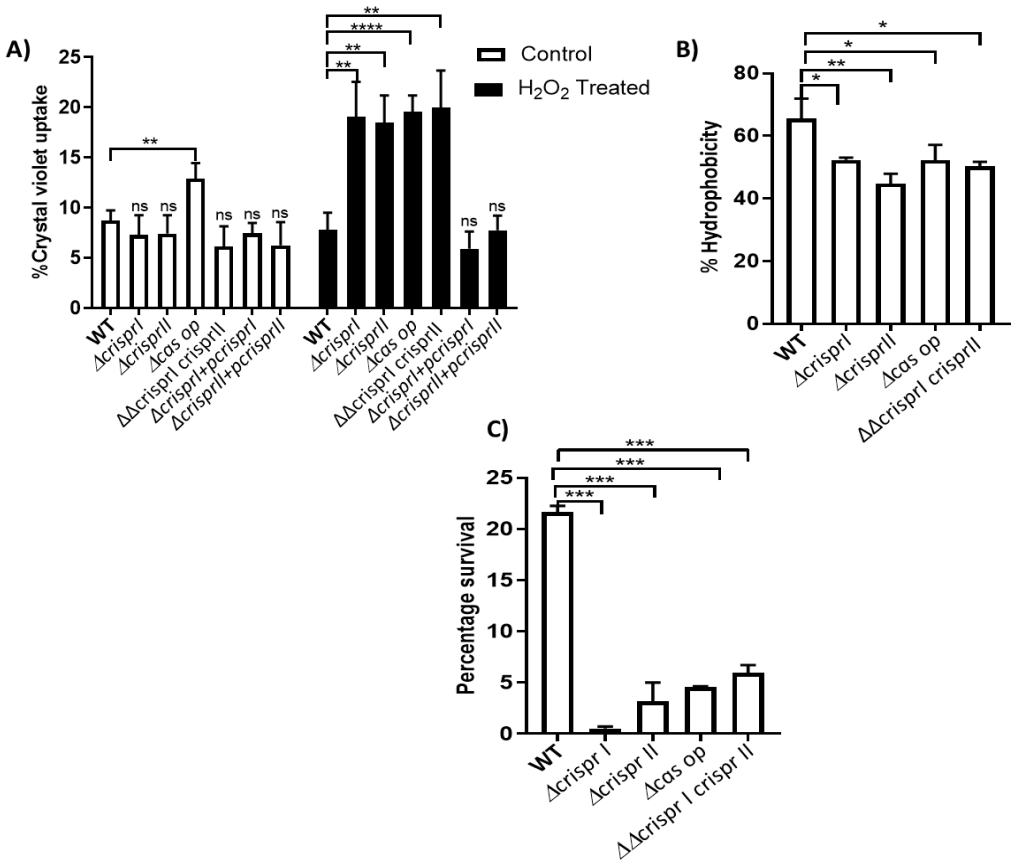

Fig. 3.5: Estimation of membrane integrity (A), cell-surface hydrophobicity (B), and antimicrobial sensitivity (C) of the CRISPR-Cas knockout strains. The *S.* Typhimurium strain 14028s wildtype (WT), CRISPR (Δ*crisprI*, Δ*crisprII*, and ΔΔ*crisprI crisprII*) and *cas operon (*Δ*cas op*) knockout strains along with their respective complement strains (Δ*crisprI*+p*crisprI* and Δ*crisprII*+p*crisprII*) were grown in F-media with and without H_2O_2 treatment (1mM) for 8 h at 37°C. **A.** Bacterial cells were harvested and treated with 10 µg/mL of crystal violet. After 20 mins of incubation, the percentage of crystal violet uptake was calculated by the formula mentioned in the materials and methods **B.** Overnight cultures were mixed with xylene in a ratio of (3:1) and incubated at RT for 30 min. The hydrophobicity of the bacterial cultures was measured using the formula mentioned in the materials and methodology section. **C**. The knockout strains were grown in MH media in presence of polymyxin B (0.5 µg/ml) for 1 h at 37°C. The bacterial suspension was plated onto LB-agar plates and susceptibility to cationic peptides was tested by normalizing the treated samples to those of the untreated control samples. An unpaired t-test was used to determine significant differences between the WT and knockout strains. Error bars indicate SD. SD. Statistical significance is shown as follows: *, $P \leq 0.05$; **, $P \leq 0.01$; ***, $P \leq 0.001$; ****, $P < 0.0001$; and ns, not significant.

upregulated *ompW* in the CRISPR-Cas knockout strains may further hamper the membrane integrity. We thus estimated the membrane permeability of the knockout strains by CV uptake assay. No difference in the percentage uptake of CV was observed in Δ*crisprI*

*and*Δ*crisprII* but Δ*cas op* and ΔΔ*crisprI crisprII* (Fig. 3.5A). However, the CV uptake was high in H_2O_2-treated samples of all the knockout strains compared to that of the wildtype (Fig. 3.5A), suggesting possible membrane damage by H_2O_2. This could be subsequently leading to their reduced viability.

The core Oligosaccharide unit of LPS is known to play a role in the cell-surface hydrophobicity (Z. Wang et al., 2015). The CRISPR-Cas knockout strains showed a decreased cell-surface hydrophobicity as per the bacterial adhesion to hydrocarbons (BATH) test. (Fig 3.5B).

The LPS modification affects bacterial susceptibility to antimicrobial peptides (AMPs) like polymyxin B (Halder et al., 2015). As the CRISPR-Cas knockout strains had altered LPS profile, we estimated the sensitivity of the knockout strains against polymyxin B. The CRISPR-Cas knockout strains showed ~60-70% reduction in their percentage survival in the presence of polymyxin B compared to that of the wildtype (Fig. 3.5C). These data clearly indicate that the membrane permeability of the bacterium is compromised in the absence of the CRISPR and *cas* genes, which is further worsened under oxidative stress.

3.5 Discussion

Cell membrane integrity is important for maintaining cellular homeostasis (Anamourlis, 2020). In Gram-negative bacteria, the plasma membrane and the peptidoglycan layer frame the cellular structure (Silhavy et al., 2010). Recently, the CRISPR-Cas system of *F. novicida* has been implicated in regulating cell membrane permeability against toxic compounds like antibiotics (Sampson et al., 2014). Similarily, we found that the CRISPR-Cas knockout strains show increased sensitivity against H_2O_2. The increased sensitivity of these strains may be a result of the increased influx of H_2O_2 *via* the increased expression of OmpW, an importer of H_2O_2 (Morales et al., 2012). The computational analysis revealed *ompW*, as one of the targets of the CRISPR1 spacer, and the RT-PCR analysis confirmed this data. H_2O_2 negatively regulates the expression of *ompW* in *S.* Typhimurium (Morales et al., 2012). In accordance, we observed that exposure to H_2O_2 reduced the fold change in the *ompW* expression in the CRISPR-Cas knockout strains leading to their improved survival against H_2O_2. Thus, we hypothesize that the CRISPR-Cas system regulates *ompW* expression and hence the sensitivity of bacteria against H_2O_2. The CRISPR-Cas system has also been reported to regulate outer membrane proteins in *S.* Typhi (Medina-Aparicio et al., 2021). As the OmpW protein is widely

distributed in the *Enterobacteriaceae* family, the question is can the CRISPR-Cas system regulate *omp* expression in other members of the *Enterobacteriaceae* family? This question needs to be explored.

The present study corroborates the finding from Chapter 2, where a few cells in the CRISPR-Cas knockout strains become filamentous at 24 h (Fig. 2.7A). This indicates a potential induction of reactive oxygen species (ROS) during biofilm formation and a few cells become filamentous in response to oxidative stress (Tran et al., 2022). As the biofilm formation progressed, the nutrient deprivation could have accelerated ROS could have been influxed in the knockout strains, resulting in their reduced viability at 24 h (Fig 2.11A). However, the increased viability at 96 hours in the biofilm state (Fig 2.11B) could be due to improved circulation of nutrients owing to thicker pellicles with wrinkled patterns and higher EPS that protects bacteria against H_2O_2 (Hahn et al., 2021).

Apart from functioning as an influx pump for H_2O_2 in *S*. Typhimurium (Morales et al., 2012), OmpW also plays a role in biofilm formation (Ye et al., 2018). Various environmental stimuli like temperature, nutrient availability, and osmolarity are known to trigger the expression of *ompW,* thereby providing the bacteria with adaptation against harsh environmental conditions (Xiao et al., 2016). In *P. aeruginosa*, Δ*ompW* mutants display impaired biofilm formation (Ritter et al., 2012). In *Cronobacter,* Δ*ompW* mutants formed better biofilm under stressed conditions like high salinity or H_2O_2, and their survival was significantly reduced due to salt and H_2O_2- induced damage (Ye et al., 2018). The results of this and the previous chapter, where we show that the knockout strains are more susceptible to H_2O_2 and show altered biofilm formation, corroborate with the above-mentioned reports.

OMP and LPS help the bacteria to tolerate different environmental stresses including H_2O_2 and AMP. The core-OS of LPS influence membrane properties like permeability, hydrophobicity, stability, biofilm formation, and adhesion (Z. Wang et al., 2015). In Chapter 2 we showed that the CRISPR-Cas strains had altered biofilm formation and LPS profile. The altered LPS profile was attributed to the differential expression of *rfa* and *rfb* gene clusters coding for LPS core synthesis and O-antigen synthesis, respectively. It is known that mutation in the O-antigen capsule makes *Salmonella* biofilms susceptible to H_2O_2 (Hahn et al., 2021). Thus, it may be possible that the altered LPS profile of the knockout strains is one of the reasons for their H_2O_2 sensitivity. LPS also influences the bacterial surface physicochemical features (Stendahl et al., 1977), and the properties of its

core oligosaccharide impact bacterial hydrophobicity and outer membrane permeability (Krasowska & Sigler, 2014; Wang et al., 2015). The reduction in the cell-surface hydrophobicity of the CRISPR-Cas knockout strains could be due to variations in their LPS profile. Taken together we presume that the altered LPS could contribute to reduced cell surface hydrophobicity of the CRISPR-Cas knockout strains. The variations in the LPS profile did not alter the membrane permeability of all the CRISPR-Cas knockout strains under normal growth conditions. The permeability was affected only for Δ*cas op* and ΔΔ*crisprI crisprII* strains. However, membrane damage was observed in all the knockout strains on H_2O_2 treatment. The alteration in LPS structure also contributes to resistance against AMP like polymyxin B. The cell-surface hydrophobicity reportedly contributes to the resistance against cationic antimicrobial peptides of *Staphylococcus aureus* (Lather et al., 2016). Furthermore, alteration in outer membrane protein along with modified LPS contributes to resistance against β-lactam antibiotics and impaired invasion ability of *S.* Paratyphi (Gutmann et al., 1988).

To summarize, the upregulated expression of OmpW in the CRISPR-Cas knockout strains resulted in an increased influx of membrane-damaging molecules (H_2O_2) inside the cell, which in turn affected the membrane permeability, leading to reduced bacterial viability. The altered LPS profile could have affected the cell surface hydrophobicity, and resistance against polymyxin B. Thus, we show that the CRISPR-Cas system regulates membrane properties like the LPS structure and OmpW expression in *S.* Typhimurium.

Chapter 4

Deletion of the CRISPR-Cas system attenuates the virulence of *Salmonella enterica* serovar Typhimurium

4.1 Introduction

The bacterial adaptive immune system, clustered regularly interspaced short palindromic repeats (CRISPR), and CRISPR-associated (Cas) endonucleases, acts against invading mobile genetic elements. Besides their canonical functions, the CRISPR-Cas systems regulate the physiology and virulence of various bacteria, including *Streptococcus*, *Enterobacter*, and *Salmonella* (Sampson & Weiss, 2014; Wu et al., 2022). For example, Cas 9 of *Francisella* targets bacterial lipoprotein (BLP) mRNA, thereby subverting the host immune response (Sampson & Weiss, 2013). Cas9 aids invasion and intracellular survival of *Campylobacter* and *Neisseria* (Heidrich et al., 2019; Louwen et al., 2013). In *Legionella*, Cas2 *is* required to infect amoebae (Gunderson & Cianciotto, 2013). The CRISPR RNA can also work independently of Cas proteins and regulate bacterial virulence. In *Listeria monocytogenes* in the absence of *cas* genes, the crRNA governs its virulence (Mandin et al., 2007). Similarly, in *Streptococcus agalactiae*, the CRISPR regulates virulence independently of Cas (Dong et al., 2021). The type IF CRISPR-Cas system of *Pseudomonas aeruginosa* regulates biofilm and virulence by targeting *lasR* transcript (Wiedenheft & Bondy-Denomy, 2017). Further, the computational analysis predicted the role of the type IE system of *E. coli* in endogenous gene regulation (Bozic et al., 2019). However, the mechanistic details are yet to be fully investigated.

Many proto-spacers of the CRISPR-Cas system in *Salmonella* were traced on the chromosome instead of its general target - phages and plasmids but the target genes were unidentified (Shariat et al., 2015). A few studies have suggested the CRISPR-Cas system's role in modulating *Salmonella enterica* subspecies *enterica* serovar Typhi's (*S.* Typhi) intracellular survival and biofilm formation. The expression of *cas7* was detected in human macrophages infected by *S.* Typhi. The transcriptome profile of bacteria displayed altered expression of *cas* genes in clinical *S.*Typhi samples, suggesting the role of the type I-E CRISPR-Cas system during *Salmonella* infection (Sheikh et al., 2011). A recent study by Cui *et al.* on *Salmonella enterica* subspecies *enterica* Enteritidis (*S.* Enteritidis) correlates the importance of the CRISPR-Cas system in regulating quorum sensing, biofilm formation, and bacterial invasion into the host (Cui et al., 2020). The study indicates the role of Cas3 nuclease in *S.* Enteritidis in regulating virulence and biofilm formation. The results of the study hint at the regulation of invasion and QS genes by Cas3. Another relevant study was performed by Stringer *et al.* ChIP seq analysis confirmed 236 crRNA- and Cascade-binding sites in *S. enterica* subsp. *enterica* serovar Typhimurium (*S.*

Typhimurium) (Stringer et al., 2020). These sites coincide with virulence gene loci - *sseA, bcsA, iroC, entE, entF, sptP* possibly suggesting the regulation of pathogenic traits by the CRISPR-Cas system.

The infection biology of *Salmonella* is well coordinated with the myriad of virulence determinants aiding adhesion, invasion, and propagation in the host cell (as detailed in section 1.3). Typically, the infection process begins *via* oral intake of *Salmonella* contaminated food. The intestinal adhesion and invasion mark the beginning of *Salmonella* pathogenesis (Darwin & Miller, 1999). Flagella-guided motility helps bacteria to reach the target host cell, playing a vital role in the intestinal phase of infection (Barbosa et al., 2017). Various environmental clues in the intestine induce the expression of the *Salmonella* pathogenicity island 1 (SPI-1) transcriptional regulator, HilD. HilD binds upstream of the master regulator, *hilA*, thereby counteracting the H-NS-mediated repression of the *hilA* promoter(Azimi et al., 2020). Following the activation of *hilA*, the structural genes and effector proteins encoded by SPI-1get activated (Azimi et al., 2020). Delivery of effectors into the host cell by SPI-1 requires the action of three translocases SipB, SipC, and SipD (Lou et al., 2019). The bacterial attachment to the host cell triggers the invasion protein, SipA, which regulates actin polymerization at the site of invasion, thereby enhancing the efficiency of bacterial entry into the host cell through membrane ruffling (Jepson et al., 2001a; Lilic et al., 2003). In addition, SipA regulates phagosome maturation and intracellular replication of *Salmonella* in non-phagocytic cells and macrophages (Brawn et al., 2007). Following membrane ruffling, *Salmonella* outer membrane proteins (Sops) control the rearrangement of the cytoskeleton while also regulating different stages of polymorphonuclear leukocyte influx (Lou et al., 2019). Among them, SopB is involved in inducing a diverse set of eukaryotic responses. For example, SopB participates in the invasion of non-phagocytic cells, early maturation of the SCV (Giacomodonato et al., 2011), and induction of iNOS (Drecktrah et al., 2005). Following the internalization of bacteria in the acidic macrophage vacuole, the SPI-2-encoded SsrAB system gets activated in response to the acidic milieu (Azimi et al., 2020). The SsrA kinase phosphorylates the key regulatory factor of SPI-2, SsrB, which in turn activates the expression of SPI-2 encoded effector proteins(Fass & Groisman, 2009b). SpiC, a SPI-2 encoded protein, inhibits endosomal trafficking and is involved in the secretion of translocon proteins SseB and SseC (Freeman et al., 2002). Another effector called PipB2 promotes *Salmonella* induced filament (SIF) extension and helps in the intramacrophage survival of *Salmonella*

(Knodler & Steele-Mortimer, 2005). Furthermore, *pipB2* is required for virulence in a mouse model of infection (Henry et al., 2006). Multiple other SPI-2 effectors govern the replication and survival of the bacteria within the host.

Herein, we aim to investigate the type IE CRISPR-Cas system's role in regulating *Salmonella's* virulence at different stages of infection.

4.2 Material and Methods

4.2.1 Bacterial strains, nematode, and culture conditions

S. Typhimurium str. 14028s was used as a parent strain. The wildtype, CRISPR *(*Δ*crisprI,* Δ*crisprII, and* ΔΔ*crisprI crisprII),* and *cas* operon *(*Δ*cas op)* knockout strains and their corresponding complement strains *(*Δ*crisprI*+p*crisprI and* Δ*crisprII*+p*crisprII)* were routinely grown in Luria-Bertani (LB, HiMedia) with appropriate antibiotics. The mCherry fluorescent derivatives of wildtype, CRISPR-Cas knockout strains, and *Escherichia coli* OP50 were obtained by electro-transformation of a plasmid. Bacterial cultures were routinely maintained on LB-Agar media along with their corresponding antibiotics (Table 4.1). A wildtype N2 strain of *Caenorhabditis elegans* (a kind gift from Vidya Devi Negi, National Institute of Technology, Rourkela) was routinely maintained at 25°C on a nematode growth medium (NGM) agar plate with *E. coli* OP50 as a food source.

4.2.2 Electrotransformation of pFPV-mCherry plasmid

For electrocompetent cell preparation, 5 mL of LB media was inoculated with 1 percent of overnight culture. Bacterial cells were harvested at 0.3 OD_{600nm} and resuspended in 5 ml of ice-cold 10% glycerol after washing with ice-cold Milli-Q. After two washes in 10 % ice-cold glycerol, cells were resuspended in 50 µL of 10 % ice-cold glycerol. 1 µg of pFPV-mCherry plasmid, a kind gift from Prof. Dipshikha Chakravorty, IISc, India, was electro-transformed into respective strains using Bio-Rad Electroporator.

4.2.3 Eukaryotic cell lines and growth conditions

The mice macrophage-like cell line RAW 264.7, and a colorectal adenocarcinoma cell line with epithelial morphology (HT-29) cells were obtained from NCCS, Pune. The cells (RAW 264.7 and HT-29) were grown in Dulbecco′s modified minimum essential medium (Gibco) and Roswell Park Memorial Institute 1640 media (Sigma Aldrich), respectively, with 10% fetal bovine serum (FBS, Himedia) at 37°C temperature inthe

presence of 5% CO_2. For polarizing the HT-29 cells, RPMI was supplemented with 2mM glutaMAX^{TM} (Gibco).

Table 4.1: List of bacterial strains and plasmids used in this study

Bacterial Strain	Genotype and Characteristics	Source
S. Typhimurium 14028s	WT 14028s	A kind gift from Prof. Dipshikha Chakravorty, IISc, India
Δ*crisprI*	WT 14028s Δ*crisprI*:: Chl (Chl^r)	This study
Δ*crisprII*	WT 14028s Δ*crisprII*:: Chl (Chl^r)	This study
Δ*cas op*	WT 14028s Δ*cas operon*:: Chl (Chl^r)	This study
ΔΔ*crisprI crisprII*	WT 14028s Δ*crisprI*:: Kan :Δ*crisprI*::Chl (Kan^r, Chl^r)	This study
Δ*sipD*	WT 14028s Δ*sipD*::Kan (Kan^r)	A kind gift from Prof. Dipshikha Chakravortty, IISc, India
E.coli-OP50		A kind gift from Vidya Devi Negi, National Institute of Technology, Rourkela
WT-mCherry	WT 14028s transformed with pFPV-mCherry Vector (Amp^r)	This study
Δ*crisprI* -mCherry	Δ*crisprI* transformed with pFPV-mCherry Vector (Amp^r)	This study
Δ*crisprII*-mCherry	Δ*crisprII* transformed with pFPV-mCherry Vector(Amp^r)	This study
Δ*cas op*-mCherry	Δ*cas op* transformed with pFPV-mCherry Vector(Amp^r)	This study
ΔΔ*crisprI crisprII*-mCherry	ΔΔ*crisprI crisprII* transformed pFPV-mCherry pQE60 vector(Amp^r)	This study
E. coli OP50-mCherry	*E. coli* OP50 transformed with pFPV-mCherry Vector(Amp^r)	This study
Δ*crisprI* +p*crisprI*	Δ*crisprI* complemented with functional CRISPR I array cloned in pQE60(Amp^r)	This study
Δ*crisprII* +p*crisprII*	Δ*crisprII* complemented with functional CRISPR II array cloned in pQE60(Amp^r)	This study

Mice peritoneal macrophages were harvested as previously described (Zhang et al., 2008). BALB/c mice were injected intraperitoneally with 1 mL of thioglycollate (Himedia).

After four days, the mice were sacrificed by cervical dislocation, 5 mL of ice-cold RPMI media was injected into the peritoneal cavity of mice, and peritoneal macrophages were withdrawn using a syringe. Cells were centrifuged and suspended in RPMI media with 10% FBS.

4.2.4 Percentage phagocytosis/invasion assay

Bacterial phagocytosis and invasion were estimated by a gentamicin protection assay in macrophages (RAW264.7 and peritoneal macrophages) and intestinal epithelial cell lines (HT-29 non-polarized and polarized cell lines), respectively. 1.5 to 3×10^5 cells were seeded into 24-well plates and incubated at 37°C with 5% CO_2 for 24 h. RAW 264.7 and peritoneal macrophages were infected with stationary phase cultures of wildtype, Δ*crisprI*, Δ*crisprII*, Δ*cas op*, and ΔΔ*crisprI crisprII* knockout strains and their respective complement strains Δ*crisprI*+p*crisprI* and Δ*crisprII*+p*crisprII* at a multiplicity of infection (MOI) 5. The HT-29 cells were infected with the log phase culture (when the SPI-1 system is active) of the strains at MOI 10. The infected cells were incubated at 37°C with 5% CO_2 for 30 min. Next, the cells were washed thrice with phosphate-buffered saline (PBS) and subjected to 100 μg/mL of gentamicin treatment for 1 h. The cells were washed again with PBS and lysed with 0.5 mL of 0.1% Triton X-100 (Sigma). The number of viable intracellular bacteria was determined by plating the lysates onto LB agar supplemented with appropriate antibiotics. Percentage phagocytosis/invasion was determined using the following formula:

$$\%\ invasion\ /phagocytosis = \frac{\text{CFU at 1 h}}{\text{CFU of pre-inoculum}} \times 100$$

4.2.5 Intracellular proliferation assay

The protocol for intracellular proliferation is similar to that mentioned above. The cells were infected with the stationary phase (RAW264.7 cells) or log phase (HT-29 cells) bacterial cultures at MOI of 5 and 10, respectively. The cells were lysed at 2 h and 16 h post-infection. The lysates were plated onto LB agar supplemented with antibiotics to obtain CFU at 2 h and 16 h. The fold proliferation 16 to 2 h was determined using the following formula:

$$Fold\ proliferation = \frac{\text{CFU at 16h}}{\text{CFU at 2 h}}$$

4.2.6 *In-vivo* infection assay

For infection studies, 6-8 weeks old BALB/c mice weighing 20-22 g raised in Central Animal Facility, Indian Institute of Science (IISc), Bangalore were used as per the guidelines of the Institutional Animal Ethics Committee at the IISc, Bangalore, India, and approved by the committee for the purpose of control and supervision of experiments on animals. All the procedures were carried out as per institutionally approved protocols (CAF/Ethics/852/2021). Five mice in five sets were orally gavaged with 10^7 bacterial cells of wildtype, Δ*crisprI,* Δ*crisprII,* Δ*cas op,* and ΔΔ*crisprI crisprII* knockout strains. After 3 days post-infection, reticuloendothelial organs like the spleen, liver, Peyer′s patch (PP), and mesenteric lymph nodes (MLN) were aseptically isolated, weighed, and homogenized in 0.5 mL of sterile PBS using a bead-beater (Bio spec products, USA). Serial dilutions of the homogenate were plated onto *Salmonella Shigella* agar (SS agar, Himedia) containing appropriate antibiotics to obtain CFU per gram weight for each organ.

4.2.7 Growth curve in F-media

Bacterial strains were grown in 25 mL F-media (37.2 mg KCl, 99 mg NH_4SO_4, 87.12 mg K_2SO_4, 195.2 mg MES buffer, 0.27% glycerol, 100 mg Casein Acid hydrolysate, and 10 µM $MgCl_2$)(pH-5.4 and 7.2) at 37°C in triplicates and optical density (O.D) at 600 nm was taken at indicated time points and plotted on the graph.

4.2.8 Measurement of intracellular reactive oxygen species (ROS)

Intracellular ROS in the infected RAW264.7 cells was determined using an oxidant-sensitive probe 2′,7′- dichlorodihydrofluorescein diacetate (H_2DCFDA, Sigma). Cells were infected with wildtype, Δ*crisprI,* Δ*crisprII,* Δ*cas op, and* ΔΔ*crisprI crisprII* knockout strains at MOI 5 as described in the above sections. 5 h post-infection, the culture supernatant was replaced with DMEM media, supplemented with a 5 µM concentration of H_2DCFDA, followed by incubation at 37°C, 5% CO_2 for 30 min. The cells were washed with sterile PBS, and fluorescence intensity was measured at (λ_{ex}) of 485 nm and (λ_{em}) at 535 nm using Fluoroskan (Thermo scientific).

4.2.9 Measurement of extracellular reactive nitrogen species (RNS)

Extracellular nitrite was measured as described previously (Vargas-Maya et al., 2021). Briefly, RAW 264.7 cells were infected, as described in the above section. 50 µL the extracellular media were collected from cells infected with wildtype, Δ*crisprI,* Δ*crisprII,* Δ*cas op, and* ΔΔ*crisprI crisprII* knockout strains at 16 h post-infection and

subjected to nitrite estimation by Griess reagents. To the culture media, 50 µL each of 1% sulphanilamide (made in 5% phosphoric acid), and 0.1% NED (N-1-naphthyl ethylenediamine dihydrochloride) (Himedia) were added and incubated in the dark at room temperature for 15 min. OD_{545nm} was measured within 30 min of the appearance of a purple-colored product.

4.2.10 Bacterial colonization assay in *C. elegans*

The mCherry-tagged bacterial strains were grown overnight in LB broth at 37°C and lawns were prepared by spreading 200 µL of overnight bacterial culture on modified NGM agar (Agar-1.7 g, NaCl-0.3 g, peptone-0.05 g). To measure the intestinal colonization of the test strains in *C. elegans*, the synchronized L4 larvae were exposed to fluorescently-tagged (m-Cherry) strains of wildtype, Δ*crisprI*, Δ*crisprII*, Δ*cas op*, ΔΔ*crisprI crisprII*, and *E. coli* OP50. After 24 h, the worms were anesthetized with 25 mM levamisole (Sigma), washed thrice with M9 buffer (KH_2PO_4, Na_2HPO_4, 5 g NaCl and 1 M $MgSO_4$), and treated with 80 µg/mL of gentamicin for 1 h followed by treatment with 25 µg/mL of gentamicin for 30 min. Finally, the worms were washed with M9 buffer and lysed with 0.2% Triton X-100 (Sigma) in a tissue lyser LT (Qiagen, India). The lysates were serially diluted and plated on LB-agar containing ampicillin to estimate bacterial burden.

4.2.11 Serum sensitivity

Bacterial strains were grown overnight in Luria broth, and 10^7 bacterial cells from an overnight culture were incubated in 20% FBS (Himedia) for 2 h at 37°C with slight agitation. Serial dilutions of these cultures were plated onto LB agar supplemented with antibiotics to determine the CFU. The percentage survival was calculated using the following formula: $\% \ survival = \frac{\text{CFU of serum treated samples}}{\text{CFU of untreated samples}} \times 100$

4.2.12 Antimicrobial killing assay

Overnight grown bacterial cultures were subcultured at a ratio of 1:40 in Luria broth and incubated at 37°C until the OD_{600nm} reached 0.3-0.4. 10^5 bacterial cells were treated with protamine sulfate (0.5µg/mL, PROTA), in TN (0.5% tryptone and 0.5% NaCl) media for 1 h at 37°C with slight agitation. Following the incubation, the mixture was plated onto LB-agar plates supplemented with appropriate antibiotics. Percentage survival was calculated with respect to the untreated samples.

Table 4.2: List of Primers used in this study

Sl. No.	Primer Name	Nucleotide Sequence
1	*rpoD* (Forward)	5′ACATGGGTATTCAGGTAATGGAAGA3′
2	*rpoD* (Reverse)	5′CGGTGCTGGTGGTATTTTA3′
3	*hilD* (Forward)	5′GACGAACCTGGGATGTTG3′
4	*hilD* (Reverse)	5′CGAAATCCATGTGGCCATTG3′
5	*hilA* (Forward)	5′TAACATGTCGCCAAACAGC3′
6	*hilA* (Reverse)	5′GCAAACTCCCGACGATGTAT3′
7	*sipA* (Forward)	5′ATGCGGGAAAGACGCTGA3′
8	*sipA* (Reverse)	5′TCGCCTCAGGAGAATCACTG3′
9	*sipD* (Forward)	5′ATTATCGCAGGCGGCTACTAA3′
10	*sipD* (Reverse)	5′CATTCAGGCTGCTGGTCAAC3′
11	*sopB* (Forward)	5′CGCTCGCCCGGAAATTATTG3′
12	*sopB* (Reverse)	5′GAGGTTATGCAGCGAGTGGT3′
13	*ssrB (Forward)*	5′CCTTATTACCCTGGCCTCA3′
14	*ssrB(Reverse)*	5′CCATTGATGCCAGGTAGACT3′
15	*H-NS (Forward)*	5′ACATCCGTACTCTTCGTG3′
16	*H-NS(Reverse)*	5′ACGAGTGCGTTCTTCCAC3′
17	*pipB2 (Forward)*	5′GGATACGTCGGAGAAATGAA3′
18	*pipB2 (Reverse)*	5′ATTCGACACGACACCCA3′
19	*spiC (Forward)*	5′TCAGGGCCGAAGGTAATAGC3′
20	*spiC (Reverse)*	5′GGTGTGCTGCAAGCAGTAGT3′
21	*sodA (Forward)*	5′ACCTGCCTGAGTTTGCC3′
22	*sodA (Reverse)*	5′GTTGTTACGCAGCACAGT3′
23	*sodCI (Forward)*	5′ATCACAGTTTCAGAGACACC3′
24	*sodCI (Reverse)*	5′TTCCCGGCATACAACTTG3′
25	*katG* (Forward)	5′GTGAAGATGTCTGGGAACC3′
26	*katG* (Reverse)	5′CCCTTCCGGGTTAACGTA3′
27	*ahpC* (Forward)	5′TTGCCCGACTGAACTGG3′
28	*aphC* (Reverse)	5′GTGCGTGAAGTGAGTATCG3′
29	*mgtC* (Forward)	5′TCTGAGCTCCATGACGAC3′
30	*mgtC* (Reverse)	5′ATCCCTTCGCGCATGAT3′

4.2.13 RNA isolation and quantitative real-time (q-RT) PCR

Bacterial strains grown overnight were subcultured at a ratio of 1:100 in LB (SPI-I inducing condition) and F media (pH 5.4, SPI-2 inducing condition). The bacterial cells

were incubated at 37°C and 150 rpm for 8 h and 4 h, respectively. At the end of the specified incubation, the RNA was isolated using TRIzol reagent (Himedia), and cDNA was synthesized using iScript^{TM} cDNA synthesis kit (Biorad). qRT-PCR was performed using PowerUp™ SYBR™ Green Master Mix (Thermo Fisher Scientific). Relative expression of the gene was calculated using the $2^{-\Delta\Delta Ct}$ method by normalizing to reference gene *rpoD*. The primers used in RT-qPCR are listed in Table 4.2.

4.2.14 Statistical analysis

Statistical analysis was performed using Prism 8 software (GraphPad, California). Unpaired Student's t-test was performed. Error bars indicate standard deviation (SD). Statistical significance is shown as follows: *,$P \leq 0.05$; **, $P \leq 0.01$; ***, $P \leq 0.001$; ****, $P < 0.0001$; and ns, not significant.

4.3 Results

4.3.1 Deletion of the CRISPR-Cas system hampers invasion and intracellular survival in cell culture infection models

An essential feature of *Salmonell*a pathogenesis relies on its ability to cross several barriers requiring invading a large variety of phagocytic and non-phagocytic cells. To understand the role of the CRISPR-Cas system in the pathogenicity of *S.* Typhimurium, we assessed infection kinetics of the wildtype and knockout strains in intestinal epithelial cells and macrophages using a gentamicin protection assay. We first evaluated the invasion and intracellular survival of CRISPR-Cas knockout strains in HT-29, a colon carcinoma intestinal epithelial cell line. The assay was performed in both non-polarized and polarized epithelial cells. The phenotypic characteristics of polarized HT-29 cells resemble intestinal epithelial lining. Hence, we decided to evaluate the invasion efficiency of CRISPR-Cas mutant strains in polarized cells as well. Compared to the wildtype strain, the knockout strains were impaired in invading the HT-29, and the invasiveness was rescued upon complementation with the knocked-out gene (Fig. 4.1A). However, the knockout strains exhibited an enhanced attenuation in percentage invasion in polarized cells (Fig. 4.1C). Though the fold replication of all the strains was less in the polarized cells, the knockout strains showed reduced replication than that of the wildtype in both the cell types (Fig. 4.1B and D). The reduction in fold replication of the knockout strains was 1.5-2 times in non-polarized HT-29 (Fig. 4.1B), while in polarized cells, the fold replication of knockout strains was ~1.3 times less than that of the wildtype strain (Fig. 4.1D).

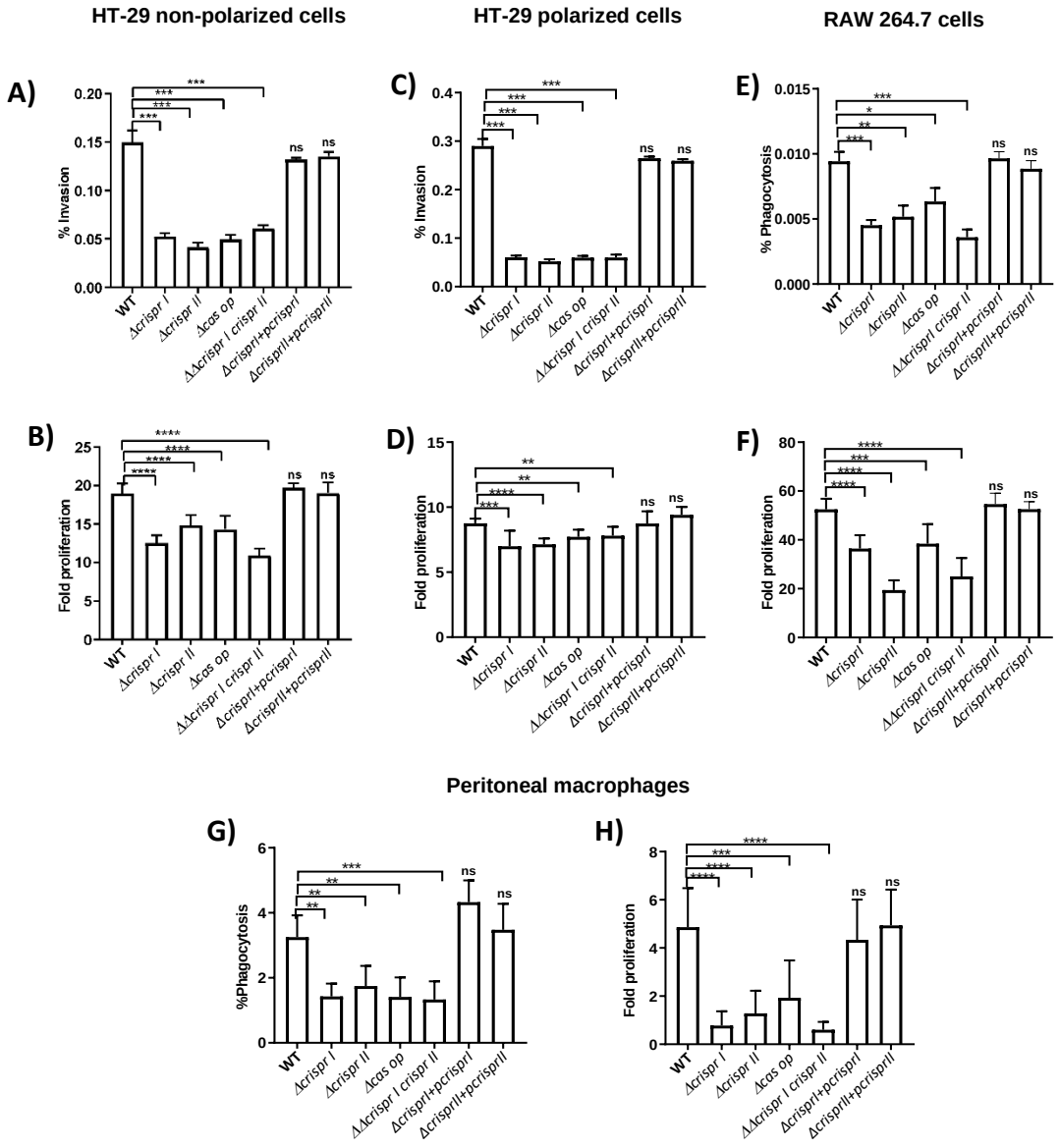

Fig. 4.1: CRISPR-Cas knockout strains show invasion and replication defects in non-phagocytic and phagocytic cell lines. A-D. Non-phagocytic (HT-29 non-polarized, HT-29 polarized) **E-H** phagocytic (RAW 264.7, peritoneal macrophages) cell lines were infected with *S.* Typhimurium strain 14028s wildtype (WT), CRISPR (Δ*crisprI*, Δ*crisprII*, and ΔΔ*crisprI crisprII)* and *cas operon (*Δ*cas op*) knockout strains along with their respective complements (Δ*crisprI*+p*crisprI* and Δ*crisprII*+p*crisprII*). The percentage of phagocytosis/ invasion in macrophages and epithelial cells, respectively was calculated using CFU analysis of the infected cell lysate. Fold proliferation was calculated by normalizing the CFU at 16 h to 2h. Error bars indicate SD. SD. Statistical significance is shown as follows: *,P ≤ 0.05; **, P ≤ 0.01; ***, P ≤0.001; ****, P < 0.0001; and ns, not significant.

After evading the intestinal epithelial barrier, *Salmonella* utilizes macrophages for its systemic dissemination. Therefore, we checked the invasion and intracellular survival of the knockout strains in RAW 264.7 macrophage cell lines and peritoneal macrophages

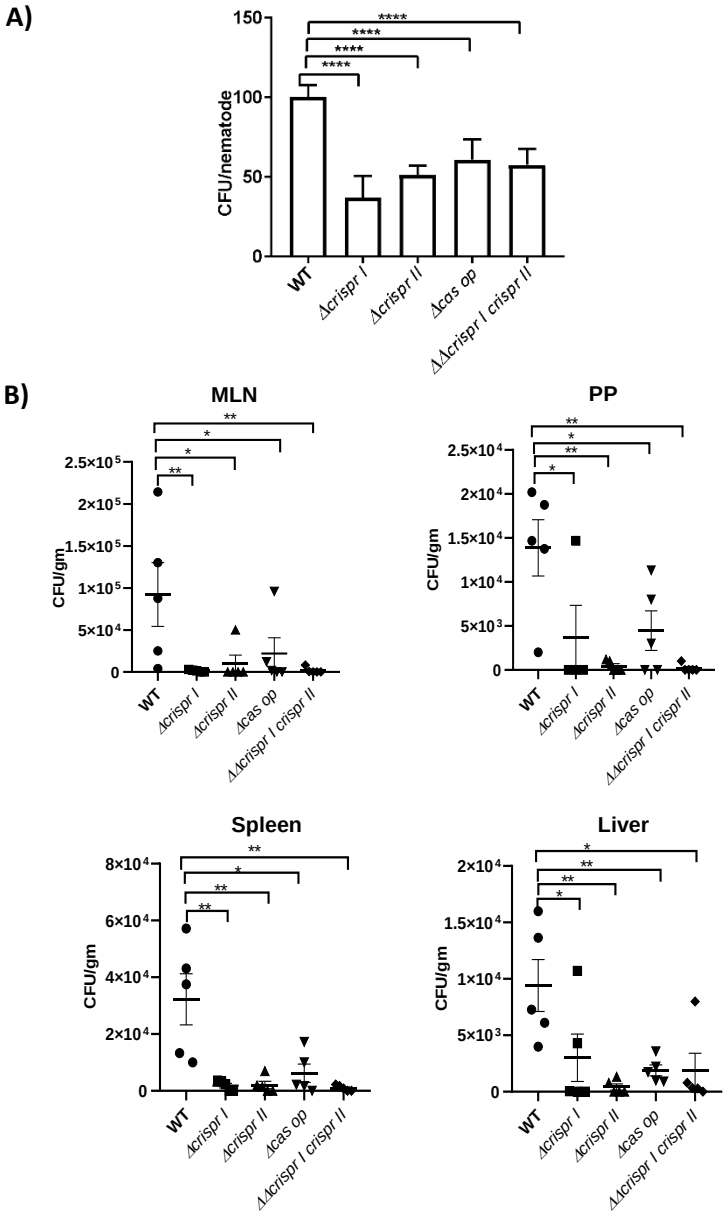

Fig. 4.2: The CRISPR-Cas knockout strains show impaired colonisation in *in-vivo* model organisms (*C. elegans* and mice) A. L4 synchronized worms were infected with mCherry tagged strains of 14028s wildtype (WT), CRISPR (Δ*crisprI*, Δ*crisprII*, and ΔΔ*crisprI crisprII)*, *cas operon (*Δ*cas op*) knockout strains, and *E. coli*-OP50 for 12 h. 24 h post-infection, worms (n=25) were crushed to estimate the bacterial burden (CFU= (No. of colonies × dilution factor×volume plated)/number of worms). **B.** Bacterial burden in different organs of the mice infected with wildtype (WT) and CRISPR-Cas knockout strains was estimated 3 days post-infection by CFU analysis. Error bars indicate SD. SD. Statistical significance is shown as follows: *,P ≤ 0.05;**, P ≤ 0.01; ***, P ≤0.001; ****, P < 0.0001; and ns, not significant

(considered immune sentinels with enhanced phagocytic activity). The percentage of phagocytosis of the knockout strains by the macrophages was reduced to ~ 35-60% of the phagocytosis of the wildtype strain (Fig. 4.1E and G). Moreover, the intracellular proliferation of CRISPR-Cas knockout strains decreased by 1.5-2.5-fold in RAW 264.7 cell lines (Fig. 4.1F) and by 2.5-5-fold in peritoneal macrophages (Fig. 4.1H). In all these infection experiments the complementation of corresponding genes in Δ*crisprI* and Δ*crisprII* showed results comparable to that of the wildtype confirming that the gene deletion process did not produce any polar effects.

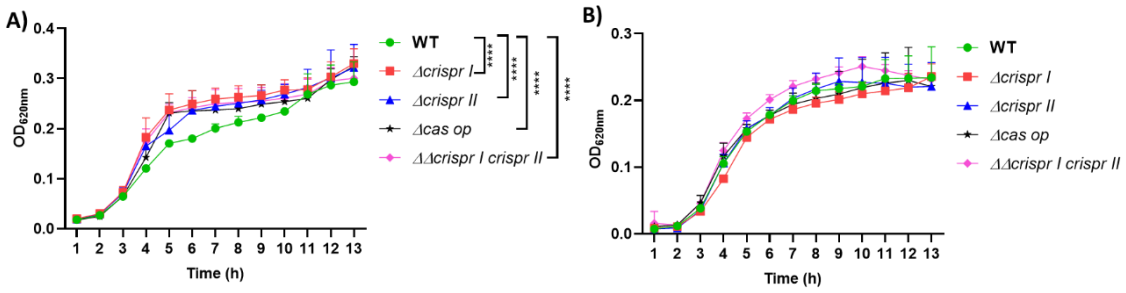

Fig. 4.3: Growth Kinetics of CRISPR-Cas knockout strains in F-media at pH-5.4 and pH- 7.2

The *S.* Typhimurium strain 14028s wildtype (WT), CRISPR (Δ*crisprI*, Δ*crisprII*, and ΔΔ*crisprI crisprII*) and *cas operon (*Δ*cas op*) knockout strains were grown overnight in Luria broth, the bacterial cultures were sub-cultured in a ratio of 1:100 in **A**. F-media, pH 5.4, and **B.** F-media, pH 7.2, and incubated at 37°C under shaking conditions. The OD_{620nm} was monitored every hour and the graph was plotted

4.3.2 Deletion of the CRISPR-Cas system led to attenuated virulence in *in-vivo* models

The impaired intracellular survival of the CRISPR-Cas knockout strains in different cell-culture infection models prompted us to look into the pathogenic potential of the CRISPR-Cas knockout strains in *in-vivo* infection models. Off-late, *C. elegans* has emerged as an attractive model host to study *Salmonella* pathogenesis. The pathogenic potential of the knockout strains was tested in *C. elegans* using the bacterial colonization assay. We observed a 40-60% reduction in the colonization of nematodes exposed to the knockout strains in comparison to those exposed to the wildtype strain (Fig. 4.2A). The observations were further validated in the mice model of typhoid fever, using BALB/c mice. To evaluate organ infiltration, the infected mice were dissected 3 days post-infection to enumerate the bacterial burden in the PP, MLN, liver, and spleen. The knockout strains displayed significantly reduced bacterial burden in all these organs (Fig. 4.2B), pointing to the role of the CRISPR-Cas system in establishing *in vivo* infection of *Salmonella.*

The attenuated proliferation of knockout strains in macrophages could be a consequence of the reduced growth rate in the stringent vacuolar compartment. To assess this, we tested the bacterial growth rate of knockout strains in F-media that mimics the SCV condition. Unexpectedly, we observed an increased growth of all the knockout strains compared to that of the wildtype (Fig 4.3A). This implies that the acidic and nutrient-deprived niche of SCV favors the growth of knockout strains.

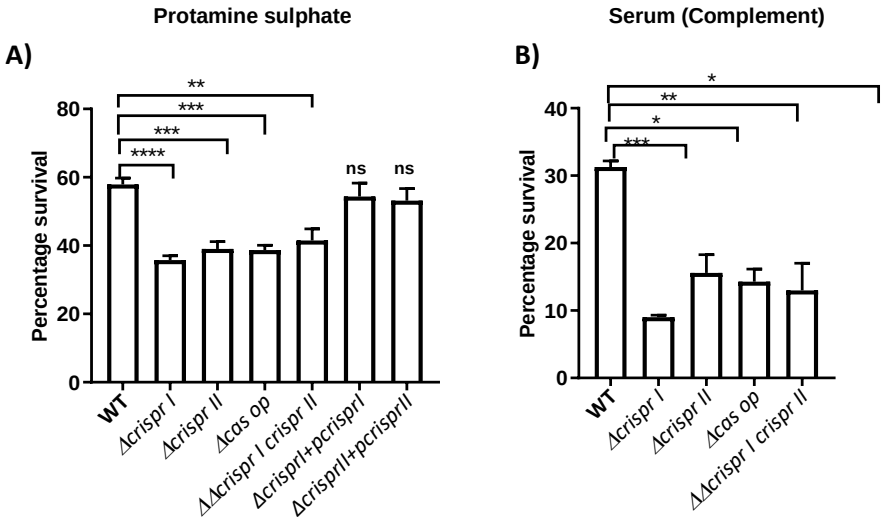

Fig. 4.4: CRISPR-Cas knockout strains show sensitivity against the AMP and serum. A. AMP sensitivity of the mutant strains against the cationic peptide, protamine sulfate was tested by survival assay. The *S.* Typhimurium strain 14028s wildtype (WT), CRISPR (Δ*crisprI*, Δ*crisprII*, and ΔΔ*crisprI crisprII*) and *cas operon (*Δ*cas op*) knockout strains along with their respective complement strains (Δ*crisprI*+p*crisprI* and Δ*crisprII*+p*crisprII*) were exposed to protamine sulfate (0.5µg/ml) for 1 h at 37°C and percentage survival was calculated using the CFU analysis. **B**. The strains were grown in the presence 20% fetal bovine serum and 20% heat-inactivated serum (56°C for 30 min, control) for 1 h. Survival was determined by normalizing the CFU of serum to CFU of heat-inactivated samples used as control. Error bars indicate SD. SD. Statistical significance is shown as follows: *,P ≤ 0.05; **, P ≤ 0.01; ***, P ≤0.001; ****, P < 0.0001; and ns, not significant.

4.3.3 The CRISPR-Cas knockout strains are susceptible to antimicrobial peptides and the complement system

The intestinal invasion by *Salmonella* evokes the innate immune responses by the host. The intestinal epithelial cells reinforce the intestinal barrier function by releasing antimicrobial peptides (AMPs), while the immunity components in serum, like lysozyme and complement (also present in the intestine), restrict microbial colonization (Broz et al., 2012). *Salmonella* shows resistance against these antimicrobials by elongating or modifying the LPS O-antigen (Murray et al., 2006; Pawlak et al., 2017). As the results from

Chapter 2 (Fig. 2.9) indicate an altered LPS profile and the knockouts strains are attenuated in virulence, we estimated the sensitivity of the knockout strains against protamine sulfate (cationic AMP) and serum (Complement). Compared to the wildtype strain, the knockout strains showed ~15-30 % reduced survival in the presence of protamine sulfate (Fig. 4.4A) and serum (Fig. 4.4B). The data indicate that the CRISPR-Cas knockout strains have an impaired ability to overcome innate immune barriers during the dissemination and intestinal infection phase.

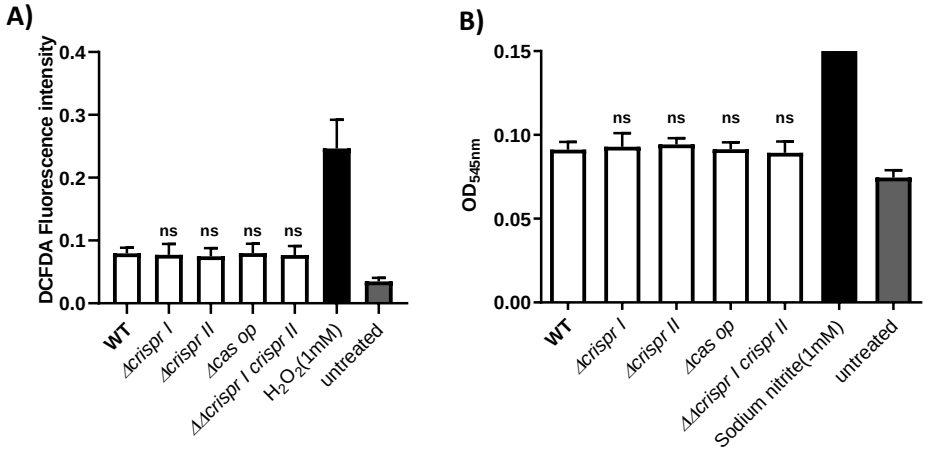

Fig. 4.5: CRISPR-Cas knockout strains induce oxidative burst comparable to that of wildtype in RAW 264.7cells. RAW 264.7 cells were infected with the *S.* Typhimurium strain 14028s wildtype (WT) and CRISPR (Δ*crisprI*, Δ*crisprII*, and ΔΔ*crisprI crisprII*) and *cas operon (*Δ*cas op*) knockout strains as described before for macrophage infection. **A**. The intracellular ROS production was estimated in infected cells. 4 h post-infection using H_2DCFDA [5 µM]. H_2O_2-treated and uninfected cells were used as controls. **B**. 12 h post-infection, the extracellular RNS production was estimated using a Griess reagent. $NaNO_2$-treated and uninfected cells supernatant were used as controls.

4.3.4 The CRISPR-Cas knockout strains induce similar oxidative response in macrophages as that of the wildtype.

Salmonella encounters oxidative and nitrosative stress inside macrophages during the early and late stages of infection (Gogoi et al., 2019). Further, in the mice model, NADPH oxidase, responsible for oxidative stress, is crucial in governing the infection dynamics (Mastroeni & Grant, 2011; Vazquez-Torres & Fang, 2001). The results from previous chapters indicate that the knockout strains are susceptible to an oxidative stressor, H_2O_2, and show an altered LPS profile (Fig. 2.9). As LPS plays an important role in inducing oxidative responses in macrophages (Rhen, 2019), we checked the ROS and RNS production in macrophages infected with the knockout strains. During the early stage of infection (4 h post-infection), the intracellular ROS produced by knockout strains-infected

macrophages was comparable to that of the wildtype infected macrophages (Fig. 4.5A). Likewise, at later stages (16 h post-infection) no significant difference was observed for the extracellular NO produced by the knockout strains-infected macrophages and wildtype infected macrophages (Fig. 4.5B).

4.3.5 The CRISPR-Cas knockout strains show altered expression of *Salmonella* pathogenicity island (SPI-1 and SPI-2) genes

To gain mechanistic insights into the regulation of pathogenesis by the CRISPR-Cas knockout strains, we checked the expression of virulent determinants like the antioxidant genes, and effectors encoded by SPI-1 and SPI-2 pathogenicity island using RT-PCR.

The SPI-1 is required during the intestinal phase of infection (Lostroh & Lee, 2001). The T3SS delivers effector proteins required for intestinal invasion and inflammation inside the host cell. As the CRISPR and Cas knockout strains were defective in the invasion, we first assessed the expression of SPI-1 regulatory genes like *hilD, hilA,* and *h-ns*. All the knockout strains showed reduced expression (~3-4 fold) of *hilA,* (Fig. 4.6A), whereas the *hilD* transcript was significantly downregulated by just 1.2 to 1.7~fold in all the knockout strains (Fig. 4.6A). The *h-ns* gene did not show any difference in the expression among all the strains (Fig. 4.6B). Next, to envisage the impaired invasion ability of the knockout strains, we analyzed the expression of a few important SPI-1 effectors, *sipA, sipD,* and *sopB*. The CRISPR-Cas knockout strains showed ~2-2.5 fold and ~1.5-2 fold reduced expression of *sipA* and *sipD,* respectively (Fig. 4.6C). However, *sopB* was downregulated by only ~ 1.4-fold in the knockout strains, except for Δ*crisprI crisprII* which showed more than two-fold downregulation (Fig. 4.6C).

Following the epithelial cell invasion, *Salmonella* employs SPI-2 encoded effector proteins to form a permissive-replicative niche in SCV (Knuff-Janzen et al., 2020). SPI-2 expression is induced within SCV and is controlled by a two-component system, SsrAB(Löber et al., 2006). The SsrB drives the expression of various SPI-2 effector proteins like PipB2, SpiC, etc. The expression of representative SPI-2 genes and its regulator SsrAB was checked in the strains grown in F-media. The expression of the SPI-2 effector, *pipB2* and *spiC*, and the transcriptional regulator, *ssrB* was downregulated by more than 2-fold in all the knockout strains (Fig. 4.7A-B).

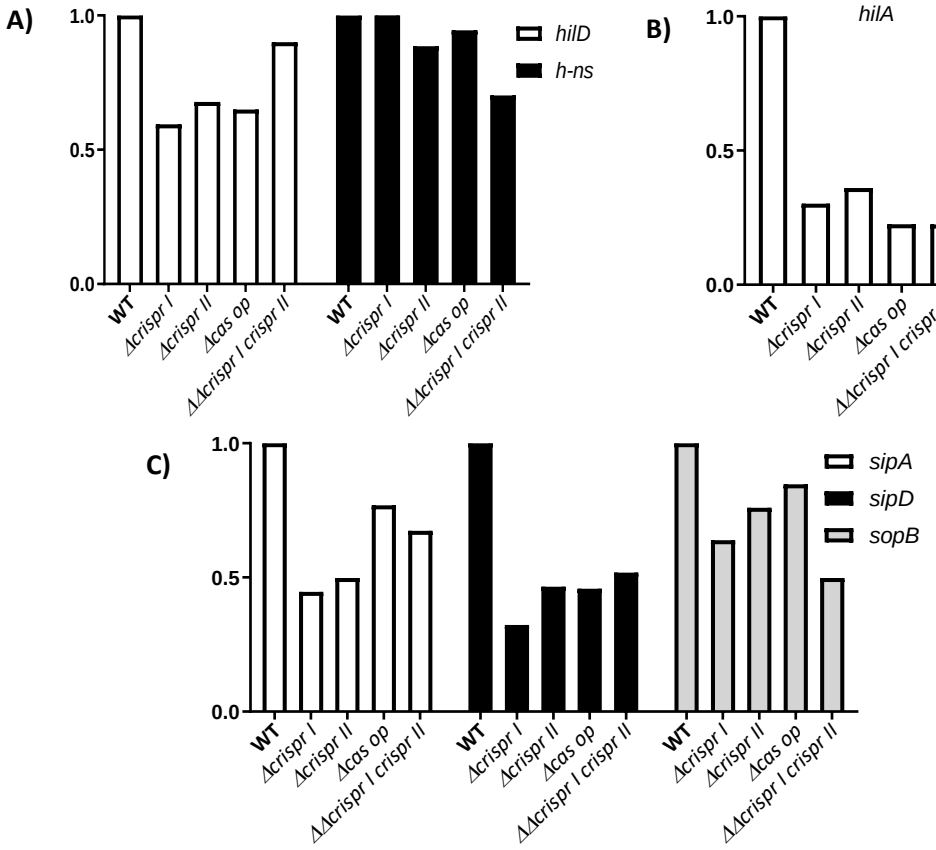

Fig. 4.6: The CRISPR-Cas system regulates SPI-1 gene expression. The CRISPR-Cas knockout strains showed no differences in the expressions of SPI-1 encoded transcriptional activator-*hilD* and global repressor, *h-ns* **(A)**. The difference in expression was observed for transcriptional regulator-*hilA* **(B),** and SPI-1 effectors **(C)**. *S.* Typhimurium strain 14028s wildtype (WT), CRISPR (Δ*crisprI*, Δ*crisprII*, and Δ*crisprI* Δ*crisprII*), and *cas* operon (Δ*cas op*.) knockout strains were grown under SPI-1 inducing condition for 7 h. qRT-PCR was performed from isolated RNA. Relative expression of the gene was calculated using the $2^{-\Delta\Delta Ct}$ method and normalized to the reference gene, *rpoD.*

The low Mg^{2+} milieu of SCV promotes MgtC expression, a virulence protein required for intracellular replication inside macrophages(J. W. Lee & Lee, 2015). Hence, we decided to evaluate the expression of *mgtC* in strains grown in F-media. All the knockout strains show ~2-fold downregulation in *mgtC* expression (Fig. 4.7C).

To combat the oxidative stress response generated by the host cell, *Salmonella* employs an array of antioxidant enzymes like superoxide dismutase, catalase, and peroxidase to detoxify ROS (Rhen, 2019). As the knockout strains are sensitive to H_2O_2 (Fig. 3.1), we analyzed the expression of antioxidant genes, *sodA, sodCI, katG,* and *ahpC* in the strains grown in F-media. All the knockout strains showed reduced expression of

these genes (Fig. 4.6 D-E) explaining the increased susceptibility of the knockout strains to H_2O_2.

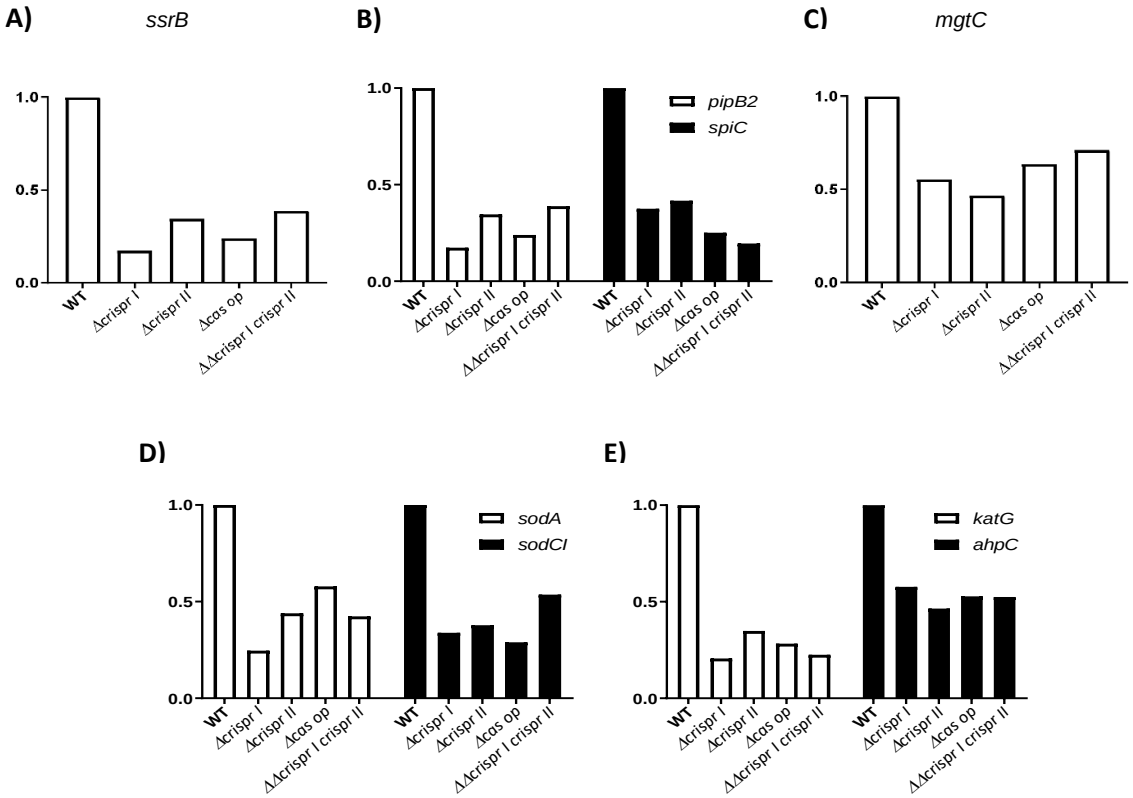

Fig. 4.7: The CRISPR-Cas system regulates SPI-2 gene expression. TheCRISPR-Cas system knockout strains showed reduced expressions of SPI-2 encoded transcriptional regulator-*ssrB* **(A)** SPI-2 effectors **(B)** SPI-3 encoded protein-*mgtC***(C)** and ROS detoxifying enzymes, superoxide dismutases-*sodCI* and *soda* **(D),** catalase-*katG* and peroxidase-*ahpC* **(E)**. *S.* Typhimurium strain 14028s wildtype (WT), CRISPR (Δ*crisprI,* Δ*crisprII,* and Δ*crisprI* Δ*crisprII*), and *cas* operon (Δ*cas op*.) knockout strains were grown in F-Media (SPI-2 inducing condition) for 5 h and qRT-PCR was performed from isolated RNA. Relative expression of the gene was calculated using the $2^{-\Delta\Delta Ct}$ method and normalized to the reference gene, *rpoD.*

4.4 Discussion

Salmonella pathogenesis is a finely tuned process coordinated by the action of virulence determinants encoded by the *Salmonella* pathogenicity islands, which in turn are regulated *via* various response regulators, like OmpR, H-NS, IHF, etc. Recently, Medina et al. reported that in *S.* Typhi, the type 1-E CRISPR-Cas system positively regulates *ompR* (Medina-Aparicio et al., 2021), a response regulator that controls the expression of *ssrAB* (A. K. Lee et al., 2000). Furthermore, Cui et al. demonstrated that the CRISPR-Cas system regulates SPI-1 expression *via* quorum sensing in *S.* Enteritidis (Cui et al., 2020).

Deletion of *cas3* in *S.* Enteritidis showed altered virulence phenotype, i.e., impaired

biofilm formation, invasiveness, and proliferation inside the host. Our study demonstrates that CRISPR-Cas knockout strains of *S.* Typhimurium show reduced invasion in nonphagocytic cells.

Salmonella invasion of non-phagocytic cells is mediated by SPI-1-encoded effectors (Gerlach & Hensel, 2007). SPI-1 translocases SipB, SipC, and SipD, are essential for the attachment of bacteria to the target cells (Lara-Tejero & Galán, 2009), and SipA is required for the efficient invasion of *S.* Typhimurium during the early stages of infection(Jepson et al., 2001b). Following membrane ruffling, *Salmonella* outer membrane proteins (Sops) control cytoskeletal rearrangement during the invasion and regulate polymorphonuclear leukocyte influx (Lou et al., 2019). *In vivo* experiments demonstrate that SopB is required during the initial invasion process but also in the later stage of murine salmonellosis (Giacomodonato et al., 2011). The knockout strains show decreased expression of the SPI-1 genes like *sipA, sipD,* and *sopB* explaining their decreased invasion phenotype. The decreased *sopB* expression in the knockout strains could also contribute to their attenuated virulence.

Adhesins like flagella and Curli inherently contribute to adhesion and invasion, helping the enteric pathogens to invade the epithelial cells (Asten et al., 2000; Sukupolvi et al., 1997). Our observations from Chapter 2 demonstrate reduced expression of the flagellar and curli genes (Fig. 2.18) in the CRISPR-Cas knockout strains, thereby explaining their attenuated invasion in both undifferentiated and differentiated epithelial (HT-29) cells. Before invading the epithelial cells, *Salmonella* must cross the mucosal barrier produced by the goblet cells (Broz et al., 2012). The differentiated HT-29 cells behave similarly to the goblet cells and produce mucin. We observed that the CRISPR-Cas knockout strains showed reduced invasion in differentiated HT-29 cells over undifferentiated cells. The flagellar subunit FljB mediates swimming motility under a highly viscous milieu, such as the gut mucosa(Yamaguchi et al., 2020). Our results in Chapter 2 showed that knockout strains have impaired swimming motility and *fljB* expression (Fig. 2.18A), thereby explaining further the reduced invasion by the knockout strains in differentiated HT-29 cells and their reduced colonization of the PP.

In addition to mucin production, the intestinal lumen houses AMPs and complement proteins (Broz et al., 2012). Our study showed that knockout strains are sensitive to serum complement and AMPs like polymyxin B (Fig3.5D) and protamine sulfate. In pathogenic bacteria including *Salmonella,* it is reported that LPS modification affects bacterial

susceptibility to complement (Murray et al., 2006) and AMPs (Salamon et al., 2020). In Chapter 2 we showed that the CRISPR-Cas knockout strains displayed an altered LPS profile with differential expression of *rfb* gene cluster coding for O-antigen synthesis (Fig. 2.18B). Thus, the increased sensitivity of the knockout strains against AMPs and complement could be attributed to the modified LPS. Nevertheless, the role of other defenses against AMPs needs further investigation.

LPS plays multifaceted roles in pathogens by also providing protection against phagocytosis (Feng et al., 2011). For example,alterations in O-antigen length impact *S.* Typhimurium uptake by macrophages (Hölzer et al., 2009; Murray et al., 2006). The altered LPS profile of the knockout strains could possibly explain the defective phagocytosis of these strains. Following bacterial uptake, the phagocytes elicit an oxidative burst. The toll-like receptors (TLRs), present on infected cells recognize *Salmonella*-derived ligands like lipoproteins (TLR1/2/6), LPS (TLR4), flagellin-FliC (TLR5), CsgA (TLR2), etc., thereby inducing a respiratory burst (Broz et al., 2012). Though our data demonstrate altered expression of PAMPs in the CRISPR-Cas knockout strains, they fail to show any differences in the induction of oxidative response in RAW 264.7 cells compared to that of the wildtype. The different ligands of the knockout strains could be acting differentially such that the net induction of the ROS or RNS is equivalent to that induced by the wildtype strain. Despite comparable induction of ROS/RNS in the macrophages infected with the knockout and wildtype, the knockout strains have attenuated proliferation possibly due to their increased susceptibility to H_2O_2 (Fig. 3.1). The upregulated *ompW* expression in the knockout strains potentiates H_2O_2 influx, thereby enhancing their killing. *Salmonella* also encounters extracellular H_2O_2 during the intestinal phase of infection (Hébrard et al., 2009), wherein it employs an array of oxidative enzymes to scavenge and degrade H_2O_2 molecules. Such enzymes include the cytoplasmic catalases (*katE, katG,* and *katN*), peroxidases (*ahpC*, *tpx*, and *tsaA*), superoxide dismutases (*sodA* and *sodB*), and the periplasmic superoxide dismutases (*sodCI*) (Rhen, 2019). The CRISPR-Cas knockout strains showed downregulation of these enzymes (one representative of each group), thereby displaying increased sensitivity against H_2O_2 and reduced survival within the macrophages and mice.

Besides the above-mentioned mechanisms, the coordinated action of other virulence determinants plays a major role in governing the survival and replication of *Salmonella* within SCV. Among them, MgtC is one such virulence factor that promotes

intra-phagosomal replication under low Mg^{2+}conditions (J. W. Lee & Lee, 2015). It also promotes *Salmonella* virulence by negatively regulating cellulose production(Pontes et al., 2015). Deletion of *mgtC* attenuates *Salmonella* virulence in the mammalian host (Pontes et al., 2015). Interestingly, our study displayed such a relation wherein all the CRISPR-Cas knockout strains showed decreased *mgtC* expression and enhanced cellulose secretion. Thus, supporting their impaired intracellular survival in phagocytic cells and *in vivo* models. The *mgtC* mutants show growth defects in low Mg^{2+} media. Contrary to this, even though the *mgtC* was downregulated in the knockout strains, they showed enhanced proliferation in F-media having low Mg^{2+} concentration. This disparity could suggest the regulation of the acid tolerance response by the CRISPR-Cas system as F-media has acidic pH. In accordance, we did not observe any difference in the growth of the knockout strains in M9 media having low Mg^{2+} concentration but neutral pH. However, these deductions need further exploration. Though the knockout strains survive better under acidic and nutrient conditions similar to that of the stomach they were defective in colonizing the PP. This could be due to increased sensitivity against intestinal AMPs and complement proteins, and the reduced invasion and proliferation of these strains in the epithelial cells.

From the intestinal lumen and PP *Salmonella* are transported to MLN, liver, and spleen either as extracellular bacteria or within the phagocytic cells(Bravo-Blas et al., 2019). Thus, the pathogen needs to overcome the innate immune barrier like resistance against AMPs and ROS to disperse systemically. Resistance against serum is also vital for the development of systemic salmonellosis. *Salmonella* achieves this through three important factors: LPS, outer membrane proteins (like PagC and Rck), and siderophores (Gao et al., 2019b). The CRISPR-Cas knockout strains show reduced survival in presence of AMPs, H_2O_2, and serum, thereby explaining their attenuated colonization and systemic spread. The altered LPS profile in the knockout strains could be one of the reasons for their increased sensitivity against AMPs and serum. However, the role of the CRISPR-Cas system in regulating other factors (outer membrane protein and siderophore) cannot be ruled out.

In the intestinal lumen, the SPI-1 transcriptional regulator, *hilD*, binds upstream of the master regulator, *hilA*, thereby counteracting its*h-ns*-mediated repression. HilA in turn regulates the expression of the T3SS'sstructural and effector proteins like Sips and Sops. In our study, the reduced expression of *hilA* in the CRISPR-Cas knockout strains may explain the other T3SS structural and effector proteins. Following the internalization of

bacteria, the SPI-2-encoded SsrAB system gets activated in response to the acidic milieu. SsrA kinase phosphorylates the key regulatory factor of SPI-2, SsrB, which in turn activates the expression of SPI-2 encoded effector proteins like SpiC, PipB2, etc. Decreased expression of these and other virulence genes like, *mgtC*, *katG*, *sod* and *ahpC* in the knockout strains could have attenuated their virulence impacting colonization in *C. elegans* and mice model of *Salmonella* infection.

Taken together our data highlights that the CRISPR-Cas system regulates SPI-1, SPI-2, and other virulence genes to aid the pathogenic lifestyle of *Salmonella*. The detailed regulatory mechanisms are to be explored further.

Chapter 5

Conclusions and Future Prospects

5.1 Conclusion

The role of the gene-editing tool, the CRISPR-Cas systems has gone beyond the canonical function of adaptive immunity. Recent bacterial research shows its potential in regulating bacterial endogenous genes thereby influencing the physiological characteristics and virulence of the bacteria. An increasing number of reports further support that the CRISPR-Cas system plays a role in biofilm formation, antimicrobial resistance, and bacterial pathogenesis. However, their underlying mechanisms are largely unclear.

The function of individual *cas* genes or the entire CRISPR-Cas system in controlling biofilm formation in *Salmonella* has been explored, but the role in governing the biofilm kinetics and the regulatory role of CRISPR arrays is less studied. Comprehensive studies on the impact of this system on pellicle biofilm is an unexplored niche. Thus, we characterized the role of the CRISPR-Cas system in regulating different stages of *Salmonella* biofilm formation. Our study focused on analysing the effects of the CRISPR-Cas system on surface-associated and pellicle biofilm formation. We demonstrate that the CRISPR array and *cas* genes modulate the expression of various biofilm-associated genes in *Salmonella*, whereby surface and pellicle biofilm formation is distinctively regulated. Our finding suggests, that the CRISPR-Cas system positively regulates the surface-attached biofilm formation by independently regulating the flagellar regulator, Yddx. While at later stages CRISPR-Cas inhibits pellicle biofilm formation by negatively regulating one of the global biofilm regulators, CRP. Thus, affecting the expression of the biofilm components like Curli and cellulose. However, it independently regulates the expression of cellulose exporter, *bcsC*, which could govern the pellicle biofilm formation. The CRISPR-Cas system also regulates the LPS modification genes, thereby impacting the LPS profile and O-antigen production and hence the ECM of the biofilm.

LPS along with outer membrane proteins maintains the bacterial cell membrane integrity. The CRISPR-Cas knockout strains showed an altered LPS profile, and modulation of membrane properties like, cell membrane permeability and hydrophobicity. The variation in the LPS profile rendered the knockout strains susceptible to LPS-specific AMP, polymyxin B. Preliminary computational analysis indicated *ompW* (H_2O_2 influx pump of *Salmonella*) as one of the targets for the CRISPR1 spacer. Consequently, we demonstrated that the CRISPR-Cas system regulates the expression of *ompW* and *Salmonella's* sensitivity against hydrogen peroxide. Thus, in a

nutshell we establish that the CRISPR-Cas system modulates the membrane properties of *Salmonella* thereby governing its defense against antimicrobial agents like hydrogen peroxide and antimicrobial peptides.

We next showed that the CRISPR-Cas system regulates *Salmonella* pathogenesis by fine-tuning the expression of various virulence factors. Using *in vivo* cell culture models, we showed that the CRISPR-Cas system regulates *Salmonella*'s invasion and replication in the intestinal and macrophage cell lines. The results were further validated using *in vivo* infection models - *C. elegans* and BALB/c mice, which showed attenuated virulence and systemic dissemination of knockout strains. We further dissected the CRISPR-Cas regulatory mechanisms in governing the virulence of the bacteria. We envisage that the regulation of LPS characteristics by the CRISPR-Cas system could possibly be controlling *Salmonella's* phagocytosis and its sensitivity against innate immune barriers like AMP and the complement system. The gene expression analysis depicts that the CRISRP-Cas system positively regulates SPI-1 encoded genes including its master regulator, *hilA*. Thus, aiding the invasion of *Salmonella* into the epithelial cells. We also found that the CRISPR-Cas system regulates the expression of the SPI-2-encoded global regulatory system, SsrAB, and the SPI-2 effector proteins like SpiC, PipB2, etc. The system also regulates the expression of other important virulence proteins. It regulates the expression of MgtC, required for survival within macrophages and virulence in the host. The survival of the bacteria against oxidative stress like hydrogen peroxide is governed by the regulation of antioxidant genes like *sodA, sodCI, katG* and *ahpC*. Thus, we conclude that the regulation of multiple virulence factors by the CRISPR-Cas system promotes the survival and systemic dissemination of *Salmonella*.

Overall, this study adds to our understanding of the role of the CRISPR-Cas system in regulating the pathogenic lifestyle of *Salmonella* by regulating various physiological features of the system.

5.2 Future prospects

In the present work, we have demonstrated that the CRISPR-Cas system regulates biofilm formation, membrane properties and virulence of *S.* Typhimurium. It provides an important correlation between the study of the CRISPR-Cas system and bacterial virulence through the regulation of endogenous genes. However, there are several aspects that could

be studied in the future to understand the CRISPR-Cas regulatory mechanisms of *Salmonella* pathogenesis.

Our study shows that the CRISPR-Cas differentially regulates *Salmonella* biofilm formation in liquid cultures. This can be extended further to understand the CRISPR-Cas mediated regulation of *Salmonella* biofilm formation under gallstone-mimicking condition. Our results demonstrated that knockout strains survive better in F-media (acidic-condition, encountered by *Salmonella* in the gastro-intestinal tract). Further studies can provide regulatory insights into the role of the CRISPR-Cas system in regulating some acid shock proteins.

It is known that the type IE CRISPR-Cas system acts by degrading DNA. Our and other studies suggest the regulation of endogenous genes by this system in *Salmonella*. As a matter of chance, one could explore, if the CRISPR-Cas system is mediating the expression of the target gene *via* mRNA degradation. However, this is a remote possibility but deserves exploration.

Our study has unveiled the role of the CRISPR-Cas system in regulating a few global regulators like the CRP and SsrB. One can probe further to confirm if some other global regulators are being regulated by the system and what is the mechanism of these regulations?

We now know that the CRISPR-Cas system is actively regulating multiple physiological aspects and is active during the pathogenic lifestyle of *Salmonella*. One could therefore explore the use of the CRISPR-Cas system as an anti-*Salmonella* strategy, wherein we can provide the *Salmonella*-specific CRISPR spacers in an array. These spacers can now guide the Cas system to target the *Salmonella* genome thereby degrading it and killing the pathogen. Furthermore, regulatory compounds could be synthesized to block the expression of the *cas* genes and use the same to decrease the virulence of bacteria.

References:

Abidi, W., Torres-Sánchez, L., Siroy, A., & Krasteva, P. V. (2022). Weaving of bacterial cellulose by the Bcs secretion systems. *FEMS Microbiology Reviews*, *46*(2). https://doi.org/10.1093/femsre/fuab051

Abulreesh, H. H., & Abulreesh, H. H. (2012). Salmonellae in the Environment. *Salmonella - Distribution, Adaptation, Control Measures and Molecular Technologies*. https://doi.org/10.5772/28201

Acheson, J. F., Derewenda, Z. S., & Zimmer, J. (2019). Architecture of the Cellulose Synthase Outer Membrane Channel and Its Association with the Periplasmic TPR Domain. *Structure*, *27*(12), 1855-1861.e3. https://doi.org/10.1016/j.str.2019.09.008

Ahimou, F., Paquot, M., Jacques, P., Thonart, P., & Rouxhet, P. G. (2001). Influence of electrical properties on the evaluation of the surface hydrophobicity of Bacillus subtilis. *Journal of Microbiological Methods*, *45*(2), 119–126. https://doi.org/10.1016/S0167-7012(01)00240-8

Ahmad, I., Cimdins, A., Beske, T., & Römling, U. (2017). Detailed analysis of c-di-GMP mediated regulation of csgD expression in Salmonella typhimurium. *BMC Microbiology*, *17*(1), 1–12. https://doi.org/10.1186/S12866-017-0934-5

Ahmad, I., Lamprokostopoulou, A., le Guyon, S., Streck, E., Barthel, M., Peters, V., Hardt, W. D., & Römling, U. (2011). Complex c-di-GMP signaling networks mediate transition between virulence properties and biofilm formation in Salmonella enterica serovar Typhimurium. *PloS One*, *6*(12). https://doi.org/10.1371/JOURNAL.PONE.0028351

Ahmad, I., Wigren, E., le Guyon, S., Vekkeli, S., Blanka, A., el Mouali, Y., Anwar, N., Chuah, M. L., Lünsdorf, H., Frank, R., Rhen, M., Liang, Z. X., Lindqvist, Y., & Römling, U. (2013). The EAL-like protein STM1697 regulates virulence phenotypes, motility and biofilm formation in Salmonella typhimurium. *Molecular Microbiology*, *90*(6), 1216–1232. https://doi.org/10.1111/MMI.12428

Altier, C., Suyemoto, M., & Lawhon, S. D. (2000). Regulation of Salmonella enterica serovar typhimurium invasion genes by csrA. *Infection and Immunity*, *68*(12), 6790–6797. https://doi.org/10.1128/IAI.68.12.6790-6797.2000

Anamourlis, C. (2020). The cell membrane. *Southern African Journal of Anaesthesia and Analgesia*, *26*(6), S1–S7. https://doi.org/10.36303/SAJAA.2020.26.6.S3.2527

Armitano, J., Mejean, V., & Jourlin-Castelli, C. (2014). Gram-negative bacteria can also form pellicles. *Environ Microbiol Rep*, *6*(6), 534–544. https://doi.org/10.1111/1758-2229.12171

Asten, F. J. A. M., Hendriks, H. G. C. J. M., Koninkx, J. F. J. G., Zeijst, B. A. M., & Gaastra, W. (2000). Inactivation of the flagellin gene of Salmonella enterica serotype enteritidis strongly reduces invasion into differentiated Caco-2 cells. *FEMS Microbiology Letters*, *185*(2), 175–179. https://doi.org/10.1111/J.1574-6968.2000.TB09058.X

Azimi, T., Zamirnasta, M., Sani, M. A., Dallal, M. M. S., & Nasser, A. (2020). Molecular Mechanisms of Salmonella Effector Proteins: A Comprehensive Review. *Infection and Drug Resistance*, *13*, 11. https://doi.org/10.2147/IDR.S230604

Barbosa, F. de O., Freitas Neto, O. C. de, Batista, D. F. A., Almeida, A. M. de, Rubio, M. da S., Alves, L. B. R., Vasconcelos, R. de O., Barrow, P. A., & Berchieri Junior, A. (2017). Contribution of flagella and motility to gut colonisation and pathogenicity of Salmonella Enteritidis in the chicken. *Brazilian Journal of Microbiology*, *48*(4), 754–759. https://doi.org/10.1016/J.BJM.2017.01.012

Bartra, S. S., Gong, X., Lorica, C. D., Jain, C., Nair, M. K. M., Schifferli, D., Qian, L., Li, Z., Plano, G. v., & Schesser, K. (2012). The outer membrane protein A (OmpA) of Yersinia pestis promotes intracellular survival and virulence in mice. *Microbial Pathogenesis*, *52*(1), 41–46. https://doi.org/10.1016/J.MICPATH.2011.09.009

Blanc-Potard, A. B., & Groisman, E. A. (1997). The Salmonella selC locus contains a pathogenicity island mediating intramacrophage survival. *EMBO Journal*, *16*(17), 5376–5385. https://doi.org/10.1093/emboj/16.17.5376

Blanc-Potard, A. B., Solomon, F., Kayser, J., & Groisman, E. A. (1999). The SPI-3 pathogenicity island of Salmonella enterica. *Journal of Bacteriology*, *181*(3), 998–1004. https://doi.org/10.1128/JB.181.3.998-1004.1999

Bourgogne, A., Garsin, D. A., Qin, X., Singh, K. v., Sillanpaa, J., Yerrapragada, S., Ding, Y., Dugan-Rocha, S., Buhay, C., Shen, H., Chen, G., Williams, G., Muzny, D., Maadani, A., Fox, K. A., Gioia, J., Chen, L., Shang, Y., Arias, C. A., … Weinstock, G. M. (2008). Large scale variation in Enterococcus faecalis illustrated by the genome analysis of strain OG1RF. *Genome Biology*, *9*(7). https://doi.org/10.1186/GB-2008-9-7-R110

Bozic, B., Repac, J., & Djordjevic, M. (2019). Endogenous gene regulation as a predicted main function of type I-E CRISPR/Cas system in E. Coli. *Molecules*, *24*(4). https://doi.org/10.3390/molecules24040784

Bravo-Blas, A., Utriainen, L., Clay, S. L., Kästele, V., Cerovic, V., Cunningham, A. F., Henderson, I. R., Wall, D. M., & Milling, S. W. F. (2019). Salmonella enterica Serovar Typhimurium Travels to Mesenteric Lymph Nodes Both with Host Cells and Autonomously . *The Journal of Immunology*, *202*(1), 260–267. https://doi.org/10.4049/JIMMUNOL.1701254/-/DCSUPPLEMENTAL

Brawn, L. C., Hayward, R. D., & Koronakis, V. (2007). Salmonella SPI1 effector SipA persists after entry and cooperates with a SPI2 effector to regulate phagosome maturation and intracellular replication. *Cell Host & Microbe*, *1*(1), 63–75. https://doi.org/10.1016/J.CHOM.2007.02.001

Brombacher, E., Baratto, A., Dorel, C., & Landini, P. (2006). Gene expression regulation by the Curli activator CsgD protein: modulation of cellulose biosynthesis and control of negative determinants for microbial adhesion. *Journal of Bacteriology*, *188*(6), 2027–2037. https://doi.org/10.1128/JB.188.6.2027-2037.2006

Brown, P. K., Dozois, C. M., Nickerson, C. A., Zuppardo, A., Terlonge, J., & Curtiss, R. (2001). MlrA, a novel regulator of curli (AgF) and extracellular matrix synthesis by Escherichia coli and Salmonella enterica serovar Typhimurium. *Molecular Microbiology*, *41*(2), 349–363. https://doi.org/10.1046/J.1365-2958.2001.02529.X

Broz, P., Ohlson, M. B., & Monack, D. M. (2012). Innate immune response to Salmonella typhimurium, a model enteric pathogen. *Gut Microbes*, *3*(2), 62. https://doi.org/10.4161/GMIC.19141

Busch, A., Richter, A. S., & Backofen, R. (2008). IntaRNA: efficient prediction of bacterial sRNA targets incorporating target site accessibility and seed regions. *Bioinformatics (Oxford, England)*, *24*(24), 2849–2856. https://doi.org/10.1093/BIOINFORMATICS/BTN544

Cabeza, M. L., Aguirre, A., Soncini, F. C., & Véscovi, E. G. (2007). Induction of RpoS degradation by the two-component system regulator RstA in Salmonella enterica. *Journal of Bacteriology*, *189*(20), 7335–7342. https://doi.org/10.1128/JB.00801-07

Calderón, I. L., Morales, E., Caro, N. J., Chahúan, C. A., Collao, B., Gil, F., Villarreal, J. M., Ipinza, F., Mora, G. C., & Saavedra, C. P. (2011). Response regulator ArcA of Salmonella enterica serovar Typhimurium downregulates expression of OmpD, a porin facilitating uptake of hydrogen peroxide. *Research in Microbiology*, *162*(2), 214–222. https://doi.org/10.1016/J.RESMIC.2010.11.001

Canton, M., Sánchez-Rodríguez, R., Spera, I., Venegas, F. C., Favia, M., Viola, A., & Castegna, A. (2021). Reactive Oxygen Species in Macrophages: Sources and Targets. *Frontiers in Immunology*, *12*. https://doi.org/10.3389/FIMMU.2021.734229

Catron, D. M., Sylvester, M. D., Lange, Y., Kadekoppala, M., Jones, B. D., Monack, D. M., Falkow, S., & Haldar, K. (2002). The Salmonella-containing vacuole is a major site of intracellular cholesterol accumulation and recruits the GPI-anchored protein CD55. *Cellular Microbiology*, *4*(6), 315–328. https://doi.org/10.1046/J.1462-5822.2002.00198.X

Chambers, J. R., & Sauer, K. (2013). Small RNAs and their role in biofilm formation. *Trends in Microbiology*, *21*(1), 39–49. https://doi.org/10.1016/J.TIM.2012.10.008

Chaudhuri, D., Chowdhury, A. R., Biswas, B., & Chakravortty, D. (2018). Salmonella Typhimurium Infection Leads to Colonization of the Mouse Brain and Is Not Completely Cured With Antibiotics. *Frontiers in Microbiology*, *9*(JUL). https://doi.org/10.3389/FMICB.2018.01632

Cheng, R. A., Eade, C. R., & Wiedmann, M. (2019). Embracing Diversity: Differences in Virulence Mechanisms, Disease Severity, and Host Adaptations Contribute to the Success of Nontyphoidal Salmonella as a Foodborne Pathogen. *Frontiers in Microbiology*, *10*(JUN). https://doi.org/10.3389/FMICB.2019.01368

Cheng, X., Zheng, X., Zhou, X., Zeng, J., Ren, Z., Xu, X., Cheng, L., Li, M., Li, J., & Li, Y. (2016). Regulation of oxidative response and extracellular polysaccharide synthesis by a diadenylate cyclase in Streptococcus mutans. *Environmental Microbiology*, *18*(3), 904–922. https://doi.org/10.1111/1462-2920.13123

Choi, S., Choi, E., Cho, Y. J., Nam, D., Lee, J., & Lee, E. J. (2019). The Salmonella virulence protein MgtC promotes phosphate uptake inside macrophages. *Nature Communications*, *10*(1). https://doi.org/10.1038/S41467-019-11318-2

Choi, U., & Lee, C. R. (2019). Distinct Roles of Outer Membrane Porins in Antibiotic Resistance and Membrane Integrity in Escherichia coli. *Frontiers in Microbiology*, *10*(APR). https://doi.org/10.3389/FMICB.2019.00953

Corcoran, M., Morris, D., de Lappe, N., O'Connor, J., Lalor, P., Dockery, P., & Cormican, M. (2014). Commonly used disinfectants fail to eradicate Salmonella enterica biofilms from food contact surface materials. *Applied and Environmental Microbiology*, *80*(4), 1507–1514. https://doi.org/10.1128/AEM.03109-13

Costa, A. F. S., Almeida, F. C. G., Vinhas, G. M., & Sarubbo, L. A. (2017). Production of bacterial cellulose by Gluconacetobacter hansenii using corn steep liquor as nutrient sources. *Frontiers in Microbiology*, *8*(OCT). https://doi.org/10.3389/fmicb.2017.02027

Crawford, R. W., Gibson, D. L., Kay, W. W., & Gunn, J. S. (2008). Identification of a bile-induced exopolysaccharide required for salmonella biofilm formation on gallstone surfaces. *Infection and Immunity*, *76*(11), 5341–5349. https://doi.org/10.1128/IAI.00786-08

Crawford, R. W., Reeve, K. E., & Gunn, J. S. (2010). Flagellated but not hyperfimbriated Salmonella enterica serovar Typhimurium attaches to and forms biofilms on cholesterol-coated surfaces. *J Bacteriol*, *192*(12), 2981–2990. https://doi.org/10.1128/JB.01620-09

Crawford, R. W., Rosales-Reyes, R., Ramírez-Aguilar, M. de la L., Chapa-Azuela, O., Alpuche-Aranda, C., & Gunn, J. S. (2010). Gallstones play a significant role in Salmonella spp. gallbladder colonization and carriage. *Proceedings of the National Academy of Sciences*, *107*(9), 4353–4358. https://doi.org/10.1073/PNAS.1000862107

Cristina Solano, B. G. J. V. C. B. J.-M. G. C. G. I. L. (2002). Genetic analysis of Salmonella enteritidis biofilm formation: critical role of cellulose. *Molecular Microbiology*, *43*(3), 793–808.

Cui, L., Wang, X., Huang, D., Zhao, Y., Feng, J., Lu, Q., Pu, Q., Wang, Y., Cheng, G., Wu, M., & Dai, M. (2020). CRISPR-cas3 of Salmonella Upregulates Bacterial Biofilm Formation and Virulence to Host Cells by Targeting Quorum-Sensing Systems. *Pathogens*, *9*(1). https://doi.org/10.3390/pathogens9010053

da Re, S., & Ghigo, J. M. (2006). A CsgD-independent pathway for cellulose production and biofilm formation in Escherichia coli. *Journal of Bacteriology*, *188*(8), 3073–3087. https://doi.org/10.1128/JB.188.8.3073-3087.2006

Darwin, K. H., & Miller, V. L. (1999). Molecular basis of the interaction of Salmonella with the intestinal mucosa. *Clinical Microbiology Reviews*, *12*(3), 405–428. https://doi.org/10.1128/CMR.12.3.405

Datsenko, K. A., & Wanner, B. L. (2000). *One-step inactivation of chromosomal genes in Escherichia coli K-12 using PCR products* (Issue 12). www.pnas.orgcgidoi10.1073pnas.120163297

Debenedictis, E. P., Liu, J., & Keten, S. (n.d.). *A P P L I E D S C I E N C E S A N D E N G I N E E R I N G Adhesion mechanisms of curli subunit CsgA to abiotic surfaces*.

Delcour, A. H. (2009). Outer membrane permeability and antibiotic resistance. *Biochimica et Biophysica Acta*, *1794*(5), 808–816. https://doi.org/10.1016/J.BBAPAP.2008.11.005

Demirbilek, S. K., & Demirbilek, S. K. (2017). Salmonellosis in Animals. *Salmonella - A Re-Emerging Pathogen*. https://doi.org/10.5772/INTECHOPEN.72192

Desai, S. K., & Kenney, L. J. (2019). Switching Lifestyles Is an in vivo Adaptive Strategy of Bacterial Pathogens. *Frontiers in Cellular and Infection Microbiology*, *9*. https://doi.org/10.3389/FCIMB.2019.00421

Desai, S. K., Padmanabhan, A., Harshe, S., Zaidel-Bar, R., & Kenney, L. J. (2019). Salmonella biofilms program innate immunity for persistence in Caenorhabditis elegans. *Proceedings of the National Academy of Sciences of the United States of America*, *116*(25), 12462–12467. https://doi.org/10.1073/PNAS.1822018116/SUPPL_FILE/PNAS.1822018116.SM03.MOV

Devi, K. P., Nisha, S. A., Sakthivel, R., & Pandian, S. K. (2010). Eugenol (an essential oil of clove) acts as an antibacterial agent against Salmonella typhi by disrupting the cellular membrane. *Journal of Ethnopharmacology*, *130*(1), 107–115. https://doi.org/10.1016/J.JEP.2010.04.025

di Domenico, E. G., Cavallo, I., Pontone, M., Toma, L., & Ensoli, F. (2017). Biofilm producing Salmonella typhi: Chronic colonization and development of gallbladder cancer. *International Journal of Molecular Sciences*, *18*(9). https://doi.org/10.3390/ijms18091887

Dong, Y., Ma, K., Cao, Q., Huang, H., Nie, M., Liu, G., Jiang, M., Lu, C., & Liu, Y. (2021). CRISPR-dependent endogenous gene regulation is required for virulence in piscine Streptococcus agalactiae. *Emerging Microbes & Infections*, *10*(1), 2113. https://doi.org/10.1080/22221751.2021.2002127

Douce, G. R., Amin, I. I., & Stephen, J. (1991). Invasion of HEp-2 cells by strains of Salmonella typhimurium of different virulence in relation to gastroenteritis. *Journal of Medical Microbiology*, *35*(6), 349–357. https://doi.org/10.1099/00222615-35-6-349/CITE/REFWORKS

Drecktrah, D., Knodler, L. A., Galbraith, K., & Steele-Mortimer, O. (2005). The Salmonella SPI1 effector SopB stimulates nitric oxide production long after invasion. *Cellular Microbiology*, *7*(1), 105–113. https://doi.org/10.1111/j.1462-5822.2004.00436.x

Edwards, R. A., & Puente, J. L. (1998). Fimbrial expression in enteric bacteria: a critical step in intestinal pathogenesis. *Trends in Microbiology*, *6*(7), 282–287. https://doi.org/10.1016/S0966-842X(98)01288-8

el Mouali, Y., Gaviria-Cantin, T., Sánchez-Romero, M. A., Gibert, M., Westermann, A. J., Vogel, J., & Balsalobre, C. (2018a). CRP-cAMP mediates silencing of Salmonella virulence at the post-transcriptional level. *PLoS Genetics*, *14*(6). https://doi.org/10.1371/JOURNAL.PGEN.1007401

el Mouali, Y., Gaviria-Cantin, T., Sánchez-Romero, M. A., Gibert, M., Westermann, A. J., Vogel, J., & Balsalobre, C. (2018b). CRP-cAMP mediates silencing of Salmonella virulence at the post-transcriptional level. *PLoS Genetics*, *14*(6). https://doi.org/10.1371/JOURNAL.PGEN.1007401

Ellermeier, C. D., Ellermeier, J. R., & Slauch, J. M. (2005). HilD, HilC and RtsA constitute a feed forward loop that controls expression of the SPI1 type three secretion system regulator hilA in Salmonella enterica serovar Typhimurium. *Molecular Microbiology*, *57*(3), 691–705. https://doi.org/10.1111/J.1365-2958.2005.04737.X

Eriksson, S., Lucchini, S., Thompson, A., Rhen, M., & Hinton, J. C. D. (2003). Unravelling the biology of macrophage infection by gene expression profiling of intracellular Salmonella enterica. *Molecular Microbiology*, *47*(1), 103–118. https://doi.org/10.1046/J.1365-2958.2003.03313.X

Espinosa, E., & Casadesús, J. (2014). Regulation of Salmonella enterica pathogenicity island 1 (SPI-1) by the LysR-type regulator LeuO. *Molecular Microbiology*, *91*(6), 1057–1069. https://doi.org/10.1111/MMI.12500

Eswarappa, S. M., Karnam, G., Nagarajan, A. G., Chakraborty, S., & Chakravortty, D. (2009). lac repressor is an antivirulence factor of Salmonella enterica: its role in the evolution of virulence in Salmonella. *PloS One*, *4*(6). https://doi.org/10.1371/JOURNAL.PONE.0005789

Fass, E., & Groisman, E. A. (2009a). Control of Salmonella pathogenicity island-2 gene expression. *Current Opinion in Microbiology*, *12*(2), 199–204. https://doi.org/10.1016/J.MIB.2009.01.004

Fass, E., & Groisman, E. A. (2009b). Control of Salmonella pathogenicity island-2 gene expression. *Current Opinion in Microbiology*, *12*(2), 199–204. https://doi.org/10.1016/J.MIB.2009.01.004

Figueira, R., & Holden, D. W. (2012). Functions of the Salmonella pathogenicity island 2 (SPI-2) type III secretion system effectors. *Microbiology (Reading, England)*, *158*(Pt 5), 1147–1161. https://doi.org/10.1099/MIC.0.058115-0

Food safety. (n.d.). Retrieved November 25, 2022, from https://www.who.int/news-room/fact-sheets/detail/food-safety

Frank, J. F., & Chmielewski, R. (2001). Inn uence of Surface Finish on the Cleanability of Stainless Steel. In *Journal of Food Protection* (Vol. 64, Issue 8).

http://meridian.allenpress.com/jfp/article-pdf/64/8/1178/1674018/0362-028x-64_8_1178.pdf

Freeman, J. A., Rappl, C., Kuhle, V., Hensel, M., & Miller, S. I. (2002). SpiC is required for translocation of Salmonella pathogenicity island 2 effectors and secretion of translocon proteins SseB and SseC. *Journal of Bacteriology*, *184*(18), 4971–4980. https://doi.org/10.1128/JB.184.18.4971-4980.2002

Frye, J., Karlinsey, J. E., Felise, H. R., Marzolf, B., Dowidar, N., McClelland, M., & Hughes, K. T. (2006). Identification of new flagellar genes of Salmonella enterica serovar typhimurium. *Journal of Bacteriology*, *188*(6), 2233–2243. https://doi.org/10.1128/JB.188.6.2233-2243.2006

Futoma-Kołoch, B., Godlewska, U., Guz-Regner, K., Dorotkiewicz-Jach, A., Klausa, E., Rybka, J., & Bugla-Płoskońska, G. (2015). Presumable role of outer membrane proteins of Salmonella containing sialylated lipopolysaccharides serovar Ngozi, sv. Isaszeg and subspecies arizonae in determining susceptibility to human serum. *Gut Pathogens*, *7*(1). https://doi.org/10.1186/S13099-015-0066-0

Galié, S., García-Gutiérrez, C., Miguélez, E. M., Villar, C. J., & Lombó, F. (2018). Biofilms in the food industry: Health aspects and control methods. In *Frontiers in Microbiology* (Vol. 9, Issue MAY). Frontiers Media S.A. https://doi.org/10.3389/fmicb.2018.00898

Gal-Mor, O. (2019). Persistent infection and long-term carriage of typhoidal and nontyphoidal salmonellae. *Clinical Microbiology Reviews*, *32*(1). https://doi.org/10.1128/CMR.00088-18/ASSET/97BA20FE-3FD8-42BF-955A-EE35F29765C9/ASSETS/GRAPHIC/ZCM0011926530004.JPEG

Gal-Mor, O., Boyle, E. C., & Grassl, G. A. (2014). Same species, different diseases: how and why typhoidal and non-typhoidal Salmonella enterica serovars differ. *Frontiers in Microbiology*, *5*(AUG). https://doi.org/10.3389/FMICB.2014.00391

Gao, R., Wang, L., Ogunremi, D., Gao, R., Wang, L., & Ogunremi, D. (2019a). Virulence Determinants of Non-typhoidal Salmonellae. *Microorganisms*. https://doi.org/10.5772/INTECHOPEN.88904

Gao, R., Wang, L., Ogunremi, D., Gao, R., Wang, L., & Ogunremi, D. (2019b). Virulence Determinants of Non-typhoidal Salmonellae. *Microorganisms*. https://doi.org/10.5772/INTECHOPEN.88904

Garmendia, J., Beuzón, C. R., Ruiz-Albert, J., & Holden, D. W. (2003). The roles of SsrA-SsrB and OmpR-EnvZ in the regulation of genes encoding the Salmonella typhimurium SPI-2 type III secretion system. *Microbiology (Reading, England)*, *149*(Pt 9), 2385–2396. https://doi.org/10.1099/MIC.0.26397-0

Gerlach, R. G., & Hensel, M. (2007). Salmonella Pathogenicity Islands in host specificity, host pathogen-interactions and antibiotics resistance of Salmonella enterica. *Berliner Und Munchener Tierarztliche Wochenschrift*, *120*(7–8), 317–327. https://doi.org/10.2376/0005-9366-120-317

Gerstel, U., Park, C., & Römling, U. (2003). Complex regulation of csgD promoter activity by global regulatory proteins. *Molecular Microbiology*, *49*(3), 639–654. https://doi.org/10.1046/J.1365-2958.2003.03594.X

Gerstel, U., & Römling, U. (2003). The csgD promoter, a control unit for biofilm formation in Salmonella typhimurium. *Research in Microbiology*, *154*(10), 659–667. https://doi.org/10.1016/J.RESMIC.2003.08.005

Gholizadeh, P., Aghazadeh, M., Ghotaslou, R., Ahangarzadeh Rezaee, M., Pirzadeh, T., Köse, Ş., Ganbarov, K., Yousefi, M., & Kafil, H. S. (2020). CRISPR- cas system in the acquisition of virulence genes in dental-root canal and hospital-acquired isolates of Enterococcus faecalis. *Virulence*, *11*(1), 1257–1267. https://doi.org/10.1080/21505594.2020.1809329

Giacomodonato, M. N., Sarnacki, S. H., Llana, M. N., & Cerquetti, M. C. (2011). SopB effector protein of Salmonella Typhimurium is translocated in mesenteric lymph nodes during murine salmonellosis. *FEMS Microbiology Letters*, *317*(1), 100–106. https://doi.org/10.1111/J.1574-6968.2011.02217.X

Gibson, D. L., White, A. P., Snyder, S. D., Martin, S., Heiss, C., Azadi, P., Surette, M., & Kay, W. W. (2006). Salmonella produces an O-antigen capsule regulated by AgfD and important for environmental persistence. *Journal of Bacteriology*, *188*(22), 7722–7730. https://doi.org/10.1128/JB.00809-06

Gogoi, M., Shreenivas, M. M., & Chakravortty, D. (2019). Hoodwinking the Big-Eater to Prosper: The Salmonella-Macrophage Paradigm. *Journal of Innate Immunity*, *11*(3), 289. https://doi.org/10.1159/000490953

Gong, T., Zeng, J., Tang, B., Zhou, X., & Li, Y. (2020). CRISPR-Cas systems in oral microbiome: From immune defense to physiological regulation. *Molecular Oral Microbiology*, *35*(2), 41–48. https://doi.org/10.1111/OMI.12279

Gonzalez-Escobedo, G., Marshall, J. M., & Gunn, J. S. (2011). Chronic and acute infection of the gall bladder by Salmonella Typhi: understanding the carrier state. *Nature Reviews. Microbiology*, *9*(1), 9–14. https://doi.org/10.1038/NRMICRO2490

Gualdi, L., Tagliabue, L., Bertagnoli, S., Ieranò, T., de Castro, C., & Landini, P. (2008). Cellulose modulates biofilm formation by counteracting curli-mediated colonization of solid surfaces in Escherichia coli. *Microbiology*, *154*(7), 2017–2024. https://doi.org/10.1099/mic.0.2008/018093-0

Guiney, D. G., & Fierer, J. (2011). The Role of the spv Genes in Salmonella Pathogenesis. *Frontiers in Microbiology*, *2*(JUNE). https://doi.org/10.3389/FMICB.2011.00129

Gunderson, F. F., & Cianciotto, N. P. (2013). The CRISPR-Associated Gene cas2 of Legionella pneumophila Is Required for Intracellular Infection of Amoebae. *MBio*, *4*(2). https://doi.org/10.1128/MBIO.00074-13

Gunderson, F. F., Mallama, C. A., Fairbairn, S. G., & Cianciotto, N. P. (2015). Nuclease activity of Legionella pneumophila Cas2 promotes intracellular infection of amoebal

host cells. *Infection and Immunity*, *83*(3), 1008–1018. https://doi.org/10.1128/IAI.03102-14

Gutmann, L., Billot-Klein, D., Williamson, R., Goldstein, F. W., Mounier, J., Acar, J. F., & Collatz, E. (1988). Mutation of Salmonella paratyphi A conferring cross-resistance to several groups of antibiotics by decreased permeability and loss of invasiveness. *Antimicrobial Agents and Chemotherapy*, *32*(2), 195–201. https://doi.org/10.1128/AAC.32.2.195

Hahn, M. M., González, J. F., & Gunn, J. S. (2021). Salmonella Biofilms Tolerate Hydrogen Peroxide by a Combination of Extracellular Polymeric Substance Barrier Function and Catalase Enzymes. *Frontiers in Cellular and Infection Microbiology*, *11*. https://doi.org/10.3389/FCIMB.2021.683081

Halder, S., Yadav, K. K., Sarkar, R., Mukherjee, S., Saha, P., Haldar, S., Karmakar, S., & Sen, T. (2015). Alteration of Zeta potential and membrane permeability in bacteria: a study with cationic agents. *SpringerPlus*, *4*(1), 1–14. https://doi.org/10.1186/S40064-015-1476-7

Hall, C. L., & Lee, V. T. (2018). Cyclic-di-GMP regulation of virulence in bacterial pathogens. *Wiley Interdisciplinary Reviews. RNA*, *9*(1). https://doi.org/10.1002/WRNA.1454

Harrell, J. E., Hahn, M. M., D'Souza, S. J., Vasicek, E. M., Sandala, J. L., Gunn, J. S., & McLachlan, J. B. (2021). Salmonella Biofilm Formation, Chronic Infection, and Immunity Within the Intestine and Hepatobiliary Tract. *Frontiers in Cellular and Infection Microbiology*, *10*. https://doi.org/10.3389/FCIMB.2020.624622

Hébrard, M., Viala, J. P. M., Méresse, S., Barras, F., & Aussel, L. (2009). Redundant Hydrogen Peroxide Scavengers Contribute to Salmonella Virulence and Oxidative Stress Resistance. *Journal of Bacteriology*, *191*(14), 4605. https://doi.org/10.1128/JB.00144-09

Heidrich, N., Hagmann, A., Bauriedl, S., Vogel, J., & Schoen, C. (2019). The CRISPR/Cas system in Neisseria meningitidis affects bacterial adhesion to human nasopharyngeal epithelial cells. *RNA Biology*, *16*(4), 390–396. https://doi.org/10.1080/15476286.2018.1486660

Henry, T., Couillault, C., Rockenfeller, P., Boucrot, E., Dumont, A., Schroeder, N., Hermant, A., Knodler, L. A., Lecine, P., Steele-Mortimer, O., Borg, J. P., Gorvel, J. P., & Méresse, S. (2006). The Salmonella effector protein PipB2 is a linker for kinesin-1. *Proceedings of the National Academy of Sciences of the United States of America*, *103*(36), 13497–13502. https://doi.org/10.1073/PNAS.0605443103

Hilker, M., Schwachtje, J., Baier, M., Balazadeh, S., Bäurle, I., Geiselhardt, S., Hincha, D. K., Kunze, R., Mueller-Roeber, B., Rillig, M. C., Rolff, J., Romeis, T., Schmülling, T., Steppuhn, A., van Dongen, J., Whitcomb, S. J., Wurst, S., Zuther, E., & Kopka, J. (2016). Priming and memory of stress responses in organisms lacking a nervous system. *Biological Reviews of the Cambridge Philosophical Society*, *91*(4), 1118–1133. https://doi.org/10.1111/BRV.12215

Hille, F., & Charpentier, E. (2016). CRISPR-cas: Biology, mechanisms and relevance. In *Philosophical Transactions of the Royal Society B: Biological Sciences* (Vol. 371, Issue 1707). Royal Society of London. https://doi.org/10.1098/rstb.2015.0496

Hölzer, S. U., Schlumberger, M. C., Jäckel, D., & Hensel, M. (2009). Effect of the O-Antigen Length of Lipopolysaccharide on the Functions of Type III Secretion Systems in Salmonella enterica. *Infection and Immunity*, *77*(12), 5458. https://doi.org/10.1128/IAI.00871-09

Horne, J. E., Brockwell, D. J., & Radford, S. E. (2020). Role of the lipid bilayer in outer membrane protein folding in Gram-negative bacteria. *The Journal of Biological Chemistry*, *295*(30), 10340–10367. https://doi.org/10.1074/JBC.REV120.011473

Hufnagel, D. A., Evans, M. L., Greene, S. E., Pinkner, J. S., Hultgren, S. J., & Chapman, M. R. (2016). The Catabolite Repressor Protein-Cyclic AMP Complex Regulates csgD and Biofilm Formation in Uropathogenic Escherichia coli. *Journal of Bacteriology*, *198*(24), 3329–3334. https://doi.org/10.1128/JB.00652-16

Hung, C., Zhou, Y., Pinkner, J. S., Dodson, K. W., Crowley, J. R., Heuser, J., Chapman, M. R., Hadjifrangiskou, M., Henderson, J. P., & Hultgren, S. J. (2013). Escherichia coli biofilms have an organized and complex extracellular matrix structure. *MBio*, *4*(5), e00645-13. https://doi.org/10.1128/mBio.00645-13

Hurley, D., McCusker, M. P., Fanning, S., & Martins, M. (2014). Salmonella-host interactions - modulation of the host innate immune system. *Frontiers in Immunology*, *5*(OCT). https://doi.org/10.3389/FIMMU.2014.00481

Ibarra, J. A., & Steele-Mortimer, O. (2009). Salmonella--the ultimate insider. Salmonella virulence factors that modulate intracellular survival. *Cellular Microbiology*, *11*(11), 1579–1586. https://doi.org/10.1111/J.1462-5822.2009.01368.X

Imlay, J. A., & Linn, S. (1986). Bimodal pattern of killing of DNA-repair-defective or anoxically grown Escherichia coli by hydrogen peroxide. *Journal of Bacteriology*, *166*(2), 519–527. https://doi.org/10.1128/JB.166.2.519-527.1986

Information for Healthcare Professionals | Typhoid Fever | CDC. (n.d.). Retrieved October 26, 2022, from https://www.cdc.gov/typhoid-fever/health-professional.html

Jahan, F., Chinni, S. v., Samuggam, S., Reddy, L. V., Solayappan, M., & Yin, L. S. (2022). The Complex Mechanism of the Salmonella typhi Biofilm Formation That Facilitates Pathogenicity: A Review. *International Journal of Molecular Sciences*, *23*(12). https://doi.org/10.3390/IJMS23126462

Jepson, M. A., Kenny, B., & Leard, A. D. (2001a). Role of sipA in the early stages of Salmonella typhimurium entry into epithelial cells. *Cellular Microbiology*, *3*(6), 417–426. https://doi.org/10.1046/J.1462-5822.2001.00124.X

Jepson, M. A., Kenny, B., & Leard, A. D. (2001b). Role of sipA in the early stages of Salmonella typhimurium entry into epithelial cells. *Cellular Microbiology*, *3*(6), 417–426. https://doi.org/10.1046/J.1462-5822.2001.00124.X

Jonas, K., Tomenius, H., Kader, A., Normark, S., Römling, U., Belova, L. M., & Melefors, Ö. (2007). Roles of curli, cellulose and BapA in Salmonella biofilm morphology studied by atomic force microscopy. *BMC Microbiology*, *7*. https://doi.org/10.1186/1471-2180-7-70

Khan, C. M. A. (2014). The Dynamic Interactions between Salmonella and the Microbiota, within the Challenging Niche of the Gastrointestinal Tract . *International Scholarly Research Notices*, *2014*, 1–23. https://doi.org/10.1155/2014/846049

Khondker, A., & Rheinstädter, M. C. (2020). How do bacterial membranes resist polymyxin antibiotics? *Communications Biology*, *3*(1). https://doi.org/10.1038/S42003-020-0803-X

Kim, K. H., Aulakh, S., & Paetzel, M. (2012). The bacterial outer membrane β-barrel assembly machinery. *Protein Science : A Publication of the Protein Society*, *21*(6), 751–768. https://doi.org/10.1002/PRO.2069

Kim, K., Kim, K. P., Choi, J., Lim, J. A., Lee, J., Hwang, S., & Ryu, S. (2010). Outer membrane proteins A (OmpA) and X (OmpX) are essential for basolateral invasion of Cronobacter sakazakii. *Applied and Environmental Microbiology*, *76*(15), 5188–5198. https://doi.org/10.1128/AEM.02498-09

Kim, W., & Surette, M. G. (2005). Prevalence of surface swarming behavior in Salmonella. *Journal of Bacteriology*, *187*(18), 6580–6583. https://doi.org/10.1128/JB.187.18.6580-6583.2005

Kiss, T., Morgan, E., & Nagy, G. (2007). Contribution of SPI-4 genes to the virulence of Salmonella enterica. *FEMS Microbiology Letters*, *275*(1), 153–159. https://doi.org/10.1111/J.1574-6968.2007.00871.X

Knodler, L. A., & Steele-Mortimer, O. (2005). The Salmonella effector PipB2 affects late endosome/lysosome distribution to mediate Sif extension. *Molecular Biology of the Cell*, *16*(9), 4108–4123. https://doi.org/10.1091/MBC.E05-04-0367

Knuff-Janzen, K., Tupin, A., Yurist-Doutsch, S., Rowland, J. L., & Finlay, B. B. (2020). Multiple Salmonella-pathogenicity island 2 effectors are required to facilitate bacterial establishment of its intracellular niche and virulence. *PLOS ONE*, *15*(6), e0235020. https://doi.org/10.1371/JOURNAL.PONE.0235020

Koczerka, M., Douarre, P.-E., Kempf, F., Holbert, S., Mistou, M.-Y., Grépinet, O., & Virlogeux-Payant, I. (2021a). The Invasin and Complement-Resistance Protein Rck of Salmonella is More Widely Distributed than Previously Expected. *Microbiology Spectrum*, *9*(2). https://doi.org/10.1128/SPECTRUM.01457-21

Koczerka, M., Douarre, P.-E., Kempf, F., Holbert, S., Mistou, M.-Y., Grépinet, O., & Virlogeux-Payant, I. (2021b). The Invasin and Complement-Resistance Protein Rck of Salmonella is More Widely Distributed than Previously Expected. *Microbiology Spectrum*, *9*(2). https://doi.org/10.1128/SPECTRUM.01457-21

Kombade, S., Kaur, N., Kombade, S., & Kaur, N. (2021). Pathogenicity Island in Salmonella. *Salmonella Spp. - A Global Challenge*. https://doi.org/10.5772/INTECHOPEN.96443

Koonin, E. v., & Makarova, K. S. (2019). Origins and evolution of CRISPR-Cas systems. *Philosophical Transactions of the Royal Society of London. Series B, Biological Sciences*, *374*(1772). https://doi.org/10.1098/RSTB.2018.0087

Koshiol, J., Wozniak, A., Cook, P., Adaniel, C., Acevedo, J., Azócar, L., Hsing, A. W., Roa, J. C., Pasetti, M. F., Miquel, J. F., Levine, M. M., Ferreccio, C., Aguayo, C. G., Baez, S., Díaz, A., Molina, H., Miranda, C., Castillo, C., Tello, A., … Hildesheim, A. (2016). Salmonella enterica serovar Typhi and gallbladder cancer: a case-control study and meta-analysis. *Cancer Medicine*, *5*(11), 3235–3310. https://doi.org/10.1002/CAM4.915

Krasowska, A., & Sigler, K. (2014). How microorganisms use hydrophobicity and what does this mean for human needs? *Frontiers in Cellular and Infection Microbiology*, *4*(AUG), 112. https://doi.org/10.3389/FCIMB.2014.00112/BIBTEX

Krzyżewska-Dudek, E., Kotimaa, J., Kapczyńska, K., Rybka, J., & Meri, S. (2022). Lipopolysaccharides and outer membrane proteins as main structures involved in complement evasion strategies of non-typhoidal Salmonella strains. *Molecular Immunology*, *150*, 67–77. https://doi.org/10.1016/J.MOLIMM.2022.08.009

Kushwaha, S. K., Bhavesh, N. L. S., Abdella, B., Lahiri, C., & Marathe, S. A. (2020). The phylogenomics of CRISPR-Cas system and revelation of its features in Salmonella. *Sci Rep*, *10*(1), 21156. https://doi.org/10.1038/s41598-020-77890-6

Labrousse, A., Chauvet, S., Couillault, C., Léopold Kurz, C., & Ewbank, J. J. (2000). Caenorhabditis elegans is a model host for Salmonella typhimurium. *Current Biology : CB*, *10*(23), 1543–1545. https://doi.org/10.1016/S0960-9822(00)00833-2

Lamas, A., Regal, P., Sanjulián, L., López-Santamarina, A., Franco, C. M., & Cepeda, A. (n.d.). *Salmonella spp*. https://www.intechopen.com/chapters/76781

Lamprokostopoulou, A., Monteiro, C., Rhen, M., & Römling, U. (2010). Cyclic di-GMP signalling controls virulence properties of Salmonella enterica serovar Typhimurium at the mucosal lining. *Environmental Microbiology*, *12*(1), 40–53. https://doi.org/10.1111/J.1462-2920.2009.02032.X

Lara-Tejero, M., & Galán, J. E. (2009). Salmonella enterica Serovar Typhimurium Pathogenicity Island 1-Encoded Type III Secretion System Translocases Mediate Intimate Attachment to Nonphagocytic Cells. *Infection and Immunity*, *77*(7), 2635. https://doi.org/10.1128/IAI.00077-09

Latasa, C., Roux, A., Toledo-Arana, A., Ghigo, J. M., Gamazo, C., Penadés, J. R., & Lasa, I. (2005). BapA, a large secreted protein required for biofilm formation and host colonization of Salmonella enterica serovar Enteritidis. *Molecular Microbiology*. https://doi.org/10.1111/j.1365-2958.2005.04907.x

le Bivic, A., Hirn, M., & Reggio, H. (1988). HT-29 cells are an in vitro model for the generation of cell polarity in epithelia during embryonic differentiation. *Proceedings*

of the National Academy of Sciences of the United States of America, *85*(1), 136–140. https://doi.org/10.1073/PNAS.85.1.136

Ledeboer, N. A., Frye, J. G., McClelland, M., & Jones, B. D. (2006). Salmonella enterica serovar Typhimurium requires the Lpf, Pef, and Tafi fimbriae for biofilm formation on HEp-2 tissue culture cells and chicken intestinal epithelium. *Infection and Immunity*, *74*(6), 3156–3169. https://doi.org/10.1128/IAI.01428-05

Lee, A. K., Detweiler, C. S., & Falkow, S. (2000). OmpR Regulates the Two-Component System SsrA-SsrB in Salmonella Pathogenicity Island 2. *Journal of Bacteriology*, *182*(3), 771. https://doi.org/10.1128/JB.182.3.771-781.2000

Lee, J., Kim, D. J., Yeom, J. H., & Lee, K. (2017). Bdm-Mediated Regulation of Flagellar Biogenesis in Escherichia coli and Salmonella enterica Serovar Typhimurium. *Curr Microbiol*, *74*(9), 1015–1020. https://doi.org/10.1007/s00284-017-1270-6

Lee, J. W., & Lee, E. J. (2015). Regulation and function of the Salmonella MgtC virulence protein. *Journal of Microbiology (Seoul, Korea)*, *53*(10), 667–672. https://doi.org/10.1007/S12275-015-5283-1

Lewis, L. A., Ngampasutadol, J., Wallace, R., Reid, J. E. A., Vogel, U., & Ram, S. (2010). The meningococcal vaccine candidate neisserial surface protein A (NspA) binds to factor H and enhances meningococcal resistance to complement. *PLoS Pathogens*, *6*(7), 1–20. https://doi.org/10.1371/JOURNAL.PPAT.1001027

Li, H., & Benghezal, M. (2017). Crude Preparation of Lipopolysaccharide from Helicobacter pylori for Silver Staining and Western Blot. *BIO-PROTOCOL*, *7*(20). https://doi.org/10.21769/bioprotoc.2585

Li, R., Fang, L., Tan, S., Yu, M., Li, X., He, S., Wei, Y., Li, G., Jiang, J., & Wu, M. (2016). Type I CRISPR-Cas targets endogenous genes and regulates virulence to evade mammalian host immunity. *Cell Research*, *26*(12), 1273–1287. https://doi.org/10.1038/CR.2016.135

Li, X., Bleumink-Pluym, N. M. C., Luijkx, Y. M. C. A., Wubbolts, R. W., van Putten, J. P. M., & Strijbis, K. (2019). MUC1 is a receptor for the Salmonella SiiE adhesin that enables apical invasion into enterocytes. *PLoS Pathogens*, *15*(2). https://doi.org/10.1371/JOURNAL.PPAT.1007566

Lilic, M., Galkin, V. E., Orlova, A., VanLoock, M. S., Egelman, E. H., & Stebbins, C. E. (2003). Salmonella sipA polymerizes actin by stapling filaments with nonglobular protein arms. *Science*, *301*(5641), 1918–1921. https://doi.org/10.1126/SCIENCE.1088433/SUPPL_FILE/LILIC.PDF

Limoli, D. H., Jones, C. J., & Wozniak, D. J. (2015). Bacterial Extracellular Polysaccharides in Biofilm Formation and Function. *Microbiology Spectrum*, *3*(3). https://doi.org/10.1128/microbiolspec.mb-0011-2014

Liu, C., Sun, D., Zhu, J., Liu, J., & Liu, W. (2020). The Regulation of Bacterial Biofilm Formation by cAMP-CRP: A Mini-Review. *Front Microbiol*, *11*, 802. https://doi.org/10.3389/fmicb.2020.00802

Liu, H., Whitehouse, C. A., & Li, B. (2018). Presence and Persistence of Salmonella in Water: The Impact on Microbial Quality of Water and Food Safety. *Frontiers in Public Health*, *6*. https://doi.org/10.3389/FPUBH.2018.00159

Liu, Z., Niu, H., Wu, S., & Huang, R. (2014). CsgD regulatory network in a bacterial trait-altering biofilm formation. *Emerging Microbes & Infections*, *3*(1). https://doi.org/10.1038/EMI.2014.1

Löber, S., Jäckel, D., Kaiser, N., & Hensel, M. (2006). Regulation of Salmonella pathogenicity island 2 genes by independent environmental signals. *International Journal of Medical Microbiology : IJMM*, *296*(7), 435–447. https://doi.org/10.1016/J.IJMM.2006.05.001

Lorenz, R., Bernhart, S. H., Höner zu Siederdissen, C., Tafer, H., Flamm, C., Stadler, P. F., & Hofacker, I. L. (2011). ViennaRNA Package 2.0. *Algorithms for Molecular Biology : AMB*, *6*(1). https://doi.org/10.1186/1748-7188-6-26

Lostroh, C. P., & Lee, C. A. (2001). The Salmonella pathogenicity island-1 type III secretion system. *Microbes and Infection*, *3*(14–15), 1281–1291. https://doi.org/10.1016/S1286-4579(01)01488-5

Lou, L., Zhang, P., Piao, R., & Wang, Y. (2019). Salmonella Pathogenicity Island 1 (SPI-1) and Its Complex Regulatory Network. *Frontiers in Cellular and Infection Microbiology*, *9*. https://doi.org/10.3389/FCIMB.2019.00270

Louwen, R., Horst-Kreft, D., de Boer, A. G., van der Graaf, L., de Knegt, G., Hamersma, M., Heikema, A. P., Timms, A. R., Jacobs, B. C., Wagenaar, J. A., Endtz, H. P., van der Oost, J., Wells, J. M., Nieuwenhuis, E. E. S., van Vliet, A. H. M., Willemsen, P. T. J., van Baarlen, P., & van Belkum, A. (2013). A novel link between Campylobacter jejuni bacteriophage defence, virulence and Guillain-Barré syndrome. *European Journal of Clinical Microbiology & Infectious Diseases : Official Publication of the European Society of Clinical Microbiology*, *32*(2), 207–226. https://doi.org/10.1007/S10096-012-1733-4

Louwen, R., Staals, R. H. J., Endtz, H. P., van Baarlen, P., & van der Oost, J. (2014). The role of CRISPR-Cas systems in virulence of pathogenic bacteria. *Microbiology and Molecular Biology Reviews : MMBR*, *78*(1), 74–88. https://doi.org/10.1128/MMBR.00039-13

Lunestad, B. T., Nesse, L., Lassen, J., Svihus, B., Nesbakken, T., Fossum, K., Rosnes, J. T., Kruse, H., & Yazdankhah, S. (2007). Salmonella in fish feed; occurrence and implications for fish and human health in Norway. *Aquaculture*, *265*(1–4), 1–8. https://doi.org/10.1016/J.AQUACULTURE.2007.02.011

Mah, T.-F. C. and O. G. A. (2001). Mechanisms of biofilm resistance to antimicrobial agents. *Trends in Microbiology*, *9*(1), 34–39.

Makarova, K. S., Haft, D. H., Barrangou, R., Brouns, S. J. J., Charpentier, E., Horvath, P., Moineau, S., Mojica, F. J. M., Wolf, Y. I., Yakunin, A. F., van der Oost, J., & Koonin, E. v. (2011). Evolution and classification of the CRISPR-Cas systems.

Nature Reviews. Microbiology, *9*(6), 467–477. https://doi.org/10.1038/NRMICRO2577

Makarova, K. S., Wolf, Y. I., Iranzo, J., Shmakov, S. A., Alkhnbashi, O. S., Brouns, S. J. J., Charpentier, E., Cheng, D., Haft, D. H., Horvath, P., Moineau, S., Mojica, F. J. M., Scott, D., Shah, S. A., Siksnys, V., Terns, M. P., Venclovas, Č., White, M. F., Yakunin, A. F., … Koonin, E. v. (2020). Evolutionary classification of CRISPR-Cas systems: a burst of class 2 and derived variants. *Nature Reviews. Microbiology*, *18*(2), 67–83. https://doi.org/10.1038/S41579-019-0299-X

Maldonado, R. F., Sa-Correia, I., & Valvano, M. A. (2016). Lipopolysaccharide modification in Gram-negative bacteria during chronic infection. *FEMS Microbiol Rev*, *40*(4), 480–493. https://doi.org/10.1093/femsre/fuw007

Malik-Kale, P., Winfree, S., & Steele-Mortimer, O. (2012). The Bimodal Lifestyle of Intracellular Salmonella in Epithelial Cells: Replication in the Cytosol Obscures Defects in Vacuolar Replication. *PLOS ONE*, *7*(6), e38732. https://doi.org/10.1371/JOURNAL.PONE.0038732

Mandin, P., Geissmann, T., Cossart, P., Repoila, F., & Vergassola, M. (2007). Identification of new noncoding RNAs in Listeria monocytogenes and prediction of mRNA targets. *Nucleic Acids Research*, *35*(3), 962–974. https://doi.org/10.1093/NAR/GKL1096

Manon, R., Nadia, A., Fatemeh, N., Isabelle, V.-P., Philippe, V., Agnes, W., Manon, R., Nadia, A., Fatemeh, N., Isabelle, V.-P., Philippe, V., & Agnes, W. (2012). The Different Strategies Used by Salmonella to Invade Host Cells. *Salmonella - Distribution, Adaptation, Control Measures and Molecular Technologies*. https://doi.org/10.5772/29979

Marraffini, L. A., & Sontheimer, E. J. (2010). CRISPR interference: RNA-directed adaptive immunity in bacteria and archaea. *Nature Reviews. Genetics*, *11*(3), 181. https://doi.org/10.1038/NRG2749

Marshall, J. M., & Gunn, J. S. (2015). The O-antigen capsule of Salmonella enterica serovar typhimurium facilitates serum resistance and surface expression of FliC. *Infection and Immunity*, *83*(10), 3946–3959. https://doi.org/10.1128/IAI.00634-15

Martynowycz, M. W., Rice, A., Andreev, K., Nobre, T. M., Kuzmenko, I., Wereszczynski, J., & Gidalevitz, D. (2019). Salmonella Membrane Structural Remodeling Increases Resistance to Antimicrobial Peptide LL-37. *ACS Infectious Diseases*, *5*(7), 1214–1222. https://doi.org/10.1021/ACSINFECDIS.9B00066

Mastroeni, P., & Grant, A. J. (2011). Spread of Salmonella enterica in the body during systemic infection: unravelling host and pathogen determinants. *Expert Reviews in Molecular Medicine*, *13*. https://doi.org/10.1017/S1462399411001840

Masuko, T., Minami, A., Iwasaki, N., Majima, T., Nishimura, S., & Lee, Y. C. (2005). Carbohydrate analysis by a phenol-sulfuric acid method in microplate format. *Anal Biochem*, *339*(1), 69–72. https://doi.org/10.1016/j.ab.2004.12.001

Medina-Aparicio, L., Dávila, S., Rebollar-Flores, J. E., Calva, E., & Hernández-Lucas, I. (2018). The CRISPR-Cas system in Enterobacteriaceae. *Pathogens and Disease*, *76*(1). https://doi.org/10.1093/FEMSPD/FTY002

Medina-Aparicio, L., Rebollar-Flores, J. E., Gallego-Hernández, A. L., Vázquez, A., Olvera, L., Gutiérrez-Ríos, R. M., Calva, E., & Hernández-Lucas, I. (2011). The CRISPR/Cas Immune System Is an Operon Regulated by LeuO, H-NS, and Leucine-Responsive Regulatory Protein in Salmonella enterica Serovar Typhi. *Journal of Bacteriology*, *193*(10), 2396. https://doi.org/10.1128/JB.01480-10

Medina-Aparicio, L., Rodriguez-Gutierrez, S., Rebollar-Flores, J. E., Martinez-Batallar, A. G., Mendoza-Mejia, B. D., Aguirre-Partida, E. D., Vazquez, A., Encarnacion, S., Calva, E., & Hernandez-Lucas, I. (2021). The CRISPR-Cas System Is Involved in OmpR Genetic Regulation for Outer Membrane Protein Synthesis in Salmonella Typhi. *Front Microbiol*, *12*, 657404. https://doi.org/10.3389/fmicb.2021.657404

Méresse, S., Unsworth, K. E., Habermann, A., Griffiths, G., Fang, F., Martínez-Lorenzo, M. J., Waterman, S. R., Gorvel, J. P., & Holden, D. W. (2001). Remodelling of the actin cytoskeleton is essential for replication of intravacuolar Salmonella. *Cellular Microbiology*, *3*(8), 567–577. https://doi.org/10.1046/J.1462-5822.2001.00141.X

Mireles 2nd, J. R., Toguchi, A., & Harshey, R. M. (2001). Salmonella enterica serovar typhimurium swarming mutants with altered biofilm-forming abilities: surfactin inhibits biofilm formation. *J Bacteriol*, *183*(20), 5848–5854. https://doi.org/10.1128/JB.183.20.5848-5854.2001

Monack, D. M., Bouley, D. M., & Falkow, S. (2004). Salmonella typhimurium persists within macrophages in the mesenteric lymph nodes of chronically infected *Nramp*1+/+ mice and can be reactivated by IFNgamma neutralization. *The Journal of Experimental Medicine*, *199*(2), 231–241. https://doi.org/10.1084/JEM.20031319

Morales, E. H., Calderán, I. L., Collao, B., Gil, F., Porwollik, S., McClelland, M., & Saavedra, C. P. (2012). Hypochlorous acid and hydrogen peroxide-induced negative regulation of Salmonella enterica serovar Typhimurium ompW by the response regulator ArcA. *BMC Microbiology*, *12*(1), 1–11. https://doi.org/10.1186/1471-2180-12-63/TABLES/1

Morgan, J. L. W., McNamara, J. T., & Zimmer, J. (2014). Mechanism of activation of bacterial cellulose synthase by cyclic di-GMP. *Nature Structural & Molecular Biology*, *21*(5), 489–496. https://doi.org/10.1038/NSMB.2803

Murray, G. L., Attridge, S. R., & Morona, R. (2006). Altering the length of the lipopolysaccharide O antigen has an impact on the interaction of Salmonella enterica serovar Typhimurium with macrophages and complement. *Journal of Bacteriology*, *188*(7), 2735–2739. https://doi.org/10.1128/JB.188.7.2735-2739.2006

Newsom, S., Parameshwaran, H. P., Martin, L., & Rajan, R. (2021). The CRISPR-Cas Mechanism for Adaptive Immunity and Alternate Bacterial Functions Fuels Diverse Biotechnologies. *Frontiers in Cellular and Infection Microbiology*, *10*. https://doi.org/10.3389/FCIMB.2020.619763

Niedergang, F., Sirard, J. C., Blanc, C. T., & Kraehenbuhl, J. P. (2000). Entry and survival of Salmonella typhimurium in dendritic cells and presentation of recombinant antigens do not require macrophage-specific virulence factors. *Proceedings of the National Academy of Sciences of the United States of America*, *97*(26), 14650–14655. https://doi.org/10.1073/PNAS.97.26.14650

Nikolaus, T., Deiwick, J., Rappl, C., Freeman, J. A., Schröder, W., Miller, S. I., & Hensel, M. (2001). SseBCD proteins are secreted by the type III secretion system of Salmonella pathogenicity island 2 and function as a translocon. *Journal of Bacteriology*, *183*(20), 6036–6045. https://doi.org/10.1128/JB.183.20.6036-6045.2001

Ogasawara, H., Yamada, K., Kori, A., Yamamoto, K., & Ishihama, A. (2010). Regulation of the Escherichia coli csgD promoter: interplay between five transcription factors. *Microbiology (Reading, England)*, *156*(Pt 8), 2470–2483. https://doi.org/10.1099/MIC.0.039131-0

Ogasawara, H., Yamamoto, K., & Ishihama, A. (2010). Regulatory role of MlrA in transcription activation of csgD, the master regulator of biofilm formation in Escherichia coli. *FEMS Microbiology Letters*, *312*(2), 160–168. https://doi.org/10.1111/J.1574-6968.2010.02112.X

Pando, J. M., Karlinsey, J. E., Lara, J. C., Libby, S. J., & Fang, F. C. (2017). *The Rcs-Regulated Colanic Acid Capsule Maintains Membrane Potential in Salmonella enterica serovar Typhimurium*. https://doi.org/10.1128/mBio

Paredes, J., Alonso-Arce, M., Schmidt, C., Valderas, D., Sedano, B., Legarda, J., Arizti, F., Gómez, E., Aguinaga, A., del Pozo, J. L., & Arana, S. (2014). Smart central venous port for early detection of bacterial biofilm related infections. *Biomedical Microdevices*, *16*(3), 365–374. https://doi.org/10.1007/S10544-014-9839-3

Paredes-Amaya, C. C., Valdés-García, G., Juárez-González, V. R., Rudiño-Piñera, E., & Bustamante, V. H. (2018). The Hcp-like protein HilE inhibits homodimerization and DNA binding of the virulence-associated transcriptional regulator HilD in Salmonella. *The Journal of Biological Chemistry*, *293*(17), 6578–6592. https://doi.org/10.1074/JBC.RA117.001421

Parry, C. M., Hien, T. T., Dougan, G., White, N. J., & Farrar, J. J. (2002). Typhoid Fever. *New England Journal of Medicine*, *347*(22), 1770–1782. https://doi.org/10.1056/NEJMra020201

Pavlova, B., Volf, J., Ondrackova, P., Matiasovic, J., Stepanova, H., Crhanova, M., Karasova, D., Faldyna, M., & Rychlik, I. (2011). SPI-1-encoded type III secretion system of Salmonella enterica is required for the suppression of porcine alveolar macrophage cytokine expression. *Veterinary Research*, *42*(1). https://doi.org/10.1186/1297-9716-42-16

Pawlak, A., Rybka, J., Dudek, B., Krzyżewska, E., Rybka, W., Kędziora, A., Klausa, E., & Bugla-Płoskońska, G. (2017). Salmonella O48 Serum Resistance is Connected with the Elongation of the Lipopolysaccharide O-Antigen Containing Sialic Acid.

International Journal of Molecular Sciences, *18*(10). https://doi.org/10.3390/IJMS18102022

Paytubi, S., Cansado, C., Madrid, C., & Balsalobre, C. (2017). Nutrient composition promotes switching between pellicle and bottom biofilm in Salmonella. *Frontiers in Microbiology*, *8*(NOV). https://doi.org/10.3389/fmicb.2017.02160

Peng, D. (2016). Biofilm Formation of Salmonella. In *Microbial Biofilms - Importance and Applications*. InTech. https://doi.org/10.5772/62905

Perov, S., Lidor, O., Salinas, N., Golan, N., Tayeb-Fligelman, E., Deshmukh, M., Willbold, D., & Landau, M. (2019). Structural insights into curli CsgA cross-β fibril architecture inspire repurposing of anti-amyloid compounds as anti-biofilm agents. *PLoS Pathogens*, *15*(8). https://doi.org/10.1371/journal.ppat.1007978

Petrova, O. E., & Sauer, K. (2012). Sticky situations: Key components that control bacterial surface attachment. In *Journal of Bacteriology* (Vol. 194, Issue 10, pp. 2413–2425). https://doi.org/10.1128/JB.00003-12

Pontes, M. H., Lee, E. J., Choi, J., & Groisman, E. A. (2015). Salmonella promotes virulence by repressing cellulose production. *Proceedings of the National Academy of Sciences of the United States of America*, *112*(16), 5183–5188. https://doi.org/10.1073/PNAS.1500989112/SUPPL_FILE/PNAS.201500989SI.PDF

Poole, K. (2005). Aminoglycoside resistance in Pseudomonas aeruginosa. *Antimicrobial Agents and Chemotherapy*, *49*(2), 479–487. https://doi.org/10.1128/AAC.49.2.479-487.2005

Prigent-Combaret, C., Rard Prensier, G. Â., le Thi, T. T., Vidal, O., Lejeune, P., & Dorel, C. (2000). Developmental pathway for biofilm formation in curli-producing Escherichia coli strains: role of flagella, curli and colanic acid. In *Environmental Microbiology* (Vol. 2, Issue 4).

Prouty, A. M., & Gunn, J. S. (2003). Comparative analysis of Salmonella enterica serovar Typhimurium biofilm formation on gallstones and on glass. *Infect Immun*, *71*(12), 7154–7158. https://doi.org/10.1128/IAI.71.12.7154-7158.2003

Prouty, A. M., Schwesinger, W. H., & Gunn, J. S. (2002). Biofilm formation and interaction with the surfaces of gallstones by Salmonella spp. *Infection and Immunity*, *70*(5), 2640–2649. https://doi.org/10.1128/IAI.70.5.2640-2649.2002

Qin, B., Fei, C., Wang, B., Stone, H. A., Wingreen, N. S., & Bassler, B. L. (2021). Hierarchical transitions and fractal wrinkling drive bacterial pellicle morphogenesis. *MICROBIOLOGY BIOPHYSICS AND COMPUTATIONAL BIOLOGY*, *118*. https://doi.org/10.1073/pnas.2023504118/-/DCSupplemental

Ranieri, M. L., Shi, C., Moreno Switt, A. I., den Bakker, H. C., & Wiedmann, M. (2013). Comparison of typing methods with a new procedure based on sequence characterization for Salmonella serovar prediction. *Journal of Clinical Microbiology*, *51*(6), 1786–1797. https://doi.org/10.1128/JCM.03201-12

Reichhardt, C., Jacobson, A. N., Maher, M. C., Uang, J., McCrate, O. A., Eckart, M., & Cegelski, L. (2015). Congo Red Interactions with Curli-Producing E. coli and Native Curli Amyloid Fibers. *PLoS One*, *10*(10), e0140388. https://doi.org/10.1371/journal.pone.0140388

Rescigno, M., Urbano, M., Valzasina, B., Francolini, M., Rotta, G., Bonasio, R., Granucci, F., Kraehenbuhl, J. P., & Ricciardi-Castagnoli, P. (2001). Dendritic cells express tight junction proteins and penetrate gut epithelial monolayers to sample bacteria. *Nature Immunology*, *2*(4), 361–367. https://doi.org/10.1038/86373

Rhen, M. (2019). Salmonella and Reactive Oxygen Species: A Love-Hate Relationship. *Journal of Innate Immunity*, *11*(3), 216. https://doi.org/10.1159/000496370

Ritter, A., Com, E., Bazire, A., Goncalves, M. D. S., Delage, L., Pennec, G. le, Pineau, C., Dreanno, C., Compère, C., & Dufour, A. (2012). Proteomic studies highlight outer-membrane proteins related to biofilm development in the marine bacterium Pseudoalteromonas sp. D41. *Proteomics*, *12*(21), 3180–3192. https://doi.org/10.1002/PMIC.201100644

Rodríguez-Rojas, A., Kim, J. J., Johnston, P. R., Makarova, O., Eravci, M., Weise, C., Hengge, R., & Rolff, J. (2020). Non-lethal exposure to H2O2 boosts bacterial survival and evolvability against oxidative stress. *PLOS Genetics*, *16*(3), e1008649. https://doi.org/10.1371/JOURNAL.PGEN.1008649

Römling, U., Bian, Z., Hammar, M., Sierralta, W. D., & Normark, S. (1998). Curli fibers are highly conserved between Salmonella typhimurium and Escherichia coli with respect to operon structure and regulation. *Journal of Bacteriology*, *180*(3), 722–731. https://doi.org/10.1128/JB.180.3.722-731.1998

Ruby, T., McLaughlin, L., Gopinath, S., & Monack, D. (2012). Salmonella's long-term relationship with its host. *FEMS Microbiology Reviews*, *36*(3), 600–615. https://doi.org/10.1111/J.1574-6976.2012.00332.X

Salamon, H., Nissim-Eliraz, E., Ardronai, O., Nissan, I., & Shpigel, N. Y. (2020). The role of O-polysaccharide chain and complement resistance of Escherichia coli in mammary virulence. *Veterinary Research*, *51*(1). https://doi.org/10.1186/S13567-020-00804-X

Salmonella Homepage | CDC. (n.d.). Retrieved October 26, 2022, from https://www.cdc.gov/salmonella/index.html

Sampson, T. R., Napier, B. A., Schroeder, M. R., Louwen, R., Zhao, J., Chin, C. Y., Ratner, H. K., Llewellyn, A. C., Jones, C. L., Laroui, H., Merlin, D., Zhou, P., Endtz, H. P., & Weiss, D. S. (2014). A CRISPR-Cas system enhances envelope integrity mediating antibiotic resistance and inflammasome evasion. *Proceedings of the National Academy of Sciences of the United States of America*, *111*(30), 11163–11168. https://doi.org/10.1073/PNAS.1323025111

Sampson, T. R., Saroj, S. D., Llewellyn, A. C., Tzeng, Y. L., & Weiss, D. S. (2013). A CRISPR/Cas system mediates bacterial innate immune evasion and virulence. *Nature*, *497*(7448), 254–257. https://doi.org/10.1038/NATURE12048

Sampson, T. R., & Weiss, D. S. (2013). Cas9-dependent endogenous gene regulation is required for bacterial virulence. *Biochemical Society Transactions*, *41*(6), 1407–1411. https://doi.org/10.1042/BST20130163

Sampson, T. R., & Weiss, D. S. (2014a). CRISPR-Cas systems: new players in gene regulation and bacterial physiology. *Frontiers in Cellular and Infection Microbiology*, *4*(APR). https://doi.org/10.3389/FCIMB.2014.00037

Sampson, T. R., & Weiss, D. S. (2014b). CRISPR-Cas systems: new players in gene regulation and bacterial physiology. *Front Cell Infect Microbiol*, *4*, 37. https://doi.org/10.3389/fcimb.2014.00037

Sana, T. G., Flaugnatti, N., Lugo, K. A., Lam, L. H., Jacobson, A., Baylot, V., Durand, E., Journet, L., Cascales, E., & Monack, D. M. (2016). Salmonella Typhimurium utilizes a T6SS-mediated antibacterial weapon to establish in the host gut. *Proceedings of the National Academy of Sciences of the United States of America*, *113*(34), E5044–E5051. https://doi.org/10.1073/PNAS.1608858113

Santos, R. L., Tsolis, R. M., Bäumler, A. J., & Adams, L. G. (2003). Pathogenesis of Salmonella-induced enteritis. *Brazilian Journal of Medical and Biological Research = Revista Brasileira de Pesquisas Medicas e Biologicas*, *36*(1), 3–12. https://doi.org/10.1590/S0100-879X2003000100002

Santos, R. L., Zhang, S., Tsolis, R. M., Kingsley, R. A., Garry Adams, L., & Bäumler, A. J. (2001). Animal models of Salmonella infections: Enteritis versus typhoid fever. *Microbes and Infection*, *3*(14–15), 1335–1344. https://doi.org/10.1016/S1286-4579(01)01495-2

Seed, K. D., Lazinski, D. W., Calderwood, S. B., & Camilli, A. (2013). A bacteriophage encodes its own CRISPR/Cas adaptive response to evade host innate immunity. *Nature*, *494*(7438), 489–491. https://doi.org/10.1038/NATURE11927

Serra, D. O., & Hengge, R. (2014). Stress responses go three dimensional - The spatial order of physiological differentiation in bacterial macrocolony biofilms. In *Environmental Microbiology* (Vol. 16, Issue 6, pp. 1455–1471). https://doi.org/10.1111/1462-2920.12483

Shariat, N., Timme, R. E., Pettengill, J. B., Barrangou, R., & Dudley, E. G. (2015). Characterization and evolution of Salmonella CRISPR-Cas systems. *Microbiology (Reading, England)*, *161*(2), 374–386. https://doi.org/10.1099/mic.0.000005

Sharma, A., Yadav, S. P., Sarma, D., & Mukhopadhaya, A. (2022). Modulation of host cellular responses by gram-negative bacterial porins. *Advances in Protein Chemistry and Structural Biology*, *128*, 35–77. https://doi.org/10.1016/BS.APCSB.2021.09.004

Sharma, N., Das, A., Raja, P., & Marathe, S. A. (2022). The CRISPR-Cas System Differentially Regulates Surface-Attached and Pellicle Biofilm in Salmonella enterica Serovar Typhimurium. *Microbiology Spectrum*, *10*(3). https://doi.org/10.1128/SPECTRUM.00202-22

Sheikh, A., Charles, R. C., Sharmeen, N., Rollins, S. M., Harris, J. B., Bhuiyan, M. S., Arifuzzaman, M., Khanam, F., Bukka, A., Kalsy, A., Porwollik, S., Leung, D. T.,

Brooks, W. A., LaRocque, R. C., Hohmann, E. L., Cravioto, A., Logvinenko, T., Calderwood, S. B., McClelland, M., … Ryan, E. T. (2011). In vivo expression of Salmonella enterica serotype Typhi genes in the blood of patients with typhoid fever in Bangladesh. *PLoS Neglected Tropical Diseases*, *5*(12). https://doi.org/10.1371/JOURNAL.PNTD.0001419

Silhavy, T. J., Kahne, D., & Walker, S. (2010). The bacterial cell envelope. *Cold Spring Harbor Perspectives in Biology*, *2*(5). https://doi.org/10.1101/CSHPERSPECT.A000414

Silva, C., Calva, E., & Maloy, S. (2014). One Health and Food-Borne Disease: Salmonella Transmission between Humans, Animals, and Plants . *Microbiology Spectrum*, *2*(1). https://doi.org/10.1128/microbiolspec.oh-0020-2013

Simm, R., Morr, M., Kader, A., Nimtz, M., & Römling, U. (2004). GGDEF and EAL domains inversely regulate cyclic di-GMP levels and transition from sessility to motility. *Molecular Microbiology*, *53*(4), 1123–1134. https://doi.org/10.1111/J.1365-2958.2004.04206.X

Singh, Y., Saxena, A., Kumar, R., Kumar Saxena, M., Singh, Y., Saxena, A., Kumar, R., & Kumar Saxena, M. (2018). Virulence System of *Salmonella* with Special Reference to *Salmonella enterica*. *Salmonella - A Re-Emerging Pathogen*. https://doi.org/10.5772/INTECHOPEN.77210

Soutourina, O., Kolb, A., Krin, E., Laurent-Winter, C., Rimsky, S., Danchin, A., & Bertin, A. P. (1999). Multiple Control of Flagellum Biosynthesis in Escherichia coli: Role of H-NS Protein and the Cyclic AMP-Catabolite Activator Protein Complex in Transcription of the flhDC Master Operon. In *JOURNAL OF BACTERIOLOGY* (Vol. 181, Issue 24). https://journals.asm.org/journal/jb

Srinandan, C. S., Elango, M., Gnanadhas, D. P., & Chakravortty, D. (2015). Infiltration of matrix-non-producers weakens the salmonella biofilm and impairs its antimicrobial tolerance and pathogenicity. *Frontiers in Microbiology*, *6*(DEC). https://doi.org/10.3389/fmicb.2015.01468

Stanaway, J. D., Parisi, A., Sarkar, K., Blacker, B. F., Reiner, R. C., Hay, S. I., Nixon, M. R., Dolecek, C., James, S. L., Mokdad, A. H., Abebe, G., Ahmadian, E., Alahdab, F., Alemnew, B. T. T., Alipour, V., Allah Bakeshei, F., Animut, M. D., Ansari, F., Arabloo, J., … Crump, J. A. (2019). The global burden of non-typhoidal salmonella invasive disease: a systematic analysis for the Global Burden of Disease Study 2017. *The Lancet. Infectious Diseases*, *19*(12), 1312–1324. https://doi.org/10.1016/S1473-3099(19)30418-9

Steenackers, H., Hermans, K., Vanderleyden, J., & de Keersmaecker, S. C. J. (2012). Salmonella biofilms: An overview on occurrence, structure, regulation and eradication. *Food Research International*, *45*(2), 502–531. https://doi.org/10.1016/j.foodres.2011.01.038

Stendahl, O., Edebo, L., Magnusson, K. E., Tagesson, C., & Hjertén, S. (1977). SURFACE-CHARGE CHARACTERISTICS OF SMOOTH AND ROUGH SALMONELLA TYPHIMURIUM BACTERIA DETERMINED BY AQUEOUS

TWO-PHASE PARTITIONING AND FREE ZONE ELECTROPHORESIS. *Acta Pathologica Microbiologica Scandinavica Section B Microbiology*, *85B*(5), 334–340. https://doi.org/10.1111/J.1699-0463.1977.TB01984.X

Stringer, A. M., Baniulyte, G., Lasek-Nesselquist, E., Seed, K. D., & Wade, J. T. (2020). Transcription termination and antitermination of bacterial CRISPR arrays. *ELife*, *9*, 1–40. https://doi.org/10.7554/ELIFE.58182

Sugawara, E., & Nikaido, H. (2012). OmpA is the principal nonspecific slow porin of Acinetobacter baumannii. *Journal of Bacteriology*, *194*(15), 4089–4096. https://doi.org/10.1128/JB.00435-12

Sukupolvi, S., Lorenz, R. G., Gordon, J. I., Bian, Z., Pfeifer, J. D., Normark, S. J., & Rhen, M. (1997). Expression of thin aggregative fimbriae promotes interaction of Salmonella typhimurium SR-11 with mouse small intestinal epithelial cells. *Infection and Immunity*, *65*(12), 5320–5325. https://doi.org/10.1128/IAI.65.12.5320-5325.1997

Taciak, B., Białasek, M., Braniewska, A., Sas, Z., Sawicka, P., Kiraga, Ł., Rygiel, T., & Król, M. (2018). Evaluation of phenotypic and functional stability of RAW 264.7 cell line through serial passages. *PloS One*, *13*(6). https://doi.org/10.1371/JOURNAL.PONE.0198943

Tahoun, A., Mahajan, S., Paxton, E., Malterer, G., Donaldson, D. S., Wang, D., Tan, A., Gillespie, T. L., O'Shea, M., Roe, A. J., Shaw, D. J., Gally, D. L., Lengeling, A., Mabbott, N. A., Haas, J., & Mahajan, A. (2012). Salmonella transforms follicle-associated epithelial cells into M cells to promote intestinal invasion. *Cell Host & Microbe*, *12*(5), 645–656. https://doi.org/10.1016/J.CHOM.2012.10.009

Tang, T., Cheng, A., Wang, M., & Li, X. (2013). Reviews in Salmonella Typhimurium PhoP/PhoQ two-component regulatory system. *Reviews and Research in Medical Microbiology*, *24*(1), 18–21. https://doi.org/10.1097/MRM.0B013E32835A9490

Toguchi, A., Siano, M., Burkart, M., & Harshey, R. M. (2000). Genetics of Swarming Motility in Salmonella enterica Serovar Typhimurium: Critical Role for Lipopolysaccharide. In *JOURNAL OF BACTERIOLOGY* (Vol. 182, Issue 22). www.genome.wustl.edu/gsc/

Tran, T. D., Ali, M. A., Lee, D., Félix, M. A., & Luallen, R. J. (2022). Bacterial filamentation as a mechanism for cell-to-cell spread within an animal host. *Nature Communications*, *13*(1). https://doi.org/10.1038/S41467-022-28297-6

Tursi, S. A., & Tükel, Ç. (2018). *Curli-Containing Enteric Biofilms Inside and Out: Matrix Composition, Immune Recognition, and Disease Implications*. https://doi.org/10.1128/MMBR

Valentini, M., & Filloux, A. (2016). Biofilms and Cyclic di-GMP (c-di-GMP) Signaling: Lessons from Pseudomonas aeruginosa and Other Bacteria. *The Journal of Biological Chemistry*, *291*(24), 12547–12555. https://doi.org/10.1074/JBC.R115.711507

van der Velden, A. W. M., Lindgren, S. W., Worley, M. J., & Heffron, F. (2000). Salmonella pathogenicity island 1-independent induction of apoptosis in infected macrophages by Salmonella enterica serotype typhimurium. *Infection and Immunity*, *68*(10), 5702–5709. https://doi.org/10.1128/IAI.68.10.5702-5709.2000

Vargas-Maya, N. I., Padilla-Vaca, F., Romero-González, O. E., Rosales-Castillo, E. A. S., Rangel-Serrano, Á., Arias-Negrete, S., & Franco, B. (2021). Refinement of the Griess method for measuring nitrite in biological samples. *Journal of Microbiological Methods*, *187*. https://doi.org/10.1016/J.MIMET.2021.106260

Vazquez-Torres, A., & Fang, F. C. (2001). Salmonella evasion of the NADPH phagocyte oxidase. *Microbes and Infection*, *3*(14–15), 1313–1320. https://doi.org/10.1016/S1286-4579(01)01492-7

Vazquez-Torres, A., Xu, Y., Jones-Carson, J., Holden, D. W., Lucia, S. M., Dinauer, M. C., Mastroeni, P., & Fang, F. C. (2000). Salmonella pathogenicity island 2-dependent evasion of the phagocyte NADPH oxidase. *Science (New York, N.Y.)*, *287*(5458), 1655–1658. https://doi.org/10.1126/SCIENCE.287.5458.1655

Velge, P., Wiedemann, A., Rosselin, M., Abed, N., Boumart, Z., Chaussé, A. M., Grépinet, O., Namdari, F., Roche, S. M., Rossignol, A., & Virlogeux-Payant, I. (2012a). Multiplicity of Salmonella entry mechanisms, a new paradigm for Salmonella pathogenesis. *MicrobiologyOpen*, *1*(3), 243–258. https://doi.org/10.1002/MBO3.28

Velge, P., Wiedemann, A., Rosselin, M., Abed, N., Boumart, Z., Chaussé, A. M., Grépinet, O., Namdari, F., Roche, S. M., Rossignol, A., & Virlogeux-Payant, I. (2012b). Multiplicity of Salmonella entry mechanisms, a new paradigm for Salmonella pathogenesis. *MicrobiologyOpen*, *1*(3), 243–258. https://doi.org/10.1002/MBO3.28

Verma, S., Senger, S., Cherayil, B. J., & Faherty, C. S. (2020). Spheres of Influence: Insights into Salmonella Pathogenesis from Intestinal Organoids. *Microorganisms*, *8*(4). https://doi.org/10.3390/MICROORGANISMS8040504

Wang, F., Deng, L., Huang, F., Wang, Z., Lu, Q., & Xu, C. (2020). Flagellar Motility Is Critical for Salmonella enterica Serovar Typhimurium Biofilm Development. *Front Microbiol*, *11*, 1695. https://doi.org/10.3389/fmicb.2020.01695

Wang, Z., Wang, J., Ren, G., Li, Y., & Wang, X. (2015). Influence of Core Oligosaccharide of Lipopolysaccharide to Outer Membrane Behavior of Escherichia coli. *Marine Drugs*, *13*(6), 3325–3339. https://doi.org/10.3390/MD13063325

Watson, K. G., & Holden, D. W. (2010). Dynamics of growth and dissemination of Salmonella in vivo. *Cellular Microbiology*, *12*(10), 1389–1397. https://doi.org/10.1111/J.1462-5822.2010.01511.X

Weiser, J. N., & Gotschlich, E. C. (1991). Outer membrane protein A (OmpA) contributes to serum resistance and pathogenicity of Escherichia coli K-1. *Infection and Immunity*, *59*(7), 2252–2258. https://doi.org/10.1128/IAI.59.7.2252-2258.1991

White, A. P., Gibson, D. L., Kim, W., Kay, W. W., & Surette, M. G. (2006). Thin aggregative fimbriae and cellulose enhance long-term survival and persistence of Salmonella. *Journal of Bacteriology*, *188*(9), 3219–3227. https://doi.org/10.1128/JB.188.9.3219-3227.2006

Whitney, J. C., & Howell, P. L. (2013). Synthase-dependent exopolysaccharide secretion in Gram-negative bacteria. In *Trends in Microbiology* (Vol. 21, Issue 2, pp. 63–72). https://doi.org/10.1016/j.tim.2012.10.001

Wiedenheft, B., & Bondy-Denomy, J. (2017). CRISPR control of virulence in Pseudomonas aeruginosa. *Cell Research*, *27*(2), 163–164. https://doi.org/10.1038/cr.2017.6

Winter, S. E., Thiennimitr, P., Winter, M. G., Butler, B. P., Huseby, D. L., Crawford, R. W., Russell, J. M., Bevins, C. L., Adams, L. G., Tsolis, R. M., Roth, J. R., & Bäumler, A. J. (2010). Gut inflammation provides a respiratory electron acceptor for Salmonella. *Nature*, *467*(7314), 426–429. https://doi.org/10.1038/NATURE09415

WORLD HEALTH ORGANIZATION Geneva ORGANISATION MONDIALE DE LA SANTÉ Genève Typhoid vaccines: WHO position paper. (2008).

World Health Organization (WHO). (2018a, January 31). *Typhoid*.

World Health Organization (WHO). (2018b, February 20). *Salmonella (non-typhoidal)*.

Worley, M. J., Nieman, G. S., Geddes, K., & Heffron, F. (2006). Salmonella typhimurium disseminates within its host by manipulating the motility of infected cells. *Proceedings of the National Academy of Sciences of the United States of America*, *103*(47), 17915–17920. https://doi.org/10.1073/PNAS.0604054103

Wu, C., Lim, J. Y., Fuller, G. G., & Cegelski, L. (2012). Quantitative analysis of amyloid-integrated biofilms formed by uropathogenic escherichia coli at the air-liquid interface. *Biophysical Journal*, *103*(3), 464–471. https://doi.org/10.1016/j.bpj.2012.06.049

Wu, Q., Cui, L., Liu, Y., Li, R., Dai, M., Xia, Z., & Wu, M. (2022). CRISPR-Cas systems target endogenous genes to impact bacterial physiology and alter mammalian immune responses. *Molecular Biomedicine*, *3*(1). https://doi.org/10.1186/S43556-022-00084-1

Xiao, M., Lai, Y., Sun, J., Chen, G., & Yan, A. (2016). Transcriptional Regulation of the Outer Membrane Porin Gene ompW Reveals its Physiological Role during the Transition from the Aerobic to the Anaerobic Lifestyle of Escherichia coli. *Frontiers in Microbiology*, *7*(MAY). https://doi.org/10.3389/FMICB.2016.00799

Xu, H., Jeong, H. S., Lee, H. Y., & Ahn, J. (2009). Assessment of cell surface properties and adhesion potential of selected probiotic strains. *Letters in Applied Microbiology*, *49*(4), 434–442. https://doi.org/10.1111/J.1472-765X.2009.02684.X

Yamaguchi, T., Toma, S., Terahara, N., Miyata, T., Ashihara, M., Minamino, T., Namba, K., & Kato, T. (2020). Structural and Functional Comparison of Salmonella

Flagellar Filaments Composed of FljB and FliC. *Biomolecules*, *10*(2). https://doi.org/10.3390/BIOM10020246

Ye, Y., Ling, N., Gao, J., Zhang, X., Zhang, M., Tong, L., Zeng, H., Zhang, J., & Wu, Q. (2018). Roles of outer membrane protein W (OmpW) on survival, morphology, and biofilm formation under NaCl stresses in Cronobacter sakazakii. *Journal of Dairy Science*, *101*(5), 3844–3850. https://doi.org/10.3168/JDS.2017-13791

Zakikhany, K., Harrington, C. R., Nimtz, M., Hinton, J. C. D., & Römling, U. (2010). Unphosphorylated CsgD controls biofilm formation in Salmonella enterica serovar Typhimurium. *Molecular Microbiology*, *77*(3), 771–786. https://doi.org/10.1111/J.1365-2958.2010.07247.X

Zegans, M. E., Wagner, J. C., Cady, K. C., Murphy, D. M., Hammond, J. H., & O'Toole, G. A. (2009). Interaction between bacteriophage DMS3 and host CRISPR region inhibits group behaviors of Pseudomonas aeruginosa. *Journal of Bacteriology*, *191*(1), 210–219. https://doi.org/10.1128/JB.00797-08

Zhang, G., Meredith, T. C., & Kahne, D. (2013). On the essentiality of lipopolysaccharide to Gram-negative bacteria. *Current Opinion in Microbiology*, *16*(6), 779–785. https://doi.org/10.1016/J.MIB.2013.09.007

Zhang, P., Ye, Z., Ye, C., Zou, H., Gao, Z., & Pan, J. (2020). OmpW is positively regulated by iron via Fur, and negatively regulated by SoxS contribution to oxidative stress resistance in Escherichia coli. *Microbial Pathogenesis*, *138*. https://doi.org/10.1016/J.MICPATH.2019.103808

Zhang, S., Kingsley, R. A., Santos, R. L., Andrews-Polymenis, H., Raffatellu, M., Figueiredo, J., Nunes, J., Tsolis, R. M., Adams, L. G., & Bäumler, A. J. (2003). Molecular pathogenesis of Salmonella enterica serotype typhimurium-induced diarrhea. *Infection and Immunity*, *71*(1), 1–12. https://doi.org/10.1128/IAI.71.1.1-12.2003

Zhang, X., Gao, J., Ling, N., Zeng, H., Tong, L., Zhang, M., Zhang, J., Wu, Q., & Ye, Y. (2019). Short communication: Roles of outer membrane protein W on survival, cellular morphology, and biofilm formation of Cronobacter sakazakii in response to oxidative stress. *Journal of Dairy Science*, *102*(3), 2017–2021. https://doi.org/10.3168/JDS.2018-14643

Zhang, X., Goncalves, R., & Mosser, D. M. (2008). The Isolation and Characterization of Murine Macrophages. *Current Protocols in Immunology / Edited by John E. Coligan ... [et Al.]*, *CHAPTER* (SUPPL. 83), Unit. https://doi.org/10.1002/0471142735.IM1401S83

Zhao, X., Zhao, F., Wang, J., & Zhong, N. (2017). Biofilm formation and control strategies of foodborne pathogens: Food safety perspectives. In *RSC Advances* (Vol. 7, Issue 58, pp. 36670–36683). Royal Society of Chemistry. https://doi.org/10.1039/c7ra02497e

Zimmer, J. (2019). Structural features underlying recognition and translocation of extracellular polysaccharides. In *Interface Focus* (Vol. 9, Issue 2). Royal Society Publishing. https://doi.org/10.1098/rsfs.2018.0060

APPENDIX

[Appendix I]

List of Publications and Conferences

Publications

From Ph.D. Thesis

- **Sharma, Nandita**, Ankita Das, Pujitha Raja, and Sandhya Amol Marathe. "The CRISPR-Cas system Differentially Regulates Surface-Attached and Pellicle Biofilm in Salmonella enterica Serovar Typhimurium." Microbiology Spectrum (2022): e00202-22.

Other Publications

- Dhingra, Divy, Sandhya Amol Marathe, **Nandita Sharma**, Amol Marathe, and Dipshikha Chakravortty. "Modeling the immune response to Salmonella during typhoid." International Immunology 33, no. 5 (2021): 281-298.

Conferences

1. **Nandita Sharma**, Ankita Das, and Sandhya Amol Marathe. Regulation of biofilm in *Salmonella enterica* subsp. *enterica* serovar Typhimurium by the CRISPR-Cas system. In: LSRIEAS- 2018, November 1st-3rd, BITS-Pilani, Pilani campus.

[Appendix II]

Biography of Dr. Sandhya Amol Marathe

Dr. Sandhya Amol Marathe is working as an Assistant Professor in the Department of Biological Sciences, Birla Institute of Technology and Science Pilani (BITS-Pilani), Pilani campus, Rajasthan since April 2017. She obtained her Bachelor's degree from Pune University. She completed her MSc. - Ph.D. integrated doctoral degree from the Indian Institute of Science (IISc), Bangalore in the area of Infection Biology. She received the Best thesis award, MCB, IISc in 2013. After her Ph.D., she worked as a research associate at MCB, IISc. She worked as visiting Assistant Professor at BITS-Pilani for 4 years starting in July 2013. Her broad areas of research interest include bacterial pathogenesis and host-pathogen interaction. Dr. Marathe has completed one research project funded by SERB-DSTas Co-Principal Investigator and one as Principal Investigator. Currently, she is having one research project as a Project coordinator as well as Principal Investigator funded by DBT. She has published more than 29 research articles in peer-reviewed journals. She has successfully guided several undergraduate and postgraduate students in their research studies. She is currently guiding as a supervisor, four students for Ph.D.

Biography of Nandita Sharma

Ms. Nandita Sharma did her Graduation Bachelor of Technology (B.Tech.) with a specialization in Industrial Microbiology from S.H.I.A.T.S Allahabad, and a Master of Engineering (ME) in Biotechnology from BITS-Pilani, Pilani. To pursue her doctoral research, she joined the research group of Dr. Sandhya Marathe at the Department of Biological Sciences, Birla Institute of Technology and Science, Pilani, Pilani Campus, India in August 2017. She possesses an active research interest in the area of infection biology with a major emphasis on Microbial Pathogenesis and Host-Pathogen Interaction.

She qualified for GATE during her master's tenure. She has published 2 research articles in journals of international repute. She has also been consistently involved in the Department of Biological Sciences, BITS Pilani, Campus teaching program.

AMERICAN SOCIETY FOR MICROBIOLOGY | Microbiology Spectrum

RESEARCH ARTICLE

The CRISPR-Cas System Differentially Regulates Surface-Attached and Pellicle Biofilm in *Salmonella enterica* Serovar Typhimurium

Nandita Sharma,[a] Ankita Das,[a] Pujitha Raja,[a] Sandhya Amol Marathe[a]

[a]Department of Biological Sciences, Birla Institute of Technology and Science (BITS), Pilani, Rajasthan, India

ABSTRACT The CRISPR-Cas mediated regulation of biofilm by *Salmonella enterica* serovar Typhimurium was investigated by deleting CRISPR-Cas components Δ*crisprI*, Δ*crisprII*, ΔΔ*crisprI crisprII*, and Δ*cas op*. We determined that the system positively regulates surface biofilm while inhibiting pellicle biofilm formation. Results of real-time PCR suggest that the flagellar (*fliC*, *flgK*) and curli (*csgA*) genes were repressed in knockout strains, causing reduced surface biofilm. The mutants displayed altered pellicle biofilm architecture. They exhibited bacterial multilayers and a denser extracellular matrix with enhanced cellulose and less curli, ergo weaker pellicles than those of the wild type. The cellulose secretion was more in the knockout strains due to the upregulation of *bcsC*, which is necessary for cellulose export. We hypothesized that the secreted cellulose quickly integrates into the pellicle, leading to enhanced pellicular cellulose in the knockout strains. We determined that *crp* is upregulated in the knockout strains, thereby inhibiting the expression of *csgD* and, hence, also of *csgA* and *bcsA*. The conflicting upregulation of *bcsC*, the last gene of the *bcsABZC* operon, could be caused by independent regulation by the CRISPR-Cas system owing to a partial match between the CRISPR spacers and *bcsC* gene. The cAMP-regulated protein (CRP)-mediated regulation of the flagellar genes in the knockout strains was probably circumvented through the regulation of *yddx* governing the availability of the sigma factor σ^{28} that further regulates class 3 flagellar genes (*fliC*, *fljB*, and *flgK*). Additionally, the variations in the lipopolysaccharide (LPS) profile and expression of LPS-related genes (*rfaC*, *rfbG*, and *rfbI*) in knockout strains could also contribute to the altered pellicle architecture. Collectively, we establish that the CRISPR-Cas system differentially regulates the formation of surface-attached and pellicle biofilm.

IMPORTANCE In addition to being implicated in bacterial immunity and genome editing, the CRISPR-Cas system has recently been demonstrated to regulate endogenous gene expression and biofilm formation. While the function of individual *cas* genes in controlling *Salmonella* biofilm has been explored, the regulatory role of CRISPR arrays in biofilm is less studied. Moreover, studies have focused on the effects of the CRISPR-Cas system on surface-associated biofilms, and comprehensive studies on the impact of the system on pellicle biofilm remain an unexplored niche. We demonstrate that the CRISPR array and *cas* genes modulate the expression of various biofilm genes in *Salmonella*, whereby surface and pellicle biofilm formation is distinctively regulated.

KEYWORDS *Salmonella*, type I-E CRISPR-Cas system, surface-attached biofilm, pellicle biofilm

The clustered regularly interspaced short palindromic repeats (CRISPR)-Cas system bestows adaptive immunity to bacteria against invading mobile genetic elements (MGE) (1). It captures protospacers from invading MGEs and incorporates them into the CRISPR array with the help of Cas proteins (2). The system has also been implicated in alternative functions like governing virulence and bacterial physiology (3). In some

Editor Justin R. Kaspar, Ohio State University

Address correspondence to Sandhya Amol Marathe, sandhya.marathe@pilani.bits-pilani.ac.in, or Nandita Sharma, nandita1991@gmail.com.

The authors declare no conflict of interest.

Received 25 January 2022
Accepted 17 May 2022
Published 9 June 2022